



HAL
open science

Pathological mechanisms of autosomal recessive centronuclear myopathy

Ivana Zivkovic Prokic

► **To cite this version:**

Ivana Zivkovic Prokic. Pathological mechanisms of autosomal recessive centronuclear myopathy. Genomics [q-bio.GN]. Université de Strasbourg, 2013. English. NNT : 2013STRAJ106 . tel-01205644

HAL Id: tel-01205644

<https://theses.hal.science/tel-01205644>

Submitted on 26 Sep 2015

HAL is a multi-disciplinary open access archive for the deposit and dissemination of scientific research documents, whether they are published or not. The documents may come from teaching and research institutions in France or abroad, or from public or private research centers.

L'archive ouverte pluridisciplinaire **HAL**, est destinée au dépôt et à la diffusion de documents scientifiques de niveau recherche, publiés ou non, émanant des établissements d'enseignement et de recherche français ou étrangers, des laboratoires publics ou privés.

ÉCOLE DOCTORALE 414

[IGBMC - CNRS UMR 7104 - Inserm U 964]

THÈSE présentée par :

[Ivana PROKIC]

soutenue le : **25 septembre 2013**

pour obtenir le grade de : **Docteur de l'université de Strasbourg**

Discipline/ Spécialité : Sciences du vivant/ Aspects moléculaires et cellulaires de la
biologie

Mécanismes pathologiques des myopathies centronucléaires
autosomales récessives

THÈSE dirigée par :

[Mr LAPORTE Jocelyn]

Docteur, université de Strasbourg

RAPPORTEURS :

[Mme SCHMIDT Anne]

Docteur, Institut Jacques Monod

[Mr FAURE Julien]

Docteur, Grenoble Institut des Neurosciences

AUTRES MEMBRES DU JURY :

[Mr CHARLET-BERGUERAND Nicolas]

Docteur, IGBMC

There are only two ways to live your life. One is as though nothing is a miracle. The other is as though everything is a miracle.

A. Einstein

ACNOWLEDGMENTS

First of all, I would like to thank the members of the jury Dr. Anne Schmidt, Dr. Julien Fauré and Dr. Nicolas Charlet-Berguerand for accepting to evaluate my work. Thank you on your on your time, patience and your openness during the preparations of the thesis.

Last four years passed fast. They were filled with great expectations, disappointments, mistakes, improvements, knowledge, laughs, tears, new acquaintances and some goodbyes. In all this I would first like to say a big THANKS to my mentor Jocelyn Laporte for accepting me to be a part of his team. Thank you on you support, thank you for sharing your knowledge and for endless patients and time that you invested. The “MAD” team was a great place to be form a career and a personal side. I would like to thank all our lab members CriCri, Belinda, Catherine, Manuela, Karim, Christos, Osorio, Hichem and Ting, for making this long journey easier.

I would like to start by thanking Belinda, my supervisor and in some way a role model. I was always stunned by her energy, efficiency and I can say “life” management! Thank you for being so positive and kind and always finding a time to discuss. And of course thank you on your superfast corrections! Manu, the Italian spirit of our lab, thank you for being a good friend, for sharing many coffees and laughs and above all for being next to me in the most difficult moments of my life. I’ll never forget that! I would like to thank CriCri on her positivity, brightness and endless mice tails cut! And thank you for making our days more colorful with your perfect garden flowers. Our artist of the lab Catherine, thank you on all French translations and on your friendship during the past years. I am still waiting for an invitation for your concert. My neighbor Karim thank you for making this trip colorful with your explanations, challenges, ideas and critics. Christos, the most positive guy of our lab thank you on your peacefulness and advices. Hichem, my first student thank you on your excellent work and enthusiasm that you showed. I would like to thank Johann for all the social activates he organized and that made our social life more field. I must thank also Osorio, our walking encyclopedia, for sharing all his more and less science related knowledge. It was great having you in the

lab! And Ting, thank you for introducing the Chinese culture in our lives. During the last four years, many people passed through our lab and all of them left a trace in my life. I must thank Leonela, a good friend and a dedicated sport buddy for all that we shared together. I will miss you to celebrate this important moment in my life! And Barbara, thank you on your friendship and talks. I would like to use this occasion to thank also Ursula, Lavanya, Nasim, Claire and Lama for coming into my life. This is the end of one journey and a beginning of a new one. I wish you all the best in your lives and careers. You will always be in my heart!

I would like to thank Jean Louis Mandel for sharing his impressive knowledge with us and above all for transferring my CV to Jocelyn. I must thank all the people in our department that were always open for discussion and good friends in need. The biggest thanks go to Ricardo and Eric, my neighbors; I could not imagine having better ones than the two of you! All the people from Charlet's (especially to Michel), Puccio's team and Gronemeyer's team thank you for sharing good humor, advices and lab equipment with me!

IGBMC was incredible environment to work in. Thanks to all the people from animal facility, histology platform (especially to Olivia, Bruno and Isabelle), phenotyping platform (especially to Roy Combe). We have amazing imaging platform and I would like to thank Marc and Pascal on their time and guidance and to Josiane for endless samples preparations! I would like to thank also to Elisabeth Toussaint and Sylviane Bronner for all the help regarding the administrative never-ending work.

I would like to thank also to our collaborators Stephane Vassilopoulos, Jeanne Laine, Arnaud Ferry and Sestina Falcone and I hope all the hard work will pay off at the end. I still owe you that!

During my PhD and through IGBMC I meet many great friends and people who I love and appreciate. Giulia, Jelena and Caitlin above all I am lucky to have you as friends! Thank you for all your support! And I cannot skip my library buddies, Yara, Alice and Thomas who shared these last difficult moments and "suffering" with me.

Finally, I would like to thank to my family without whose support I could have never achieved this. THANK YOU my dear loving husband, for supporting me in the thought moments and for believing in me. It wasn't always easy. Thank you for your sense of humor, endless energy and all the trips to the clouds and back. This thesis is our work. Mom, thank you for encouraging me to follow my dreams and for teaching me that impossible doesn't exist. Dad, this thesis was written with you in my heart and thoughts every single day. You would be proud of me. I know. I miss you endlessly... My dear belle mère and beau père, thank you on all your kind advices, support and positive energy. I could not imagine having better parents in law than the two of you. My best sister in the world, Jelena thank you for being with me in all the ups and downs and for backing me up. Finally, I want to thank Gaga, Rada, Sandra and Mladen for all that you've been going through with me and for being the most best friends one can imagine! I love you all!

SUMMARY

BIN1 is a membrane tubulating protein and it consists of the BAR domain which binds membranes and has tubulating property; the PI motif which binds phosphoinositides and is expressed only in skeletal muscle; the CLAP domain binds clathrin and AP2 and is present exclusively in brain isoforms of BIN1; the MBD is involved in c-Myc binding and the SH3 domain is involved in interactions with prolin-rich proteins. BIN1 is an ubiquitously expressed protein with the highest expression in skeletal muscle. Mutations in amphiphysin 2 / BIN1 were found to cause autosomal recessive centronuclear myopathy (ARCNM, OMIM 255200). Mutations in patients were found in all the protein domains and include two mutations leading to a premature stop codon in the last exon 20. The PI motive, encoded by exon 11, is upregulated during myogenesis. The aim of this research was to better understand the role of BIN1 in healthy muscle and in the pathology of CNM. For this purpose, by using targeted homologous recombination in ES cells, we generated two knockout mouse models: BIN1 exon 11 and BIN1 exon 20, with exon 11 and 20 deleted, respectively. The deletion of exon 20 disrupts the SH3 domain, involved in interactions with different proteins, amongst which is dynamin 2 and induced a considerable loss of the total BIN1 protein expression. The total and muscle specific deletions of exon 20 were perinatally lethal. A disrupted T-tubules organization was observed in knockout mice, showing an importance of BIN1 during the T-tubule biogenesis. Interestingly, deletion induced in adult mice did not affect muscle function and organization. In order to understand the role of the muscle specific PI motif, we characterized the BIN1 exon 11 KO mice. Even at 12 months of age the muscle function in mice was not compromised by this deletion. However, further examination showed impairment of skeletal muscle regeneration. This work revealed that *in vivo*, BIN1 is necessary during the T-tubules biogenesis and dispensable for muscle maintenance, whereas the skeletal muscle specific PI motif of BIN1 is involved in muscle regeneration. Its function in muscle is tightly regulated by isoform switch and intramolecular binding. Understanding these features will help us step forward towards successful therapy in ARCNM and MD patients.

TABLE OF CONTENTS

LIST OF ABBREVIATIONS	1
LIST OF FIGURES	6
LIST OF TABLES	7
INTRODUCTION	8
1. Skeletal muscle	8
1.1. Skeletal muscle organization	8
1.1.1. Sarcomere	8
1.1.1.1. The thick filament structure	8
1.1.1.2. The thin filaments structure	10
1.1.1.3. Organization of the membrane system of the muscle cell	11
1.1.1.3.1. Sarcolemma	11
1.1.1.4. T-tubules	12
1.1.1.5. Sarcoplasmic reticulum	13
1.1.2. Triads, the place of excitation-contraction coupling	17
1.1.3. Excitation-contraction coupling	18
1.1.3.1. Modulating the E-C coupling	19
1.2. Development of the membrane system	20
1.2.1. ER to SR transition and maturation	21
1.2.2. T-tubules development	22
1.2.3. Triad and Calcium release units (CRUs) formation	23
1.2.4. Molecular players in triad biogenesis	24
1.2.4.1. RyR and DHPR	24
1.2.4.2. Dysferlin	26
1.2.4.3. Junctophilins	26
1.2.4.4. Mitsugumins	28
1.2.4.5. Triadin and junctin	29
1.2.5. CRUs formation summary	30
1.3. Muscle maintenance, regeneration and aging	30

1.4.	Muscle regeneration	30
1.5.	Maintenance and aging.....	32
2.	Centronuclear Myopathy	33
2.1.	X-linked centronuclear myopathy.....	33
2.1.1.	Clinical description and prognosis	33
2.1.2.	Histology	34
2.1.3.	Myotubularin 1.....	34
2.1.4.	Role of myotubularin 1	35
2.2.	Autosomal dominant centronuclear myopathy	38
2.2.1.	Clinical description and prognosis	38
2.2.2.	Histology	38
2.2.3.	Dynamin 2	39
2.2.4.	Role of dynamin 2	40
2.3.	Autosomal recessive centronuclear myopathy.....	42
2.3.1.	Clinical description and prognosis	42
2.3.2.	Histology	42
2.3.3.	BIN1 and its functions	43
3.	Review in preparation: Amphiphysin 2 (BIN1) in physiology and diseases	44
3.1.	Introduction	45
3.2.	<i>BIN1</i> gene organization and expression	45
3.3.	BIN1 domain organization and protein regulation	46
3.4.	BIN1 cellular functions	48
3.5.	Physiological functions of BIN1 and physiopathology of related diseases	52
3.6.	Conclusion and pending questions	58
	MATERIALS and METHODS	59
	RESULTS	68
	Results I: Characterization of the <i>Bin1</i> exon 20 knockout mouse model	68
1.1.	Introduction.....	68
1.2	Aim	69
1.3	Results.....	69
1.4	Conclusion.....	74

Results II: Is BIN1 involved in skeletal muscle maintenance?.....	86
II.1. Introduction.....	86
II.2. Aim	86
II.3. Results.....	86
II.4. Conclusion.....	88
Results III: Characterization of the Bin1 exon 11 knockout mouse model	92
III.1. Introduction.....	92
III.2. Aim	92
III.3. Results.....	92
III.4. Conclusion.....	96
Results IV: Altered splicing of the BIN1 muscle-specific exon in humans and dogs with a highly progressive centronuclear myopathy.....	109
IV.1. Introduction.....	109
IV.2. Aim	109
IV.3. Results	109
IV.4. Conclusion and contribution to the study.....	109
DISCUSSION and PERSPECTIVES	130
1. Role of BIN1 in skeletal muscle.....	130
1.1. BIN1 and muscle maturation.....	131
1.2. BIN1 in skeletal muscle maintenance	132
1.3. Conclusion and perspectives	134
2. BIN1 and pathophysiology.....	136
2.1. What can murine models tell us about ARCNM.....	136
2.2. Pathological mechanism of ARCNM.....	138
2.3. The pathological mechanism in centronuclear myopathy and myotonic dystrophies	141
2.4. Conclusion and perspectives	142
3. CONCLUSION	142
REFERENCES.....	144
APPENDIX I: Resume de la these de doctorat.....	179

LIST OF ABBREVIATIONS

AAV: Adeno-associated virus

Abp1: Actin binding protein

Ach: Acetylcholine

AD: Alzheimer disease

ADCNM: Autosomal dominant centronuclear myopathy

ADP: Adenosine diphosphate

ARCNM: Autosomal recessive centronuclear myopathy

ATP: Adenosine triphosphate

BAR: BIN/Amphiphysin/Rvs

bHLHLZ: basic helix-loop-helix-leucine zipper

BIN1: Briding integrator 1 or Amphiphysin 2

Ca²⁺: calcium

CASQ: Calsequestrin

CAV 3: Caveloin 3

CC: colid-coil

CHO: Chinese hamster ovary

CICR: Calcium induced calcium release

CK: Creatine kinase

CMV: *Cytomegalovirus*

CNM: Centronuclear myopathy

CO₂: Carbon dioxide

COS: CV-1 (simian) in Origin, and carrying the SV40 genetic material

CRU: Calcium release units

DAPI: 4',6-diamidino-2-phenylindole

DHPR: Dihydropyridine receptor

DiIC16: a fluorescent lipid analogue that marks the plasma membrane and all externally connected membranes, such as T-tubules

DMBA: 7,12-Dimethylbenz(a)anthracene

DNM2: Dynamin 2

E-C: Excitation-contraction

EDL: *Extensor digitorum longus*

EM: Electron microscopy

eMHC: embryonic Myosin heavy chain

ER: Endoplasmic reticulum

FDB: Flexor digitorum brevis

GED: GTPase effector domain

GRAM-PH: Pleckstrin Homology/ Glucosyltransferase, Rab-like GTPase Activator and Myotubularins

GST: Glutathione S-transferase

GTP: Guanosine triphosphate

HE: Hematoxylin-Eosin staining

HRC: Histidine rich Ca^{2+} binding protein

HSA: Human Skeletal Actin

HSA-ER^{T2}: Human Skeletal Actin tamoxifen dependent

IC: Immunohistochemistry

IP3R: IP3 receptors

ISH: In Situ hybridization

JP: Junctophilin

jSR: Junctional Sarcoplasmic reticulum

jT: junctional tubules

K⁺: potassium

KD: knockdown

KI: knockin

KO: knockout

LOAD: Late- onset Alzheimer disease

MAD: Myotubularin1-Amphiphysin2-Dynamin 2

MB: Myc Binding

MG: Mitsugumin

Mg²⁺: magnesium

MHC: Myosin heavy chain

MID: Middle domain

MTJ myotendinous junction

MTM1: Myotubularin 1

Na⁺: sodium

NADH-TR: NADH-tetrazolium reductase

NHEJ: Non-homologous end-joining

nMHC: neonatal Myosin Heavy Chain

NMJ: Neuromuscular junction

nsSNP: Non-synonymous Single-nucleotide polymorphism

OMIM: Online Mendelian Inheritance in Man

PBS: Phosphate buffered saline

PDZ-BM: PDZ binding motif

PH: Pleckstrin homology domain

PI motif: Phosphatidylinositol binding motif

Pi: orthophosphate

PI: Phosphoinositides

PRD: Prolin rich domain

PtdIns(3,5)P₂: Phosphatidylinositol 3,5 -biphosphate

PtdIns(4,5)P₂: Phosphatidylinositol 4,5-biphosphate

PtdIns: Phosphatidylinositol

PtdIns3P: Phosphatidylinositol 3-Phosphate

PtdIns5P: Phosphatidylinositol 5-Phosphate

PTP/DSP: Protein Tyrosine Phosphatase and Dual-Specificity Phosphatase

Q: Quadriceps

RID: Rac-Induced recruitment Domain

RSS: Radial strands of sarcoplasmic reticulum

RT: Room temperature

RyR: Ryanodine receptor

SDH: Succinic dehydrogenase

SEM: Standard error of the mean

SERCA: Sarco(endo)plasmic reticulum Ca²⁺ ATPase

SET: Suvar3-9, Enhancer-of-zeste, Trithorax

SH3: Src homology 3

SOL: Soleus

SR: Sarcoplasmic reticulum

TA: Tibialis anterior

TEM: Transmission electron microscopy

Tg: Transgenic

TNNT 2: Troponine T type 2

T-tubules: Transversal tubules

VGCR: voltage-gated calcium release

VICR: Voltage induced calcium release

WT: wild type

XLCNM: X-linked centronuclear myopathy

LIST OF FIGURES

Figure	Page
1. An illustration of muscle fiber and sarcomere organization	9
2. Mechanism of muscle contraction	10
3. An illustration of neuromuscular junction and organization of membrane system involved in excitation-contraction coupling relative to myofiber organization	11
4. Schema of DHPR domain organization	12
5. Structure of Calcium Release Units in adult skeletal muscle fibers	13
6. Myofibrils, sarcoplasmic reticulum and T-tubules organization in mouse diaphragm during muscle development	21
7. Models for T-tubule formation	22
8. Models for triad formation	23
9. The sequence of CRU differentiation	29
10. Satellite cell fate in regeneration	30
11. Muscle regeneration following a crush injury	31
12. Histology of neonatal X-linked myotubular myopathy and protein domains and disease-causing mutations in the myotubularin 1	34
13. Muscle histology of DNM2-related CNM, schema of dynamin 2 domain organization and its tubulation	38
14. A biopsy from a patient diagnostified with BIN1-related CNM together with schema of BIN1 protein domain organization and a schema showing BAR domains dimerization	42
15. Muscle biopsy sections of patients with severe X-linked myotubular myopathy, DNM2- and BIN1-related CNM patients	43
16. Amphiphysin 2 (BIN1) functional domains and tissue-specific isoforms	46
17. BIN1 cellular roles and proposed mechanisms of linked diseases	52
18. Model of BIN1 tubulation mechanism in normal muscle and KO models	134

LIST OF TABLES

Table	Page
1. Amphiphysin 2 (BIN1) interactors and regulated functions	48

INTRODUCTION

1. Skeletal muscle

1.1. Skeletal muscle organization

Skeletal muscle is a specialized organ that is involved in both voluntary and automatic movements, such as breathing and head and body posture. Muscles are surrounded by the epimysium and fascia which protects and isolates them from the surrounding. Skeletal muscles are composed of myofibers, assembled and connected by the tendon to the bone, which gives it a scaffold to contract and generate force.

Myofibers are multinucleated cells with a high internal organization. They are composed of hundreds of thousands of myofibrils, which are made out of sarcomeres. The sarcomere is the basic contractile unit of the skeletal muscle (Figure 1).

1.1.1. Sarcomere

The most striking feature of the skeletal muscle is its striated pattern. The striation has periodicity of 2-3 μm . The repetition unit is called sarcomere and it is the fundamental contractile unit of the skeletal muscle. One sarcomere is defined by two Z-lines, I (isotrope) band either side of it and in the middle A (anisotrope) band with the H zone and M line in the center (Figure 1). Attachment of the sarcomere occurs at the Z and M lines through the cytoskeletal complexes called costamers. Costamers are composed predominantly of intermediate filaments. Numerous proteins are involved in sarcomere organization, but the most abundant are cytoskeletal actin proteins and myosin motor proteins. Together they comprise around 70% of myofibrillar proteins.

1.1.1.1. The thick filament structure

Thick filaments are made from myosin II polymers (Figure 1). Myosin II belongs to a group of protein motors and it is the most abundant of the myofibrillar proteins. On the electron microscopy (EM) they appear as cross bridging the thick and thin filaments, giving a murky staining of the A band. Myosin functions as both, a structural protein (role of the myosin tail) and an enzyme (role of the myosin head). It moves from the M

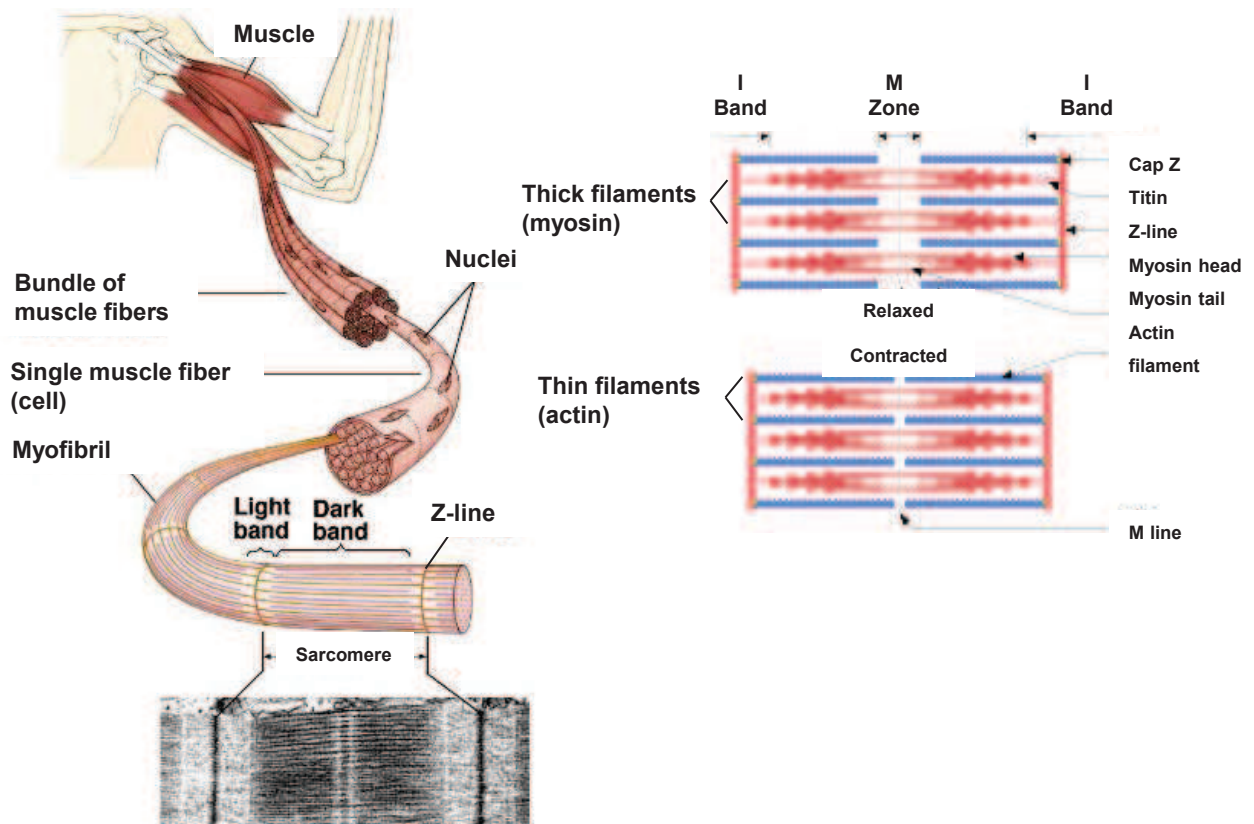


Figure 1. A schematic illustration of muscle fiber and sarcomere organization. A skeletal muscle is made of bundles of muscle fibres. Muscle fibres are long multinucleated cells, composed of myofibrils and a sarcomeres are the basic structural unites making them. Sarcomeres are aligned giving a skeletal muscle its striated appearance. The ends of each sarcomere are defined by the Z-line and thin, I band (isotropic) and thick A band (anisotropic) are composed out of actin and myosin filaments, respectively. (from <http://themedicalbiochemistrypage.org/muscle.php>)

line, along the A band and it represents the thick filament in the myofiber. Tails of the protein are joined to make the backbone of the filament, while the heads are soluble and globular. Its ATPase hydrolyzing activity is the main force of the muscle contraction. ATP binding to myosin head it followed by ATP hydrolysis to ADP and orthophosphate (Pi). Energy released in this process activates the myosin head and cocks it into a “high” energy position (Figure 3). Cocked head crossbridges the actin filament. Further the ADP and Pi are released which causes the myosin head to return to a “low” energy state and pull the actin filament (Figure 2). This process leads to contraction and is called the power stroke. Only new ATP binding destabilizes the crossbridge and detaches the myosin. Again ATP binding will result in its hydrolysis and a new cycle of contraction if the actin binding sites are available (Figure 2).

Myosin associated proteins have mainly structural role in the organization of the thick filaments (Figure 1). M protein binds and bridges the myosins on the both sides of M line. Myomesin links the titin and myosin, and the enzyme creatine kinase buffers the ATP-ADP conversion by catalyzing the regeneration of ATP from ADP during muscle contraction. Myosin-binding proteins C, H and X (MyBP-C, -H, -X) have important roles during myofibrillogenesis (Gilbert, Cohen et al. 1999). When muscle development is complete, these proteins act to stabilize thick filaments and additionally may modulate the contraction (Hofmann, Greaser et al. 1991).

Titin is one of the biggest proteins identified. It spreads from the Z-line and all the way until the M-line. It defines the length and organization of the myosin filament. The N-terminal of titin is anchored to the Z-line and interacts with a protein named titin cap (T-cap). The elastic region then spans the half of the sarcomere and C-terminal at the M-line will bind myomesin and MyBP-C. Titin is one of the first proteins to assemble into the nascent myofibril and it provides molecular template for the assembly of the thick and thin filaments (Person, Kostin et al. 2000; van der Ven, Bartsch et al. 2000). In the mature muscle titins elasticity maintains the sarcomere integrity and filament order in both the relaxed and active states.

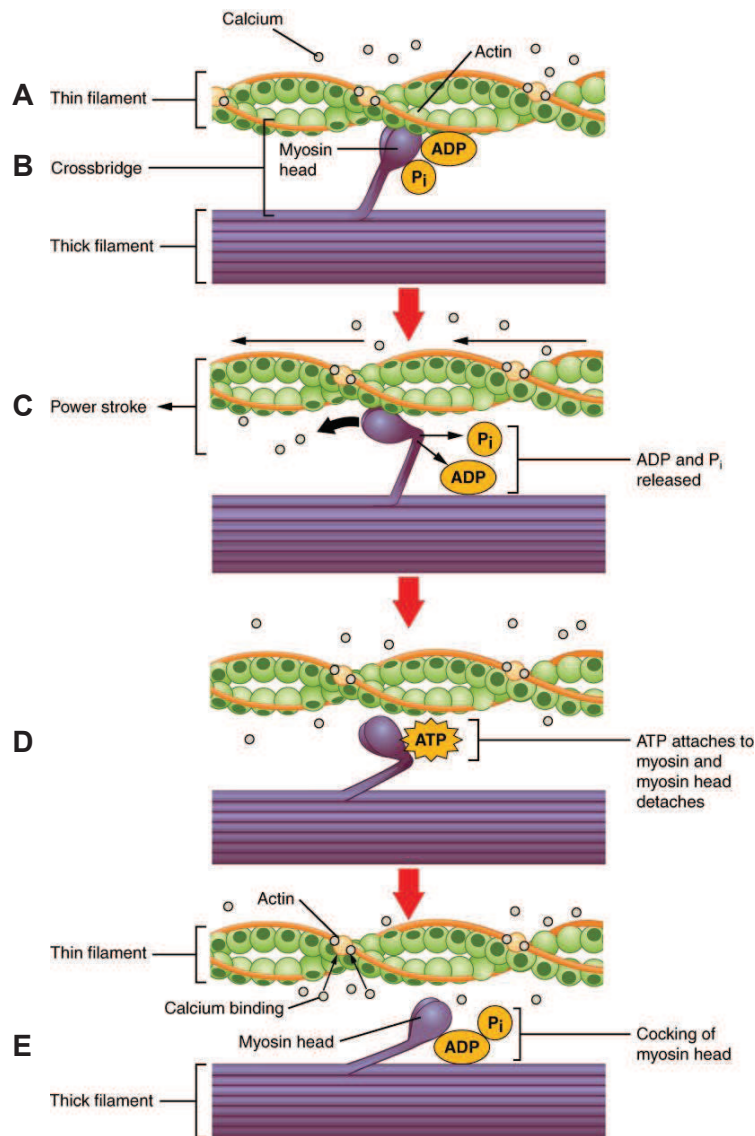


Figure 2. (A) The active site on actin is exposed as calcium binds to troponin. (B) The myosin head is attracted to actin, and myosin binds actin at its actin-binding site, forming the cross-bridge. (C) During the power stroke, the phosphate generated in the previous contraction cycle is released. This results in the myosin head pivoting toward the center of the sarcomere, after which the attached ADP and phosphate group are released. (D) A new molecule of ATP attaches to the myosin head, causing the cross-bridge to detach. (E) The myosin head hydrolyzes ATP to ADP and phosphate, which returns the myosin to the cocked position.

(from <http://cnx.org/content/m46447/latest/?collection=col11496/latest>)

1.1.1.2. The thin filaments structure

Actin filaments are the thin filaments of skeletal muscle that are anchored in the Z-line and span until the H band (Figure 1). The actin protein family is divided into 3 groups: α -actins are expressed in muscle cells and β and γ isoforms are prominent in non-muscle cells. Different isoforms are expressed in the heart, skeletal and smooth muscle. In the skeletal muscle actin filaments are capped on both sides- at the Z-line side α -actin is capped by CapZ, and at the M-line by tropomodulin. Although the capping of proteins stabilizes the length of the filament, this regulation is relatively dynamic. Exchange of actin subunits at both ends is occurred while the length is maintained (Littlefield, Almenar-Queralt et al. 2001).

Two important proteins implicated in the regulation of the actin filaments are tropomyosin and troponin. They are at regular intervals attached to the actin backbone and they regulate actin contraction. Troponin directly regulates the myosin binding to the actin filaments. Troponin is comprised of 3 subunits. The TnI is the inhibitory subunit, where the inhibition does not come from a direct interaction with actin but by its position over the filament together with the tropomyosin with whom it interacts. The TnC is a Ca^{2+} binding subunit. Binding of the Ca^{2+} released from sarcoplasmic reticulum (SR) changes its conformation allowing the myosin heads to interact with actin which results in muscle contraction. The TnT is the third subunit that provides a scaffold and connects the first two subunits with tropomyosin and actine. The main role of tropomyosin is to position troponin and to stabilize and strengthen the actin filaments. Nebulin is the second biggest protein in muscle. It is associated with the actin thin filaments and it spans the entire length of the thin filaments. The N-terminus is placed in the A-band near the tips of the thin filament and C-terminus is integrated into the Z-disk (Labeit and Kolmerer 1995).

The Z-line has a well-defined role in the structural maintenance of muscle fibers cross linking the actin and titin filaments (Figure 1). A key protein of the Z-line is the α -actinin, which binds several proteins. Its interaction with actin and titin defines the alignment of the sarcomere into the linear arrays.

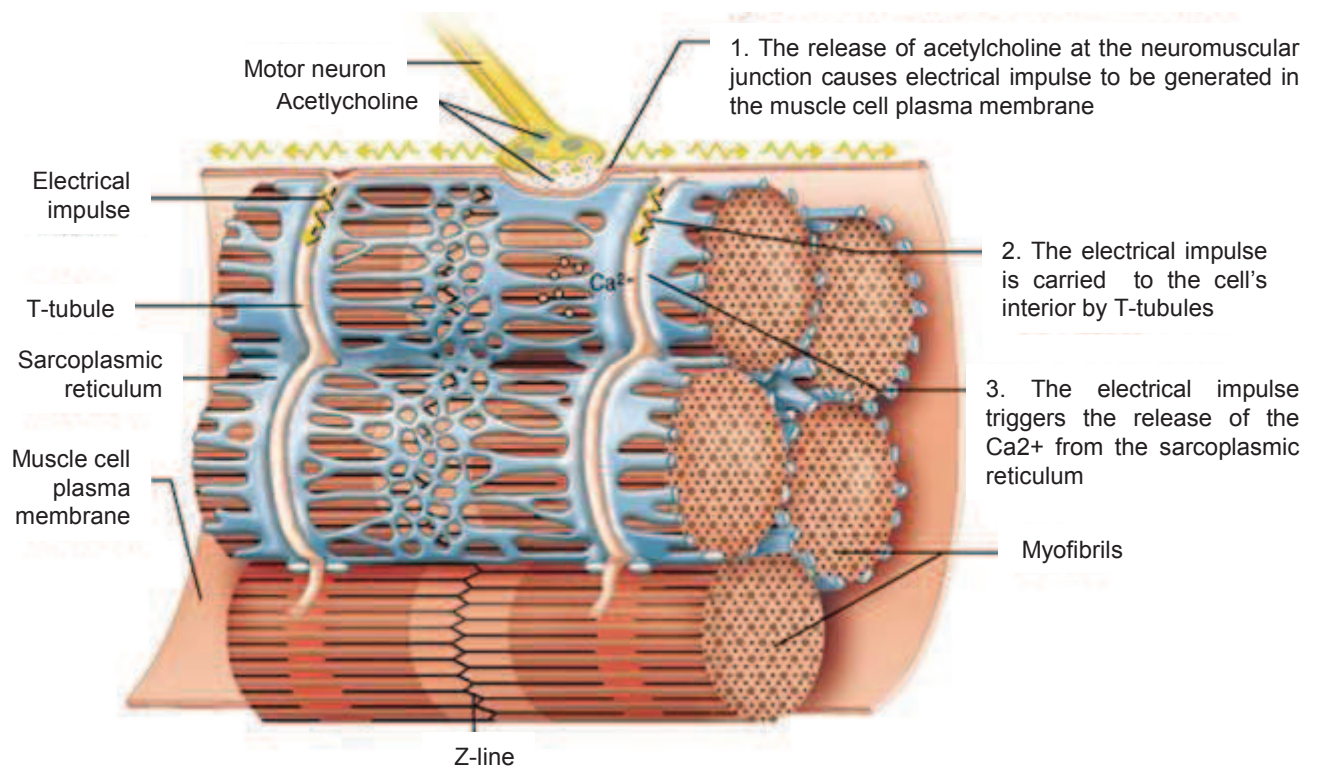


Figure 3. A schematic illustration of neuromuscular junction and organization of membrane system involved in excitation-contraction coupling relative to myofiber organization (from: <http://www.studyblue.com/notes/n/anatomy-quiz-4-muscles-/deck/1292451>)

1.1.1.3. Organization of the membrane system of the muscle cell

1.1.1.3.1. Sarcolemma

The sarcolemma is the plasma membrane of skeletal muscle. Organization of the sarcolemma is not uniform as it contains several specialized domains, including neuromuscular and myotendonous junctions, caveolae and T-tubules, described below.

Neuromuscular junction (NMJ) is comprised of motoneuron which provides a presynaptic membrane, the synaptic space and the postsynaptic membrane, provided by the skeletal muscle side (Figure 3). The action potential transmitted through the axon of the motoneuron opens the voltage-dependent calcium channels. Opening allows extracellular Ca^{2+} ions to enter the cytosol, causing the neurotransmitter-containing vesicles to fuse to presynaptic membrane and release of acetylcholine (Ach) into the synapse. Ach binds the nicotinic acetylcholine receptors on the postsynaptic membrane. The receptors are ligand-gated ion channels and Ach binding opens them and allow sodium and potassium exchange, inducing the depolarization of the motor end plate. The depolarization spreads and activates through excitation-contraction (E-C) coupling, increase of Ca^{2+} in skeletal muscle cytosol, which is followed by contraction (Figure 3).

Another type of junction is the **myotendinous junction (MTJ)**, which is located where the sarcoplasmic membrane connects to the collagen fiber bundles, known as tendons. In this case the sarcolemma penetrates into the myofibers and forms digitized-folds that are parallel to the fiber. The MTJ allows the tension generated by a muscle contraction is transmitted from the intracellular contraction of muscle proteins to extracellular proteins (Tidball 1991).

Caveolae are specialized lipid rafts localized on the cytoplasmic surface of the sarcolemmal membrane. Caveolae are fixed elements of the surface membrane and have important role in the maintenance of plasma membrane integrity. Besides serving as reservoirs of membranes, they constitute specific macromolecular complexes that provide highly localized regulation of ion channels, and regulate vesicular trafficking and signal transduction. In skeletal muscle, the main structural assembly of caveolae is mediated by caveolin 3, which is one of the 3 members of a caveolin family. It has been

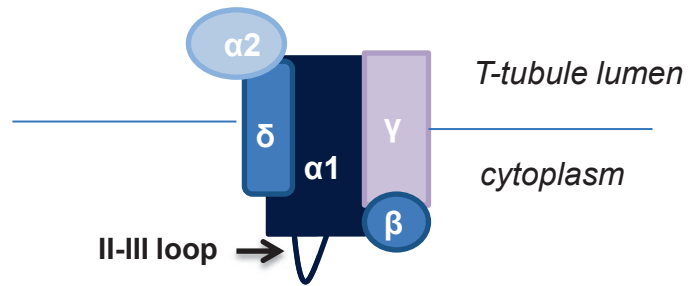


Figure 4. Schema of DHPR domain organization. The $\alpha 1$ subunit is the pore forming one. The cytosolic domain of $\alpha 1$ subunit (II-III loop) interacts with the β subunit. The γ and $\alpha 2$ - δ dimer are anchored in the T-tubule membrane and associate with the pore forming subunit.

suggested that caveolae, by further tubulation could participate in the T tubule formation (Zampighi, Vergara et al. 1975).

1.1.1.4. T-tubules

Transverse or T-tubules are invaginations which go deep into the muscle fiber between the myofibrils, and allow the action potential to be transmitted throughout the entire fiber (Figure 3). They are placed in defined and organized regions of the sarcomere, on either side of the Z-line or the A-I junction level, and as their name suggests they are positioned transversally to the muscle fiber in vertebrates. T-tubules are often not placed only transversally and longitudinal tubules can be found as well. This provides more flexibility during contraction. Although longitudinal tubules are predominant in immature fibers, in adult muscle some remain, forming a complex tubule network. T-tubules consist of free and junctional tubules (jT). In adult muscle, all longitudinal T-tubules form part of the free regions and by transmission electron microscopy (EM) they appear rounder, compared to the jT. jT are places of contact with another specialized muscle compartment, sarcoplasmic reticulum. One T-tubule and two SRs form a structure named the triad. Triads allow excitation-contraction (E-C) coupling to occur, which stimulates skeletal muscle contraction. Junctional T-tubules are present in a higher number in fast-twitch muscles, compared to slow muscles due to the faster reaction time and contraction reaction needed (Dauber 1979; Eastwood, Franzini-Armstrong et al. 1982).

Dihydropyridine receptor (DHPR) is L-type calcium channel and a voltage sensing protein that responds to the change of the action potential. Action potential goes across the membrane surfaces and into the T-tubules. DHPR receptors are located in the T-tubules, provide the link to the SR and allow Ca²⁺ release upon stimulation from action potential. DHPR is composed of $\alpha 1$, β , γ and $\alpha 2/\delta$ subunits (Figure 4) (Jay, Sharp et al. 1991).

The $\alpha 1$ subunit is the channel-forming and DHP-binding portion of the molecule (Tanabe, Takeshima et al. 1987; Morton, Caffrey et al. 1988; Mikami, Imoto et al. 1989; Nakayama, Taki et al. 1991; Perez-Reyes, Castellano et al. 1992). It consists of six α -

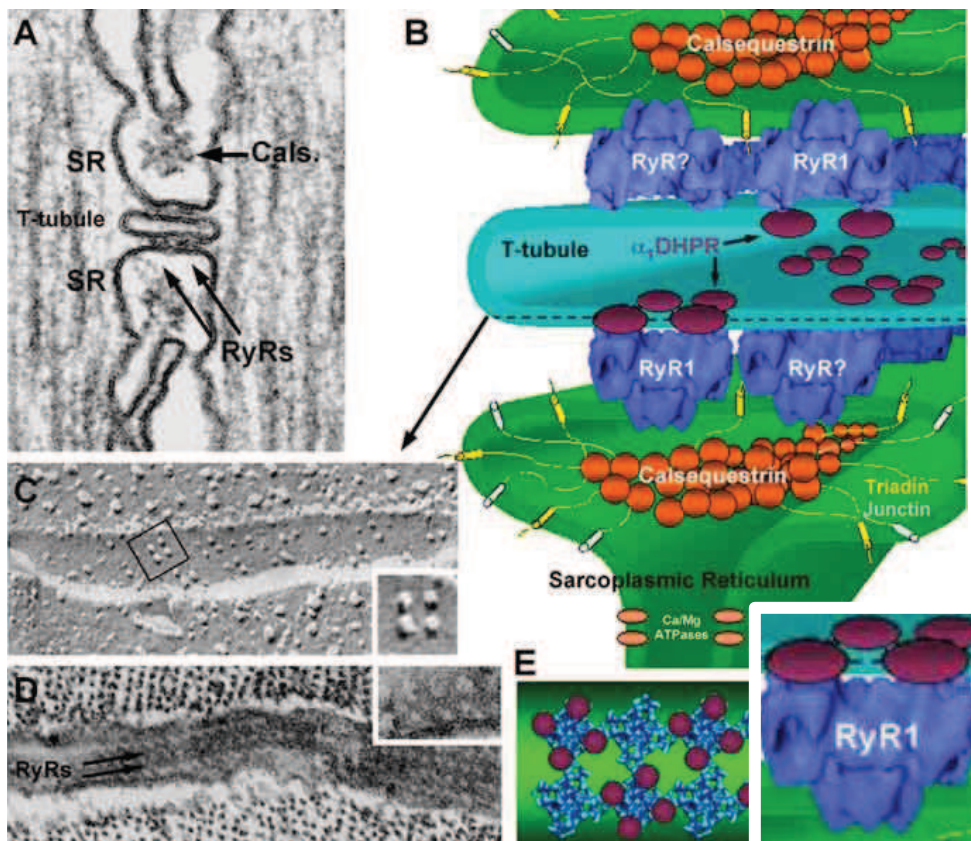


Figure 5. Structure of Calcium Release Units in adult skeletal muscle fibers. In adult skeletal muscle, junctions are mostly triads: two SR elements coupled to a central T-tubule. (A) A triad from the toadfish swimbladder muscle in thin section EM: the cytoplasmic domains of RyRs, or feet, and calsequestrin are well visible. (B) A tri-dimensional reconstruction of a skeletal muscle triad showing the ultrastructural localization of RyRs, DHPRs, Calsequestrin, Triadin, Junctin, and $\text{Ca}^{2+}/\text{Mg}^{2+}$ ATPases. Note the localization of DHPRs in the T-tubule membrane: DHPRs are intramembrane proteins that are not visible in thin section EM but can be visualized by freeze fracture replicas of T tubules (see panel C). (C) DHPRs in skeletal muscle DHPRs form tetrads, group of four receptors (see enlarged detail), that are linked to subunit of alternate RyRs (see models in B and E). (D) In sections parallel to the junctional plane, feet arrays are clearly visible (toadfish swimbladder muscle): feet touch each other close to the corner of the molecule (see enlarged detail). (E) Model that summarizes finding of panels C and D: RyRs form two (rarely three) rows and DHPRs form tetrads that are associated with alternate RyRs (RyRs in blue; DHPRs in purple; T-tubule in green) (EM courtesy of Clara Franzini-Armstrong; 3D reconstruction of RyRs courtesy of T. Wagenknecht). (Adapted from Protasi F. et al., *Front Biosci.* 2002)

helical transmembrane segments (S1-S6) in each of the four homologous domains (I-IV). Segments 5 and 6 of each of the homologous domain form the pore of the channel (Catterall 2000). Loops II and III are responsible for the interaction with the ryanodine receptor (RyR). RyR is located in the SR and loops II and III provide a mechanical link between the T-tubules and the SR. In skeletal muscle 3 α 1 isoforms have been detected (De Jongh, Warner et al. 1991) while only one isoform in cardiac muscle has been identified (Mikami, Imoto et al. 1989). The β subunit of DHPR in the cytoplasm is needed for the transport, insertion and localization of the subunit α 1 into the membrane (Schredelseker, Di Biase et al. 2005) where it is involved in kinetics regulation of the skeletal calcium channel (Lacerda, Kim et al. 1991; Andronache, Ursu et al. 2007). The γ subunit is a transmembrane subunit associated mainly with a regulatory role of the E-C. It can inhibit the DHPR channel, as well as regulate the quantity of free Ca^{2+} following hyper-depolarization of the fiber (Andronache, Ursu et al. 2007). The α 2 and δ subunits form a dimer, in which α 2 is weakly associated to α 1 and this exposes the delta subunit to the outer face of the complex. The role of this dimer has not been well studied, but interestingly mutations in α 1 and α 2 subunits lead to malignant hyperthermia (Iles, Lehmann-Horn et al. 1994). The mutations increase the RyR sensitivity by abolishing the inhibitory effect of DHPR III-IV loop on RyR1 (Weiss, O'Connell et al. 2004).

1.1.1.5. Sarcoplasmic reticulum

The sarcoplasmic reticulum (SR) is a smooth membranous structure that spans between the myofibrils (Figure 3). The main function of the SR inside the muscle cell is to regulate Ca^{2+} levels by serving as calcium storage unit and it controls Ca^{2+} release and uptake.

SR is made out of a network of tubules and cisterns. It has two distinctive domains- the longitudinal SR and the terminal cisterns. The longitudinal part or free SR surrounds the A band. This is the main site of calcium uptake in the muscle cell. The terminal cisterns are the dilated part of the SR, located each side of the longitudinal SR. Terminal cisterns are placed on the A-I border, where it couples with the T-tubules via

RyR. Coupling area defines the junctional SR (jSR) (Porter and Palade 1957; Peachey 1965).

SR contains a plethora of Ca^{2+} regulatory proteins. These proteins can be classified into 3 major groups: luminal Ca^{2+} binding proteins (calsequestrin, histidine-rich Ca^{2+} -binding protein, junctate and sarcolumenin); Ca^{2+} release channels (ryanodine receptor type 1 (RyR1) and IP3 receptors) and SR Ca^{2+} ATPase (SERCA), which is a pump for the Ca^{2+} uptake.

✚ Luminal binding or Ca^{2+} storage proteins

Calsequestrin (CASQ) (Figure 5) is the most abundant luminal protein and it makes up to 27% of the Ca^{2+} storage proteins (Costello, Chadwick et al. 1986). CASQ is aptly named due to its low-affinity and high capacity for Ca^{2+} binding (MacLennan and Wong 1971) therefore to sequestering calcium in the SR. In the free lumen, calsequestrin exists as a polymer. About a third of calsequestrin residues are acidic and are found at the C-terminus of the protein. They play an important role in Ca^{2+} binding, by forming a net surface or a pocket which binds the Ca^{2+} (Wang, Trumble et al. 1998). The polymer is not membrane bound (Fliegel, Ohnishi et al. 1987) but rather anchored to the jSR through the interactions with junctin, triadin and RyR (Zhang, Kelley et al. 1997) (Figure 5). Calsequestrin polymers can be observed by EM in the terminal SR (Franzini-Armstrong, Kenney et al. 1987).

Triadin is located in the lumen of the SR (Figure 5) (Knudson, Stang et al. 1993) and it interacts with junctin, RyR1 and calsequestrin (Zhang, Kelley et al. 1997; Kobayashi, Alseikhan et al. 2000). To date, four isoforms have been detected (Peng, Fan et al. 1994; Marty, Thevenon et al. 2000; Vassilopoulos, Thevenon et al. 2005). In skeletal muscle the most abundant isoforms of triadin are Trisk 95 and Trisk 51 (Marty, Thevenon et al. 2000). In skeletal muscle the interaction of Trisk 95/51 with other proteins is Ca^{2+} sensitive and in vitro the strongest interaction occurs in vitro in the absence of calcium (Lee, Kang et al. 2001) implying that aside from Ca^{2+} buffering, it could have a secondary role in triad regulation. Triadin also binds DHPR (Caswell,

Brandt et al. 1991). This interaction might have both, functional and structural importance.

Junctin contains as well luminal RyR and calsequestrin binding domains (Figure 5) (Jones, Zhang et al. 1995; Zhang, Kelley et al. 1997; Wei, Gallant et al. 2009). Together with triadin it anchors the calsequestrin (Figure 4). Triadin and junctin have high similarity in organization: both have a similar single membrane spanning domain, an N-terminus that is short and cytoplasmic and a C-tail is luminal and highly conserved between the two proteins (Zhang, Kelley et al. 1997; Sato, Ferguson et al. 1998). C-tail contains putative interaction site with triadin and other interaction proteins (Zhang, Kelley et al. 1997; Zhang, Franzini-Armstrong et al. 2001).

Junctate, junctin and aspartil- β hydroxylase are results of the alternative splicing of the same gene (Treves, Feriotto et al. 2000). Junctate has the initial N-terminal domain identical to junctin, the middle, single pass transmembrane domain and negatively charged C-terminal domain that is located in the lumen of the SR. C-terminal has the ability to bind calcium (Treves, Feriotto et al. 2000). Unlike calsequestrin and HCR, Ca^{2+} binding sites of junctate are tethered close to the sites of jSR membrane via its anchoring transmembrane C-terminal domain.

Histidine rich Ca^{2+} binding protein (HRC) is less abundant in the lumen compared to calsequestrin and probably functions as a secondary Ca^{2+} binding protein (Kim, Shin et al. 2003). A central histidine rich domain is involved in both the binding of calcium and protein-protein interactions (Hofmann, Goldstein et al. 1989).

Sarcalumenin is another Ca^{2+} binding protein, however unlike the other SR proteins described here sarcalumenin is located in the longitudinal SR (Leberer, Timms et al. 1990). Interestingly sarcalumenin colocalizes with SERCA, suggesting that this protein might have a role in influencing the Ca^{2+} reuptake (Leberer, Timms et al. 1990; Yoshida, Minamisawa et al. 2005).

All of the calcium binding proteins have a high-capacity and moderate to low affinity for Ca^{2+} binding and can be modulated in different ways in order to regulate the

binding properties. This complicates the understanding of their roles of individual proteins and their regulation of the calcium storage/release properties.

🚦 **Ca²⁺ release channels**

IP3 receptors (IP3R) contribute to a long lasting calcium elevation in nucleoplasmic calcium and therefore influence calcium- dependent gene transcription (Cardenas, Liberona et al. 2005). Nevertheless expression of this channel appears to be very low in skeletal muscle and its activation much slower compared to RyR. It is generally accepted that IP3R does not contribute to the E-C (Kockskamper, Zima et al. 2008). IP3R function has been subject of many debates. In C2C12 cells by over expression or photolysis it was shown that the IP3 –IP3R system does not appear to affect global calcium levels (Blaauw, del Piccolo et al. 2012). Nevertheless pharmacological prevention of IP3 production or inhibition of IP3R channel activity abolishes stress-induced Ca²⁺ sparks in skeletal muscle (Tjondrokoesoemo, Li et al. 2013). Additionally it has been proposed that in dystrophic skeletal muscle the pathological consequence of altered Ca²⁺ signals observed was associated with abnormal IP3R distribution (Balghi, Seville et al. 2006).

Ryanodine receptor type 1 (RyR1) is responsible for primary calcium release during the activation of the E-C coupling (Figure 5). RyR1 is located in the junctional regions within the triads where it forms a physical link with DHPR localized in the membrane of the T-tubules (Block, Imagawa et al. 1988). There are 3 ryanodine isoforms. RyR1 is predominantly found in the skeletal muscle, RyR2 is a cardiac muscle expressed isoform and RyR3 is found in the various tissues (Fill and Copello 2002), including skeletal muscle, however in this case always outside of the triad and E-C coupling unit (Lai, Dent et al. 1992; Giannini and Sorrentino 1995; Protasi, Takekura et al. 2000). RyR1 is a 565 KDa protein formed by homo tetramers of RyR proteomers. The C-terminal is involved in RyR1 anchoring to the terminal SR, and the majority of the RyR1 protein lays in the lumen between the SR and T-tubules where, besides the DHPR interaction, RyR1 interacts with many other with junctional regulatory proteins (Fill and Copello 2002). RyR3 plays a less direct role in the E-C coupling, and probably is being activated after RyR1 (Rios, Ma et al. 1991). Cryo-EM and 3D reconstructions

show that RyR1 is composed of two main structural components: a membrane transversal segment- the basal platform and a large cytoplasmic domain formed by 80% of the protein. The cytoplasmic domain, which has a square shape, represents the feet structures observed by EM (Block, Imagawa et al. 1988; Wagenknecht, Grassucci et al. 1989).

✚ Calcium reuptake

Sarco(endo)plasmic reticulum Ca^{2+} ATPase (SERCA) is the main protein involved in calcium clearance from the cytoplasm (Figure 5). SERCA pumps use the energy derived from ATP hydrolysis to transport ions across a biological membrane. It pumps two Ca^{2+} ions from the cytoplasm into the SR/ER lumen for each molecule of ATP hydrolyzed (Inesi, Kurzmack et al. 1980). Multiple isoforms of protein exist. SERCA1 is predominantly found in the fast-twitch skeletal muscle, whilst SERCA2 is present in cardiac, slow-twitch and neonatal muscle as well as in smooth muscle and some non-muscle tissues (Wuytack, Raeymaekers et al. 1992; Wu, Lee et al. 1995). SERCA3 is found in platelets, lymphoid cells and mast cells (Wuytack, Raeymaekers et al. 1992; Wuytack, Papp et al. 1994).

The most abundant isoform in skeletal muscle is SERCA1. It is located in both SR membranes- longitudinal and terminal cistern but outside of the E-C unit (Zhang, Fujii et al. 1995). Free SR has a uniform distribution of SERCA. The cytoplasmic domain of SERCA is composed of three globular domains, A, P and N. Domain A represents the transduction domain, domain P is the phosphorylated domain, and the N domain represents the nucleotide (ATP) binding domain. The transmembrane region contains ten hydrophobic helices (M1 to M10). Transmembrane and cytoplasmic domains are connected by intermediated region, which is called the stalk (MacLennan, Brandl et al. 1985; Brandl, Green et al. 1986).

1.1.2. Triads, the place of excitation-contraction coupling

Triads are components of the excitation-contraction (E-C) coupling and are comprised of 2 terminal cisterns of sarcoplasmic reticulum and a T-tubule (Figure 5). Although the number of triads varies between different species and within muscles, no

variability exists within a given fiber and their localization is highly organized. There are two other types of SR coupling with external membranes: dyads and peripheral couplings. Dyads are composed of one T-tubule and one terminal cistern, whereas in the case of peripheral coupling the connection is made between the jSR and plasma membrane. Dyads are more often seen in the fully formed cardiac muscle and developmental stages of skeletal muscle. Peripheral couplings precede the formation of the triads and in some muscles they disappear with maturation. Together with dyads and peripheral couplings they belong to the Ca^{2+} release units (CRUs).

Junction itself is spanned by *feet* (cytoplasmic domains of RyR) (Figure 5). Feet spans the gap between the T-tubules and SR and maintains the constant distance. They are the first part of the triad to be described and are composed of cytoplasmic domains of four large subunits of RyR. Each of the four subunits apparently contributes equally to the formation of the foot and the channel regions. The complete tetramer is necessary for ryanodine binding and channel activity (Lai, Erickson et al. 1988). Closely associated with feet are the regions of exterior membranes containing the DHPR (Flucher, Morton et al. 1990; Jorgensen, Shen et al. 1993). In normal muscle RyR1 feet are placed tetragonally, and groups of four DHPRs, called *tetrads* (Figure 5), are associated with alternate RyRs forming a related array (Franzini-Armstrong and Nunzi 1983; Protasi, Franzini-Armstrong et al. 1997). Tetrads are visible in freeze-fracture replicas, that form orderly clusters either on the surface membrane, presumably at sites of peripheral couplings or in the junctional region of T tubules.

1.1.3. Excitation-contraction coupling

Besides the striking structural features of E-C coupling, its functional side is as equally complex. Contraction information is transmitted within milliseconds and throughout the thickness of muscle fiber Ca^{2+} will be released synchronically. Its intracellular level raises several orders of magnitude.

In skeletal muscle contraction can occur in the absence of the external calcium, and DHPR directly activates the transduction of membrane depolarization into the muscle

contraction, called excitation-contraction (E-C) coupling. This observation is confirmed in dysgenic skeletal muscle (lacking $\alpha 1$ DHPR subunit, which leads to DHPR absence) which lack charge movement and E-C activation (Tanabe, Beam et al. 1988; Adams and Beam 1990). Membrane depolarization will cause DHPR to change its conformation, and through process of voltage-gated calcium release (VGCR) to activate the calcium release units (CRUs) (Figure 5). CRUs are structures that will mediate rapid release of calcium from internal stores in response to the depolarization of the external membranes (plasma membrane and T-tubules) (Franzini-Armstrong and Jorgensen 1994; Flucher and Franzini-Armstrong 1996). Relaxation of the muscle occurs when the calcium is pumped back in SR through SERCA (Fill and Copello 2002).

In cardiac muscle entry of external calcium through DHPRs is required for E-C coupling in cardiac and invertebrate muscles. DHPRs are clustered in the proximity of RyR but not physically connected and thus not forming the tetrads (Sun, Protasi et al. 1995; Protasi, Sun et al. 1996). Cardiac muscle Ca^{2+} flux through the DHPR acts on already adjacent RyRs by a different mechanism to skeletal muscle called “calcium induced calcium release” (CICR).

1.1.3.1. Modulating the E-C coupling

DHPR has the strongest impact on modulating RyR activity. It is interesting that it can activate RyR over a wide range of calcium concentrations (Posterino and Lamb 2003) and it can fully deplete SR calcium, resulting in the dramatic change in calcium levels during the E-C coupling (Kurebayashi and Ogawa 1991; Posterino and Lamb 2003)

RyR1 channel activity is dually regulated- cytosolic and luminal calcium can change its activity. Low levels of calcium (1-10 μ M) activate calcium release, whereas high concentrations (1-10mM) inhibit it (Copello, Barg et al. 1997). However concentrations of calcium as high as needed for the inhibition are rarely found under normal conditions and are more likely to be associated with pathological conditions. Since the RyR, calcium channel has a low selectivity towards the monovalent cations, such as Mg^{2+} , Na^+ and K^+ (Fill and Copello 2002), it is likely that specificity is important, in the case of

high cytoplasmic Mg^{2+} binding to a nonspecific low-affinity binding site (Laver, Baynes et al. 1997).

Calcium from the lumen of the SR can regulate RyR1 through 2 mechanisms: A feed through mechanism, in which calcium released from through RyR will bind the activating and inactivating sites on the cytoplasmic side of the protein (Tripathy and Meissner 1996) and a luminal calcium sensing which can increase activity if the channel when SR calcium reaches the mM level (Hidalgo and Donoso 1995). The precise mechanism of luminal regulation is not completely understood. It has been suggested that both the direct interaction (Sitsapesan and Williams 1997; Ching, Williams et al. 2000) and calcium-mediated conformational coupling through by the complex of calsequestrin, RyR, junction and triadin, are possible (Beard, Sakowska et al. 2002; Beard, Casarotto et al. 2005).

Finally, calcium release during the EC coupling can be modulated by various ranges of soluble molecules, such as Mg^{2+} , ATP (Smith, Coronado et al. 1985; Coronado, Morrissette et al. 1994; Copello, Barg et al. 1997), other associated proteins include FKBP12, calmodulin, protein kinase A and calmodulin kinase II (Jayaraman, Brillantes et al. 1992; Herrmann-Frank and Varsanyi 1993; Hain, Nath et al. 1994; Tripathy, Xu et al. 1995; Wang, Trumble et al. 1998) and pharmacological agents such as caffeine, ryanodine and ruthenium red (Sitsapesan and Williams 1990; Buck, Zimanyi et al. 1992; Ma, Anderson et al. 1993; Callaway, Seryshev et al. 1994).

1.2. Development of the membrane system

The first step in membrane system development is the ER transition to muscle specialized form, sarcoplasmic reticulum and its subsequent specialization to free and junctional SR (Takekura, Flucher et al. 2001). This process is followed by formation of peripheral couplings and T- tubules network elongation. Finally jSR associated with the T-tubules and forms the CRUs (Takekura, Flucher et al. 2001). This step circles the formation process, resulting in the skeletal muscle organization that we know.

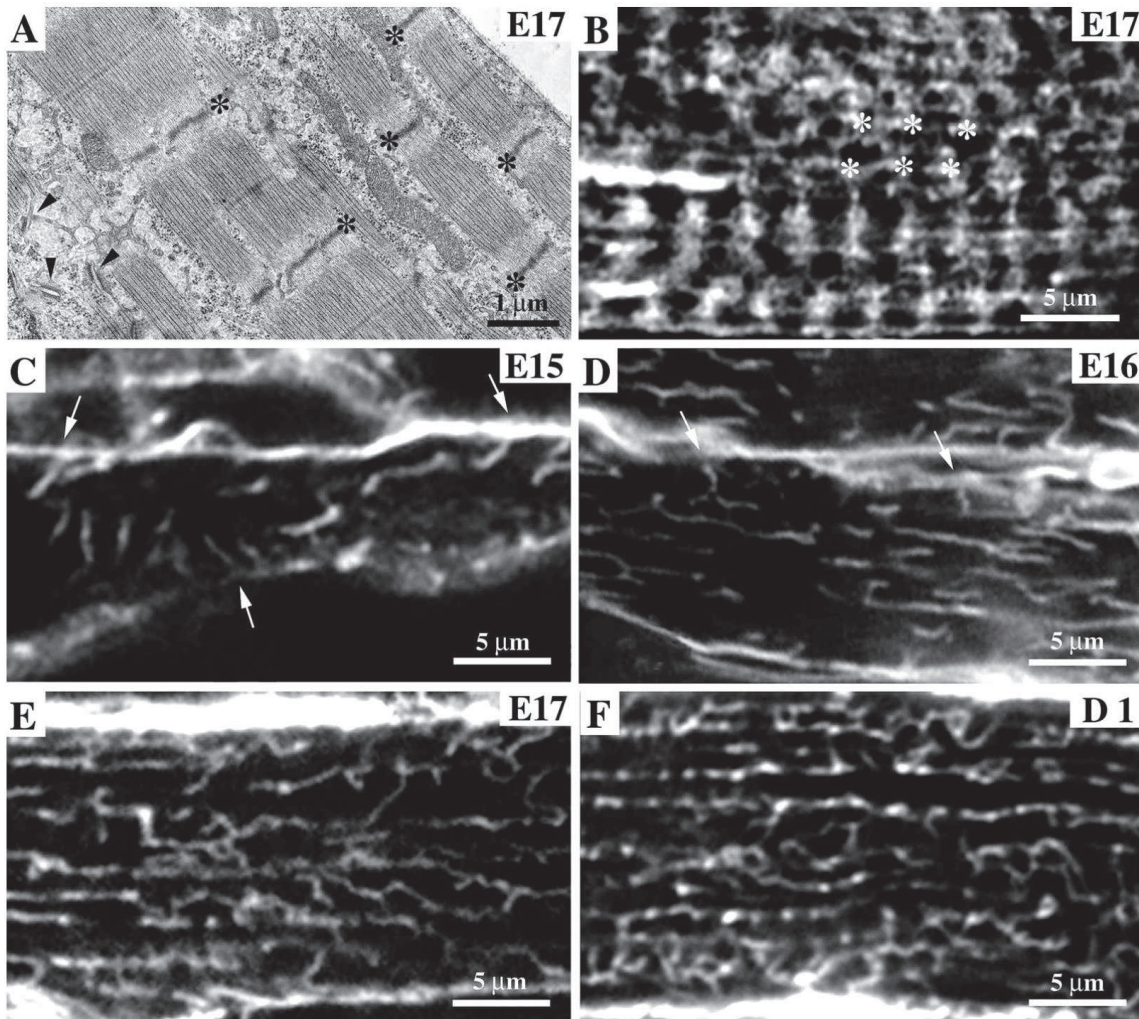


Figure 6. (A) Early organization of myofibrils and SR in developing mouse diaphragm muscle. At E17, the myotube to myofiber transition has just occurred. The myofibrils are mostly aligned with each other, forming cross striations, but occasional shifts are present (asterisks, see also (B)). Three CRUs (arrowheads) are located near the A-I border, but their orientation is not transverse. (B) SERCA immunolabeling at E17 outlines the SR and shows a transverse banding pattern, due to the preferential association of the SR networks with the I-bands of myofibrils. Asterisks indicate a cross striation shift similar to the one shown in (A). (C–F) Organization of T tubules. Confocal images of DilC16[3]-labeled muscle fibers detect the first T tubules at E15 in the form of short invaginations penetrating myotubes from the periphery (arrows, C). At E16, the great majority of T tubules run in a longitudinal orientation, and are connected to the surface by short transverse segments (arrows, D). At E17, the T tubules penetrate across the entire fiber and have a predominantly longitudinal orientation (E). At birth, the T tubule network is denser but is still predominately longitudinal with some transverse connecting elements (F).
(from Takekura H et al., Dev. Bio. 2001)

1.2.1. ER to SR transition and maturation

There are two models explaining the SR formation and specialization from ER (Boland, Martonosi et al. 1974; Martonosi 1982).

- ✚ The first model proposes that random incorporation of different SR specialized proteins (such as Ca^{2+} ATPase, SERCA, and the Ca^{2+} handling proteins) that eventually outnumber the residential ER proteins. This process gives rise to the SR as a highly specialized Ca^{2+} regulating organelle.
- ✚ The second model proposes that distinctive membranes could outgrow from ER and that the SR specific proteins could be either synthesized in the rough ER and then transported into SR forming tubules by lateral displacement or that the proteins could be transported in vesicles derived from the Golgi.

In either case the process seems like the SR and ER keep the membrane continuous through development and in the adulthood (Flucher, Takekura et al. 1993). The major SR specific proteins are upregulated early during myogenesis in parallel with myofibrillogenesis (Flucher, Takekura et al. 1993; Flucher, Andrews et al. 1994). CASQ is one of the earliest proteins to be expressed in the differentiating ER/SR (Zubrzycka and MacLennan 1976). Moreover when overexpressed in skeletal muscle CASQ segregates into the SR subdomains (Gatti, Podini et al. 1997; Jones, Suzuki et al. 1998; Sato, Ferguson et al. 1998). Together with the SR specialization, peripheral CRUs are being assembled. Using EM, in mouse diaphragm the first SR cisternae, without feet, can be seen by EM at embryonic day 14 (E14), together with the start of myofibrillar development (Takekura, Flucher et al. 2001). At E16, RyR clusters are abundant throughout most myotubes, but their labeling is weak and uneven (Takekura, Flucher et al. 2001). At this point the association with A-I junctions starts to be seen. Interestingly free SR organization, identified by SERCA labeling is already longitudinal and aligned with myofibrils. During maturation (E17-E18) the number of RyR clusters increases and they become predominantly transvers (Figure 6). The SR reaches its final position earlier in development compared to T-tubules, and it seems that association with the myofibrils is most likely driven by the formation of the CRUs (Takekura, Flucher et al.

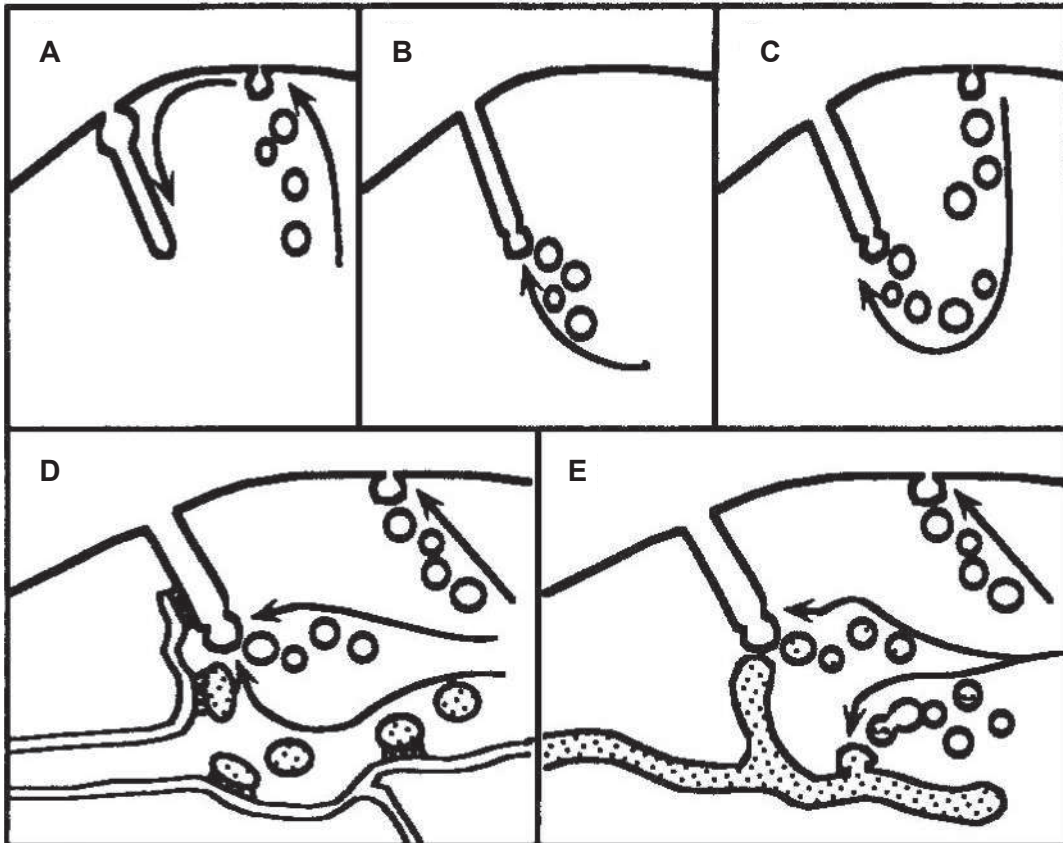


Figure 7. Models for T-tubule formation. (A) According to the “pull- in” model T-tubules derive from the plasma membrane, by a mechanism similar to endocytosis. (B) According to the “add-on” model T- tubules form by addition of new membranes by a mechanism similar to exocytosis. (C) A combination of the two principal models has been proposed, by which endocytosed plasma membrane vesicles are being added onto growing T-tubules. (D and E) Variations of the add-on model based on immunocytochemical experiments, suggesting that T-tubules are synthesized by a pathway distinct from that of the plasma membrane. (D) Junctional and nonjunctional T-tubules are transported in separate vesicles. The latter fuse directly with the plasma membrane to form T-tubules, whereas junctional T-tubule vesicles first assemble with junctional SR to form triad precursors and subsequently become incorporated in the developing T-system. (E) Transport vesicles for T-tubules are capable of fusing with the plasma membrane to form the open T-system as well as with one another to form an internal tubular system. Both systems later merge into a single open T-tubule system. (from Flucher BE et al., *Developmental biology*, 1992)

2001). At birth RyR containing elements already have a mature organization (Takekura, Flucher et al. 2001).

1.2.2. T-tubules development

After the SR development is complete and peripheral CRUs have formed, first invaginations of T-tubules can be visualized (Flucher, Takekura et al. 1993; Takekura, Flucher et al. 2001). Early T-tubules show extensive longitudinal networks that start from the periphery of the fiber and spreads towards the center. With time this network becomes more and more complex (Flucher, Takekura et al. 1993). In mouse diaphragm, the first T-tubules can be seen at E15 (Takekura, Flucher et al. 2001). At E16, T-tubules are considerably longer and make a network, penetrating deep into the fiber. The network is mostly longitudinal in orientation, which is maintained at birth (Figure 6) (Takekura, Flucher et al. 2001). The maturation of the network happens postnatally and occurs gradually throughout the next 3 weeks (Franzini-Armstrong 1991).

There are two main models explaining the T-tubule formation:

- ✚ “Pull-in” model: T-tubules are derived from the plasma membrane and are being formed by a process similar to endocytosis, but without the final step of cutting the tubes to form vesicles (Ishikawa 1968). This model proposes that no newly formed membranes that are being inserted into the growing tubules, but rather the membranes that build up the T-tubules come exclusively from the plasma membrane, together with the residential sarcolemmal proteins (Figure 7) (Schiaffino, Cantini et al. 1977).
- ✚ “Add-on” model: the appearance and elongation of the T-tubules occurs through the process of vesicle fusion and exocytosis. Vesicles are produced in the Golgi apparatus and transported to the elongated T-tubules (Figure 7).

Nevertheless two models are not mutually exclusive and may both occur to form T-tubules. T-tubule formation could start with the process of endocytosis and the elongation of the plasma membrane, together with the addition of the new vesicles at the tip of the T-tubules (Figure 7) (Malouf and Wilson 1986).

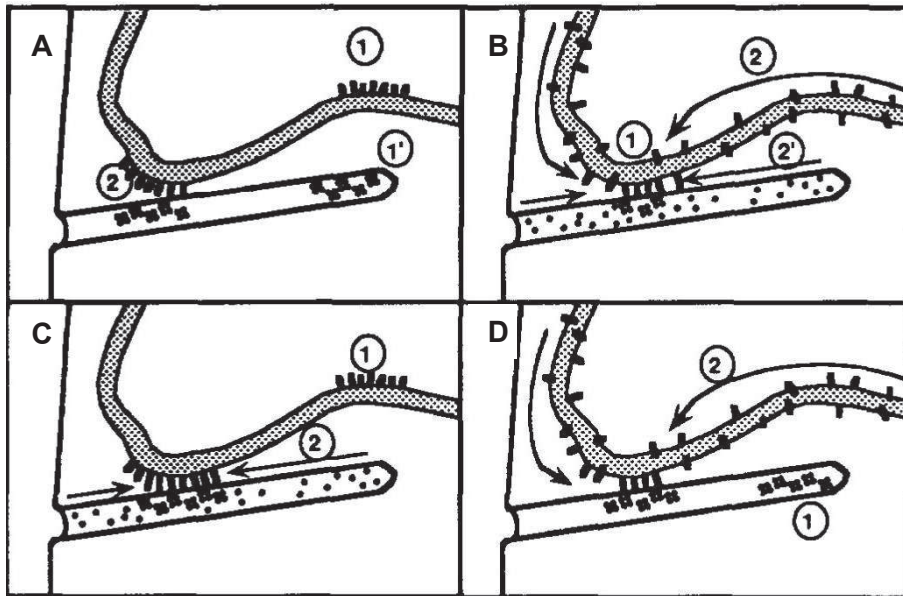


Figure 8. Models for triad formation. (A) The junctional membrane domains of the SR (1) and the T-tubules (1') differentiate independently from one another and subsequently associate to form the triad junction (2). (B) Components of undifferentiated SR and T-tubules interact with one another at (random) contact sites, leading to the association of the two membrane systems and to the initial immobilization of junctional proteins (1). Additional membrane proteins of both systems diffuse into the contact zones and become trapped as the junction differentiates (2 and 2'). (C and D) The junctional domain of one membrane system is formed autonomously (1) and upon contact with the other system induces the specialization of its junctional domain by a diffusion-trap mechanism (2). This process could originate in the SR (C) or in the T-tubules (D).

(from Flucher BE et al., *Developmental biology*, 1992)

Specific T-tubule marker proteins are absent from the plasma membrane and specific membrane proteins are absent from the T-tubules. This can be seen even at early stages and before the triad formation (Yuan, Arnold et al. 1990; Flucher, Terasaki et al. 1991). In the model explanation in newly fused myoblasts a closed tubular system has also T-tubule which contained specific proteins that was not attached to external membranes, therefore inaccessible to the DiIc16 (a fluorescent lipid probe marker of the external membranes). 48h after myoblast fusion this internal system was attached to the external membrane (Flucher, Terasaki et al. 1991).

1.2.3. Triad and Calcium release units (CRUs) formation

The link between the triad components, T-tubules and SR is so strong that even after mechanical fractionation it remains intact (Lau, Caswell et al. 1977; Kim, Caswell et al. 1990). Even after the separation of the heavy SR vesicles and the junctional T-tubules triads will maintain the ability for self-assembly (Corbett, Caswell et al. 1985). The mechanism underlying this assembly remains to be answered.

There are multiple proposed mechanisms of triad segregation and formation. (Figure 8) (Flucher 1992).

- ✚ Specialized domains on the T-tubules and SR may appear separately, after which, those domains will associate forming a functional triad
- ✚ Specific binding properties of SR and T-tubules will associate to one another. This association will trigger triad specific proteins to be concentrated at these specific points
- ✚ Junctional domains of SR and T-tubule are independently organized and will interact with the junctional domain and induce passive assembly of the counterpart membrane.

Peripheral couplings precede delivery of most of the junctional proteins (Carl, Felix et al. 1995; Protasi, Sun et al. 1996). Nevertheless in cardiac muscle it has been reported that docking is not needed for the formation of jSR complex (Engel and Franzini-Armstrong 2004). Interestingly the increased formation of the internal CRUs is

accompanied by the disappearance of the peripheral couplings (Yuan, Arnold et al. 1990; Takekura, Sun et al. 1994). It is not known what triggers this shift.

1.2.4. Molecular players in triad biogenesis

1.2.4.1. RyR and DHPR

RyR and DHPR are expressed early during the myogenesis (Marks, Taubman et al. 1991) and interestingly both become incorporated into the membranes at the same time (Flucher, Takekura et al. 1993; Flucher, Andrews et al. 1994). Mouse models of dysgenic (α 1DHPR null) and dyspedic (RyR1 null) mutant and the double KO of the two, greatly helped in understanding triad biogenesis and RyR/DHPR involvement. Studying the dysgenic muscle, it was shown that α 1 subunit is necessary for the DHPR assembly at the triads and that SR and T-tubules are not being assembled separately (Flucher, Terasaki et al. 1991). Triads and dyads are often missing, but the once which are formed have normal disposition of feet and calsequestrin (Pincon-Raymond, Rieger et al. 1985; Franzini-Armstrong 1991). In cultured dysgenic myotubes L-type Ca^{2+} current and intramembranous charge movement associated with the voltage-sensing in the E-C coupling, were also reported to be disrupted (Beam, Knudson et al. 1986; Adams and Beam 1990). The question underlying this observation was whether the interaction between voltage the sensing DHPR and calcium release RyR is required for the triad formation. Nevertheless although the formed triads appeared normal in dysgenic fibers and dysgenic myotubes in culture, E-C coupling was severely disrupted (Rieger, Pincon-Raymond et al. 1987; Franzini-Armstrong 1991). Indicating proper DHPR positioning is not needed for the triad formation. Furthermore dysgenic triads contained RyR and CASQ, showing that their targeting is independent of DHPR (Franzini-Armstrong 1991).

A knockout model of RyR1 has demonstrated, that in the absence of RyR1, SR can make junctions with the exterior membranes, and therefore RyR1 is not required for the initial docking of SR (Protasi, Franzini-Armstrong et al. 1998). Junctions contain triadin located at the CRUs and DHPR but lack the feet (RyR1). Although DHPR is expressed in RyR KO muscle it does not associate into tetrads, as seen in normal

muscle (Protasi, Franzini-Armstrong et al. 1998). Rescue of the myotubes lacking RyR1 and RyR3 (1B5 line), with RyR1 or RyR3 independently, has shown that both proteins are able to be appropriately targeted to the junctional sites and CRUs independently, but only RyR1 is able to restore the tetrad formation of DHPR (Protasi, Takekura et al. 2000). This confirms that the physical link to DHPR is not needed for DHPR clustering at the junction, but for tetrad-like organization.

Moreover skeletal muscle from double knockout mice for RyR and DHPR α 1 showed the junctional gap distance was smaller and no feet were visible in the gap, but SR-surface docking, targeting of triadin and CSQ to the jSR domains and the structural organization of the two latter proteins was not affected by lack of DHPR and RyR (Felder, Protasi et al. 2002). In non-muscle cells, overexpressed RyR and DHPR localizes to the ER and plasmalema (labeling peripheral junctions), but this does not lead to the formation of CRUs (Flucher and Franzini-Armstrong 1996). All together published data indicates that initial docking of the jSR to the plasmalema and T-tubules is necessary for the formation of the CRUs and this step does require RyR-DHPR interaction.

Caveolae may be involved in triad biogenesis. Newly formed T-tubules are continuous with clusters of caveolae and caveolar activity is very high during the start of T-tubule formation (Ishikawa 1968). One of the possible proteins implicated in the start of the formation of triads is caveolin 3. **Caveolin 3 (CAV 3)**, a member of caveolin family is most highly expressed in muscle tissues and is induced during the differentiation of skeletal myoblasts in culture (Tang, Scherer et al. 1994). One of the earliest hypothesis was T-tubules arise from the repeated budding of caveolae (Ishikawa 1968). CAV 3 has been shown to associate with newly developing T-tubules, both in vitro and in vivo (Parton, Way et al. 1997; Galbiati, Engelman et al. 2001). Cholesterol disrupting agents induce caveolin redistribution to endosomes and were found to affect T-tubule formation in vitro (Carozzi, Ikonen et al. 2000). The mice lacking CAV 3 have no clinical symptoms up to 30 weeks of age and only mild myopathic changes were identified at this age (Hagiwara, Sasaoka et al. 2000; Galbiati, Engelman et al. 2001). Nevertheless T-tubules, although present, were swollen and run in irregular

directions and DHPR and RyR exhibited a diffuse expression pattern (Galbiati, Engelman et al. 2001). Patients with limb-girdle muscular dystrophy 1C, despite having up to 95% reduction in *CAV 3* expression, have a relatively mild severity of the disease considering that patients had clinically mild to moderate proximal muscle weakness and muscle histology and biochemistry revealed only moderate non-specific myopathic changes. Most of the mutations are dominantly inherited. (Minetti, Sotgia et al. 1998).

1.2.4.2. **Dysferlin**

Dysferlin is a 230 KDa protein that belongs to a ferlin family. The C-terminal is a transmembrane domain and its multiple C2 domains are implicated in calcium binding and calcium dependent membrane fusion and repair (Rizo and Sudhof 1998; Klinge, Laval et al. 2007). In adult skeletal muscle it mainly localizes at the sarcolemma, and a minor portion is associated with the T-tubule system (Ampong, Imamura et al. 2005; Lo, Cooper et al. 2008). In contrast to normal mature skeletal muscle, during regeneration, dysferlin relocates to the cytoplasm, and increased expression observed at the T-tubules (Klinge, Harris et al. 2010). *In vitro*, dysferlin labels T-tubules during their development (Klinge, Laval et al. 2007). Additionally one of the primary defects in dysferlin deficient mice are alterations in T-tubule morphology, proving its importance in this process (Bittner, Anderson et al. 1999). Dysferlin may be involved in T-tubule formation through its interaction with caveolin 3 and it could have a role in fusion of caveolin-3 containing vesicles during T-tubule biogenesis. This mechanism is based on the interaction of dysferlin with the DHPR in adult skeletal muscle and the known interaction of dysferlin with caveolin 3 (Matsuda, Hayashi et al. 2001; Ampong, Imamura et al. 2005). Moreover patients born with mutations in dysferlin, have a subsarcolemmal accumulation of vacuoles which stay attached with to the T-tubule system (Selcen, Stilling et al. 2001).

1.2.4.3. **Junctophilins**

Junctophilins (JP) are a group of proteins that may play a role in stabilizing the interaction between SR and external membranes. They have a C- terminal hydrophobic domain, a middle single membrane passing domain, and a N- terminal cytoplasmic

domain. Within the cytoplasmic region is the MORN motif (Membrane Occupation and Recognition Nexus), which is responsible for T-tubule binding, either through phospholipids or membrane specific proteins (Takeshima, Komazaki et al. 2000). There are 4 different junctophilin isoforms (JP1-4). JP1 and JP2 are co-expressed in the skeletal muscle and JP2 is also found in cardiac muscle (Takeshima, Komazaki et al. 2000). JP1 and JP2 are needed for the maintenance of the triad and E-C coupling.

Suppression of JP1 and JP2 in skeletal myotubes leads to uncontrolled intracellular Ca^{2+} release and decreased extracellular Ca^{2+} entry (Hirata, Brotto et al. 2006). Knock out JP1 mice die perinatally from an inability to feed. They exhibit abnormal swelling of SR structures and a reduction in the number of triads. Experiments performed on muscle from the KO mice, in the short life span, show reduced contractile force and abnormal sensitivity to extracellular Ca^{2+} (Ito, Komazaki et al. 2001; Komazaki, Ito et al. 2002). During embryonic development at E14 formation of the SR and T-tubules was comparable between the KO and WT littermates. At E17 besides some triads being mispositioned there were no major alterations detected. At this time point JP1 levels start to rise significantly and expression peaks at perinatal day 1 (P1). Accordingly, P1 KO muscle morphology revealed swallowed terminal cisterns of SR and a reduced number of triads formed, together with the inefficient E-C coupling (seen by EMG) (Ito, Komazaki et al. 2001; Komazaki, Ito et al. 2002). The most recent studies have shown JP1 and JP2 are part of a large protein complex that, includes DHPR, CAV 3 and RyR1, and that JP1 and JP2 facilitate the assembly of DHPR with other proteins of the E-C coupling machinery (Golini, Chouabe et al. 2011). JP45 is another family member found to be specifically expressed in skeletal muscle (Zorzato, Anderson et al. 2000). JP45 can directly bind calcequestrin and I and II loop and C-terminus of the $\text{DHPR}\alpha 1\text{S}$ subunit. Over expression of JP45 in C2C12 myotubes does not change the properties of the voltage-activated Ca^{2+} current whereas the amplitude of depolarization-induced Ca^{2+} transient was decreased (Gouadon, Schuhmeier et al. 2006). Both knock down of JP45 in myotubes and chronic ablation of JP45 expression in JP45 KO mice have reduced DHPR protein expression in microsomal vesicles containing T tubule membranes, as well as DHPR peak molecular charge movement (~40%) in myotubes and mature muscle fibers (Anderson, Altafaj et al. 2006; Delbono, Xia et al. 2007). This

suggests JP45 is involved in the regulation of E-C coupling and proper positioning of the triads. (Anderson, Treves et al. 2003; Anderson, Altafaj et al. 2006).

1.2.4.4. **Mitsugumins**

Another player in CRUs formation is ***Mitsugumin 29 (MG29)***. MG29 is a 29kDa protein and which is located in the triad junction (Komazaki, Nishi et al. 1999). MG29 is a member of the synaptophysin family (Takeshima, Shimuta et al. 1998). The N- and C-terminus are cytoplasmic and the central region contains 4 transmembrane segments. MG29 is expressed prior to T-tubule formation where it is associated with the formation of the SR (Komazaki, Nishi et al. 1999). Following SR formation, the formation of triad occurs, it starts localizing on the junctional region of triads, where in the adult muscle is located predominately (Komazaki, Nishi et al. 1999) Interestingly expression of MG29 in amphibian embryonic cells caused excess formation of tubular ER in the cytoplasm (Komazaki, Nishi et al. 1999). MG29 KO mice had reduced muscle mass and fiber diameter. KO mice had lower twitch force, increased fatigability and reduced Ca^{2+} uptake (Nishi, Komazaki et al. 1999; Komazaki, Nishi et al. 2001; Brotto, Nagaraj et al. 2004). Ultrastructure of the skeletal muscle showed incompletely developed and immature SR network and swollen T-tubules (Nishi, Komazaki et al. 1999; Komazaki, Nishi et al. 2001). These observations suggests that MG29 has a role in both the early formation of jSR and its connection to T-tubules (Komazaki, Nishi et al. 1999), as well as proper E-C coupling (Nishi, Komazaki et al. 1999; Brotto, Nagaraj et al. 2004).

Another ***mitsugumin family member MG53*** has been identified as a key player in intracellular membrane trafficking and membrane repair in striated muscles (Cai, Masumiya et al. 2009). MG53 KO mice show progressive myopathy and reduced exercise capability, associated with defective membrane-repair capacity (Cai, Masumiya et al. 2009). In addition to its specific expression in striated and cardiac muscle, MG53 was shown to bind to dysferlin and caveolin 3, two proteins directly implicated in T-tubule biogenesis (Cai, Weisleder et al. 2009). More recently it was shown to interact with SERCA1a and attenuate its activity during muscle contraction and relaxation, but not during the resting state (Lee, Park et al. 2012). In order to investigate more general approach in repairing the “leaky cell membranes” in myotonic dystrophy hamster model,

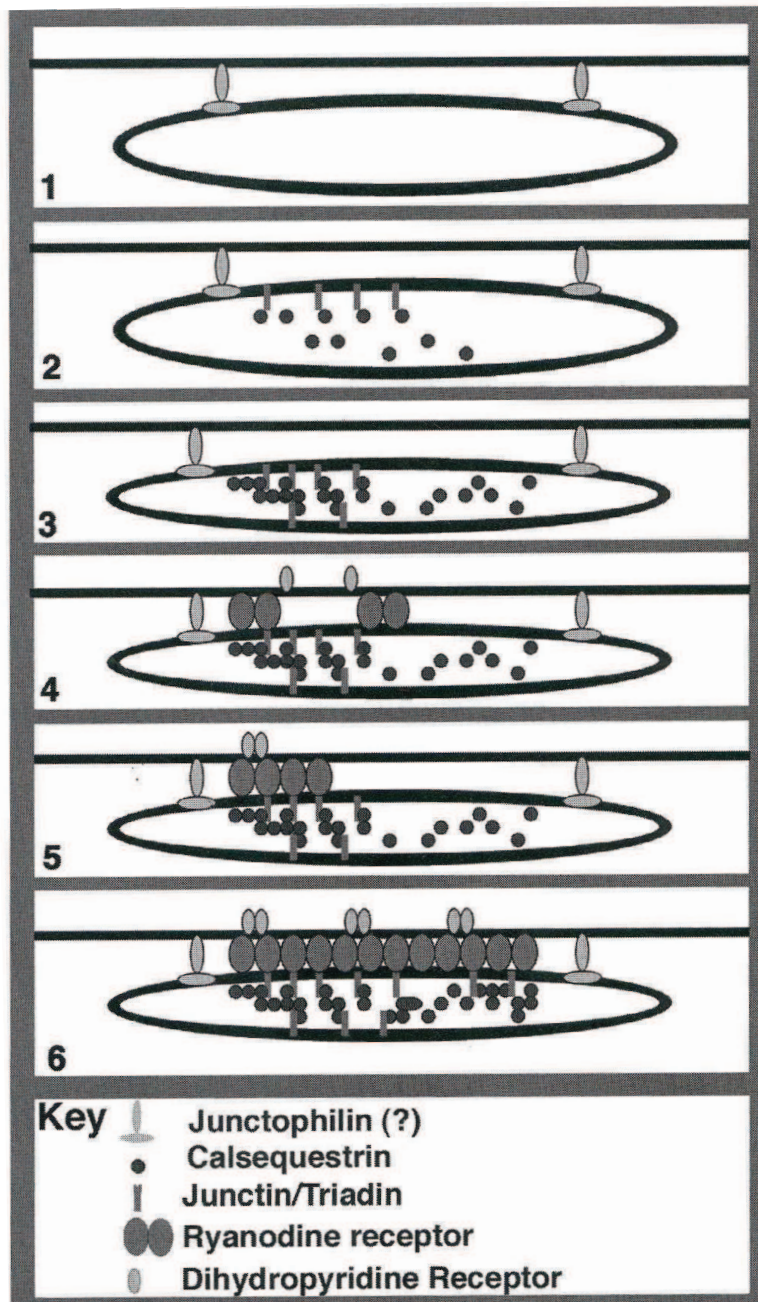


Figure 9. The sequence of CRU differentiation events involves (1) an initial docking due to junctophilin; (2) arrival of junctin/triadin and calsequestrin; (3) bundling of calsequestrin by triadin/junctin; (4) trapping of RyRs and DHPRs (5) self-assembly of RyR into arrays and linking of DHPR to RyR; and (6) maturation by the addition of more junctional protein.

Myology book, 2006

systemic delivery and muscle-specific over-expression of human MG53 gene by recombinant adeno-associated virus (AAV) vectors was used. MG53 overexpression enhanced membrane repair, ameliorated pathology, and improved muscle and heart function in the hamster model of myotonic dystrophy (He, Tang et al. 2012). Injection of recombinant human MG53 decreased muscle pathology in the mdx dystrophic mouse model (Weisleder, Takizawa et al. 2012) showing that it is a promising target for the membrane restoration defects in dystrophy patients.

1.2.4.5. **Triadin and junctin**

Other proteins that might facilitate the process of triad formation are ***triadin and junctin***. Knockdown of triadin in C2C12 cells inhibits depolarization induced Ca^{2+} release (Rezgui, Vassilopoulos et al. 2005; Wang, Li et al. 2009). Conversely overexpression of triadin in non-myogenic cells resulted in drastic modifications of ER structure. ER rope-like structures were associated with large reorganization of the microtubule (MT) network, and moreover the MTs could not be depolymerized by nocodazole (Faure J. et al 2009, (Fourest-Lieuvin, Rendu et al. 2012), suggesting a novel role for triadin. High Ca^{2+} depolymerized the MTs and triadin could be the missing link which normally stabilizes them and maintains the SR shape (Marty, Faure et al. 2009). Nevertheless, triadin KO mice present no obvious functional phenotype, but exhibited 30% of misorganized T-tubules and have reduced amplitude of Ca^{2+} transient (Shen, Franzini-Armstrong et al. 2007; Oddoux, Brocard et al. 2009). This shows that besides regulating Ca^{2+} homeostasis, triadin plays a role in triad organization. Interestingly triadin has been shown to bind CAV 3. This interaction has been proposed to regulate of Ca^{2+} levels, through modulation of the RyR- CAV 3 interaction (Vassilopoulos, Oddoux et al. 2010). The impact that this might have on triad biogenesis has not yet been explored.

Junctin is a structurally similar to triadin, and may have a complementary role in Ca^{2+} regulation. A recent study comparing single and double mutants for triadin and junctin has showed that, triadin and not junctin function as an anchorage point for the CASQ in the jSR (Boncompagni, Thomas et al. 2012). Double KO triadin/junctin mice

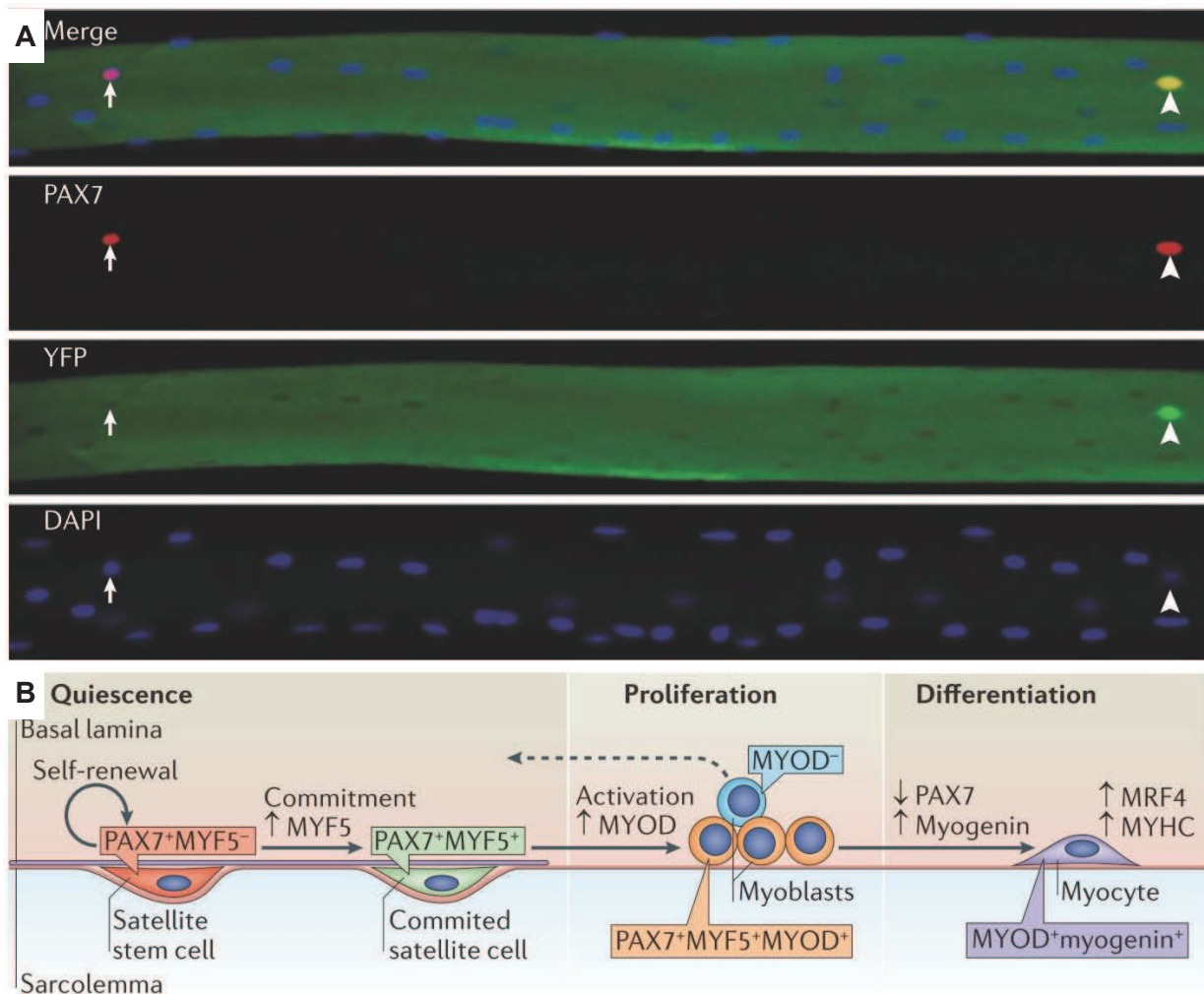


Figure 10. Satellite cell fate in regeneration. (A) Immunofluorescence micrograph of quiescent satellite cells on a resting extensor digitorum longus (EDL) muscle fibre isolated from a MYF5–Cre R26R–YFP transgenic mouse, in which MYF5 expression is marked by yellow fluorescent protein (YFP; green). Satellite cells represent <math><5\%</math> of all nuclei (labelled with DAPI; blue) in skeletal muscle and express the transcription factor paired-box 7 (PAX7; red). Although most satellite cells (~90%) are committed to the muscle lineage and have expressed Myf5 at some point in their ancestry (arrowhead), a subpopulation (~10%) has never expressed Myf5 and remains YFP negative (arrow). (B) In quiescence, satellite cells are a heterogeneous population residing between the basal lamina and the sarcolemma of their host fibres; ~90% are committed satellite cells (PAX7 + MYF5 +), whereas ~10% are satellite stem cells (PAX7 + MYF5 -). Following activation, committed satellite cells upregulate myoblast determination protein (MYOD; PAX7 + MYF5 + MYOD + cells), re-enter the cell cycle to proliferate as myoblasts and then progress into differentiation by downregulating PAX7 and upregulating myogenin as myocytes (MYOD + myogenin + cells). Regeneration of myofibres requires the fusion of myocytes into new myotubes or with host fibres (not shown). During proliferation, heterogeneity regarding MYOD expression suggests that some MYOD - myoblasts are able to reverse into quiescence (dashed arrow). MRF4, muscle-specific regulatory factor 4; MYHC, myosin heavy chain (from Yu Xin Wang YX et al., *Nat Rev Mol Cell Bio*, 2012).

exhibited a strong defect in terminal cisternae structure and almost a complete absence of CASQ localized in jSR (Boncompagni, Thomas et al. 2012).

1.2.5. CRUs formation summary

Taken together, it is believed that sequence of events leading to triad formation (figure 3) start with SR docking, probably via JP family involvement. This is followed or slightly preceded by CASQ accumulation due to the junctin/triadin accumulation. RyR and DHPR appear simultaneously and RyR self-assembly will direct DHPR arrangement into tetrads (Figure 9) (Engel and Franzini-Armstrong 2004).

1.3. Muscle maintenance, regeneration and aging

Muscle tissue is exposed daily to various environmental pressures and almost constantly goes remodeling. This remodeling is required for muscle maintenance and in more extreme cases requires muscle regeneration. During aging, the muscle is less able to respond to environmental stress and injuries. The damage accumulates, leading gradually to deterioration and eventually muscle wasting. Muscle regeneration can be compromised in different muscle diseases such as muscular dystrophies (Piccolo, Moore et al. 2000; Lo, Cooper et al. 2008), myotubular myopathy (Lawlor, Alexander et al. 2012), etc.

1.4. Muscle regeneration

Process of skeletal muscle regeneration has different phases (Figure 10). Following the injury, signaling from the damaged tissue, initiates rapid recruitment of neutrophils from the circulation (Tidball 1995). 24-48h later, signaling from the neutrophils and satellite cells (SCs) population attracts monocytes (Chazaud, Sonnet et al. 2003). These monocytes initially have a pro inflammatory role and they phagocytose cellular debris. Following this, SCs start to proliferate and migrate to the site of injury. Further, the monocyte population then become anti-inflammatory, by differentiating into macrophages, which clear cellular debris and stimulate myoblasts (activated satellite cells) to fuse to form newly regenerating fibers or fuse to damaged and regenerating fibers (Arnold, Henry et al. 2007). The total time taken from activation until myoblast

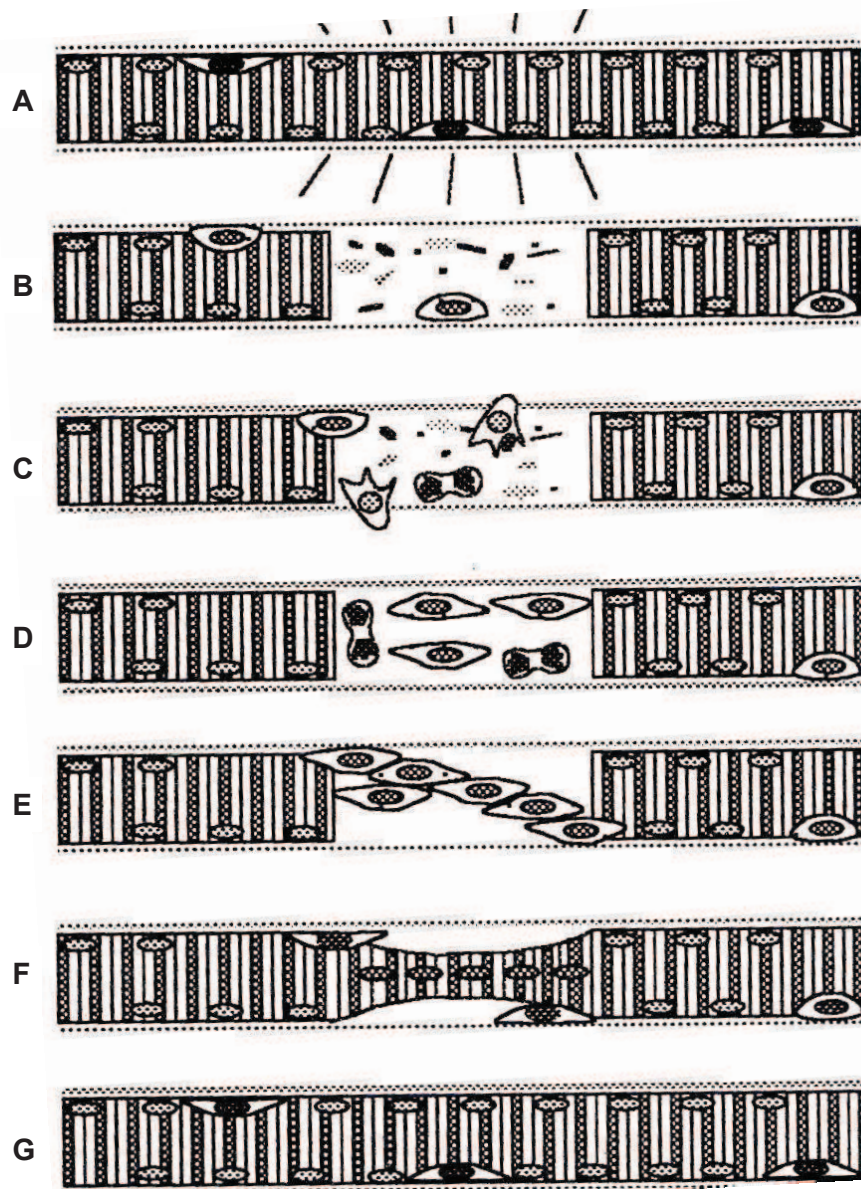


Figure 11. Muscle regeneration following a crush injury. (A) Mechanical trauma destroys the integrity of the myofiber plasmamlemma, leading to ingress of extracellular calcium. (B) The myofiber undergoes necrosis and autodigestion by intrinsic proteases, but the endomysial tube and satellite cells remain. Segments of the myofiber adjacent to the injury may heal over and remain viable. (C) Macrophages, derived from the blood monocytes, penetrate the endomysial tube and complete the removal of necrotic debris. Satellite cells become activated and enter the cell cycle. (D) The cells proliferate while attached to the inner surface of the basal lamina. (E and F) Satellite cells begin to withdraw from the cell cycle and fuse to form multinucleated myotubes. These may subsequently fuse with the surviving stump myofibers, thus providing continuity across the injury. (G) The original myofibers and complement of the satellite cells are restored. (from Yu Xin Wang YX et al., *Nat Rev Mol Cell Bio*, 2012).

fusion, in mouse takes around 7 days (Zammit, Heslop et al. 2002). Muscle maturation then continues with myofibrils being formed and aligned, together with the rest of the contractile machinery (SR, T-tubules, triads). Interestingly most of the embryonic myogenic program is repeated (reviewed in the chapter 2.4).

Satellite cells (SCs) are primary progenitors involved in muscle regeneration. They have the ability to self-renew, classifying them as muscle stem cells. The name satellite cells comes from their location between the basal lamina that surrounds each muscle fiber and the plasma membrane of the muscle fiber (Mauro 1961). An important role of satellite cells is to contribute to the growth of muscle fibers, which in adults contain 6 to 8 times more nuclei per fiber than in neonates (Engel and Franzini-Armstrong 2004). Interestingly the number of satellite cells decreases with time. In mice this starts from the age of 2 months, and in humans it happens after the 9th year of life (Engel and Franzini-Armstrong 2004). Quiescent satellite cells represent 2.5-6% of total nuclei per muscle fiber, however muscle injury leads to their activation, and they can proliferate and generate large numbers of new myofibers within a few days (Whalen, Harris et al. 1990). Some quiescent SCs through asymmetrical cell division maintain the progenitor pool giving rise to a new population of quiescent and activated SCs. The activated population continues to proliferate giving rise to myogenic precursor cells and myoblasts (Figure 11).

Different models to induced muscle damage have been used to study muscle regeneration. The most commonly used are toxin injections, downhill running and needle wounding. Toxin injections are very often used, as it induces massive degeneration of the muscle where it is injected. The two most used toxins are notexin and cardiotoxin (Harris, Johnson et al. 1974; Lin Shiau, Huang et al. 1976). Both are given intramuscularly and therefore injuring a single muscle. Downhill running is the most physiologically relevant model, as this causes eccentric contraction of the muscle, which induces damage to the muscle. This type of exercise will damage different muscles, but to a smaller extend than toxin injections. Finally needle wounding is the most subtle form, that causes localized injury within the muscle, and it is the most appropriate to what is seen under the normal conditions. However the toxin induced

approach is the most common used, since it stresses the muscle in higher extend. Regeneration is a gradual and continuous process, but nevertheless it can be separated in different phases. In mice the phases are well defined. Three days after degeneration, the immune system is activated. At this stage pro-inflammatory macrophages are active clearing the cellular debris. Two days later, the macrophage population already switched to have an anti-inflammatory role, stimulating the satellite cells migration and fusion. By day 7 the response from SCs is mainly complete and this is followed by muscle maturation. At 14 days, most of the cells have regenerated and contain centralized nuclei and with numerous fibers expressing embryonic or neonatal myosin heavy chain (eMHC/nMHC), which is normally characteristic for fetal muscle development. At 28 days, regeneration is complete, with some centralized nuclei, and eMHC or nMHC expression has diminished.

1.5. Maintenance and aging

Muscle maintenance relies on the capability of muscle to overcome the constant challenges and continuously repair the damaged fibers. Aging of the skeletal muscle is accompanied by numerous changes- differences in MHC expression (Frontera, Suh et al. 2000; D'Antona, Pellegrino et al. 2003; Kadi, Charifi et al. 2004), a decline in respiratory chain function (Boffoli, Scacco et al. 1994), reduction of the stress response proteins (Doran, Donoghue et al. 2009), reduction of the protein synthesis (Balagopal, Schimke et al. 2001) and impairment in the E-C coupling (Wang, Messi et al. 2000). All this leads to reduced specific force both in vitro and in vivo (Larsson, Li et al. 1997; D'Antona, Pellegrino et al. 2003; Trappe, Gallagher et al. 2003). This is why certain pathologies although genetically based, can have a late onset phenotype (Galbiati, Engelman et al. 2001; Durieux, Vignaud et al. 2010). The difference in penetrance or a late penetrance can come as a result of compensatory mechanisms within muscle, accumulation of the damage over time and the capability of muscle to handle these changes.

2. Centronuclear Myopathy

Centronuclear myopathies (CNM) are a group of inherited muscle disorders that belongs to a larger group of congenital myopathies. Although heterogeneous, all congenital myopathies are inherited muscle disorders, clinically characterized by early onset. Some of the common features are delayed motor development and stable or slowly progressive muscle weakness (Romero and Clarke 2013).

CNM is characterized by a high number of muscle cells with centrally located nuclei which are not in the process of regeneration. Type I fiber predominance and fiber atrophy is observed. There are three main forms of CNM: X-linked or myotubular myopathy (XLCNM, OMIM 310400), caused by mutations in myotubularin 1 (*MTM1*); autosomal dominant form (ADCNM, OMIM 160150) caused by mutations in dynamin 2 (*DNM2*) and an autosomal recessive form (ARCNM, OMIM 255200) caused by mutations in amphiphysin 2/*BIN1* (Blondeau, Laporte et al. 2000; Bitoun, Maugenre et al. 2005; Toussaint, Nicot et al. 2007).

2.1. X-linked centronuclear myopathy

X-linked or myotubular myopathy (XLCNM, OMIM 310400), was the first form of CNM to be discovered. Mostly it affects males, but a few female cases have been described (Tanner, Orstavik et al. 1999). In total, more than 200 mutations, spread throughout the *MTM1* gene have been reported (Laporte, Biancalana et al. 2000).

2.1.1. Clinical description and prognosis

The first cases of XLCNM were described already in 1966 (Spiro, Shy et al. 1966). Onset of the disease can be seen even in utero, due to reduced foetal movements and polyhydramnios (excess of amniotic fluid in the amniotic sac). At birth, newborns are usually weak and floppy. They have feeding difficulties and frequently need respiratory assistance (Romero 2010; Romero and Bitoun 2011). Ptosis and limited eye movement are common as well as facial diplegia (inability to move facial muscles). Often there is no cardiac involvement and cognitive development is normal. A high number of patients die within the first year of life, due to respiratory failure. The

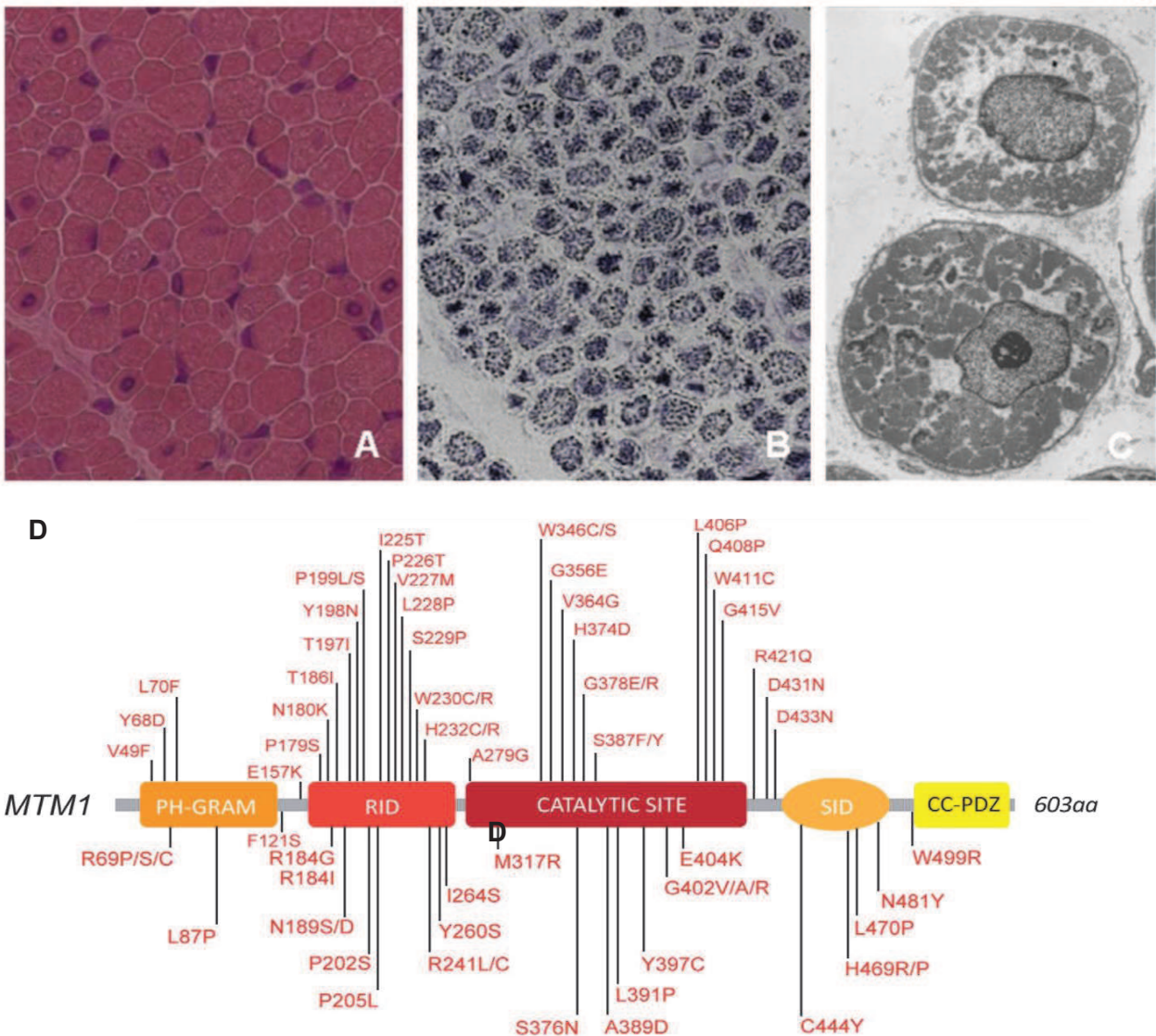


Figure 12. Histology of neonatal X-linked myotubular myopathy and protein domains and disease-causing mutations in the myotubularin. (A and B) Histology of transverse muscle sections from the XLCNM patient show (A; HE) numerous fibres with central nuclei resembling myotubes. (B) NADH-TR staining reveals the fibres with a dark central region which are frequently surrounded by a paler peripheral halo. (C) Electron micrograph of transverse section shows the nuclei in the centre of the fibre often bordered by mitochondria, glycogen and zone with reduction of myofilaments (*from Romero NB, Neuromuscular Disorders, 2010*) (D) Myotubularin contains a PH-GRAM domain that may bind lipids and a coil-coiled-PDZ binding site to form homo- and hetero-dimers with other members of the myotubularin family. Only the disease-causing missense mutations in MTM1 are represented, based on the international UMD-MTM1 database (*from Cowling BS et al., PLOS Genetics, 2012*).

disease in non or mildly progressive, and with a respiratory support (needed in more than 70% of the cases) (McEntagart, Parsons et al. 2002) and regular check-ups (respiratory infections are common), prognosis is much more promising and patients have better chances for longer survival. In the case of missense mutations, life span of the patients is more diverse and can reach even more than 60 years (Biancalana, Caron et al. 2003).

2.1.2. Histology

In addition to the classical CNM features mentioned previously, histology reveals fibres which can appear rounder and resemble foetal myotubes (Spiro, Shy et al. 1966). In longitudinal sections, long chains of nuclei are seen in the centre of the fibre. Succinic dehydrogenase (SDH) and nicotinamide adenine dinucleotide tetrazolium reductase (NADH-TR) staining reveal the fibres with a dark central region which are frequently surrounded by a paler peripheral halo ring (Figure 12). Using EM to look at the ultrastructure shows that the central areas of the fibres correspond either to centrally placed nuclei or empty regions surrounded by mitochondria aggregates and glycogen granules. Myofilaments are lacking from this region and are only found at the periphery (Figure 12). Immunocytochemistry (IC) shows DHPR and RyR1 are located in the central areas of the muscle fibers. All cytoplasm was positive for desmin, with more prominent central staining, and Cav3 is normally observed at the sarcolemma (Figure 15) (Romero and Bitoun 2011).

2.1.3. Myotubularin 1

Linkage analysis related myotubular myopathy to X chromosome (Darnfors, Larsson et al. 1990; Thomas, Williams et al. 1990) and this was followed by discovery of myotubularin 1 (MTM1) and its involvement in CNM (Laporte, Hu et al. 1996). MTM1 is a phosphoinositide phosphatase located on Xq28. With 13 other family members, it belongs to a myotubularin family of phosphatases (Laporte, Bedez et al. 2003). MTM1 dephosphorylates, *in vivo* and *in vitro*, PtdIns3P and PtdIns (3,5)P₂ by removing the phosphate from the D3 position to produce PI and PtdIns5P (Blondeau, Laporte et al. 2000; Schaletzky, Dove et al. 2003). PI and PtdIns5P are important molecules

involved in endocytosis and membrane trafficking (Laporte, Bedez et al. 2003; Dang, Li et al. 2004).

Myotubularin 1 has six different domains: GRAM-PH, RID, PTP/DSP, SID, CC and PDZ-BM domain (Figure 12). The GRAM-PH (Pleckstrin Homology/Glucosyltransferase, Rab-like GTPase Activator and Myotubularins) domain is a phosphoinositide-protein interaction domain. This domain binds PtdIns(3,5)P₂ and PtdIns5P, and the interaction is important for phosphatase activity (Schaletzky, Dove et al. 2003; Tsujita, Itoh et al. 2004). The RID (Rac-Induced recruitment Domain) domain is necessary for the recruitment of myotubularin and homologues to plasma membrane ruffles upon Rac1 activity (Laporte, Blondeau et al. 2002). The PTP/DSP contains the CX5R motif acting as a catalytic pocket and harbouring cysteine and arginine residues important for its phosphatase function. The catalytic pocket is a place of dephosphorylation of the substrate. The aspartate residue located near the top of the substrate pocket is involved in the release of the dephosphorylated product (Begley and Dixon 2005). The SID (SET (Suvar3-9, Enhancer-of-zeste, Trithorax) interacting domain) has a paired-helical motif. SET containing proteins are implicated in gene silencing due to the methyltransferase activity (Yeates 2002). The last feature made a glimpse on the possibility of myotubularin involvement in epigenetic regulation (Cui, De Vivo et al. 1998), but this feature needs to be further explored. The CC domain determines the specificity of the phosphatase (Srivastava, Li et al. 2005). The PDZ-BM (PDZ binding motif) acts as a scaffold for the formation of the signalling complex (Zimmerman et al 2006). This domain is potentially necessary for interaction with PDZ domain containing proteins, which further acts as a scaffold. In XLCNM plethora of mutations are located within the GRAM domain (Herman, Kopacz et al. 2002), nevertheless mutations in XLCNM have been spread throughout the entire gene, meaning that each domain is essential for the proper functioning of the protein (Herman, Kopacz et al. 2002; Laporte, Blondeau et al. 2002; Biancalana, Caron et al. 2003).

2.1.4. Role of myotubularin 1

Phosphoinositides (PIs) are lipid second messengers involved in membrane trafficking. Based on the inositol sugar ring and phosphorylation of phosphatidylinositol,

7 different PtdIns can be formed. Their turnover is regulated by PtdIns kinases and phosphatases. PtdIns define the membranes (Di Paolo and De Camilli 2006). Presence of specific PtdIns will attract particular proteins, involved in different pathways, further guiding the specific processes (Nicot and Laporte 2008). PtdIns3P localizes at the early endosome and the internal vesicles of the multivesicular body (MVB). It plays a role in the recruitment of the endocytic machinery (Gillooly, Morrow et al. 2000). PtdIns(3,5)P₂ is enriched at the early endosome and in the outer membrane of MVB, and proposed to be involved in the regulation of vacuolar volume. Its levels are elevated in yeast in response to osmotic stress (Dove, Cooke et al. 1997) where PtdIns(3,5)P₂ plays a major role in controlling the size and shape of the vacuole and in mediating its fragmentation (Bonangelino, Nau et al. 2002; Dove and Johnson 2007).

Consistent with the role of MTM1 in vesicular transport, overexpression of MTM1 in COS cells induced large endosomal structures and impaired growth factor trafficking from late endosome to the lysosome compartment (Tsujita, Itoh et al. 2004). Overexpression in HeLa cells confirmed this association with the early endosome pool, showing that MTM1 can control endosomal fusion and morphology (Cao, Laporte et al. 2007). *Mtm1* downregulation, using morpholino in zebrafish, induced myopathic phenotype and motor function of these mutants was severely affected (Dowling, Vreede et al. 2009). Histological analysis showed that muscle fibres were hypotrophic and many fibres had abnormal nuclei. In addition, EM reveals a large number of abnormal mitochondria, areas depleted of organelles, and unusual membranous structures. Functional analysis by electrical stimulation shows E-C coupling to be defective as well. PtdIns3P level was also increased (Dowling, Vreede et al. 2009).

Murine model analysis identified that MTM1 is ubiquitously expressed. However the expression level in skeletal muscle is higher compared to the other tissues (Buj-Bello, Laugel et al. 2002). Moreover in mice, the *Mtm1* gene is expressed during the skeletal muscle development, and it is upregulated in the first weeks of postnatal life (Buj-Bello, Fougousse et al. 2008). Immunogold labelling revealed that MTM1 localizes mainly on SR (Amoasii, Hnia et al. 2013). A mouse model of MTM1 deficiency reproduced faithfully most of the features found in patients, proving it to be a good

research tool for better understanding of the disease (Buj-Bello, Laugel et al. 2002). *Mtm1* KO mice are viable, and seem unaffected at birth. First signs of disease start are visible at 2-3 weeks of age. After this, disease has a rapid progression and mice die between 6th and 12th week (Buj-Bello, Laugel et al. 2002). This model, together with muscle specific deletion, has proved that the primary affected tissue is skeletal muscle and that the disease comes from a defect in muscle maintenance and not myogenesis (Buj-Bello, Laugel et al. 2002). Histology reproduces findings in patients, showing mislocalized nuclei and central oxidative accumulation by SDH. Ultrastructure examination discovers Z-line mislocalization, mitochondria and triad defects (Buj-Bello, Laugel et al. 2002; Al-Qusairi, Weiss et al. 2009; Hnia, Tronchere et al. 2011). E-C coupling was also affected (Al-Qusairi, Weiss et al. 2009). Rescue in muscle structure of TA was observed with inactive mutant of MTM1 (the defect in the catalytic domain, and therefore unable to perform phosphatase function). This shows that not only the phosphatase function of MTM1 plays an important role, but also its protein-protein interactions are equally important (Amoasii, Bertazzi et al. 2012). Overexpression of MTM1 in WT mice, leads to abnormal accumulation of SR honeycomb-like structures (Amoasii, Hnia et al. 2013). This confirms the effect of MTM1 on membrane remodelling, especially important in the case of SR membranes. Recent studies in vivo and in vitro have indicated a role for MTM1 in the ubiquitin proteasome system and autophagy (Al-Qusairi, Prokic et al. 2013; Fetalvero, Yu et al. 2013), which is consistent with its function in membrane trafficking. Deletion of *Mtm1* in adult skeletal muscle in mice, confirmed its involvement in the maintenance of the skeletal muscle (Joubert, Vignaud et al. 2013).

There is no therapy for XLCNM and a few therapy approaches have been used in mice. One of which is AAV mediated MTM1 enzyme replacement therapy. It seems to be efficient in the mouse (Lawlor, Alexander et al. 2012) and trials with a naturally occurring dog model of XLCNM (Beggs, Bohm et al. 2010) are on-going. Besides AAV approach pharmacological inhibition of autophagy pathway in *Mtm1* KO mice was shown to improve the phenotype (Fetalvero, Yu et al. 2013). Additionally acetylcholinesterase inhibitors have been shown to slightly improve the muscle function in patients (Robb, Sewry et al. 2011).

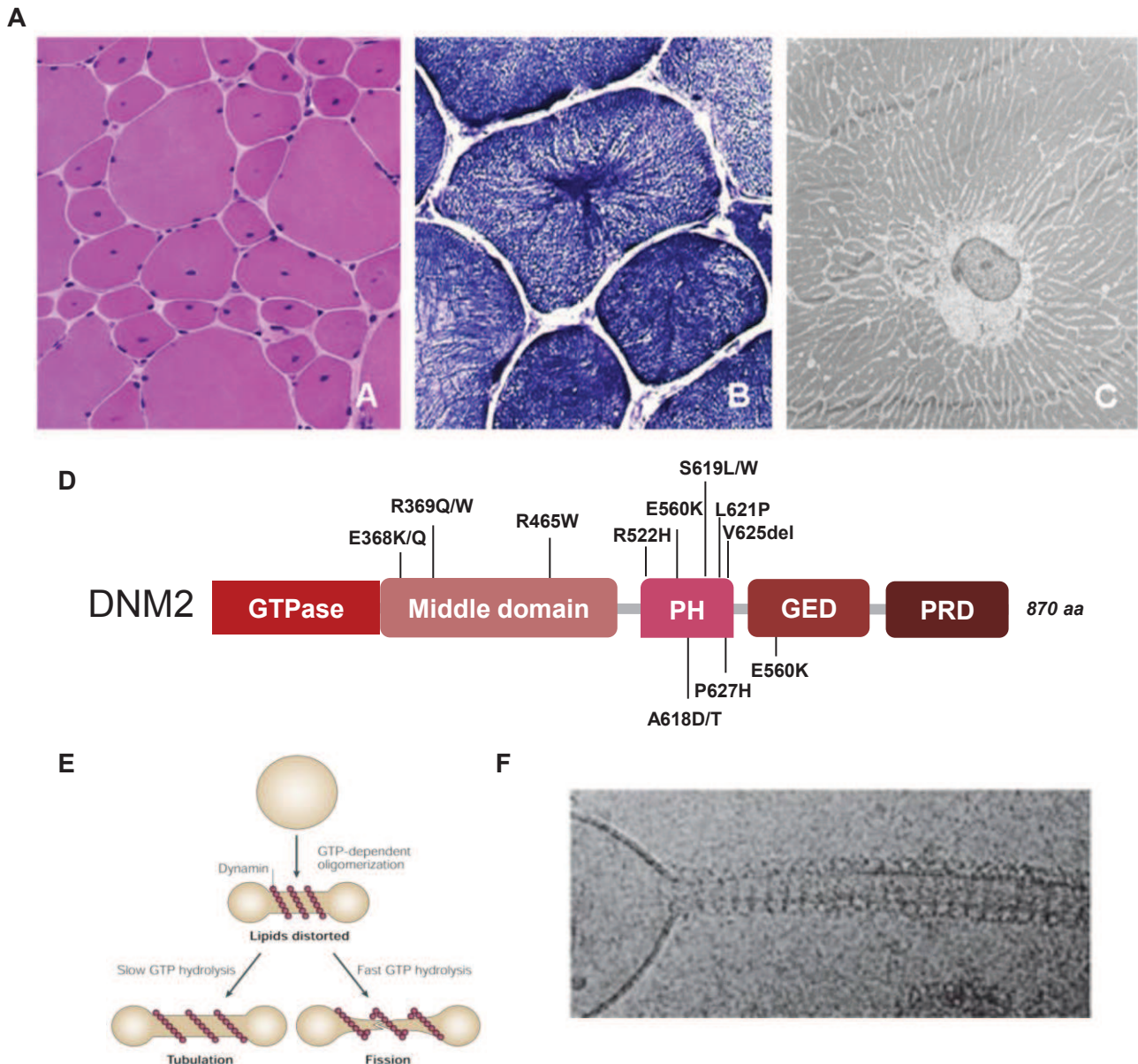


Figure 13. Muscle histology of DNM2-related CNM, schema of dynamin 2 domain organization and its tubulation. (A and B) Transverse muscle sections of ADCNM patient show (A; HE) centralised nuclei especially in small fibres. (B) Typical aspect of radiating sarcoplasmic strands is seen on NADH-TR. (C) Electron micrograph of transverse section shows the nucleus in the centre of the fibre and the radial distribution of sarcoplasmic strands (*from Romero NB, Neuromuscular Disorders, 2010*). (D) DNM2 contains a GTPase domain, a central middle (MID) domain, a Pleckstrin Homology (PH) domain, a GTPase Effector Domain (GED), and a C-terminal Proline Rich Domain (PRD). Mutations presented were found in patients of ADCNM. (E) When Dynamin 2 binds lipid vesicles, slow or uncooperative GTPase activity leads to an extension of the helix, which results in stretching and subsequent tubulation, whereas fast and cooperative dynamin GTPase activity leads to a rapid extension of the helix and fission of the tube (*from Praefcke GJK et al., Nat Rev Mol Cell Bio, 2004*). (F) Cryo-EM image showing a helical polymer of purified dynamin that has driven the formation of a tubule from a liposome. (*from Ferguson SM et al., Nat Rev Mol Cell Bio, 2012*)

2.2. Autosomal dominant centronuclear myopathy

The gene causing the autosomal dominant form (ADCNM, OMIM 160150) (Bitoun, Maugenre et al. 2005) of centronuclear myopathy was recently discovered and this form of the disease accounts for approximately 50% of CNM patients (Romero 2010; Romero and Bitoun 2011). Most often the disease has a late onset and it is clinically mild (Bitoun, Maugenre et al. 2005). Nevertheless some very severe cases have been reported (Bitoun, Bevilacqua et al. 2007).

2.2.1. Clinical description and prognosis

ADCNM is clinically milder and patients have moderate skeletal muscle weakness. External ophthalmoplegia and ptosis are constant (Fischer, Herasse et al. 2006). Few cases have prominent calf muscle hypertrophy (Jeannet, Bassez et al. 2004). Mutations in *DNM2* are missense mutations and normally mutations in the middle domain are associated with a milder onset and good prognosis, as the majority of patients maintain ambulatory independence up to 60 years of age (Bitoun, Maugenre et al. 2005; Fischer, Herasse et al. 2006). The more severe are *de novo* mutations in the pleckstrin homology domain (PH) which have neonatal onset, however muscle performance can gradually improve over time (Bitoun, Bevilacqua et al. 2007)

2.2.2. Histology

Looking at the muscle organization, the most prominent feature is a high number of centrally and internally placed nuclei, type I fibre predominance, atrophy and radial strands of sarcoplasmic reticulum (RSS) seen by NADH-TR (Figure 13). Ultrastructure of the fibres confirms radial distribution of the intermyofibrillar sarcoplasmic strands observed in numerous fibres. The central inter nuclear space is occupied by mitochondria, SR, Golgi complex and glycogen particles (Figure 13). They can be also observed between the myofibrils. Usually, the myofibril diameter is decreasing from the periphery to the centre, giving rise to the radiating appearance (Fischer, Herasse et al. 2006). Immunohistochemistry shows desmin, RyR1 and DHPR staining diffused in the whole cytoplasm, with more prominent central staining. Caveolin 3 staining was sarcolemmal (Figure 15) (Romero and Bitoun 2011).

2.2.3. Dynamin 2

Dynamin 2 is a large GTPase localized on chromosome 19p13.2. It has an important and well characterized role in membrane tubulation and endocytosis, membrane trafficking, actin assembly and centrosome function (Warnock and Schmid 1996; Praefcke and McMahon 2004; Bitoun, Maugendre et al. 2005). Dynamin 2 belongs to the dynamin family, which has 3 members: DNM1, expressed exclusively in neurons where it is mainly associated with membranous organelles (Nakata, Iwamoto et al. 1991; Noda, Nakata et al. 1993), DNM2, which is ubiquitously expressed (Cook, Urrutia et al. 1994), and DNM3, which is expressed in testis, brain and lungs (Nakata, Takemura et al. 1993; Cook, Urrutia et al. 1994).

DNM2 is comprised of an N-terminal GTPase domain, a MID or middle domain, plectrin homology domain (PH), a GTPase effector domain (GED), and a terminal proline rich domain (PRD) (Figure 13). The GTPase domain has GTPase activity. The MID domain is involved in self-assembly (Smirnova, Shurland et al. 1999) and GTP induced conformational change of the protein (Chen, Zhang et al. 2004). The role of the PH domain due to its interaction with membrane PtdIns (mainly PtdIns(4,5)P₂) is in targeting DNM2 to specific membranes (Dong, Misselwitz et al. 2000). Oligomerisation appears crucial for the high affinity (Klein, Lee et al. 1998). The GED domain acts as a GTPase-activating protein and it is involved in self-assembly (Sever, Muhlberg et al. 1999). The C-terminal PRD domain, has multiple Src homology 3 binding motifs (SH3) and mediated protein-protein interactions. Some of the interacting proteins are amphiphysins (David, McPherson et al. 1996), profilin (Witke, Podtelejnikov et al. 1998) and syndapin 1 (Qualmann, Roos et al. 1999), which are members of remodelling system (Praefcke and McMahon 2004). Most of the mutations found in patients are located in the PH and the MID domain (Bitoun, Maugendre et al. 2005; Bitoun, Bevilacqua et al. 2007).

DNM2 has the ability to self-oligomerize, a feature that stimulates its GTPase activity (Warnock, Baba et al. 1997; Eccleston, Binns et al. 2002). Oligomerization of DNM2 enhances in the presence of microtubules or phospholipid vesicles, especially those containing the PI(4,5)P₂ (Lin, Barylko et al. 1997; Warnock, Baba et al. 1997). Self-

oligomerization is mediated by interaction of the GED domains with the GTPase and MID domains in intra-chain and inter-chain reactions (Muhlberg, Warnock et al. 1997; Zhang and Hinshaw 2001), whereas PH and PRD domains function as the regulators of this assembly (Muhlberg, Warnock et al. 1997). Interestingly the PRD is the domain that interacts with the SH3 domain of amphiphysin and it was suggested that this interaction might lead to the conformational change, which will overcome the PRD inhibitory effect on GTP hydrolysis (Zhang and Hinshaw 2001). Moreover, GTPase activity of dynamin can determine the enzyme ability to tubulate liposomes and/or lead to membrane fission. At the low hydrolysis activity, the enzyme tubulates membranes, whereas at high GTPase activity scission would occur (Figure 13) (Praefcke and McMahon 2004).

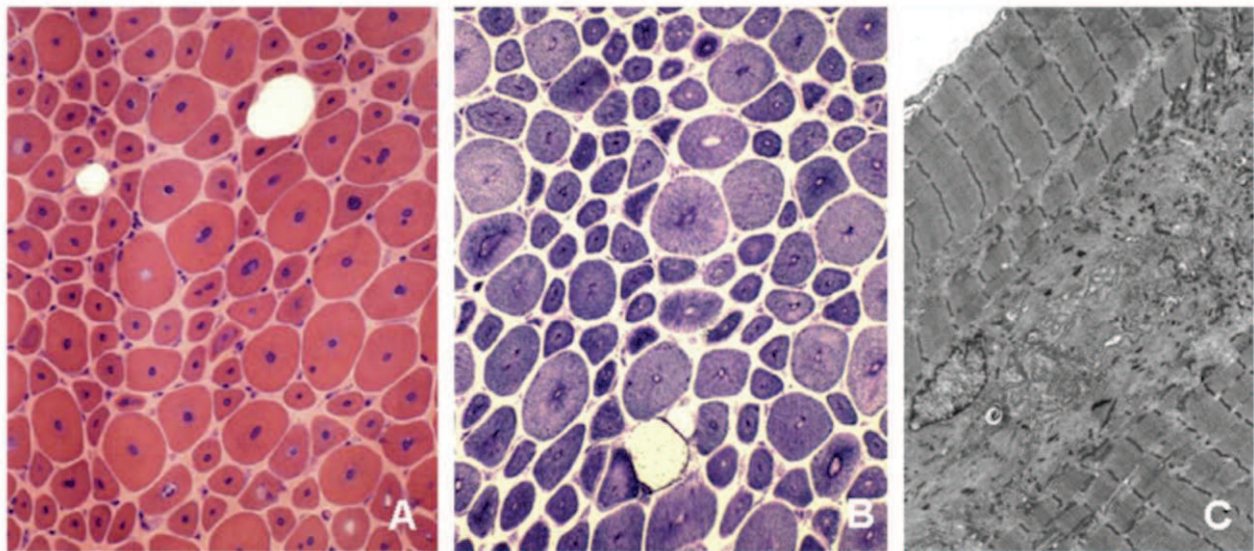
2.2.4. Role of dynamin 2

Endocytosis and membrane trafficking. The most studied role for DNM2 is in endocytosis, where DNM2 is implicated in the formation of the clathrin-coated pits (Warnock, Baba et al. 1997). Anchorage to the membrane occurs through interaction with the membrane phosphoinositide PtdIns(4,5)P₂ (Zoncu, Perera et al. 2007) and BAR domain proteins such as amphiphysin 1, amphiphysin 2 and sorting nexin 9 (David, McPherson et al. 1996). Binding promotes oligomerization and neck formation around the nascent vesicles which are then pinched off (Hinshaw and Schmid 1995; Warnock, Baba et al. 1997; Takei, Slepnev et al. 1999). Besides clathrin mediated endocytosis, dynamin is involved in clathrin independent endocytosis, during the formation of phagosomes and caveolae (Henley, Krueger et al. 1998; Gold, Underhill et al. 1999) and in coat-independent endocytosis such as micro and macropinocytosis (Cao, Laporte et al. 2007; Liu, Surka et al. 2008). *Dnm2* KO mice die in utero, between day 8 and 12 (Ferguson, Raimondi et al. 2009), but studies on a fibroblast cell line lacking DNM2 showed a drastic impairment of endocytosis seen through a lack of transferrin uptake and increase number of endocytic clathrin-coated pits which were clustered (Liu, Surka et al. 2008). DNM2 is predominantly found at the trans-Golgi network (Maier, Knoblich et al. 1996) and knockdown or overexpression of DNM2 disrupts vesicle formation from the trans-Golgi network (Jones, Suzuki et al. 1998; Kreitzer, Marmorstein et al. 2000). These results were confirmed in the KO cells from *Dnm2* (Liu, Surka et al.

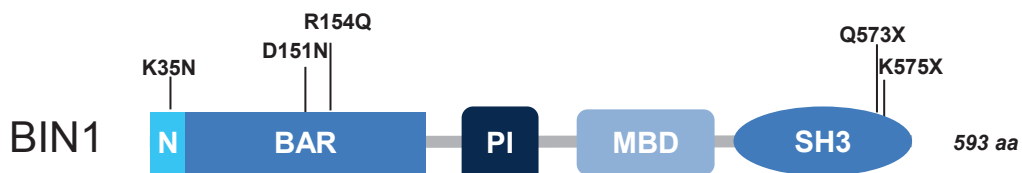
2008). *In vitro* studies of ADCNM patient mutations showed impairment of clathrin-mediated endocytosis (Bitoun, Durieux et al. 2009). Homozygote knockin (KI) mice for the most common mutation found in ADCNM patients, R465W, die just after the birth, probably from clathrin-mediated endocytosis defect and increased autophagy (Durieux, Vignaud et al. 2010; Durieux, Vassilopoulos et al. 2012). Heterozygote R465W mice are viable and progressively develop a myopathy. In addition to the defect in T-tubule and reticular network, a slight increase in autophagy was observed (Durieux, Vignaud et al. 2010). The same mutation overexpressed using AAV in the wild type (WT) TA mouse showed that the disease is muscle specific as it reproduced most of ADCNM features (Cowling, Toussaint et al. 2011). As overexpression in the WT adult muscle leads to the disease, it is likely that the disease arises as a result of gain of function of the mutated DNM2 and that DNM2 plays an important role in adult muscle maintenance.

Actin dynamics. Actin-based dynamics are important for vesicle formation and in the last steps of endocytosis. DNM2 interacts with at least 2 actin-binding proteins, actin-binding protein 1 (Abp1) and cortactin (Kessels, Engqvist-Goldstein et al. 2001; Weaver, Karginov et al. 2001; Schafer, Weed et al. 2002). Abp1 is a Src kinase which provides a link between the endocytosis machinery and the cortical actin network (Kessels, Engqvist-Goldstein et al. 2001), and cortactin binds the F-actin and the ARP2/3 complex, which is the essential molecular machine for nucleating actin filament assembly (Weed, Karginov et al. 2000). The link between the DNM2 and actin cytoskeleton may be relevant, not only in endocytosis, but in membrane tubule generation as well.

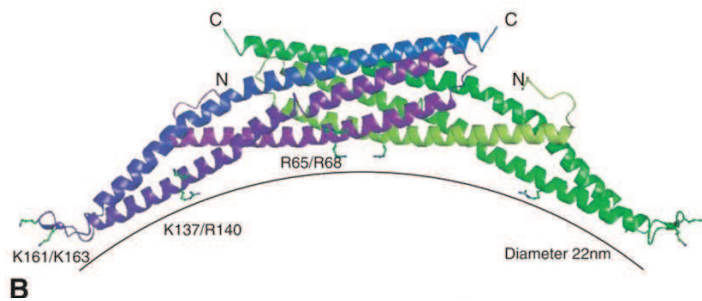
Microtubule network. DNM2 was first isolated as a microtubules (MT) binding protein (Shpetner and Vallee 1989). It interacts with microtubules (MT) through its PRD (Lin, Barylko et al. 1997; Hamao, Morita et al. 2009). Its downregulation by siRNA, increases the amount of acetylated tubulin in MT and reduces their growth capacity (Tanabe and Takei 2009). This interaction seems to be important in Golgi apparatus cohesion (Tanabe and Takei 2009). Additionally, DNM2 has been identified as a component of the microtubule organizing centre (MTOC), where it binds γ -tubulin with



D



E



B

Figure 14. A biopsy from a patient diagnosed with BIN1-related CNM together with schema of BIN1 protein domain organization and a schema showing BAR domains dimerization. (A and B) Histology of a ARCNM patient done on a transverse muscle sections show (A; HE) a large majority of rounded fibres with centralised nuclei and increase of endomysial fibrosis; some fibres have clusters of centrally placed nuclei. (B) NADH-TR staining reveals a central zone with dark border corresponding to the nuclear area. (C) Electron micrograph of longitudinal sections shows amorphous material in the centre of the fibre containing nucleus, mitochondria, sarcotubular profiles and glycogen particles (*from Romero NB, Neuromuscular Disorders, 2010*) (D) BIN1 possess an N-BAR domain able to sense and eventually curve membrane and a C-terminal SH3 domain binding to proteins with proline-rich domains, such as dynamins. In addition some isoforms have clathrin-binding and Myc-binding domains (CBD, MBD); a phosphoinositide-binding motif is present between the BAR and MBD domains specifically in skeletal muscle. (E) Structure of BAR domain of *Drosophila* amphiphysin. The BAR domain is a homodimer of α -helical bundles. The two subunits are colored green and purple. The ends and concave surface have several basic residues, some of which are shown here. (*from Zimmerberg J. et al., Curr Biol, 2004*)

its middle domain (Thompson, Cao et al. 2004). Knockdown of *Dnm2* points to its role in the centrosome cohesion (Thompson, Cao et al. 2004).

2.3. Autosomal recessive centronuclear myopathy

The autosomal recessive form (ARCNM, OMIM 255200) (Toussaint, Nicot et al. 2007) of CNM is the most rare form of CNM. The severity and onset are intermediate to XLCNM and ADCNM with onset of the disease usually in early childhood.

2.3.1. Clinical description and prognosis

Typically seen in ARCNM are facial weakness and rarely there is severe involvement of the masticatory muscles (Zanoteli, Guimaraes et al. 2000). Often there are ocular abnormalities such as ptosis and external ophthalmoplegia (Jungbluth, Wallgren-Pettersson et al. 2008). Depending on clinical symptoms ARCNM is classified into three subgroups: an early onset form with ophthalmoparesis, an early onset form without ophthalmoparesis, and a late onset form without ophthalmoparesis (Jeannet, Bassez et al. 2004). Although BIN1 has been associated with cardiomyopathy (Hong, Cogswell et al. 2012) as up to now cardiac involvement has been described only in one ARCNM patient (Bohm, Yis et al. 2010).

2.3.2. Histology

Biopsies show numerous rounded and small type I fibres. Central nuclei are present in the majority of the fibres and it is common to observe several nuclei in the central part clustered together (Figure 14). Staining for NADH-TR activity reveals fibres showing a clear central zone with a dark border. Central zone corresponds to the nucleus (Figure 14). Typical RSS fibres are rarely observed (Claeys, Maisonobe et al. 2010) and an increase in connective tissue and fibro-adipose replacement is consistently present. Electron microscopy shows centrally placed nuclei and internuclear space occupied by amorphous material containing mitochondria, sarcotubular structures and glycogen particles.

IC labelling of DHPR and RyR1 shows a collapsed, central staining pattern which surrounds nuclei. Desmin staining had colourless areas with dark dotted underlining

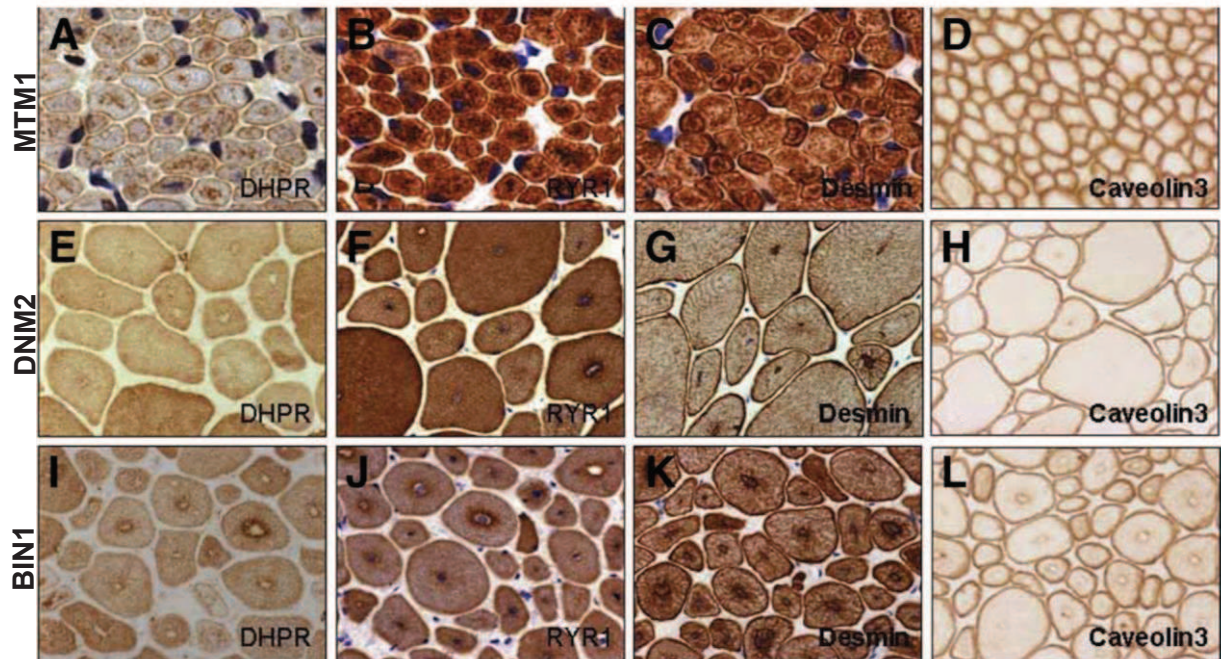


Figure 15. Muscle biopsy sections of patients with severe X-linked myotubular myopathy (A, B, C, D) and DNM2- (E, F,G, H) and BIN1-related CNM patients (I, J, K, L) showing immunohistochemical findings of DHPR (A, E, I), RYR1 (B,F, J), desmin (C, G, K), and caveolin3 (D, H, L). Muscle sections in A, B, and C (MTM1-) demonstrate muscle fibers with positive expression of either of DHPR, RYR1, and desmin with a labeling increased in the central areas of the fibers. Muscle sections in E, F, and G (DNM2-) reveal in general a relatively homogeneous and diffuse labeling of the cytoplasm. However, muscle sections in I, J, and K (BIN1-) show a labeling strictly increased in the central areas of the fibers with an intense coloration in the cytoplasm. Noticeably, the immunolabeling for caveolin3 was observed normally in the sarcolemma in MTM1- (D) and DNM2- (H) related CNM, but it was peculiarly associated with increased staining in the central areas of the fibers in BIN1-related CNM (L) (*from Romero NB et al., Semin Pediatr Neurol, 2011*).

mainly around the central nuclei. Additionally to sarcolemma labelling, caveolin 3 was observed in the central area of the fibre as well (Figure 15) (Romero and Bitoun 2011).

2.3.3. BIN1 and its functions

BIN1 and its role is reviewed separately in the chapter III.

3. Review in preparation: Amphiphysin 2 (BIN1) in physiology and diseases

Ivana Prokic^{1,2,3,4,5}, Jocelyn Laporte^{1,2,3,4,5}

¹IGBMC (Institut de Génétique et de Biologie Moléculaire et Cellulaire), Illkirch, France

²Inserm, U964, Illkirch, France

³CNRS, UMR7104, Illkirch, France

⁴Université de Strasbourg, Illkirch, France

⁵Collège de France, chaire de génétique humaine, Illkirch, France

Correspondence to: jocelyn@igbmc.fr

Abstract

Amphiphysin 2, also named BIN1 (Bridging integrator-1) or SH3P9, has been recently implicated in rare and common diseases affecting different tissues and physiological functions. BIN1 downregulation is linked to cancer progression and also correlates with ventricular cardiomyopathy and arrhythmia preceding heart failure, increased expression appears as a major susceptibility for late-onset Alzheimer, altered splicing may account for the muscle compound of myotonic dystrophies, and recessive germinal mutations cause centronuclear myopathy. While, it undoubtedly underlines the relevance of BIN1 in human diseases, the molecular and cellular bases leading to such different diseases are unclear at present. BIN1 is a key regulator of endocytosis and membrane recycling, cytoskeleton regulation, DNA repair, cell cycle progression and apoptosis. In light of the recent findings on the molecular, cellular and physiological roles of BIN1, we discuss potential pathological mechanisms and highlight both common disease pathways and tissue-specific regulations. Next challenges will be to validate BIN1 as a prognostic marker for the related diseases and as a potential therapeutic target.

3.1. Introduction

Amphiphysin 2, also named BIN1 (Box- dependent MYC-interacting protein-1 or Bridging integrator-1) or SH3P9, is a nucleocytoplasmic protein ubiquitously expressed that was identified as a partner of the transcription factor MYC and in parallel as an interactor of a tyrosine kinase SRC SH3 ligand peptide (Sparks, Hoffman et al. 1996).

BIN1 is a key regulator of different cellular functions, as endocytosis and membrane recycling, cytoskeleton regulation, DNA repair, cell cycle progression and apoptosis. BIN1 alteration is also of strong medical relevance as it was linked to cancer progression, several myopathies as centronuclear myopathy and myotonic dystrophy, heart failure, and late onset Alzheimer disease. The aim of this review is to focus on the different roles of BIN1 in specific tissues, in relation to the different associated diseases.

3.2. *BIN1* gene organization and expression

BIN1 is located on human chromosome 2q14 (Negorev, Riethman et al. 1996) and mouse 18q32 (Mao, Steingrimsson et al. 1999). The mouse and human coding sequence have approximately 89% similarity at the DNA level and 95% at the protein level (Mao, Steingrimsson et al. 1999). Human Bin1/Amphiphysin 2 and amphiphysin 1 are part of the amphiphysin family. Amphiphysins 1 and 2 share an overall 49% amino acid sequence homology (Leprince, Romero et al. 1997; Owen, Wigge et al. 1998). Amphiphysin 1 is a neuronal protein involved in synaptic vesicle endocytosis (Bauerfeind, Takei et al. 1997). Orthologues have been studied in *Caenorhabditis elegans*, drosophila and zebrafish. The amphiphysins are structurally related to the yeast RVS 167, which is involved in endocytosis (Munn, Stevenson et al. 1995) and is a negative regulator of the cell cycle in *S. cerevisiae* (Bauer, Urdaci et al. 1993).

The highest expression of *BIN1* is found in the skeletal muscle and brain (Sakamuro, Elliott et al. 1996; Butler, David et al. 1997). The regulatory sequence in the promoter region of human BIN1 encompasses myogenin/myoD, Sp1 and serum response factor (SRF) binding sites (Mao, Steingrimsson et al. 1999). Sp1 and SRF sites are conserved in mouse and probably responsible for the muscle specific expression whereas the myogenin/myoD sites are not conserved and are substituted by

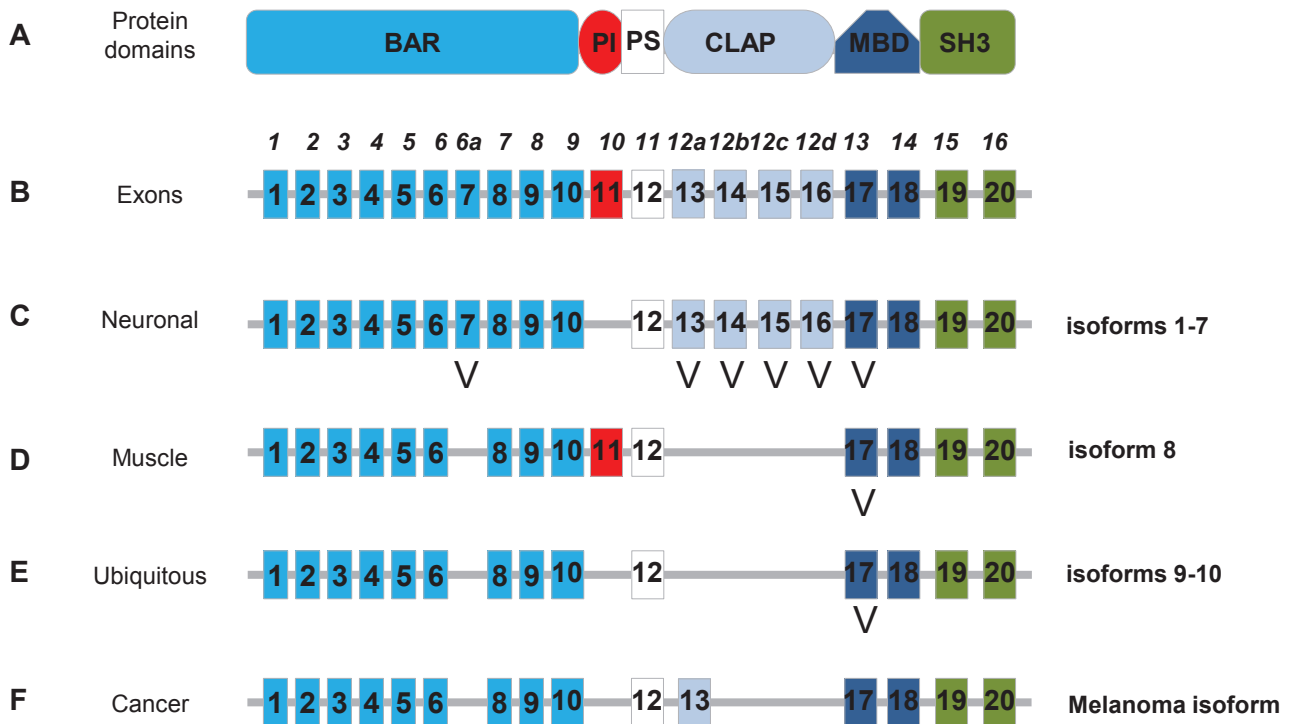


Figure 16. Amphiphysin 2 (BIN1) functional domains and tissue-specific isoforms. (A) Protein domains of BIN1; The BAR domain is involved in membrane binding and tubulation; The PI motif is skeletal muscle specific and it is involved in phosphoinositides binding; The PS motif is a Proline-Serine rich region encoded by exon 12 and present in all the isoforms; The CLAP domain is involved in clathrin and AP2 binding and is only present in neuronal isoforms; The MB domain binds c-Myc and it is involved in its regulation; The SH3 domain interacts with Proline rich proteins such as dynamin 2. (B) The gene organization of BIN1. The main nomenclature used is from NCBI and in *Italic* are placed names of the exons by Weschler-Reya et al.,1997. (C) The exon expression of main neuronal BIN1 isoform 1 with alternatively spliced exons in other neuronal isoforms (isoforms 2-7). (D) The expression of exons in muscle specific BIN1 isoform 8. Exon 17 is alternatively spliced. (E) Exons expression in ubiquitous isoform 9 and another ubiquitous isoform 10 is made without the exon 17 (F) The melanoma isoform exon expression.

Mef2 and Tef sites (Mao, Steingrimsson et al. 1999). Moreover, in both human and mouse, a strong NF- κ B binding site is conserved in the promoter region (Mao, Steingrimsson et al. 1999). Additionally, E2F1 and c-MYC were found to modulate transcription of BIN1 (Cassimere, Pyndiah et al. 2009; Pyndiah, Tanida et al. 2011).

The *BIN1* gene has in total 20 exons and can be spliced into multiple isoforms (Figure 16). We will use thereafter the NCBI nomenclature and the correspondence with numbering used in some published works is indicated in Figure 16. Exons 7, 13, 14, 15 and 16 are brain specific (Butler, David et al. 1997; Tsutsui, Maeda et al. 1997; Ellis, Barrios-Rodiles et al. 2012) whereas exon 11 is a muscle specific exon (WechslerReya, Sakamuro et al. 1997; Mao, Steingrimsson et al. 1999). Splicing of the particular isoforms is tightly regulated and it plays a crucial role in defining the specific functions of the protein. Missplicing of exon 7 and 11 (inclusion of exon 7 and exclusion of exon 11) was seen in muscles from patients with myotonic dystrophy (Fugier, Klein et al. 2011), and exon 17 is often misspliced in cancer, resulting in inhibition of c-MYC binding (Ge, DuHadaway et al. 1999). Isoforms 1-7 are expressed in brain and the most studied neuronal isoform is the isoform 1. The muscle specific isoform is isoform 8, whereas isoforms 9 and 10 are ubiquitously expressed.

3.3. BIN1 domain organization and protein regulation

BIN1 has several distinctive protein domains (Figure 16). The N-BAR (BIN-amphiphysin/Rvs) domain encoded by exons 1 to 10 is ubiquitously expressed, binds lipid membranes and has a role in generating and sensing membrane curvature (Frost, Unger et al. 2009). The N-terminal amphipathic helix inserts into the membrane and curvature is maintained by an interaction between the negatively charged membrane and positively charged surface of the BAR domain (Peter, Kent et al. 2004). Differential splicing of this domain (exon 7) was shown to be able to modulate the interaction with the SH3 domain binding partners as dynamin (Ellis, Barrios-Rodiles et al. 2012). The BAR domain is also involved in homo and hetero dimerization (with amphiphysin 1) (Wigge, Kohler et al. 1997; Ramjaun and McPherson 1998; Slepnev, Ochoa et al. 1998) and the formation of the “banana” shape sensing curvature (Peter, Kent et al. 2004).

The PI (phosphoinositide binding) motif is a short polybasic sequence, encoded by exon 11 and mainly expressed in muscle isoforms (Butler, David et al. 1997; WechslerReya, Sakamuro et al. 1997; Nicot, Toussaint et al. 2007). It was shown that the PI motif increases BIN1 affinity towards the negatively charged lipids PtdIns(4,5)P₂ (Lee, Marcucci et al. 2002) and/or PtdIns3P and PtdIns5P (Fugier, Klein et al. 2011). This motif may potentially target BIN1 to membrane compartments such as T-tubules in muscle. Additionally it could provide a muscle specific regulation of BIN1 conformation through binding with phosphoinositides (PI) (Kojima, Hashimoto et al. 2004). Noteworthy, its inclusion correlates with the translocation of BIN1 from the nucleus in proliferating muscle cells to the cytosol in differentiating cells (Wechsler-Reya, Elliott et al. 1998).

The CLAP (clathrin and AP2 binding) domain encoded by exons 13-16 is found only in brain isoforms of BIN1 (Butler, David et al. 1997; Ramjaun, Micheva et al. 1997; Tsutsui, Maeda et al. 1997) and it is responsible for binding to clathrin and AP2 (Ramjaun and McPherson 1998), proteins involved in endocytosis.

The Myc binding domain (MBD) is constitutively expressed and it is encoded by exons 17 and 18. Both exons are needed for the interaction with c-MYC (Sakamuro, Elliott et al. 1996). Interestingly exon 17 is alternatively spliced, in different tissues (Toussaint, Cowling et al. 2011), leading to the disruption of the domain and loss of interaction (WechslerReya, Sakamuro et al. 1997).

The SH3 (Src homology 3) domain is encoded by the last two exons (19 and 20), and present in all isoforms. SH3 domains bind proline-rich motifs (Yu, Chen et al. 1994). The SH3 domains of amphiphysin 1 and 2 differ to other SH3 domains due to a large patch of negative electrostatic potential and an unusually extended n-Src loop (Owen, Wigge et al. 1998).

BIN1 functions are regulated both through specific isoform expression and by phosphorylation (Marks and McMahon 1998). Three proline-directed protein kinases phosphorylate amphiphysin 1 on a proline-rich domain, including cdk5/p35, mitogen-activated protein kinase (MAPK), and Dyrk1A/minibrain kinase, while experimental

NCBI gene name	Protein	Interaction site	Function	Reference
ITGB1	Integrin alpha 3 beta 1		endocytosis	Wixler et al., 1999
ACTA1	Actin alpha 1		sarcomere assembly	Fernando et al., 2009
AMPH1	Amphiphysin 1	BAR	endocytosis	Wigge et al., 1997
AP1	AP-1, adaptin	CLAP	endocytosis	Huser et al., 2013
AP2	AP-2, adaptin	CLAP	endocytosis	Wigge et al., 1997
BIN1	Amphiphysin 2	BAR with BAR	membrane tubulation	Ramjaun et al., 1999
BIN1	Amphiphysin 2	BAR+PI with SH3	endocytosis, membrane tubulation	Kojima et al. 2004; Royer et al., 2013
ABL1	c-ABL	SH3	tumor suppressor	Kadlec and prendergast 1997
PP3C/R	Calcineurin		endocytosis	Cousin et al., 2001
CACNA1C	CAV1.2, voltage-dependent calcium channel		Cav 1.2 transport	Hong et al., 2010
CDK5	Cyclin-dependent kinase 5		sarcomere assembly	Fernando et al., 2009
CLTC	Clathrin heavy chain	CLAP	endocytosis	Ramjaun et al. 1998
CLIP1	CLIP170, CAP-Gly domain-containing linker protein	BAR	cytoskeleton	Meunier et al. 2008
MYC	c-MYC	MBD	tumor suppressor	Sakamuro et al. 1996
DNM1	Dynamin 1	SH3	endocytosis	Grabs et al., 1997
DNM2	Dynamin 2	SH3	endocytosis	Dong et al. 2000; Kojima et al. 2004
EHD1	EPS15 homology-domain containing protein	SH3	endocytosis	Pant et al. 2009
SH3GL2	Endophilin A1	SH3	endocytosis	Micheva et al. 1997a
SH3GLB1	Endophilin B1	SH3	endocytosis	Micheva et al. 1997a
PTK2	FAK, focal adhesion kinase	SH3	cellular adhesion	Messina et al., 2003
KU	Ku	BAR	DNA repair	Ramalingam et al. 2007
MTM1	Myotubularin	BAR+SH3	membrane remodeling	Royer et al., 2013
MHC	Myosin heavy chain		sarcomere assembly	Fernando et al., 2009
MYCN	N-MYC	MBD	tumor suppressor	Hogarty et al. 2000
PARP1	Poly (ADP ribose) polymerase 1	BAR	DNA repair	Pyndiah et al., 2011
PLD1	Phospholipase D1		signal transduction	Lee et al., 2000
PLD2	Phospholipase D2		signal transduction	Lee et al., 2000
RIN2	Ras and Rab interactor 2	SH3	endocytosis	Kajiho et al., 2003
RIN3	Ras and Rab interactor 3	SH3	endocytosis	Kajiho et al., 2003
SNX4	Sorting nexin 4	SH3	endocytosis	Leprince et al., 2003
SOS1	Son of sevenless homolog 1		endocytosis, signal transduction	Lapince et al. 1997
SOS2	Son of sevenless homolog 2		endocytosis, signal transduction	Lapince et al. 1997
SYNJ1	Synaptojanin 1	SH3	endocytosis	McPherson et al. 1996
TTN	Titin		sarcomere assembly	Fernando et al., 2009
XRCC4	X-ray repair cross-complementing protein 4		DNA repair	Grelle et al., 2006

Table 1. Amphiphysin 2 (BIN1) interactors and regulated functions.

evidence remains to be obtained for BIN1 that contains a similar proline-rich region encoded by exon 12 and present in all isoforms. Open and close conformations of BIN1 have been suggested to be regulated in part by inclusion of the PI motif and integrity of the SH3 domain (Kojima, Hashimoto et al. 2004; Royer, Hnia et al. 2013). In the case of isoform 8, the BAR+PI domains bind the SH3 domain and compete with BIN1 interactors. PtdIns(4,5)P₂ binding to the PI motif favors the open conformation and interactions with protein effectors on PtdIns(4,5)P₂ enriched membranes (Kojima, Hashimoto et al. 2004). Mutations found in myopathies in the SH3 domain affect BIN1 conformation and binding to effectors (Royer, Hnia et al. 2013).

3.4. BIN1 cellular functions

Membrane trafficking

The most characterized function of amphiphysins is linked to the endocytosis. Amphiphysin 1 is involved in endocytosis in neuronal cells (David, McPherson et al. 1996; Bauerfeind, Takei et al. 1997; Shupliakov, Low et al. 1997). *In vivo*, the interaction between amphiphysin 1 and 2 is well documented (Leprince, Romero et al. 1997; Ramjaun, Micheva et al. 1997; Wigge, Kohler et al. 1997) and in brain, both amphiphysins colocalize and form a stable heterodimer (Wigge, Kohler et al. 1997) while deletion of *AMPH1* lead to loss of both AMPH1 and BIN1 in this tissue (Di Paolo, Sankaranarayanan et al. 2002). Amphiphysins interact with several proteins associated with clathrin-coated pits: dynamin (David, McPherson et al. 1996), AP2 adaptor complexes (David, McPherson et al. 1996; Wigge, Kohler et al. 1997), clathrin (McMahon, Wigge et al. 1997; Ramjaun, Micheva et al. 1997), synaptojanin (McPherson, Garcia et al. 1996) and endophilin/SH3GL2 (Micheva, Ramjaun et al. 1997; Ringstad, Nemoto et al. 1997) (Table 1). Dephosphorylation by calcineurin of both amphiphysin 1 and amphiphysin 2 is necessary to induce endocytosis (Marks and McMahon 1998). Moreover, exogenous expression of isolated amphiphysins SH3 domain inhibit dynamin induced endocytosis and transferrin uptake (Owen, Wigge et al. 1998). The role of amphiphysin may be conveyed through its interaction with clathrin and AP2 to recruit dynamin and synaptojanin to the sites of membrane fission (Taylor, Perrais et al. 2011). The mutual exclusivity for clathrin or dynamin binding may be

functionally linked to the correct targeting of dynamin and clathrin to non-overlapping sites at the clathrin-coated pit (McMahon, Wigge et al. 1997) or to sequential action of amphiphysins.

Interestingly, knockdown (KD) of *BIN1* in HeLa and knockout (KO) in MEF cells did not change the kinetics of transferrin uptake, but increased the intracellular transferrin level (Muller, Baker et al. 2003; Pant, Sharma et al. 2009). KD in HeLa cells shows that this intracellular increase is due to defect in the recycling of transferrin receptor (Pant, Sharma et al. 2009). Similarly, the *C. elegans* orthologue named AMPH-1 colocalizes and directly interacts with RME-1 (dynamin-like protein and EHD orthologue) to initiate endosome tubulation and membrane recycling (Pant, Sharma et al. 2009). Thus, depending on the context, amphiphysins control endocytosis and/or recycling.

Tubulation

The role of BIN1 in membrane trafficking reflect its property to tubulate membrane. In vitro studies have shown that the BAR domain of amphiphysin binds and evaginates lipid membranes into narrow tubules (Takei, Slepnev et al. 1999; Farsad, Ringstad et al. 2001; Razzaq, Robinson et al. 2001). In a liposome-binding assay, the BAR domain together with the muscle-specific PI motif encoded by exon 11 binds strongly to PtdIns4P and PtdIns(4,5)P₂ (Lee, Marcucci et al. 2002). Additionally, lipid-dot blot assays and colocalization of BIN1 with PI probes suggested a higher affinity of muscle BIN1 towards PtdIns5P compared to PtdIns(4,5)P₂, whereas isoform lacking the PI motif has a very low binding affinity for PIs (Fugier, Klein et al. 2011). Overexpressing amphiphysin 1 and brain BIN1 isoform in the Chinese hamster ovary (CHO) cells showed diffused and cytosolic distribution. Overexpression of BIN1 muscle isoform 8 in CHO and C2C12 muscle cells lead to its strong concentration at the cell surface and formation of numerous narrow tubules that is prevented by cholesterol depletion. Deletion of the PI motif strongly decreased but did not abrogate membrane tubulation (Meunier, Quaranta et al. 2009; Fugier, Klein et al. 2011). Electron microscopy (EM) and correlative microscopy (CLEM) identified that the tubules are connected to the plasma membrane (Lee, Marcucci et al. 2002; Spiegelhalter, Tosch et al. 2010).

Cytoskeleton network

The potential of BIN1 to regulate actin cytoskeleton remains to be confirmed and is based on the following data. Amphiphysin 1 directly binds N-WASP (Yamada, Padilla-Parra et al. 2009) and regulates actin polymerization during phagocytosis (Yamada, Ohashi et al. 2007). Moreover, the yeast amphiphysin orthologue RVS167 is involved in actin dynamics regulation in response to environmental signals (Bauer, Urdaci et al. 1993; Colwill, Field et al. 1999).

BIN1 may also modulate the microtubule (MT) network through binding to CLIP170, a plus-end protein involved in MT stability and recruitment of dynactin (Meunier, Quaranta et al. 2009). The domains coordinating the interaction were identified as the BAR domain of BIN1 and the coiled-coil region of CLIP170 (Meunier, Quaranta et al. 2009). BIN1 membrane tubulation in HeLa cells was nocodazole sensitive and depletion of CLIP170 decreased BIN1 tubulation capacity (Meunier, Quaranta et al. 2009). Moreover, in human neuroblastoma cells and in mouse brain, BIN1 colocalizes and interacts with TAU, a microtubule-associated protein promoting microtubule assembly and stabilization and implicated in Alzheimer disease (Chapuis, Hansmannel et al. 2013).

DNA repair, cell cycle and apoptosis

In addition to cytosolic functions, BIN1 has several roles in the nucleus. BIN1 isoform 9 that lacks the PI motif and maintains a functional MYC-binding domain (-exon 11 +exon 17) was reported to locate mainly in the nucleus of cultured cells (Wechsler-Reya, Sakamuro et al. 1997). Indeed, BIN1 was identified as an interactor of c-MYC, a transcription factor with the basic helix-loop-helix-leucine zipper (bHLH-LZ) structure that plays a central role in cell growth, apoptosis and malignancy (Sakamuro, Elliott et al. 1996). BIN1 and c-MYC interact through their MBD and MB1 binding domains, respectively (Sakamuro, Elliott et al. 1996). The SH3 domain is also a low affinity interaction site (Pineda-Lucena, Ho et al. 2005), however it is not sufficient by itself to bind c-MYC *in vivo* (Sakamuro, Elliott et al. 1996). Only isoforms of BIN1 which localize in the nucleus can activate the programmed cell death (Ge, DuHadaway et al.

1999; Elliott, Ge et al. 2000). Overexpression of BIN1 in malignant but not in non-malignant cells induced apoptosis (Elliott, Ge et al. 2000; DuHadaway, Sakamuro et al. 2001).

BIN1 can inhibit cell transformation in a caspase-independent cell death process through both Myc-dependent and Myc-independent mechanisms (Elliott, Sakamuro et al. 1999). The cell death program engaged by BIN1 is susceptible to the serine protease inhibitor AEBSF and to inhibition by the SV40 large T antigen (Elliott, Ge et al. 2000). In addition, BIN1 interacts with the proto-oncogene c-ABL and its overexpression results in morphological transformation of NIH 3T3 fibroblasts in a c-ABL-dependent manner (Kadlec and Pendergast 1997). Moreover, BIN1 is part of the transforming pathway induced by the adenovirus gene product E1A. E1A can inactivate the tumor suppressor Retinoblastoma protein (RB), leading to the release of the DNA-binding factor E2F1 and the subsequent inhibition of BIN1 transcription (Kinney, Tanida et al. 2008). The downregulation of BIN1 liberates c-MYC activity for cell cycle progression. Interestingly, while BIN1 is an inhibitory interactor of c-MYC, it is possible that BIN1 impacts directly on the activation of c-MYC target genes. Additionally in transformed cells, c-MYC can repress *BIN1* transcription which further facilitates cell transformation (Pyndiah, Tanida et al. 2011).

Other studies suggested that BIN1 plays an important role on DNA repair as an inhibitor of the poly ADP-ribose polymerase PARP1, a key component of the base excision repair pathway (Meyer-Ficca, Meyer et al. 2005). Indeed, BIN1 interacts with PARP1 through its BAR domain. Depletion of endogenous BIN1 abolished cisplatin-induced cell death via inhibition of c-MYC and PARP1 (Pyndiah, Tanida et al. 2011). *BIN1* downregulation also reduces cell sensitivity to the DNA-damaging chemotherapeutic agents etoposide and doxorubicin (Pyndiah, Tanida et al. 2011). Sakamuro et al. concluded that BIN1 diminution of intrinsic PARP1 activity is the most likely mechanism whereby it sensitizes cancer cells to DNA damage. In addition, BIN1 interacts with two other proteins important for DNA repair in the non-homologous end-joining (NHEJ) pathway, Ku and XRCC4 (Grelle, Kostka et al. 2006; Ramalingam, Farmer et al. 2007), strengthening a role for BIN1 as a regulator of DNA repair.

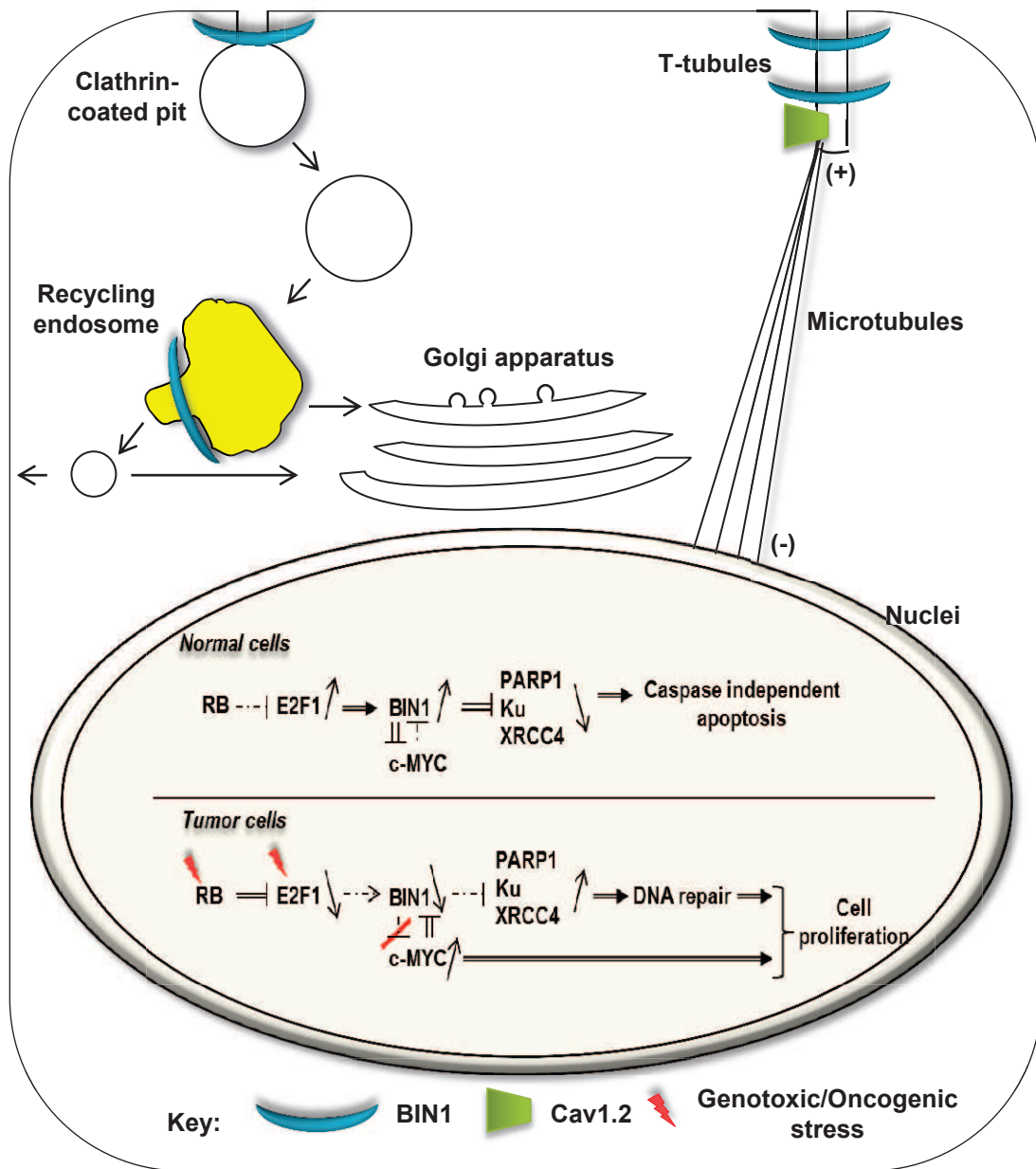


Figure 17. BIN1 cellular roles and proposed mechanisms of linked diseases. BIN1 is involved in clathrin-mediated endocytosis and in recycling endosomes fission. Membrane trafficking is important for T-tubules biogenesis and maintenance. Through interaction with microtubules BIN1 could be involved in correct positioning of CAV 1.2 in heart. BIN1 isoforms localized in the nucleus are involved in cell cycle and apoptosis regulation. The thickness of arrows indicates the strength of interaction.

Additional evidence of a role for BIN1 in cell cycle regulation came from studies of the fission yeast homologue *hob1* (*homologue of Bin1*). Hob1p was shown to be dispensable for actin organization and endocytosis but mutants were hypersensitive to starvation or genotoxic stress (Routhier, Donover et al. 2003). In particular, *hob1* mutants were more susceptible to DNA damage and failed to undergo G1 arrest after DNA damage (Routhier, Donover et al. 2003). BIN1 but not Amphiphysin 1 rescued this phenotype, confirming an evolutionary conserved role for BIN1 in cell cycle regulation (Routhier, Donover et al. 2003).

3.5. Physiological functions of BIN1 and physiopathology of related diseases

🚩 BIN1 and cancer

BIN1 expression is reduced or altered in several cancer types as breast, colon, prostate and lung cancers, hepatocarcinoma and neuroblastoma (Chang, Boulden et al. 2007; Ghaneie, Zemba-Palko et al. 2007; Zhong, Hoelz et al. 2009; Pan, Liang et al. 2012). Loss of heterozygosity or missplicing of BIN1 also correlates with cancer prognosis and increased metastasis (Ge, DuHadaway et al. 1999; Ge, DuHadaway et al. 2000; Ge, Minhas et al. 2000; Ghaneie, Zemba-Palko et al. 2007).

In an elegant model of mosaic *Bin1*-null mouse, Chang and colleagues mammary gland specific *Bin1* deletion has no effect on mammary gland function or remodeling during the pregnancy, and it didn't increase tumor susceptibility (Chang, Boulden et al. 2007). Nevertheless, when tumor formation was initiated by the carcinogen DMBA, mice lacking *Bin1* developed more aggressive tumors which were characterized by an increase in proliferation, survival and motility (Chang, Boulden et al. 2007). In addition, mosaic *Bin1*-null mice showed increased inflammation in several tissues and increased incidence of spontaneous lung tumors and hepatocellular carcinomas.

BIN1 can inhibit MYC transformation and tumor growth and BIN1 is absent from various advanced tumor cell lines (Sakamuro, Elliott et al. 1996; Kennah, Ringrose et al. 2009). Indeed, MYC mutations, overexpression, rearrangement and translocation have been associated with a variety of hematopoietic tumors, leukemias and lymphomas,

including Burkitt lymphoma. Moreover, BIN1 regulates another member of MYC family of oncogenes, MYCN (Hogarty, Liu et al. 2000), which with MYC shares the N-terminal domain and MYC box 1 needed for the interaction with BIN1 (Sakamuro, Elliott et al. 1996). MYCN is highly expressed in neurons and overexpressed in aggressive neuroblastoma (Brodeur, Seeger et al. 1984; Seeger, Brodeur et al. 1985). In 6 out of 8 neuroblastoma cell lines overexpressing MYCN, BIN1 was found strongly downregulated while its overexpression led to apoptosis (Seeger, Brodeur et al. 1985).

The frequent loss of *BIN1* may contribute to malignant development via the loss of processes required for terminal differentiation (through downregulation of p21 and p53), and by contributing to Myc deregulation and loss of control over NHEJ repair. Cisplatin-based chemotherapy is a commonly used therapy-approach for the various human malignancies but many cancer patients respond poorly to this treatment (Brabec and Kasparkova 2005). *BIN1* downregulation was shown to increase resistance to this therapy, most likely through loss of control over the DNA repair mechanism (Pyndiah, Tanida et al. 2011). Quantification of *BIN1* expression may thus be an important marker to predict cisplatin sensitivity. Additionally, increasing the expression of *BIN1* may be a novel therapeutic strategy for treatment of cisplatin-resistant cancers (Tanida, Mizoshita et al. 2012).

Altogether, it appears that *BIN1* loss does not strongly increase the risk of tumor formation but favors tumor progression (Prendergast G.C 2009). Apart from its nuclear functions discussed above, its roles in cytoskeleton and membrane remodeling may be implicated in tumor cell migration and invasion.

BIN1 in skeletal muscle and myopathies

BIN1 is implicated in two myopathies: centronuclear myopathy (CNM) and myotonic dystrophy (DM). Germline mutations cause autosomal recessive centronuclear myopathy (ARCNM), a rare congenital myopathy associated to non-progressive muscle weakness with onset at birth or infancy (Nicot, Toussaint et al. 2007; Claeys, Maisonobe et al. 2010; Bohm, Vasli et al. 2013). Muscle histology of all patients shows a strong increase in the number of centralized nuclei and fiber atrophy

(Romero and Bitoun 2011; Bohm, Vasli et al. 2013; Romero and Laporte 2013). No history of cancer has been noted and potential cardiac involvement was reported in only one patient (Nicot, Toussaint et al. 2007; Bohm, Yis et al. 2010; Claeys, Maisonobe et al. 2010; Bohm, Vasli et al. 2013). So far, the following homozygous mutations were reported: missense changes in the amphipatic helix and BAR domain (K35N, D151N and R154C) (Nicot, Toussaint et al. 2007; Claeys, Maisonobe et al. 2010), stop codon mutations in the last exon truncating the SH3 domain, and a mutation in the exon 11 donor splice site leading to exon 11 skipping (Bohm, Vasli et al. 2013). While they do not appear to change the level of BIN1 protein, mutations in N-BAR or skipping of the PI motif strongly decrease the membrane tubulation properties of BIN1, while the SH3 truncations impair both intramolecular binding and binding to dynamin 2, a well characterized interactor of BIN1 implicated in cytoskeleton and membrane remodeling (Nicot, Toussaint et al. 2007; Bohm, Vasli et al. 2013). Noteworthy, these mutations potentially affect different BIN1 functions, all important for skeletal muscle integrity.

Myotonic dystrophies are multisystemic diseases characterized by progressive muscle wasting, myotonia, cataracts and heart conduction defects. Congenital myotonic dystrophy (CDM1) and myotonic dystrophy of type 1 (DM1) or of type 2 (DM2) are caused by the expression of mutant RNAs containing expanded CUG or CCUG repeats that sequester splicing factors as Muscleblind-like-1 (MBNL1), resulting in aberrant splicing of other mRNAs, including *BIN1*. In DM muscles, *BIN1* isoform is reverted to the embryonic isoform containing exon 7 and lacking exon 11 (Fugier, Klein et al. 2011). As centronuclear myopathy and myotonic dystrophy share several clinical and histopathological features as muscle weakness and centralization of nuclei in muscle fibers, alteration of BIN1 represents a potential common molecular mechanism.

BIN1 is highly expressed in skeletal muscle, its level increases during in vitro differentiation of muscle cells, and *Bin1* knockdown inhibited myoblast fusion and differentiation (Sakamuro, Elliott et al. 1996; Butler, David et al. 1997; Wechsler-Reya, Elliott et al. 1998; Lee, Marcucci et al. 2002). The inclusion of the muscle-specific PI motif during muscle differentiation and its importance for the membrane tubulating properties of BIN1 also point to a significant role of BIN1 on membrane remodeling in

skeletal muscle (Butler, David et al. 1997; Wechsler-Reya, Elliott et al. 1998). In addition, BIN1 localizes to the T-tubules, muscle-specific plasma membrane invaginations sustaining the excitation-contraction (EC) coupling machinery (Butler, David et al. 1997).

Several studies in animal models revealed the physiological importance of BIN1 for skeletal muscle. Deletion of the unique amphiphysin orthologue in flies (*amph*) is viable but flies are flightless and generally sluggish (Razzaq, Robinson et al. 2001). In *Drosophila melanogaster* AMPH is localized on the postsynaptic membrane of the neuromuscular junction and on the T-tubule network, and adult *amph* mutants had severe structural defects in T-tubule organization and EC coupling, while they do not have strong defects in synaptic vesicle endocytosis or recycling suggesting *Drosophila* AMPH is functionally closer to mammalian BIN1 than to AMPH1 (Razzaq, Robinson et al. 2001). Concordantly, knockdown of *Bin1* in adult mouse flexor digitorum brevis (FDB) muscle led to alteration of T-tubule structure and Ca^{2+} levels (Tjondrokoesoemo, Park et al. 2011). Similarly, U7-antisense induced exon 11 skipping in mouse tibialis anterior induced a defect in T-tubule organization and DHPR distribution and a decrease in specific muscle strength while muscle mass and fiber size were not affected (Fugier, Klein et al. 2011). Recently, a spontaneous BIN1 model was reported in dog where a splice site mutation affecting exon 11 and reducing the overall protein level was linked to the Inherited Myopathy of Great Danes, a late onset and very progressive myopathy (Bohm, Vasli et al. 2013). Histological and ultrastructural analyses revealed a high number of centrally located nuclei, reminiscent of centronuclear myopathy, the presence of sarcolemmal invaginations which contained basement membranes and often pointed towards the centralized nuclei, and alteration of T-tubules (Bohm, Vasli et al. 2013). T-tubule defects and alteration in the localization of T-tubule markers as RYR1, DHPR and caveolin3 are also noted in patients with centronuclear myopathy (Toussaint, Cowling et al. 2011; Bohm, Vasli et al. 2013). Taking together the molecular function of BIN1 as a membrane tubulating protein and the similar data from animal models and patients, it appears BIN1 is a key for the remodeling and positioning of T-tubules in muscle. It does not exclude that BIN1 has additional role in skeletal muscle, like for sarcomere organization as suggested through transgenic overexpression of BIN1 SH3

domain in mice (Fernando, Sandoz et al. 2009) or autophagosome maturation (Bohm, Vasli et al. 2013).

✚ BIN1 in heart and cardiac failure

A decrease in BIN1 has been observed in patients with ventricular arrhythmia. Plasma BIN1 level correlated with disease progression and advanced heart failure in a small cohort of patients (Hong, Smyth et al. 2012). Moreover, BIN1 expression is significantly decreased in failing cardiomyocytes at both mRNA and protein levels (Hong, Smyth et al. 2012). BIN1 also localizes to T-tubules in cardiac muscle. *Bin1* knockdown in cardiomyocytes reduces the distribution of DHPR (CAV1.2) to the T-tubules and delays calcium transient (Hong, Smyth et al. 2010). Thus, in addition to a structural role at the T-tubules, BIN1 was proposed to regulate the transport of DHPR to the T-tubules. Preliminary data sustained a physiological role of BIN1 in heart function. Injection of a *bin1* morpholino antisens in zebrafish induced a strong cardiac phenotype, with altered calcium transient and contractility and a significant decrease in the heart rate (Hong, Smyth et al. 2012). In mouse, complete KO of *Bin1* is perinatal lethal (Muller, Baker et al. 2003). Heart analysis identified markedly increased thickness and occlusion of both ventricular chambers, leading to the suggestion that mice died from ventricular cardiomyopathy. As another *Bin1* mouse KO model dies perinatally from specific skeletal muscle defects (Prokic and Laporte, unpublished), the contribution of the heart phenotype in survival remains to be confirmed.

Overall, several studies indicated that both membrane remodeling and trafficking functions of BIN1 are important for cardiac muscle, and suggested that BIN1 may be a predictive biomarker for future ventricular arrhythmias.

✚ Role of BIN1 in brain and implication in Alzheimer disease

Recently large scale genome-wide association studies (GWAS) have linked *BIN1* to late-onset Alzheimer disease (LOAD) (Seshadri, Fitzpatrick et al. 2010; Carrasquillo, Belbin et al. 2011; Hu, Pickering et al. 2011; Lambert, Zelenika et al. 2011; Lee, Cheng et al. 2011; Wijsman, Pankratz et al. 2011; Masoodi, Al Shammari et al. 2013) . Alzheimer's disease (AD) is the most common cause of dementia, affecting 13% of the

population older than 65 years of age and 30-50% older than 80 years. LOAD is characterized by a large number of senile plaques and neurofibrillary tangles in the brain, and it is the most prominent form of dementia in elderly (Schaeffer et al. 2011). *BIN1* is currently the most important susceptibility locus for LOAD after APOE (<http://www.alzgene.org/>) (Tan, Yu et al. 2013). SNPs upstream of *BIN1* correlate with a higher risk to develop LOAD, and to increased *BIN1* transcript levels, albeit the causative nucleotide change remains to be confirmed (Chapuis, Hansmannel et al. 2013; Tan, Yu et al. 2013). Altered expression of *BIN1* was demonstrated in aging mice, transgenic AD models and AD brains. Whether *BIN1* can be a biomarker, or a therapeutic target for Alzheimer's disease remain to be investigated. Mammalian models to confirm *BIN1* implication in Alzheimer are lacking to date. For example the role of *BIN1* in mammalian brain is not known; of note the *Amph1* KO mice have a concomitant decrease in *BIN1* in brain and showed impaired cognitive ability and fatal seizures in the first months of age (Di Paolo, Sankaranarayanan et al. 2002).

To decipher the pathological mechanism linking *BIN1* to LOAD, Chapuis et al. used drosophila and could show that *BIN1* interacts with TAU and that, while altered *amph* expression did not modify the A β 42-induced rough eye and neurodegeneration phenotype, loss of *amph* was able to suppress TAU-induced neurotoxicity (Chapuis, Hansmannel et al. 2013). As TAU (MAPT) is a microtubule-associated protein, they hypothesized *BIN1* overexpression could disrupt vesicle transport at the synapse and favor TAU sequestration at the membrane. Importantly, these data place *BIN1* modulation of the AD pathogenesis at the level of the TAU pathway. *BIN1* and several proteins recently linked to AD appear interconnected through multiple interacting proteins and share related functions on membrane trafficking, sustaining a potential central role of *BIN1* in AD (Raj, Shulman et al. 2012). A recent study pointed for a role of PtdIns3P, a regulator of membrane trafficking, in AD. Interestingly, PtdIns3P is also implicated in centronuclear myopathy as the PtdIns3P phosphatase myotubularin is mutated in severe forms of CNM (Hnia, Vaccari et al. 2012). These findings suggest the existence of a PtdIns3P-*BIN1* pathway common to both centronuclear myopathy and Alzheimer's disease.

3.6. Conclusion and pending questions

BIN1 downregulation is linked to increased cancer progression and also correlates with ventricular cardiomyopathy and arrhythmia preceding heart failure, increased expression appears as a main susceptibility for late-onset Alzheimer, altered splicing may account for the muscle compound of the multisystemic phenotypes in myotonic dystrophies, and germinal mutations cause centronuclear myopathy. While it undoubtedly underlines the importance of BIN1 in human diseases, the molecular and cellular bases leading to such different diseases linked to alterations in BIN1 are unclear at present and represent an exciting area of future research. A more precise definition of BIN1 isoforms, tissue-specific regulation and interactors will be needed, together with the generation of mammalian models to test the pathological hypotheses summarized in this review. Future translational research will also aim to validate BIN1 as a prognostic marker for the related diseases and as a potential therapeutic target.

Acknowledgements

We apologize to colleagues whose work was not cited because of space limitations. We acknowledge B.S. Cowling for discussions. This study was supported by the Institut National de la Santé et de la Recherche Médicale, the Centre National de la Recherche Scientifique, Strasbourg University, Collège de France and Association Française contre les Myopathies.

Table 1: Amphiphysin 2 (BIN1) interactors and regulated functions

Figures legends

Figure 16: BIN1 functional domains and tissue-specific isoforms.

Figure 17: BIN1 cellular roles and proposed mechanisms of linked diseases.

MATERIALS and METHODS

✚ MATERIALS

Primary antibodies used were: mouse anti-DHPR α 1 (Cav 1.1) subunit (MA3–920; Affinity Bioreagents or ab58552; Abcam), α -actinin (EA-53, Sigma-Aldrich), BIN1 c99d clone (B9428; Sigma-Aldrich), RyR1 (clone 34C; Sigma-Aldrich) DNA polymerase (sc-373884, Santa Cruz) and glyceraldehyde-3-phosphate dehydrogenase (GAPDH, MAB374; Chemicon) monoclonal antibodies; and rabbit anti-RYR1 (a kind gift from Isabelle Marty, Grenoble Institut des Neurosciences, France). Rabbit anti-DNM2 antibodies (R2680 and R2865, characterized in (Cowling BS et al., 2011), anti-MTM1 (R2827) (Hnia K et al., 2011) and anti-BIN1 (R2444 and 2405, characterized in Nicot et al., 2007) were made onsite at the polyclonal antibody facility of IGBMC. Alexa-conjugated secondary antibodies were purchased from Invitrogen. Secondary antibodies against mouse and rabbit IgG, conjugated with horseradish peroxidase (HRP) were purchased from Jackson ImmunoResearch Laboratories. The following products were purchased: Hoechst nuclear stain (B2883, Sigma-Aldrich), ECL chemiluminescent reaction kit (Pierce), LipofectamineTM (Life Technologies), Tamoxifen (Sigma-Aldrich), Notexin (Latoxan).

✚ METHODS

Generation of *Bin1* exon 11 and *Bin1* exon 20 homozygote mice. The targeting vector was created with LoxP sites flanking exon 11 of *Bin1* in case of *Bin1* exon 11 KO (Results 3, Figure 1A) and exon 20 in case of *Bin1* exon 20 KO mouse (Results 1, Figure 1A), then linearized and electroporated into embryonic stem (ES) cells. Recombinant ES cells were injected into C57BL/6 blastocysts that were implanted in pseudo-pregnant females and germline transmission determined. Recombination was triggered using CMV or HSA promoter. Mice bred and analyzed were B6J strain. In case of time-inducible recombination the HSA ER¹² promoter was used. To trigger the recombination, 7 week old mice were injected daily, for 5 consecutive days with 100 μ l of tamoxifen solution (tamoxifen was diluted in 90% vegetable oil and 10% ethanol in the concentration of 1mg/100 μ l).

Animal experiments. Animal experimentation was approved by the institutional ethical committee Com'Eth IGBMC-ICS (2012-128). Animals were housed in a temperature-controlled room (19–22°C) with a 12:12-h light/dark cycle. Mice were weighed weekly until one year of age. Mice were humanely killed when required by CO₂ inhalation followed by cervical dislocation, according to national and European legislations on animal experimentation. Muscles and other tissues were dissected (TA muscle under anesthesia when required for TEM) and frozen in nitrogen-cooled isopentane and liquid nitrogen for histological and immunoblot assays, respectively. In case of isolated fibres muscle were first fixed, then dehydrated and only after frozen on -80 (detailed protocol in: Immunofluorescence on isolated fibers).

Phenotyping of *Bin1* exon 11 homozygote and *Bin1* exon 20 heterozygote mice. Mice aged 10-15 weeks were phenotyped under the EUMODIC phenotyping program (<http://www.eumodic.eu/>) with results made publicly available (<http://www.euophenome.org/>). In both cases male and female mutant mice were compared to the WT littermates. Blood chemistry, ECG measurements, Dexascan, and qNMR presented here for male mice (n= minimum 10 per group) were performed as part of pipelines 1 and 2 of the EUMODIC phenotyping program, at the Institut Clinique de la Souris (ICS, Illkirch, France, <http://www.ics-mci.fr/>).

In vivo regeneration test. 12 week old male BIN1 exon 11 KO and WT mice were used for the in vivo regeneration study. A cycle of degeneration and regeneration was induced and studied in Tibialis Anterior (TA) by intramuscle injection of notexin (notexin was diluted in PBS in concentration: 10g/ml and 20µl was then injected into the right leg). The contralateral TA muscle was used as the control. At various time-points after the injections, mice were killed by cervical dislocation. The TA muscles of both hindlimbs were immediately removed, snap frozen in isopentane cooled in liquid nitrogen, mounted in OCT, and 8µm longitudinal sections were cut and mounted onto SuperFrost Plus slides.

String, grip (2 and 4 paws), hang and rotarod tests. String test: Mice are suspended on a wire by their forelimbs, and allowed 20 seconds to climb their hindlimbs onto the wire. Three trials per mouse were performed, with 5 minutes rest between

trials. A fall was considered equal to 20 seconds (n=minimum 5 mice per group). Grip strength tests: Performed by placing the 2 front paws or all 4 paws on the grid of a dynamometer (Bioseb, Chaville, France) and mice were pulled by the tail in the opposite direction. The maximal strength exerted by the mouse before losing grip was recorded. Three trials per mouse were performed, with 30 seconds rest between trials (2 paw test, n=minimum 5 mice per group; 4 paw test, n=5-7 mice per group). Hanging test: mice were suspended from a cage lid for a maximum of 60 seconds. The time the mouse fell off the cage was recorded for each trial. Three trials per mouse were performed. Rotarod test: Coordination and whole body muscle strength and fatigability were tested using an accelerated rotating rod test (Panlab, Barcelona, Spain). Mice were placed on the rod which accelerated from 4 to 40 rpm during 5 minutes. Three trials per day, with 5 minutes rest between trials were performed for day 1 (training day) then 4 days which were recorded. Animals were scored for their latency to fall (in seconds). The mean of the three trials was calculated for each experiment listed above (n=5-7 mice per group).

TA muscle contractile properties. Muscle force measurements were evaluated by measuring in situ muscle isometric contraction in response to nerve and muscle stimulation, as described previously (Vignaut A et al., 2005; Vignaut A et al., 2010). Results from nerve stimulation are shown (n=5-11 mice per group). After contractile measurements, the animals were killed by cervical dislocation. TA muscles were then dissected and weighed to determine specific maximal force.

Echocardiography. Pregnant mice were studied on day 17.5-18.5 of gestation (E17.5-18.5) (where 18.5 days is full term), and a total of 19 WT and KO embryos (4 pregnant mice in total were used and the results from HZ mice data were excluded from the analysis) were observed. A vevo 2100 (VisualSonics, Incorporated -Toronto, Canada) system with a 40-MHz. Transducer (lateral and axial resolutions of 68 and 38 μm , respectively) was used for ultrasound interrogation of the mouse fetuses. Pregnant female mice were anesthetized with isoflurane anesthesia (1.5% isoflurane in medical air containing 21% oxygen) and laid supine in a petri dish filled with physiological solution with the right forearm and left hindlimb implanted with electrocardiogram (ECG) electrodes subcutaneously for heart rate monitoring (450–550 beats/min). Body

temperature and physiological solution temperature were both monitored via a thermometer (rectal thermometer for body temperature) and maintained at 36–38°C using a lamp (for the mouse) and a heating pad (for the saline solution). The obtention of proper imaging plane involved externalization of the uterus into the warm physiological solution bath followed by placement of the transducer directly on the uterine wall where pre warmed ultrasound gel was applied. M-mode imaging produces excellent images that can provide the most accurate measurements of ventricular wall thickness and shortening fraction in fetal mouse heart measuring 2–5 mm. In this mode, the improved frame rate of up to 1,000 frames/sec allowed end systole and end diastole to be measured with ease. At the end of the procedure, the pregnant mouse was killed by cervical dislocation and biopsies of the fetuses were taken for genotyping.

Glucose mesurment. Blood glucose concentration was determined by the use of a glucometer and test strips (One touch ultra) both purchased from Lifescan.

In Situ Hibridization. In situ hybridizations were performed on whole-mount wild type embryos at E14.5 and E18.5 day. Probe used for BIN1 was made for Euroexpress program (<http://www.euroexpress.org/ee/>)

BIN1 probe sequence:

TACCTAGGCCAGTTCCCTGATATCAAGTCGCGCATTGCCAAGCGGGGGCGGAAGC
 TGGTGGACTATGACAGTGCCCGGCACCACTATGAGTCTCTTCAAACCGCCAAAA
 GAAGGATGAAGCCAAAATTGCCAAGCCTGTCTCGCTGCTTGAGAAAGCCGCCCCC
 CAGTGGTGCCAAGGCCAACTACAGGCTCATCTTGAGCTCAAATAACCTGCTCCG
 AAATCAGGCAGAAGAGGAGCTCATCAAAGCCCAGAAGGTGTTTCGAGGAGATGAAC
 GTGGATCTGCAGGAGGAGCTGCCATCCCTGTGGAACAGCCGTGTAGGTTTCTATG
 TCAACACGTTCCAGAGCATCGCGGGTCTGGAGGAAAACCTTCCATAAAGAGATGAG
 TAAGCTCAATCAGAACCTCAATGATGTCCTGGTCAGCCTAGAGAAGCAGCACGGG
 AGCAACACCTTCACAGTCAAGGCCCAACCCAGTGACAATGCCCTGAGAAAGGGA
 ACAAGAGCCCGTACCTCCTCAGATGGCTCCCCTGCTGCTACCCCTGAGATCAG
 AGTGAACCATGAGCCAGAGCCGGCCAGTGGGGCCTCACCCGGGGCTACCATCCC
 CAAGTCCCCATCTCAGCTCCGGAAAGGCCACCTGTCCCTCCGCCTCCCAAACAC
 ACCCATCCAAGGAGATGAAGCAGGAGCAGATTCTCAGCCTTTTTGATGACGCATT
 TGTCCCTGAGATCAGCGTGACCACCCCTCCAGTTTGAGGCCCTGGGCCTTTC
 TCAGAGCAGGCCAGTCTACTAGACCTGGACTTCGAGC.

Histology on newborns. Day-18.5 fetuses were skinned, fixed in Bouin's fluid for at least a week and decalcified in rapid decalcifier DC3 (Labonord) 24 hours with 2

changes, washed 24 hours with 3 changes in 96% ethanol, dehydrated in absolute ethanol (1 day with 3 changes), cleared in Histolemon (1 day with 3 changes), then embedded in paraplast (4 days with 4 changes). Serial sections, 7 μ m thick, were deparaffinized with Histosol (Shandon) then stained with either Groat's hematoxylin (Gabe, 1968) followed by Mallory's trichrome (Ganter and Jollès, 1970) or either Hematoxylin and Eosin according to standard protocols.

Primary cell culture. Primary myoblasts from WT newborn mice were prepared using a protocol adapted from De Palma et al., 2010. After hind limb muscles isolation, muscles were minced and digested for 1.5 hours in PBS containing 0.5 mg/ml collagenase – Sigma - and 3.5 mg/ml dispase – Gibco. Cell suspension was filtered through a 40 μ m cell strainer and pre-plated in DMED-10%FBS (Gibco), to discard the majority of fibroblasts and contaminating cells, for 3 hours. Non adherent-myogenic cells were collected and plated in IMDM (Gibco)-20% FBS-1% Chick Embryo Extract (MP Biomedical) onto 1:100 Matrigel Reduced Factor (BD) in IMDM coated fluorodishes. Differentiation was triggered by medium switch in IMDM + 2% horse serum and 24 hours later a thick layer of matrigel (1:3 in IMDM) was added. Myotubes were treated with 80 μ g/mL of agrin, or explanted spinal cords from E12 mouse embryos, and the medium was changed every 2 days. Cells in culture were prepared, fixed and stained with antibodies to BIN1-R2444 (1:100) and BIN1-C99D (1:50) and DNM2-R2680 (1:200).

Histological and immunofluorescence analysis of skeletal muscle. Longitudinal and transverse cryosections (8 μ m) sections of mouse skeletal muscles were prepared, fixed and stained with antibodies to DHPR α 1 (1:100), RYR1 (1:200), α -actinin (1:1,000), DNM2-R2680 (1:200), MTM1-R2827 (1:200), BIN1-C99D (1:50) and BIN1-R2444 (1:100). Nuclei were detected by costaining with Hoechst (Sigma-Aldrich) for 10 min. Samples were viewed using a laser scanning confocal microscope (TCS SP5; Leica Microsystems, Mannheim, Germany). Air-dried transverse sections were fixed and stained with haematoxylin and eosin (HE), succinate dehydrogenase (SDH), NADH-TR or Sirius red/fast green staining and image acquisition performed with a slide scanner NanoZoomer 2 HT equipped with the fluorescence module L11600-

21 (Hamamatsu Photonics, Japan) or a DMRXA2 microscope (Leica Microsystems GmbH). Cross-sectional area (CSA) was analyzed in HE sections from TA mouse skeletal muscle, using FIJI image analysis software. CSA (μm^2) was calculated (>500 fibres per mouse) from 4-7 mice per group. The percentage of TA muscle fibres with centralized or internalized nuclei was counted in >500 fibres from 4-6 mice using the cell counter plugin in ImageJ image analysis software.

Immunofluorescence on isolated fibers. Muscles dissected from mouse wild type and knockout for *Bin1* exon 11 and *Bin1* exon 20 KO were fixed in 4% PFA for 30 min at RT, and then incubated in PBS supplemented with 0.1M glucose for 30min at RT and afterwards in PBS supplemented with 30% sucrose at 4°C overnight. Muscles were then frozen at -80°C. Thawed entire muscles were dissected in PBS to isolate fibers. Fibers were permeabilised in PBS supplemented with 50mM NH₄Cl and 0.5% Triton X100 for 30 min at RT and then saturated in PBS supplemented with 50mM NH₄Cl, 0.5% donkey serum and 0.1% Triton X100 for 1 hour at RT. Immunocytochemistry was performed as described above at 4°C overnight, using MTM1-R2827 (1:200), BIN1 (1:50, C99D), DHPR (1:150, Abcam) and RYR1 antibody (1:150, Sigma-Aldrich). Fibers were then incubated with donkey anti-mouse or donkey anti-rabbit secondary antibodies (Alexa Fluor 488/594, Life technologies) diluted in 1:250 (v/v).

RT-PCR and Quantitative RT-PCR. Total RNA was purified from hind limb muscles in case of *Bin1* exon 20 KO mice and TA and Q in case of *Bin1* exon 11 KO mice using TRIzol reagent (Invitrogen) according to manufacturer's instructions. cDNA was synthesized from 1–2 μg of total RNA using SuperScript II reverse transcriptase (Invitrogen) and random hexamers. Quantitative PCR amplifications of cDNA were performed on a Light-Cycler 480 instrument (Roche). Gene expression is considered as dysregulated when fold change is higher than 1,3 and p value is ≤ 0.05 . Following primers were used (from 5'-3'):

Bin1 exon7 F: ACTATGAGTCTCTTCAAACCGCC

Bin1 exon7 R: TCCACGTTTCATCTCCTCGAACACC

Bin1 exon9 F: TCAACACGTTCCAGAGCATC

Bin1 exon19 R: GTGTAATCATGCTGGGCTTG

Bin1 exon18,19 F : CATGTTCAAGGTTCAAG

Bin1 exon20 R: TGATTCCAGTCGCTCTCCTT

CASQ 2 F: GCCCAACGTCATCCCTAACA

CASQ 2 R: GGGTCACTCTTCTCCGCAA

TNNT 2 F: GCCATCGACCACCTGAATGA

TNNT 2 R: GCTGCTTGAACTTTTCTGC

JP 2 F: ACGGAGGAACCTATCAAGGC

JP 2 R: CTTGAGAAAGCTCAAGCGGC

Pax 7 F: GGCACAGAGGACCAAGCTC

Pax 7 R: GCACGCCGGTTACTGAAC

MyoD F: CTACGAGGACAGCTATGTGCACCC

MyoD R: AACTGCCCTGTCCCTCTAAGCGG

Myogenin F: CACCCTGCTCAACCCCAAC

Myogenin R: CAGCCCCACTTAAAAGCCC

eMHC F: AGATGGAAGTGTGGCATA

eMHC R: GGCATACACGTCCTCTGGCT

GAPDH F: TTGTGATGGGTGTGAACCAC

GAPDH R: TTCAGCTCTGGGATGACCTT

Western blotting. To extract whole muscle proteins, muscle was homogenized using a Ultra-Turrax (IKA-WERKE) homogenizer in 50 mM Tris, 10% glycerol, 50 mM KCl, 0.1% SDS, 2% Triton X 100 and a set of protease inhibitors: 1 mM EDTA, 10 mM NaF, 1 mM Na₃VO₄, 1 mM PMSF (phenylmethylsulphonyl fluoride), 1 μM pepstatin, 10 μM leupeptin. The homogenate was kept at 4°C for 2 hours, and clarified by centrifugation at 13000 rpm for 10 min. Protein concentration of the supernatant fraction was quantified with the Biorad Protein Assay (Biorad laboratorie GmbH) and lysates analyzed by SDS-PAGE and western blotting on nitrocellulose membrane. Primary antibodies used were DNM2-R2680 (1:500), DNM2-R2865 (1:500), BIN1-R2405 (1:5000), BIN1-R2444 (1:500), GAPDH (1:10,000) and DNA polymerase

(1:1000); secondary antibodies were anti-rabbit HRP or anti-mouse HRP (1:10,000). Western blot films were scanned and band intensities were determined using ImageJ software (Rasband, W.S., ImageJ, U. S. National Institutes of Health, Bethesda, Maryland, USA, <http://rsb.info.nih.gov/ij/>, 1997-2009). Densitometry values were standardized to corresponding total GAPDH values and expressed as a fold difference relative to the listed control (n=3-5 mice per group).

Transmission electron microscopy. Mice were anesthetized by intraperitoneal injection of 10 μ L/g of ketamine (20 mg/mL; Virbac) and xylazine (0.4%, Rompun; Bayer). Muscle biopsy specimens from hind limbs were fixed with 2.5% glutaraldehyde in 0.1 mol/L cacodylate buffer (pH 7.2) and processed as described (Buj-Bello A. et al., 2002). For T-tubule analysis, Potassium ferrocyanide staining was performed as described previously (Al-Qusairi L. et al., 2009).

Immunogold staining. Pre-embedding immunogold electron microscopy Deeply anaesthetized (pentobarbital 60mg/kg) mice were transcardially perfused with 4% paraformaldehyde, 0.1M phosphate buffer. Dissected anterior tibialis were further post-fixed in 4% paraformaldehyde and cut in 100 μ m thick longitudinal sections with a vibratome. A standard free-floating immunocytochemical procedure was followed, using 0.1M saline phosphate buffer as diluent and rinsing liquids. After preincubation in 5% normal goat serum, 5% BSA, sections were overnight incubated at 4° in 1/500 anti-BIN1 antibody. A further 4 hour incubation in ultra-small gold conjugate of goat anti-mouse IgG (1/20; Aurion, Netherlands) was followed by extensive washings, 10 min post-fixation in 2% glutaraldehyde and 0.70nm gold beads were then silver enhanced (HQ silver; Nanoprobes, Stony Brook, NY). After 15' post-fixation in 1 % OsO₄, sections were dehydrated in graded acetone and finally embedded in Epon resin. Ultrathin sections were examined with a Philips CM120 electron microscope, operated at 80kV and imaged with a SIS Morada digital camera.

Microscopy and statistical analysis. All microscopy was performed at the IGBMC Imaging Centre. All samples for microscopy were mounted in Fluorsave reagent (Merck) and viewed at room temperature. Light microscopy was performed using a fluorescence

microscope (DM4000; Leica microsystems) fitted with a color CCD camera (Coolsnap cf colour, Photometrics) camera. Confocal microscopy was performed using a confocal laser scanning microscope (TCS SP2 or SP5; Leica Microsystems, Mannheim, Germany). ImageJ (Rasband, W.S., ImageJ, U. S. National Institutes of Health, Bethesda, Maryland, USA, <http://rsb.info.nih.gov/ij/>, 1997-2009) and FIJI analysis software were used for image analysis. Statistical analysis was performed using the unpaired student's T-test unless stated otherwise. p-values of <0.05 were considered significant.

RESULTS

Results I: Characterization of the *Bin1* exon 20 knockout mouse model

I.1. Introduction

BIN1 is a membrane tubulating protein. It is present in all the tissues, but not equally expressed. BIN1 has 20 exons and in a tissue specific manner it is spliced in to a minimum of 12 different isoforms. The highest BIN1 expression level is in the skeletal muscle. The muscle specific isoform, isoform 8, has several distinctive domains. The N-terminus is composed of the BAR domain which involved in binding and tubulating membranes. The PI motif is encoded by exon 11 and it is a muscle specific exon, although its function is not well defined it may be involved in intra protein binding and regulation. It was shown that it can bind its SH3 domain, as well as bind PtdIns(4,5)P₂ and/or PtdIns3P and PtdIns5P (Lee, Marcucci et al. 2002; Fugier, Klein et al. 2011). The MBD (Myc Binding Domain) is encoded by exons 17 and 18 and it is involved in c-Myc binding (Sakamuro, Elliott et al. 1996). Exon 17 splicing is regulated in an unknown manner and when missing it abolishes the interaction. The SH3 domain is encoded by exons 19 and 20, and it is involved in various interactions.

Mutations in BIN1 are associated with different muscle diseases. Missense mutations in the BAR domain and a stop codon mutation in the SH3 domain are known to be associated with the Autosomal recessive Centronuclear myopathy (ARCNM). Missplicing of exon 7 of the BAR domain and exon 11 of the PI motive have been observed in myotonic dystrophy. Additionally, patients with a decreased level of BIN1 have a predisposition for ventricular cardiomyopathy. The importance of BIN1 in muscle is not fully understood and characterized but importance of BIN1 in this tissue is evident.

I.2 Aim

The aim of this study was to investigate the role of BIN1 and its SH3 domain in mouse skeletal muscle and contribute to a better understanding of BIN1 in muscle development.

I.3 Results

Investigation of BIN1 expression and localization. In order to confirm a expression of BIN1 we performed in situ hybridization on mice at 14,5 and 18,5 days in utero. Our results clearly showed that the highest expression was seen in the skeletal muscle, diaphragm, eye and cortex (Figure 1A) which confirmed previously published data (Butler, David et al. 1997). To identify the exact localization of BIN1 in muscle in collaboration with Stéphane Vassilopoulos we did immunogold labeling using a BIN1 antibody in adult mouse skeletal muscle. Interestingly BIN1 was specifically localized on triads (Figure 1B).

Creation of CMV *Bin1* exon 20 knockout (CMV *Bin1* x20 KO) mice. We created *Bin1* exon 20 knockout mice by targeting exon 20 of BIN1 (Figure 2A). We used recombinase under the cytomegalovirus (CMV) promoter to induce deletion of exon 20 constitutively in all tissues (see methods section for details). Interestingly no KO mice were found in the litter genotyped at 2 weeks of age. We genotyped in total 131 mice. From 131 pups 85 were heterozygote (HZ) and 46 wild type (WT). After genotyping at birth and at 18.5 days in utero (E18.5) we saw that CMV *Bin1* x20 KO mice were alive in utero (Figure 2B) but were mostly dying within first 20h. Interestingly, Newborns were indistinguishable from the WT littermates and weight of the CMV *Bin1* x20 KO mice was comparable to the WT littermates at birth (Figure 5A). Using Western blot we could see that CMV *Bin1* exon 20 deletion led to a strong decrease in protein level (Figure 2C). Since the recombination between the loxP sites was predicted to delete the last exon, exon 20, together with the stop codon and poly-A tail, we believe that the rest of the protein is expressed doesn't have the exon 20 but we had no ways of determine the exact sequence of the region expressed after the end of exon 19. Program ORF Finder from Bioinformatics (http://www.bioinformatics.org/sms/orf_find.html) predicted the first

stop codon was only 7 amino acids after the exon 19 (data not shown). The deletion did not induce the difference in protein size of BIN1 on Western blot (Figure 2C). Taken together, this shows that exon 20 deletion led to a strong decrease in BIN1 protein and perinatal lethality.

Heart characterization of CMV *Bin1* exon 20 KO mice. Since complete deletion of *Bin1* by Muller AJ et al. has been shown to be lethal in the same manner and since the authors concluded that death was due to ventricular cardiomyopathy we wanted to see if CMV *Bin1* x20 KO mice die from the same cause. There was no alteration in the heart mass in the KO compared to the WT hearts (Figure 3B). Histology of the heart followed through 7 μ m cross did not reveal any abnormalities (Figure 3A). After this we wanted to see if heart function was compromised. We performed Echocardiography in utero on day 18.5 days old mice (E18.5) and we could see that the frequency of the heart beats together with systolic and diastolic ratios of the contractions was not impaired (Figure 3C). Expression of the muscle specific proteins involved in muscle contraction and Ca²⁺ handling when checked on mRNA level by RT-qPCR did not show any difference (Figure 3D). Additionally, heterozygote mice were genotyped through the EUMODIC phenotyping program (for further details see methods section and <http://www.eumodic.eu/>) and on all metabolic and motor tests HZ KO mice were comparable to WT. Homozygote CMV deletion of exon 20 of *Bin1* did not induce any alteration in heart function and heterozygote mice did not show any phenotype.

Creation of muscle specific *Bin1* exon 20 knockout (HSA *Bin1* x20 KO) mice. In *Bin1* exon 20 L2/L2 knockout mice line (Figure 4A) Cre recombinase under Human skeletal actin (HSA) promoter was introduced in order to obtain homozygote muscle specific *Bin1* exon 20 KO mice (HSA *Bin1* x20 KO). This approach allowed us to investigate the primary role of BIN1 in skeletal muscle. Surprisingly, we have seen the same effect as when the deletion was induced using the CMV promoter, as no HSA *Bin1* x20 KO mice were found in the litter genotyped at 2 weeks of age. We repeated the approach used for CMV *Bin1* x20 KO mice and once again we saw that HSA *Bin1* x20 KO mice were dying within the first 20h. At the protein level, the decrease of BIN1 was comparable to what was observed in the CMV model. Taken together results

underlined the importance of BIN1 during development and pointed to the probable skeletal muscle defect being the common cause of peri-lethality in total and muscle-specific *Bin1* exon 20 KO.

Skeletal muscle analysis on CMV *Bin1* exon 11 KO mice. Perinatal lethality triggered by a skeletal muscle defect can be caused either by a breathing or a feeding defect. We performed floating test to see if the KO mice breathe efficiently. When immersed into PBS KO mice were floating as well as the WT mice, which showed lungs were able to inflate and initial breathing was possible (data not shown). To further examine diaphragm organization and muscle structure we used histological examination of longitudinal cuts of E18.5 KO and WT mice muscle (Figure 5B). Diaphragm thickness and organization (Figure 5B left panel) together with organization of other tissues with a focus on the skeletal muscle (Figure 5B right panel) did not show any gross structural abnormalities.

Interestingly we observed that CMV *Bin1* x20 KO newborns unlike WT and HZ mice did not have any milk in their stomach (data not shown). We examined the glucose level in the blood and we could see that in all but one case, KO Newborns had very low glucose levels (Figure 5D). To make sure that this decrease in glucose was due to a lack of feeding and was not metabolically or pregnancy related, we checked glucose levels at E18.5 days (Figure 5C). KO, HZ and WT mice did not have significantly different glucose levels. Interestingly in utero glucose showed variable levels, but this was not genotype related (Figure 5C). Overall we concluded that KO mice probably die from hypoglycemia caused by an inability to feed. Mice might additionally have undetectable breathing problems but we did not have any means in order to investigate this further.

BIN1 localization in CMV *Bin1* exon 20 KO mice. BIN1 localization was investigated using two different techniques and two different pan antibodies. We used isolated fibres to look at the BIN1 organization and its longitudinal pattern. We could see that compared to the WT littermates which had pronounced tubular staining of BIN1 that was previously shown to belong to the T-tubules (Lee, Marcucci et al. 2002). CMV *Bin1* x20 KO fibers were faintly stained for BIN1, which was diffuse and not specific for T-

tubules (Figure 6A). Using two different antibodies we saw that BIN1 in KO mice was concentrated towards the center of the fibers (Figure 6B). Interestingly the same pattern was observed in ARCNM BIN1 patients (Romero and Bitoun 2011).

Triad structure and myotubularin1/dynamin 2 localization in CMV *Bin1* exon 20 KO mice. We have already showed that BIN1 localizes to the T-tubule system (Figure 1B) and therefore we continued with analysis of triad markers. DHPR staining on transversal sections colocalized with BIN1 and in the KO was collapsed towards the center of fibre in the same way as BIN1 organization (Figure 7A). Longitudinal staining done on isolated fibres showed in WT muscle that DHPR organization had staining pattern seen in the skeletal muscle of adult mice (Figure 7B) whereas BIN1 was still longitudinal, labeling a dense network within the fibres (Figure 7B). This pattern was expected and previously confirmed by other studies (Franzini-Armstrong 1991). Interestingly BIN1 stained tubules were at certain points clearly seen colocalizing with DHPR which points to BIN1 connection to the T-tubule system (Figure 7B). Staining in the KO fibers was similar to what was observed on transversal sections, which was aggregated and collapsed towards the centralized nuclei (Figure 7B). RyR1 staining on the transversal sections showed the same type of collapse (Figure 8A). Further we wanted to analyze myotubularin 1 and dynamin 2 localization since in both, mutations causing centronuclear myopathy were found. Myotubularin1 localizes on sarcoplasmic reticulum (SR) and in CMV *Bin1* x20 KO mice its localization was altered (Figure 8B, right panel). This would be expected if T-tubules were missing and this resulted in inability of SR and T-tubules connections and triad formation. Further this might have led to the collapse of SR network with DHPR segregation on it. BIN1 interacts with dynamin 2 through its SH3 domain. BIN1 reduction and SH3 deletion did not cause the mislocalization of dynamin 2 (Figure 8B, left panel). Therefore we could see that dynamin 2 localization is not BIN1 dependent. To summarize, we concluded that homozygote deletion of exon 20 together with BIN1 protein reduction caused strong T-tubules and SR alterations but did not affect dynamin 2 localization.

Dynamin 2 localization in WT differentiating fibres. Interestingly, when we looked at the dynamin 2 localization in skeletal muscle of WT newborns we noticed that

the certain population of fibres exists in which both BIN1 and dynamin 2 were still longitudinal (Figure 9A, bottom panel). It was already shown that BIN1 through its SH3 domain interacts with dynamin2 in vitro, but in vivo in skeletal muscle those two proteins were never seen in a proximity by localization. When both reach its final positions in the adult muscle, BIN1 is seen at the triads and dynamin 2 on the Z-line (Figure 9A, upper panel). We decided to check localization of those patterns in the primary culture of the differentiating myoblasts derived from the satellite cells from WT mice. This system due to its homogeneity and ability to manipulate is suitable for the further understanding of this interaction. 8 days from the start of the differentiation we could clearly see BIN1 and dynamin 2 colocalization in the numerous myotubes examined (Figure 9B). The interaction might be needed in the short time window, possibly during T-tubules formation. We wanted to verify this hypothesis under Notexin induced muscle regeneration. Notexin is a snake venom, commonly used to induce muscle damage in mice. Injecting it into TA of WT mice allows us to follow the regeneration process of the muscle. 7 days after the damage induced in TA muscle, we could see the T-tubule network being formed and at numerous places BIN1 and dynamin 2 colocalized (Figure 10). At 14 days the network was almost fully developed, resembling what was seen in adult muscle (Figure 10).

BIN1 - dynamin 2 interaction in WT skeletal muscle. Since we did not see any alterations in dynamin 2 localization, we measured the dynamin 2 protein level in skeletal muscle of CMV *Bin1* x20 KO mice (Figure 11A). The protein expression of dynamin 2 was not altered compared to the WT littermates (Figure 11A,B). Recently it was reported that exon 7 inclusion in the BIN1 BAR domain resulted in increased binding to dynamin 2 (Ellis, Barrios-Rodiles et al. 2012). In MD patients exon 7 missplicing resulted in its elevated inclusion in skeletal muscle specific isoform of BIN1 (Fugier, Klein et al. 2011). This missplicing may lead to the maintenance of the interaction found in the fetal muscle. We checked if the exon 7 expression was increased in embryonic (E 18.5 days) compared to the adult (12 weeks) skeletal muscle, since this might explain the colocalization observed. Indeed, RT-PCR showed that when comparing the ratio of the isoform with exon 7 compared to the isoform

without of it, its inclusion was significantly increased for approximately 50% (Figure 11B).

I.4 Conclusion

In this study we showed that BIN1 and its intact SH3 domain are necessary for proper muscle function and for T-tubule development and no significant defects on heart development and function were observed. Homozygote exon 20 deletion caused strong reduction of BIN1 protein level resulting in perinatal lethality. *Bin1* x20 KO mice have strong SR and T-tubules defects. Additionally we could see that BIN1 and dynamin 2 colocalize in immature muscle which can be explained by increase inclusion of exon 7 in the BAR domain of BIN1. The interaction might be crucial during T-tubule development and might be related to the missing T-tubule network in *Bin1* x20 KO mice. This hypothesis needs to be explored in more detail.

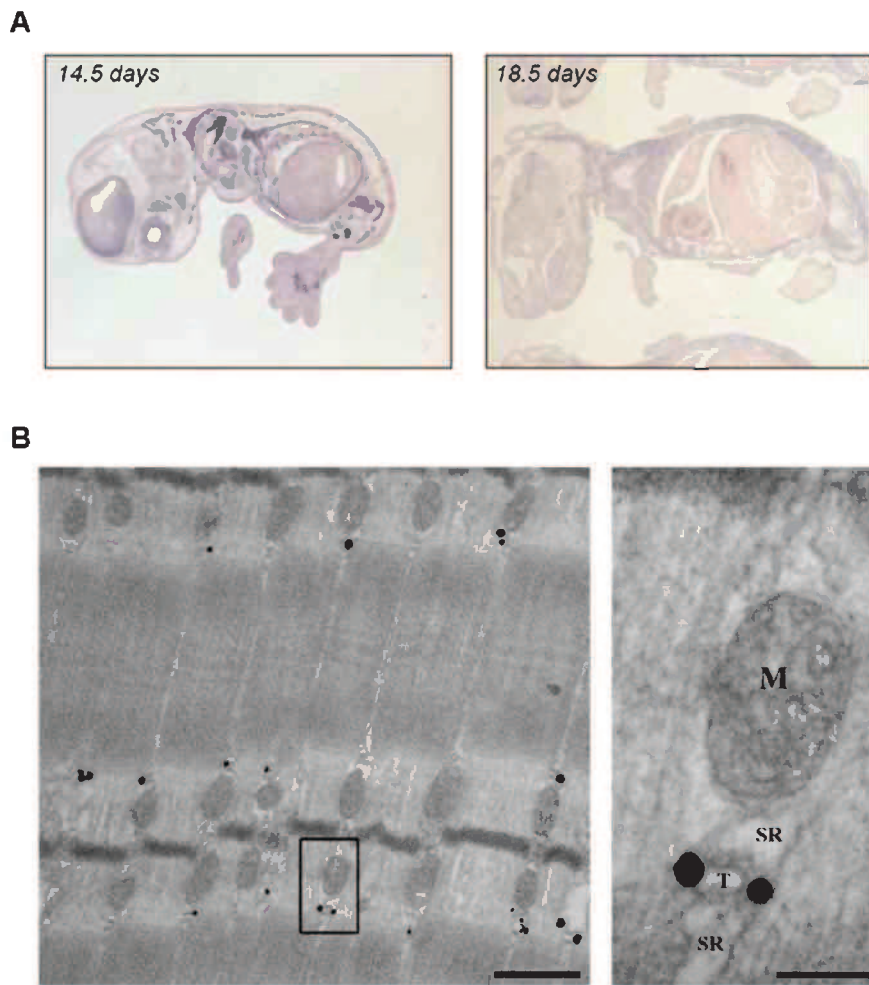


Figure 1. BIN1 expression and localization. (A) In situ BIN1 labeling in WT mouse at embryonic day 14.5 (E14.5) and 18.5 (E18.5). (B) Immunogold labeling using BIN1 antibody on a Tibialis anterior (TA) muscle from a WT adult mouse showing specific triad localization.

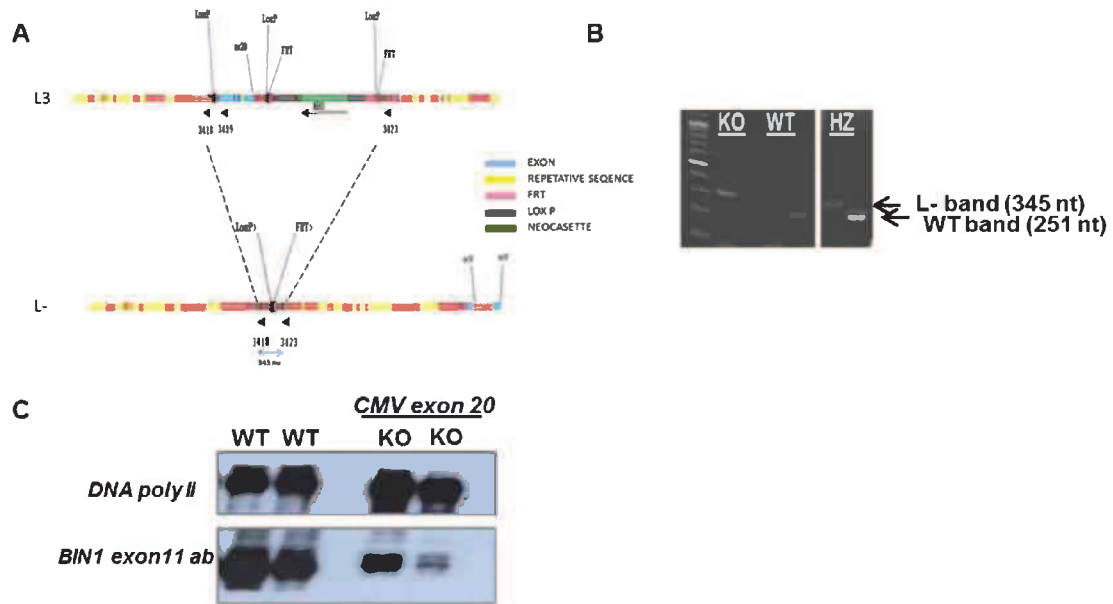


Figure 2. Targeted disruption of mouse *Bin1* exon 20 to create *Bin1* homozygous (*Bin1*^{x20} ^{-/-}). CMV promoter was used in order to induce recombination in all tissues. (A) The genomic region surrounding the targeted exon 20 of *Bin1* in mice. (B) PCR from WT (+/+), KO (-/-) and HZ(+/-) mice. (C) Western blot using anti-BIN1 exon 11 antibody on skeletal muscle protein extracts shows that deletion of exon 20 induced the reduction of total BIN1 protein level.

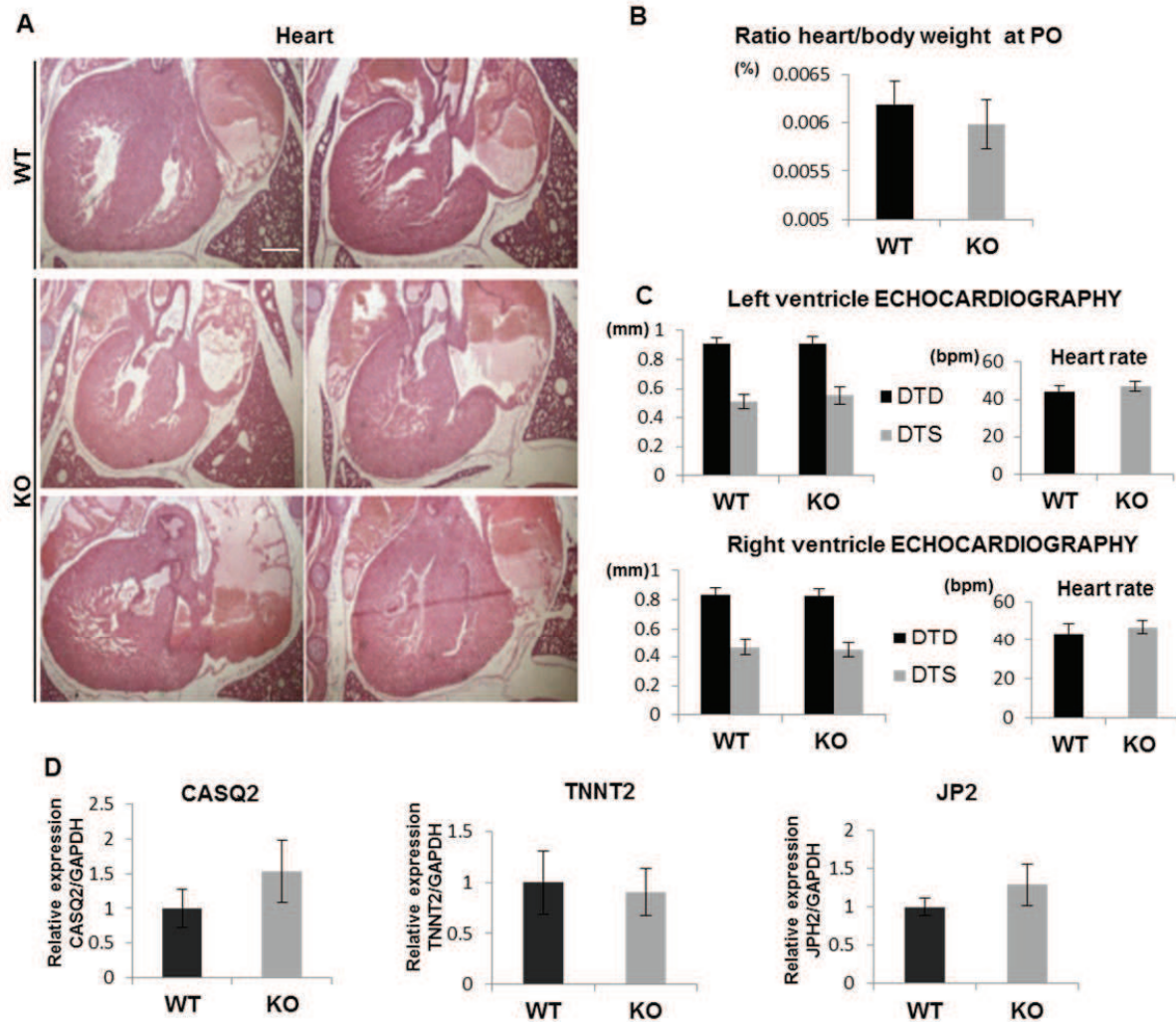


Figure 3. Heart characterization in CMV *Bin1* exon 20 KO mice. (A) Histology of the heart in Newborn WT and KO mice. Scale bar 200 μ m. (B) Ratio of the heart weight compared to the body weight (n=minimum 7 mice per group). (C) Echocardiography done in utero on E18.5 embryos showing no difference in the systolic (DTS) and diastolic (DTD) contraction in left (upper panel) or right (lower panel) ventricle as well as in frequency of heart beats (n=minimum 8 mice per group). (D) RT-qPCR on the heart from P0 days old embryos showing no difference in relative expression of the calsequestrin 2 (CASQ2), troponin T 2 (TNNT2) and junctophilin 2 (JP2) (n=minimum 3 mice per group).

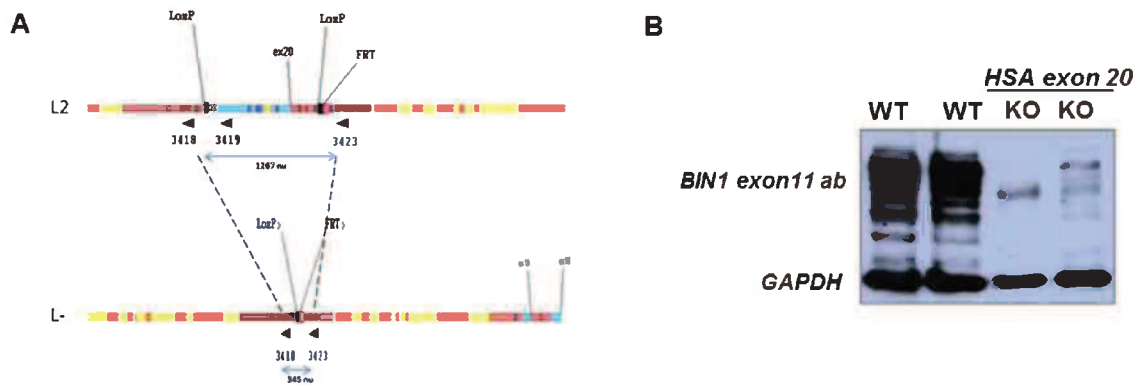


Figure 4. Targeted disruption of mouse *Bin1* exon 20 to create *Bin1* homozygous (*BIN1x20* L2/L2) mice. HSA promoter was used in order to induce deletion specifically in skeletal muscle. (A) The genomic region surrounding the targeted exon 20 of *BIN1* in mice is shown. (B) Western blot using anti-*BIN1* exon 11 antibody on skeletal muscle extract shows that skeletal muscle specific (HSA) deletion of exon 20 induced the reduction of *BIN1* protein level, similar to total *Bin1* exon 20 KO (CMV).

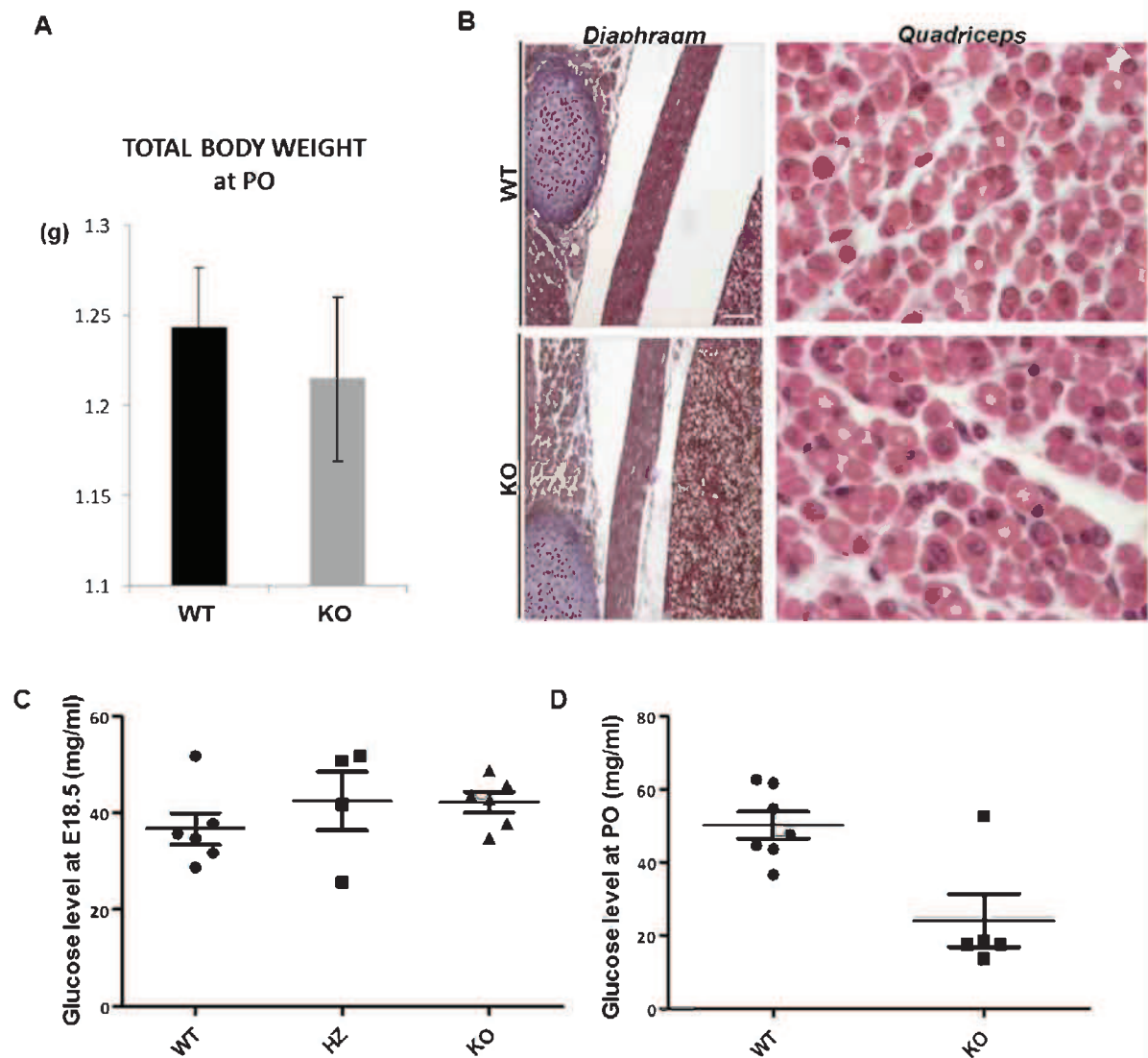


Figure 5. Characterization of the cause of death in newborn CMV *Bin1* exon 20 KO mice. (A) Total body weight of the newborn KO and WT mice is not significantly different (n= minimum 8 mice per group). (B) Histology of the diaphragm and quadriceps in Newborn WT and KO mice. Scale bar 200 μ m. (C) Glucose level measurement from the blood of E18.5 embryos showing no difference in the glucose level between the WT, HZ and KO mice (n=minimum 4 mice per group). (D) Glucose level measurement from the blood of P0 newborns after birth, presumably after mice have fed. WT mice showed higher glucose level compared to all but one KO. (n=minimum 5 mice per group).

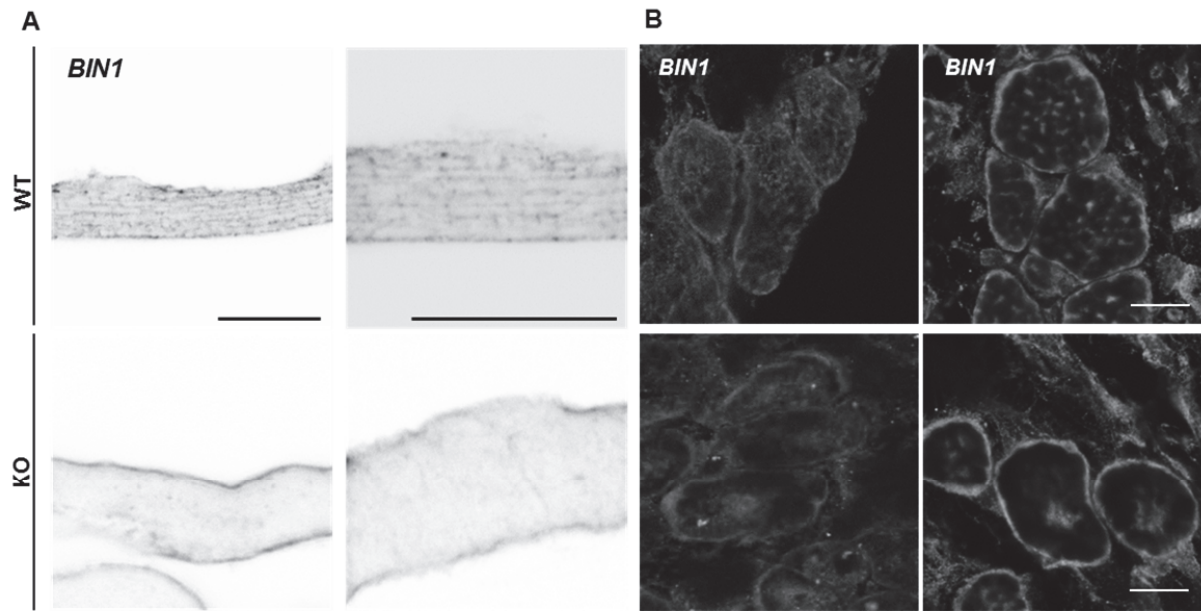


Figure 6. Localization of BIN1 in skeletal muscle of CMV *Bin1* exon 20 KO and WT mice. (A) BIN1 localization in WT and KO mice isolated fibres and imaged by confocal microscopy. Staining in KO is very faint and the extensive network inside of the fibres is lacking compared to WT littermates. (B) Transverse muscle sections were stained with two different BIN1 antibodies and imaged by confocal microscopy. The left panel shows sections stained with C99D antibody which recognizes the exon 17 of the MBD. The right panel shows staining with R2444 antibody which is specific for exon 19 which belongs to the SH3 domain of BIN1. In the KO mouse staining is strongly collapsed towards the center of the fibre. Scale bar 10 μm (transverse) or 5 μm (longitudinal images).

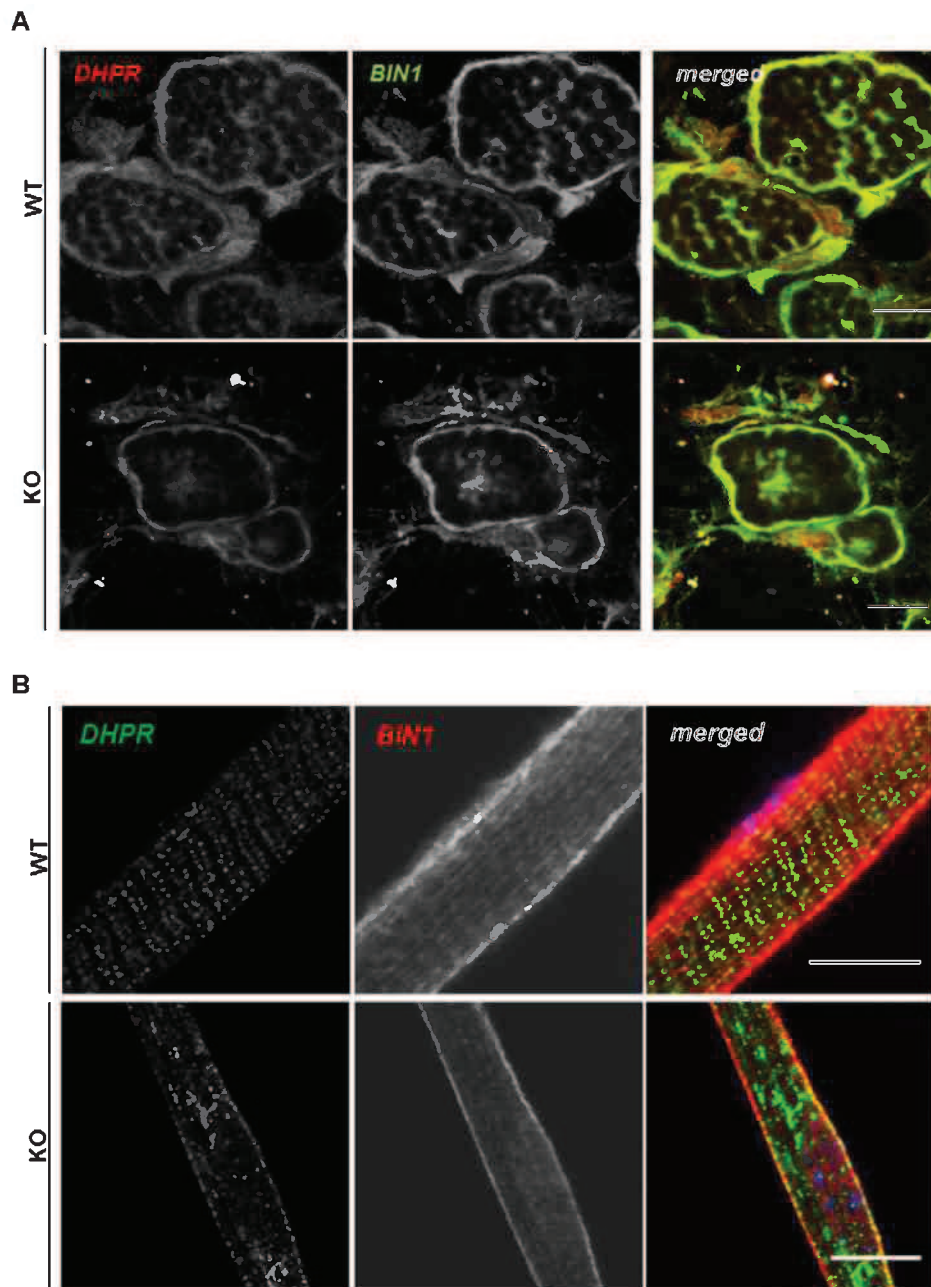


Figure 7. Localization of T-tubules markers in CMV *Bin1* exon 20 KO mice and WT littermates. (A) Transverse muscle sections were costained with DHPR (red, T-tubules) and BIN1 (green, T-tubules) antibodies and imaged by confocal microscopy. In WT and KO muscle DHPR and BIN1 (pan antibody, anti-exon 19) staining colocalize. Staining in KO muscle was collapsed towards the center of the fibres. (B) DHPR (green, T-tubules) and BIN1 (red, T-tubules) (pan antibody, C99D) staining on isolated fibres and imaged by confocal microscopy. Staining of DHPR and residual BIN1 appeared disrupted in KO muscle compared to WT littermates. Scale bar 10 μm (transverse) or 5 μm (longitudinal images).

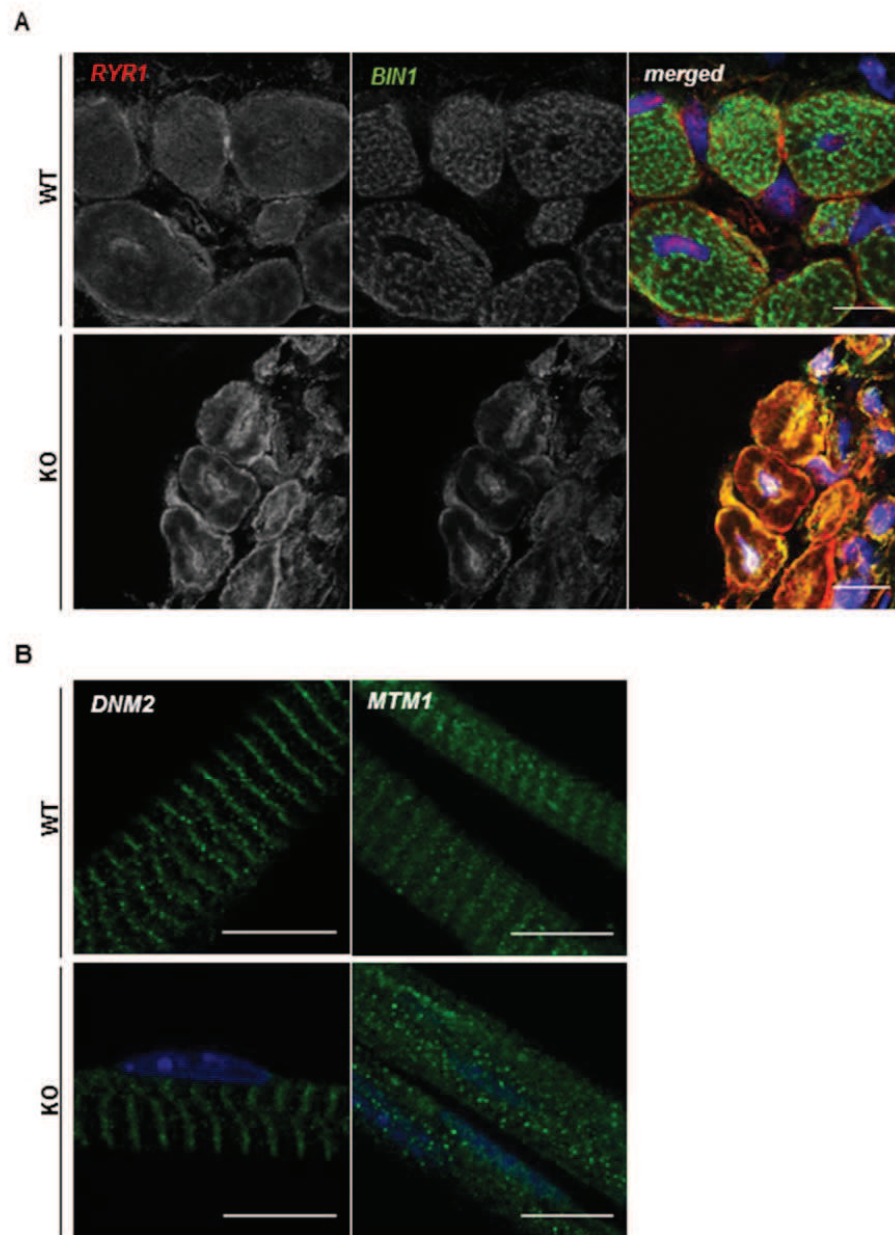


Figure 8. Localization of different markers in the CMV *Bin1* exon 20 KO mice and WT littermates. (A) Transverse muscle sections from hind leg costained with RYR1 (red, SR) and BIN1 (green, T-tubules) antibodies and imaged by confocal microscopy. Staining of RYR1 and BIN1 in KO muscle was collapsed towards the center of the fibres. (B) Dynamin 2 (Z-line) and myotubularin 1 (MTM1) (SR) localization in isolated fibres and imaged by confocal microscopy. Dynamin 2 staining was not altered, whereas myotubularin 1 was altered. Alteration in MTM1 localization was expected in case of altered SR morphology. Scale bar 10 μm (transverse) or 5 μm (longitudinal images).

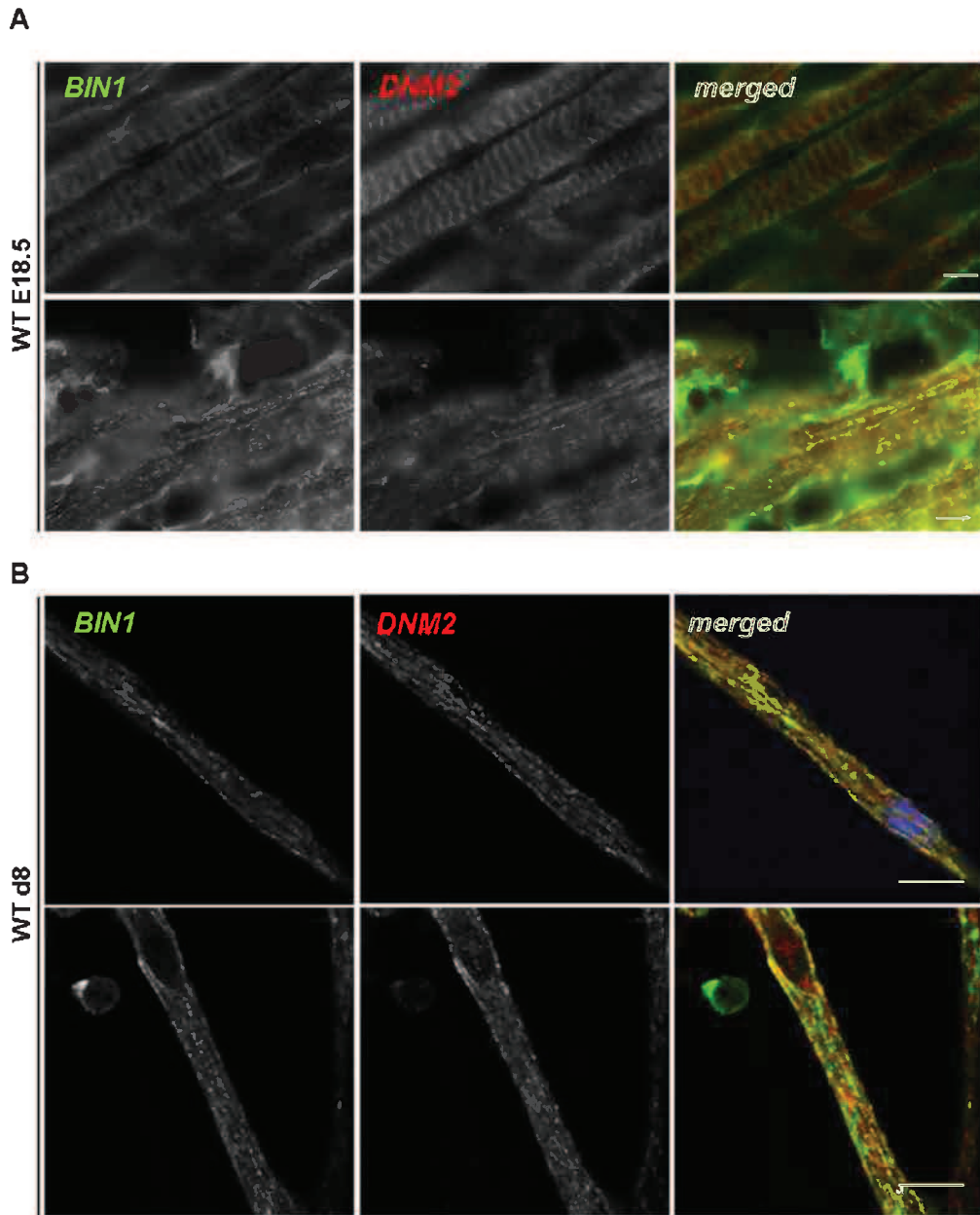


Figure 9. Dynamin 2 and BIN1 localization in the muscle sections of E18.5 WT mouse and in differentiated WT myoblasts. (A) Longitudinal muscle sections costained with DNM2 (red) and BIN1 (green) antibodies and imaged by epifluorescent microscopy. BIN1 and DNM2 staining overlaps in immature fibres (bottom panel) but not in mature muscle (upper panel). Scale bar 20 μm (B) BIN1 and DNM2 colocalize during the differentiation of primary myoblasts in culture (day 9 of the differentiation) when imaged by confocal microscopy. Scale bar 10 μm .

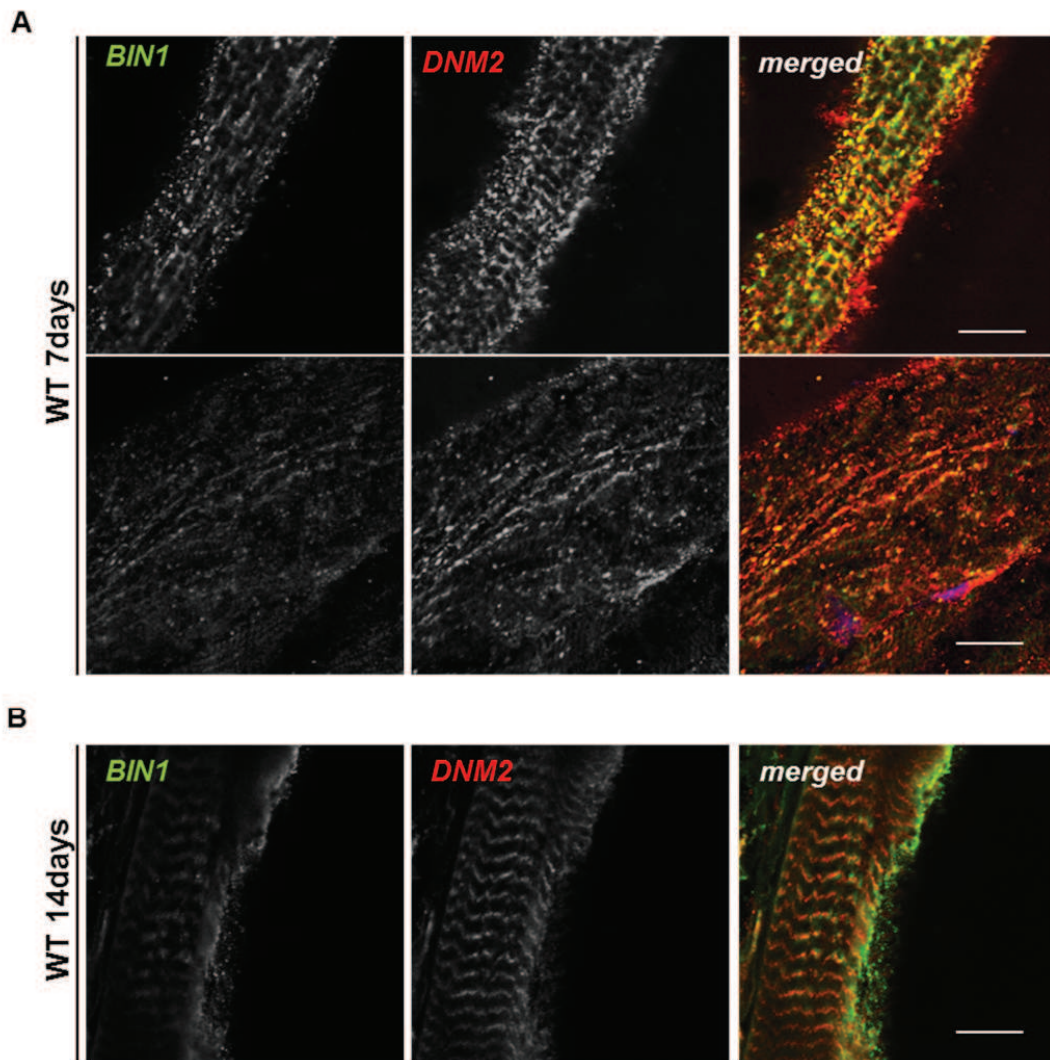


Figure 10. BIN1 and DNM2 localization in regenerating TA muscle of 12 weeks old WT mice. Longitudinal muscle sections were costained with DNM2 (red) and BIN1 (green) antibodies and imaged by confocal microscopy. (A) Regenerating TA muscle analyzed 7 days after the notexin induced damage. BIN1 and DNM2 colocalize in regenerating muscle, most likely during T-tubule network development. (B) Regenerating TA muscle analyzed 14 days after the notexin damage. At this time point BIN1 and DNM2 are not colocalizing anymore. Scale bar 10 μ m.

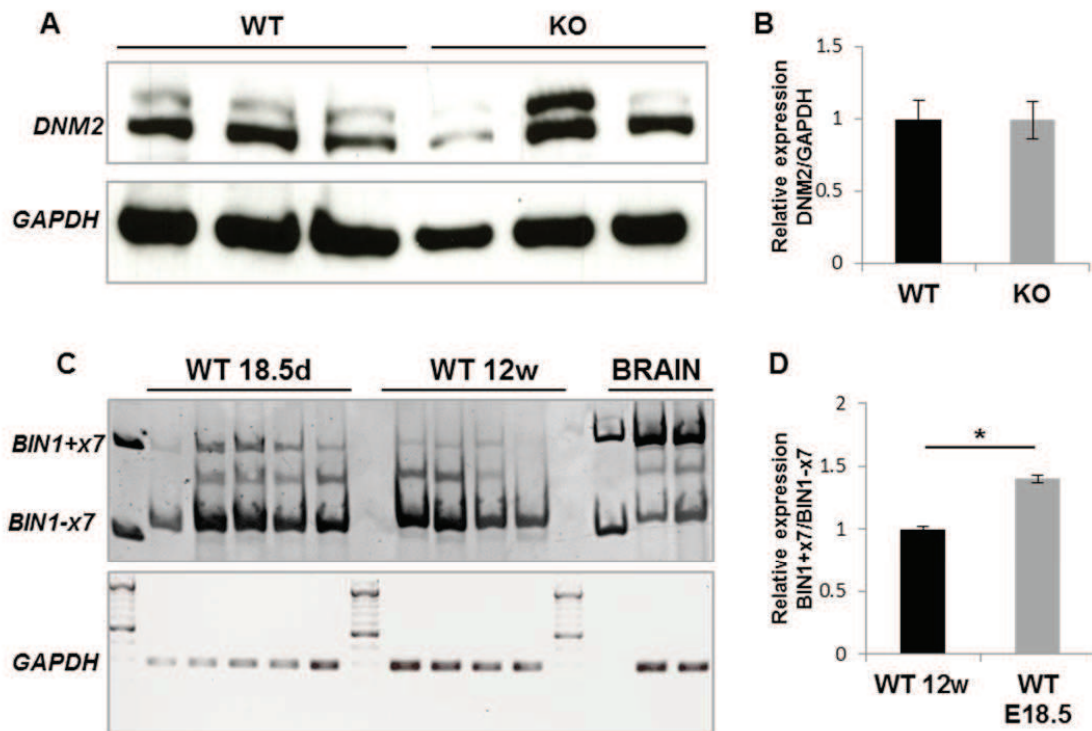


Figure 11. Understanding mechanisms underlying BIN1 and DNM2 colocalization. (A) Western blot for DNM2 performed on KO and WT muscle protein extracts. (B) Densitometry analysis of DNM2 protein expression normalized to GAPDH in CMV BIN1 exon 20 KO and WT littermates. (C) RT-PCR showing the amplification of exon 7 of BIN1, showing increased expression in E18.5 mice. (D) Relative expression of BIN1 isoform containing exon 7 normalized to expression level of BIN1 isoform lacking exon 7. Immature WT muscle shows significantly higher level of expression of exon 7 inclusion compared to adult WT muscle. Graph depicts mean \pm s.e.m (* $p < 0.05$).

Results II: Is BIN1 involved in skeletal muscle maintenance?

II.1. Introduction

As previously described (in Results 1) embryonic deletion of exon 20 in skeletal muscle of mice was neonatally lethal, highlighting the importance of BIN1 during myogenesis in fetal muscle. To determine the importance of BIN1 in adult muscle maintenance, we induced knockout of BIN1 in adult mice.

II.2. Aim

Aim of this study was to investigate the involvement of BIN1 and impact of exon 20 deletion in the maintenance of adult skeletal muscle.

II.3. Results

Muscle specific deletion in adult *Bin1* exon 20 knockout (mKOi) mice. Inducible *Bin1* exon 20 muscle-specific knockout mice were generated using HSA-Cre-ER^{T2} mice crossed with *Bin1* exon 20 floxed (*Bin1* exon 20 L2/L2) mice. A schematic of the *Bin1* exon 20 L2/L2 transgene is presented in Figure 1A. We used the HSA promoter to drive skeletal muscle-specific expression of the Cre recombinase to allow us to decipher the skeletal muscle specific role of BIN1. At 7 weeks of age mice were daily injected for 5 days intra peritoneal with tamoxifen, which triggered the recombination and therefore excision of exon 20. By genotyping we could see the mKOi mice had amplification of the DNA fragment expected after the recombination occurred. The same band was absent from the control group (Figure 1B). As a positive control CMV exon 20 KO DNA was used (Figure 1A). Already 5 weeks after tamoxifen injection we identified that recombination was efficient in both Tibialis anterior (TA) and quadriceps (Q) muscles by RT-qPCR (Figure 1C). The residual expression in TA and Q could be due to the reduced efficiency of the tamoxifen inducible system. Additionally, muscle is also composed of non-muscle and satellite cells in which recombination will not occur. The difference in level of excision between the Q and the TA muscle may be due to the number of non-muscle and satellite cells, which could be different between the two muscles and/or the total number of fibers, could have an impact, as the Q is

considerably bigger and has more fibers in which excision needs to be done. All further analysis was continued on the TA muscle. Five weeks after tamoxifen injection we could see a slight decrease in BIN1 protein expression (Figure 1D). 15 weeks after the injection BIN1 protein decrease was much stronger and this level was maintained 25 weeks after tamoxifen injection (Figure 1E,F). At the latest time point, at 25 weeks we checked the BIN1 protein level in the heart using the BIN1 pan antibody and we could see that there was no decrease in the BIN1 protein level in the heart and decrease was characteristic for skeletal muscle (Figure 1F), confirming excision was specific for skeletal muscle.

Phenotyping of *Bin1* mKOi mice. Mice were analyzed 5, 15 and 25 weeks after the tamoxifen injection. Due to a lack of difference between the mKOi and control littermates, only the results on the final time point (25 weeks) are presented. Body weight of the mKOi mice was not different from the control group (Figure 2A), and there was no reduction in muscle mass (Figure 2B). Furthermore we wanted to examine the muscle function using different tests. The two paws GRIP test, string and hanging tests did not show any weakness or alterations in muscle performance in mKOi mice (Figure 2 C,D,E).

Histological features in mKOi mice. CNM presents histologically with mislocalized internal nuclei and muscle fiber atrophy. Histological analysis by HE staining showed normal muscle organization with also occasional nuclei mislocalization (Figure 3A, upper panel) and NADH-TR staining was normal (Figure 3A, middle panel). We checked if there was increased fibrosis in the TA muscle by Sirius red/Fast green staining that emphasizes the fibrotic tissue by coloring it red compared to the dark blue stained muscle fibers. *Bin1* exon 20 KOi did not induce an increase in the fibrotic tissue (Figure 3A, bottom panel). To assess if muscle atrophy was present we analyzed the fibre size of the TA, but we did not find any alterations in the fiber size (Figure 3B). Further we quantified nuclei mislocalization and we saw a slight increase in mislocalized nuclei in the TA of control group compared to the mKOi (Figure 3C). Interestingly the same increase was seen at 15 days after the tamoxifen injection (data not shown). Muscle ultrastructure morphology was also assessed by transmission electron

microscopy (TEM) and no difference in sarcomere organization was noticed (Figure 3D). Overall *Bin1* exon 20 KOi mice showed that *Bin1* deletion did not have an impact on muscle fiber structure and function, indicating BIN1 is not implicated in muscle maintenance.

II.4. Conclusion

Similar to total and muscle-specific induced recombination of exon 20 of *Bin1*, inducible exon 20 deletion induced a strong reduction of total BIN1 protein level and not only deletion of exon 20. The deletion did not affect muscle mass, histology or muscle function even 25 weeks after tamoxifen injection, which is contrary to what was seen when BIN1 was excised during embryogenesis and was neonatally lethal. Therefore BIN1 is essential for muscle development but is not needed for muscle maintenance if we consider that the deletion rate of tamoxifen-inducible system was efficient.

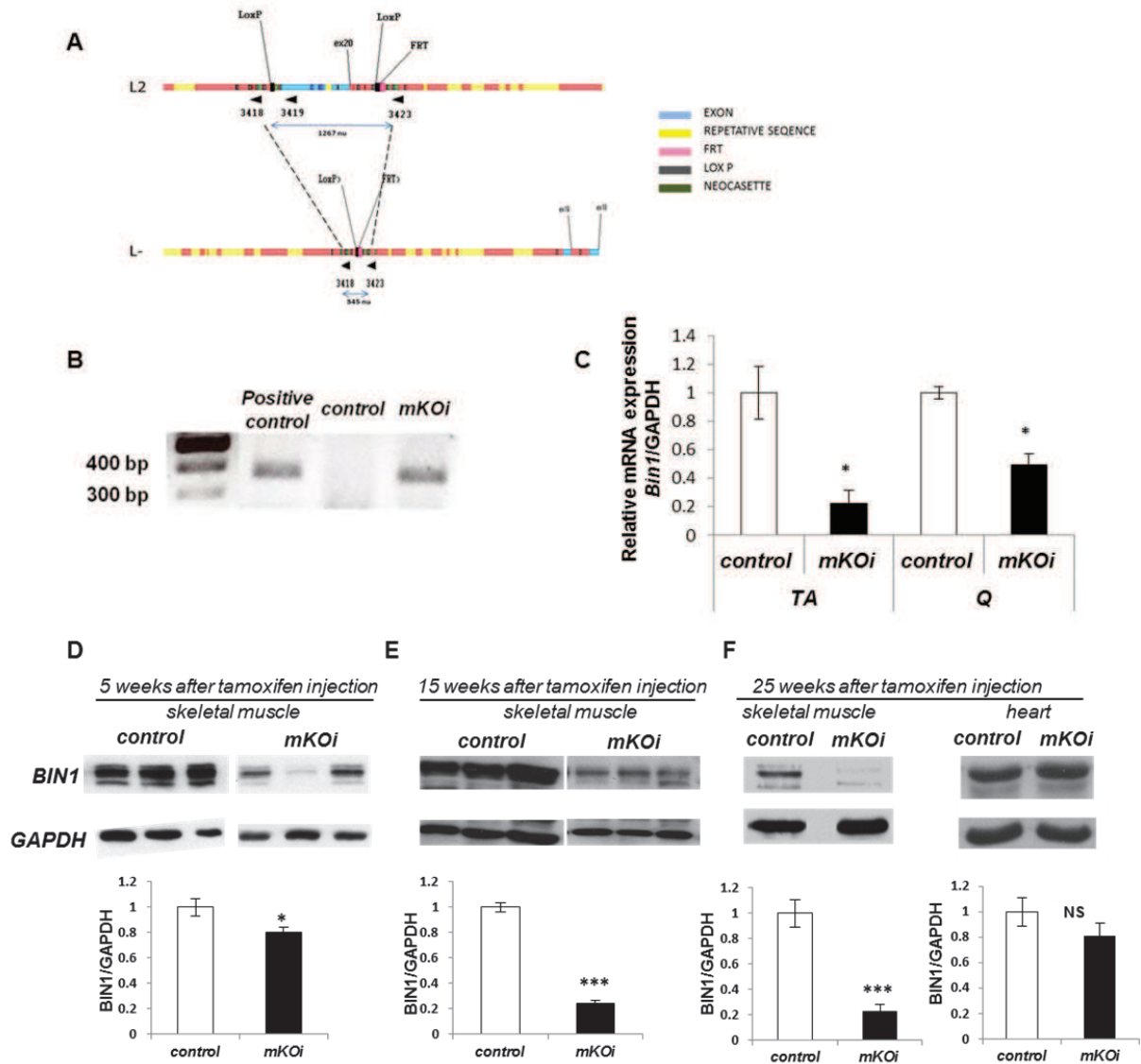


Figure 1. Tamoxifen induced *Bin1* exon 20 deletion at 7 weeks of age. (A) The genomic region with two Lox P recombination sites, surrounding the targeted exon 20 of BIN1 in mice. (B) PCR showing the excision from the positive control (CMV exon 20 KO), control (L2 HSA Cre ERT²⁻) and mKOi (L2 HSA Cre ERT²⁺) (C) RT-qPCR from control and mKOi mice on Tibialis anterior (TA) and Quadriceps (Q) 5 weeks after the tamoxifen injections. Stronger excision is seen in the TA compared to the Q. BIN1 protein level 5 weeks (D), 15 weeks (E) and 25 weeks (F) after tamoxifen injection *intraperitoneal* (IP). All graphs depict mean \pm s.e.m. (* $p < 0.05$, ** $p < 0.01$, *** $p < 0.001$) (n=minimum 3 mice per group).

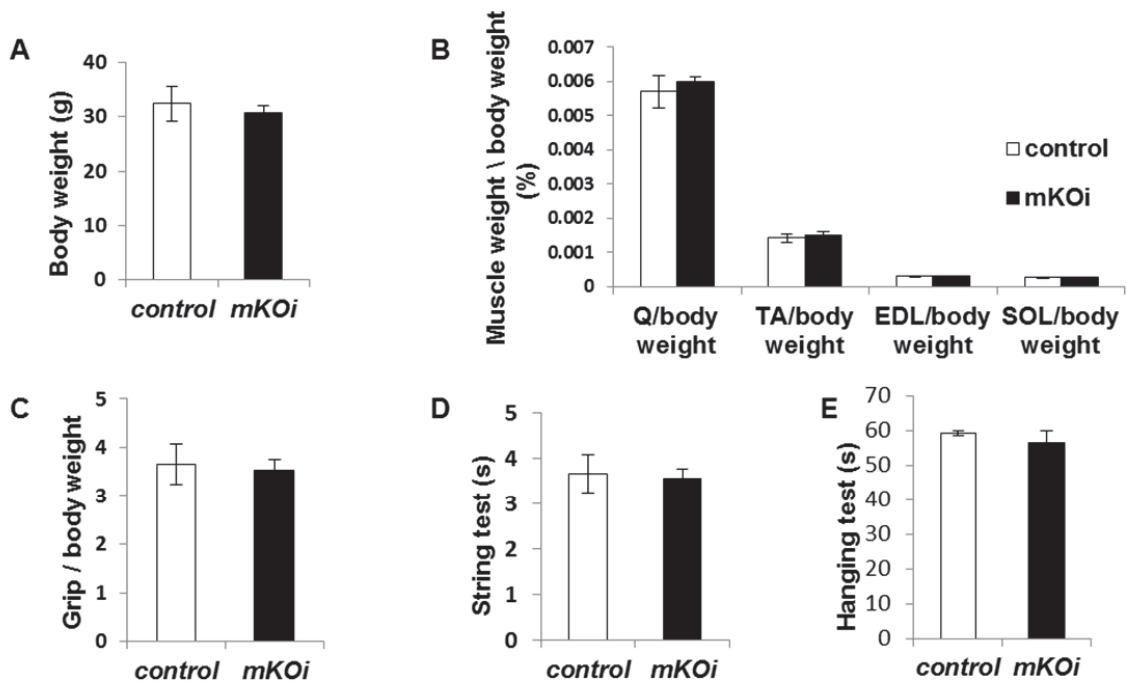


Figure 2. Phenotyping of *Bin1* mKOi mice 25 weeks after tamxifen injection. (A) Body weight of the mKOi mice is comparable to the control littermates. (B) Ratio of muscle/body weight of different muscle shows no significant difference between the groups. (C) The GRIP test was performed using 2 paws and shows no difference when measured by GRIP strength. String test (time taken to rise hind limbs to wire) (D) and hanging test (time mice is suspended from cage. Max time 60sec) (E) show the comparable performance between the control and mKOi groups. All graphs depict mean \pm s.e.m. (* $p < 0.05$, ** $p < 0.01$, *** $p < 0.001$) (n=minimum 6 mice per group).

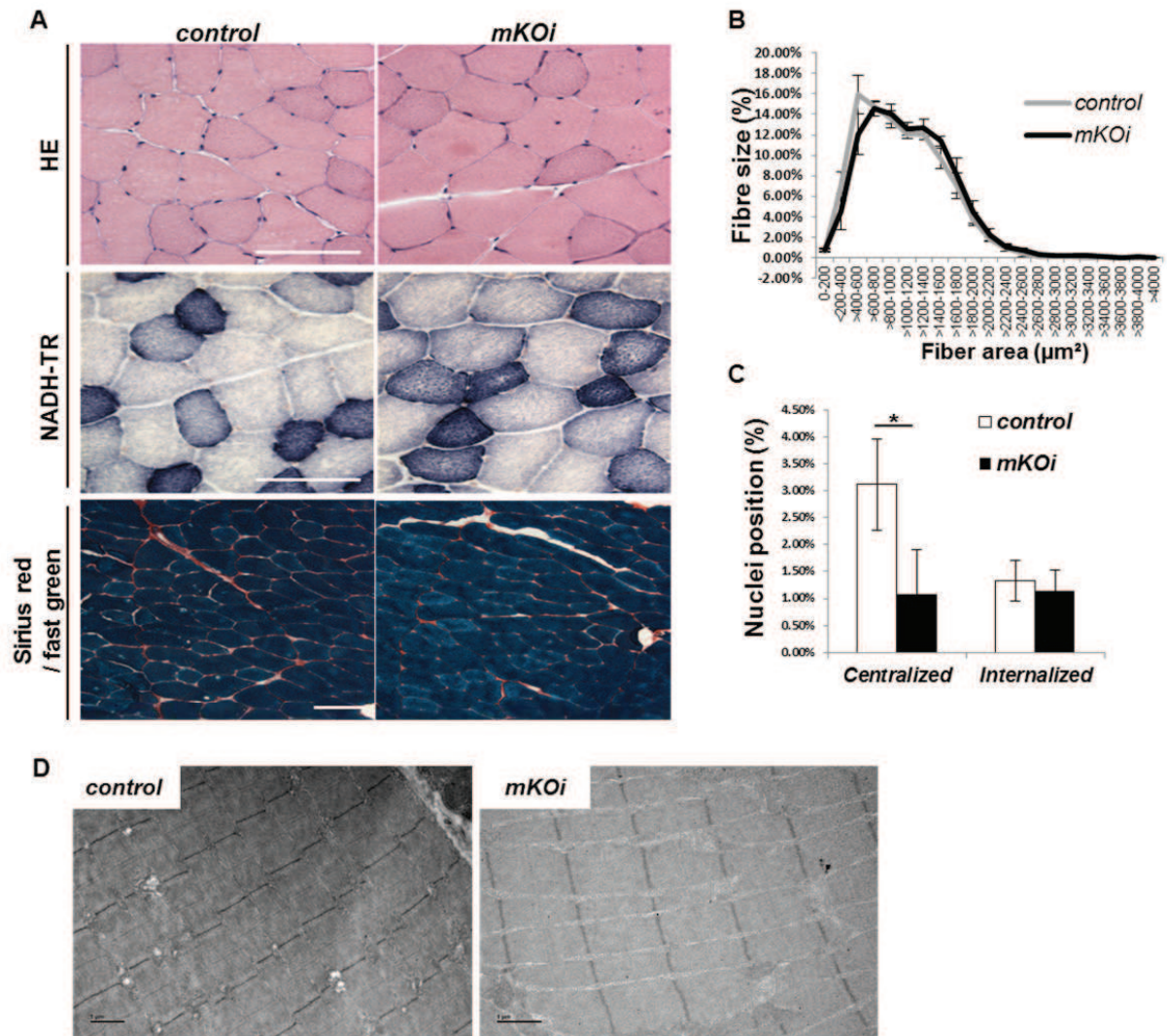


Figure 3. Characterization of the CNM histological features in *Bin1* exon 20 mKOi mice 25 weeks after tamoxifen injection. (A) Histology of the TA muscle seen by haematoxylin and eosin (HE) (upper panel), NADH-tetrazolium reductase (NADH-TR) (middle panel) or sirius red/ fast green (lower panel) and (D) viewed by transmission electron microscopy (TEM). Magnification scale bar 100 μm and in the case of TEM 1 μm . (B) TA muscles were analyzed for fibre area. Fibre size is grouped into 200 μm^2 intervals, and represented as the percentage of total fibres in each group (n= minimum 5 mice). (C) The frequency of fibres with internal or central nuclei were scored (n= minimum 5 mice). Internal nuclei are defined as not subsarcolemmal nor central. All graphs depict mean \pm s.e.m. (* $p < 0.05$, ** $p < 0.01$, *** $p < 0.001$).

Results III: Characterization of the Bin1 exon 11 knockout mouse model

III.1. Introduction

BIN1 is a ubiquitously expressed protein with highest expression in skeletal muscle. Skeletal muscle isoform exclusively contains exon 11 encoding the PI binding motif. Exon 11 expression and integration are upregulated in the final phases of fetal development. Myotonic dystrophy patients show alteration of the splicing of exon 11, which may contribute to the skeletal muscle weakness. Recently splice site exon 11 mutations were described in a patient and in a naturally occurring dog model. Interestingly, BIN1 isoform without exon 11 overexpressed in C2C12 cells does not tubulate membranes. It was shown that the PI motif of BIN1 can bind PtdIns(4,5)P₂ and/or PtdIns3P and PtdIns5P (Lee, Marcucci et al. 2002; Fugier, Klein et al. 2011). PI coordinates intra protein SH3 domain binding, therefore regulating its ability to interact with other proteins (Kojima, Hashimoto et al. 2004). The exact role, function and importance of exon 11 in skeletal muscle are not fully understood or characterized.

III.2. Aim

The aim of this study was to investigate the role of exon 11 in mouse skeletal muscle and provide a better understanding of the importance of the muscle specific isoform.

III.3. Results

Creation of *Bin1* exon 11 knockout (KO) mice. We created *Bin1* exon 11 knockout (*Bin1* x11 KO) mice by targeting exon 11 of *Bin1* (Figure 1A). The deletion was induced using the cytomegalovirus (CMV) promoter which is expressed constitutively, therefore in all tissue (see methods section for details). We found no difference on the Mendelian distribution of mice genotypes. From 116 pups 28 were KO (24%), 55 heterozygote (HZ) (48%) and 33 wild type (WT) (28%). The deletion of exon 11 is predicted to produce a full length protein without the PI binding domain, which is encoded by exon 11. RT-PCR (Figure 1D) and sequencing (Figure 1C) confirmed that

the deletion was exon 11 specific. Analysis at the protein level using an in house antibody raised against exon 11, we confirmed that exon 11 was also absent from the protein (Figure 1E), this also confirmed the specificity of this BIN1 antibody. Antibody against the ubiquitously expressed exon 19 showed that BIN1 protein was still present although in a slight reduced level (Figure 1E). Taken together, this shows that exon 11 deletion was specific and did not strongly alter the splicing of neighboring exons, nevertheless the deletion of exon 11 reduced BIN1 protein level expression.

Phenotyping of *Bin1* exon 11 KO mice. At birth *Bin1* exon 11 KO mice were indistinguishable from the WT littermates. At 12 weeks of age body weight (Figure 2A) and body length (Figure 2B) were not significantly different. DEXA scan did not show any difference in the lean mass or quantity of fat amount (Figure 2C). The life expectancy of the mice was not reduced compared to the control group (data not shown). Homozygote mice were additionally analyzed under the EUMODIC phenotyping program (for further details see methods section and <http://www.eumodic.eu/>) and on all metabolic and motor activity tests KO mice were comparable to WT. Overall, we did not see any defects after the exon 11 deletion on whole body analysis.

CNM-like histological features *Bin1* exon 11 KO mice. CNM presents histologically with mislocalized internal nuclei and muscle fibre atrophy. First we determined if the muscle mass of individual muscles when normalized to the body weight was altered. The TA, EDL and soleus (SOL) mass to body weight ratios were comparable to WT littermates (Figure 3A). HE of the TA muscle staining showed normal muscle organization with occasional nuclei mislocalization (Figure 3B, upper panel) and SDH staining was normal (Figure 3B, bottom panel). To assess the possible muscle atrophy observed in patients, we analyzed the fiber size of the TA, but we did not find any alterations in the distribution of the fiber size (Figure 3C). The nuclei position was quantified in different muscles. Nuclei mislocalization was slightly but significantly increased in all muscles analyzed, with the quadriceps and TA muscles more affected compared to the soleus (Figure 3D). Ultrastructure of the TA muscle by transmission electron microscopy (TEM) and again no difference in sarcomere organization was

noticed (Figure 3E). Z-lines were aligned correctly and mitochondria and triads had no obvious defects. Taken together *Bin1* x11 KO mice exhibited only slight increase of the centralized nuclei. All the other characterized features were comparable to the WT littermates.

Muscle function of *Bin1* exon 11 KO mice. To determine if the muscle function was affected by BIN1 exon 11 deletion we performed various tests. GRIP strength was performed with two front paws (Figure 4A) or all four paws (Figure 4B) and no difference was observed. Rota rod latency to fall did not identify any difference (Figure 4C). Finally to examine if there might be some specific muscle defects we measured the absolute (total) and specific (relative to muscle mass) muscle force. Absolute force (data not shown) and specific (Figure 4D) were comparable to the WT littermates. Exon 11 deletion therefore did not appear to alter muscle strength.

Triad structure of *Bin1* exon 11 KO mice. In C2C12 cells muscle specific BIN1 isoform was shown to induce membrane tubulation and it was shown that those tubules were membrane connected (Lee, Marcucci et al. 2002). Additionally, U7 skipping of exon 11 in mouse induced T-tubules defects (Fugier, Klein et al. 2011). This indicated that muscle specific isoform of BIN1 may be responsible for T-tubules formation in skeletal muscle. Therefore we wanted to examine the structure of triads in our model. Exon 11 deletion did not alter BIN1 localization as determined with the PAN BIN1 antibody (Figure 5A). Triad markers, RyR1 (SR) and DHPR (T-tubules) also showed normal localization (Figure 5A). To look in more detail, triad organization was checked by potassium ferrocyanide labeling which labels external membranes and invaginations including T-tubules and no obvious changes in the KO mice were seen (Figure 5B). These data confirm that *Bin1* exon 11 KO mice have no T-tubules alterations seen by immunofluorescence or ultrastructure labeling.

Phenotyping of 12 month old *Bin1* exon 11 KO mice. As at 12 weeks of age, *Bin1* exon 11 KO mice did not show any phenotype besides a slight increase in nuclei centralization (Figure 7C). I wanted to look in older mice in order to see if a phenotype develops. Therefore we characterized 10 and 12 month old mice (to both I will later refer as aged mice). At 12 months, *Bin1* x11 KO mice were slightly but significantly heavier

than WT littermates (Figure 6A) but did not differ in the muscle mass relative to body weight (Figure 6B). Further using qNMR, we observed that the increase in weight came from the increase percentage of fat and free body fluid and not due to an increase in the lean mass (Figure 6C). Additionally we have compared the muscle mass to the lean mass and confirmed that indeed there is no difference in the muscle abundance (Figure 6D).

CNM-like histological features and muscle function analysis in aged *Bin1* exon 11 KO mice. The histology of TA was analyzed and neither HE nor SDH staining showed any obvious difference compared to the control group (Figure 7A). Fiber size analysis did not show any alteration (Figure 7B) and only slight increase in the KO mice of mislocalized nuclei was noticed (Figure 7C). This increase was higher than at 12 weeks of age but increase was not massive (Figure 7C). Nevertheless the previously noted fat increase might come from the reduced ambulatory movement and muscle function impairment. We measured the absolute and specific muscle force. Again, absolute force (data not shown) and specific muscle force (Figure 7D) of the TA were comparable to the control WT group.

Triad and sarcomere organization of aged *Bin1* exon 11 KO mice. To determine if exon 11 deletion had an effect on triad organization in aged mice we analyzed isolated fibers from EDL muscles of 10 month old mice. BIN1, DHPR and RYR1 localizations were not altered (Figure 8). Moreover immunofluorescence labeling with titin and alpha-actinin antibodies did not show any sarcomere misalignment (Figure 9A) and this was confirmed by TEM (Figure 9B). Taken together analysis of the aged *Bin1* exon 11 KO mice did not show any strong defects in structure or function compared to the WT littermates.

Regeneration test in 12 weeks old *Bin1* exon 11 KO mice. The only phenotype observed of *Bin1* exon11 KO mice was nuclei mislocalization. Due to a significant increase in abnormally positioned nuclei and in order to see response to stress we wanted to test regeneration capacity of the muscle. For this reason we used notexin, a snake poison, to induce TA muscle injury, and we then followed the regeneration process. The TA muscle was analyzed 3,5,7,14,21 and 28 days after the

notexin-induced injury for both muscle histology and recovery. The first steps of the regeneration are characterized by muscle inflammation and necrosis (3 and 5 days after the injury), which is followed by satellite cells activation and proliferation (5 and 7 days after the injury). Activated satellite cells then start to differentiate and fuse either together to form a new myofiber or with damaged muscle cells in order to contribute to regeneration of existing fiber (process is observed between 5 and 7 days after the toxin induced injury). Finally fibers undergo maturation (14, 21 and 28 days after the notexin injection). By comparing the muscle mass of the injured versus control, non-injected leg we could see that the muscles of both groups were equally damaged and in the first steps (inflammation and satellite cells activation) muscle mass was comparable (Figure 10A and 10B). After this, at 14 days a delay in the muscle mass increase was observed in the KO (Figure 10B) and this difference remained constant until the final time point checked, 28 days after notexin injection (Figure 10B). We observed a shift towards the smaller fibers in the BIN1 x11 KO mice 14 and 28 days post injection (Figure 10C,D). In order to better understand the primary cause of altered regeneration observed, we characterized muscle, at 14 days post injection (the first time point with a significant difference in muscle mass and fibre size), following markers for satellite cells and regenerating fibers by RT-qPCR (Figure 11). Relative expression of Pax7 (quiescent and activated satellite cell marker) and MyoD (a marker of activated satellite cells and myoblasts) were not altered (Figure 11A,B). When we checked relative expressions of Myogenin and embryonic Myosin Heavy Chain (eMHC), characteristic of myoblasts and regenerating fibers, we saw increased expression of both (Figure 11C,D). Nevertheless the TA mass and fiber size was reduced (Figure 10C, D). In *Bin1* exon 11 KO mice the final steps of fusion and/or muscle maturation seem to be delayed, showing the need of the muscle specific isoform of BIN1 during the muscle injury.

III.4. Conclusion

We have extensively characterized *Bin1* exon 11 KO mice. Mice exhibited no obvious phenotype apart from a slight mislocalization in nuclei positioning. Nuclei mislocalizations are commonly seen in regenerating muscle. Indeed we could see that *Bin1* exon 11 KO mice show impairment in final steps of regeneration fail to increase in

mass as WT does together with a higher expression of regenerative markers of immature fibers. Therefore, we can conclude that exon 11 is important during regeneration processes of skeletal muscle.

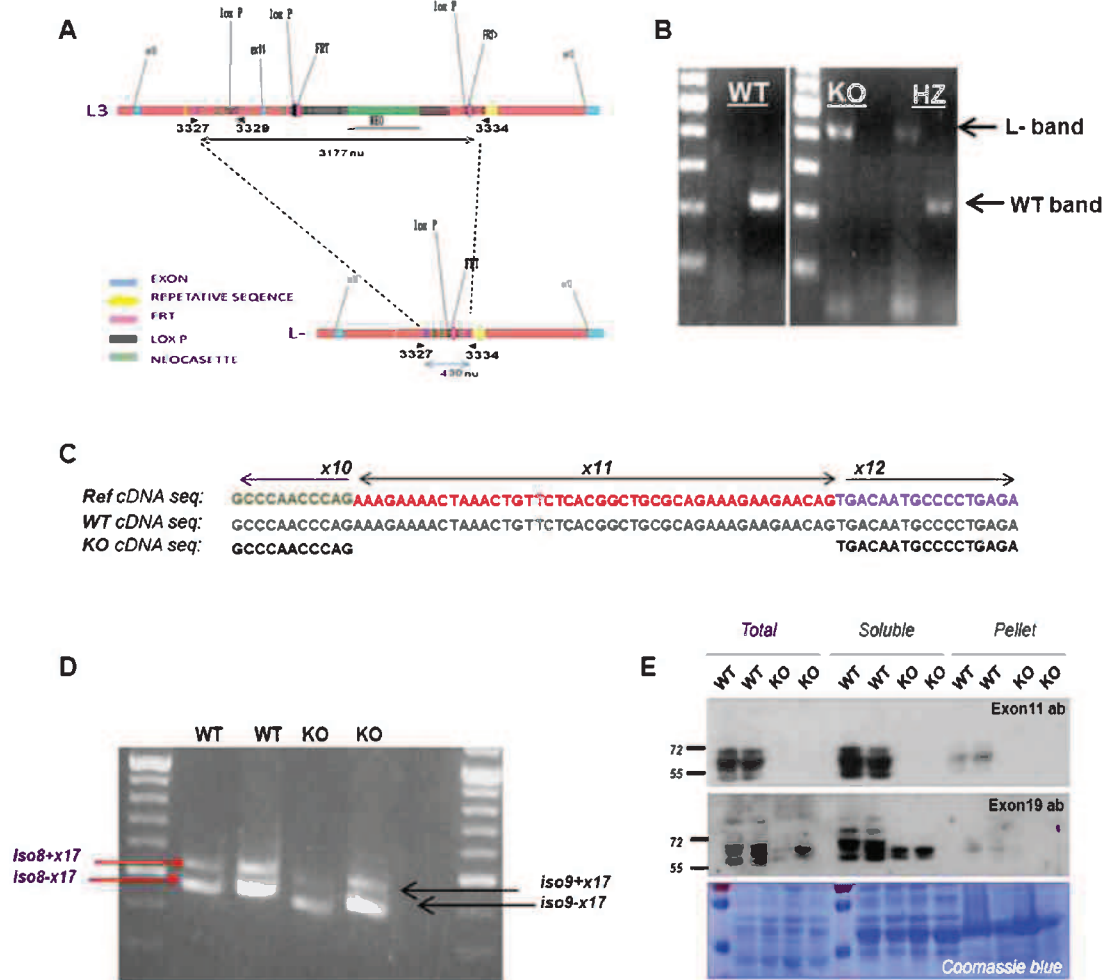


Figure 1. Targeted disruption of mouse *Bin1* exon 11 to create *Bin1* homozygote (*Bin1* x11^{-/-}) mice. (A) The genomic region surrounding the targeted exon 11 of *Bin1* in mice. Deletion of exon 11 is predicted to lead to an in frame transcript which is lacking only exon 11. BIN1 without of exon 11 is named isoform 9. (B) PCR from the WT (+/+), KO (-/-) and HZ(+/-) mice. (C) Sequences performed on cDNA from WT and *Bin1* x11 KO mice, showing that exon 11 is removed and the neighboring exons are intact. (D) Agarose gel with RT-PCR from the TA of WT and KO mice of the region between exons 9 and 19. Bands from the KO mice are lower compared to the WT, indicating expected shift in the size. (E) Western blot using anti-*Bin1* exon 11 antibody shows complete lack of exon 11 (top panel). Pan-BIN1 antibody (for exon 19) shows that the protein is present but decreased (middle panel). Equal loading was checked using Coomassie blue (lower panel).

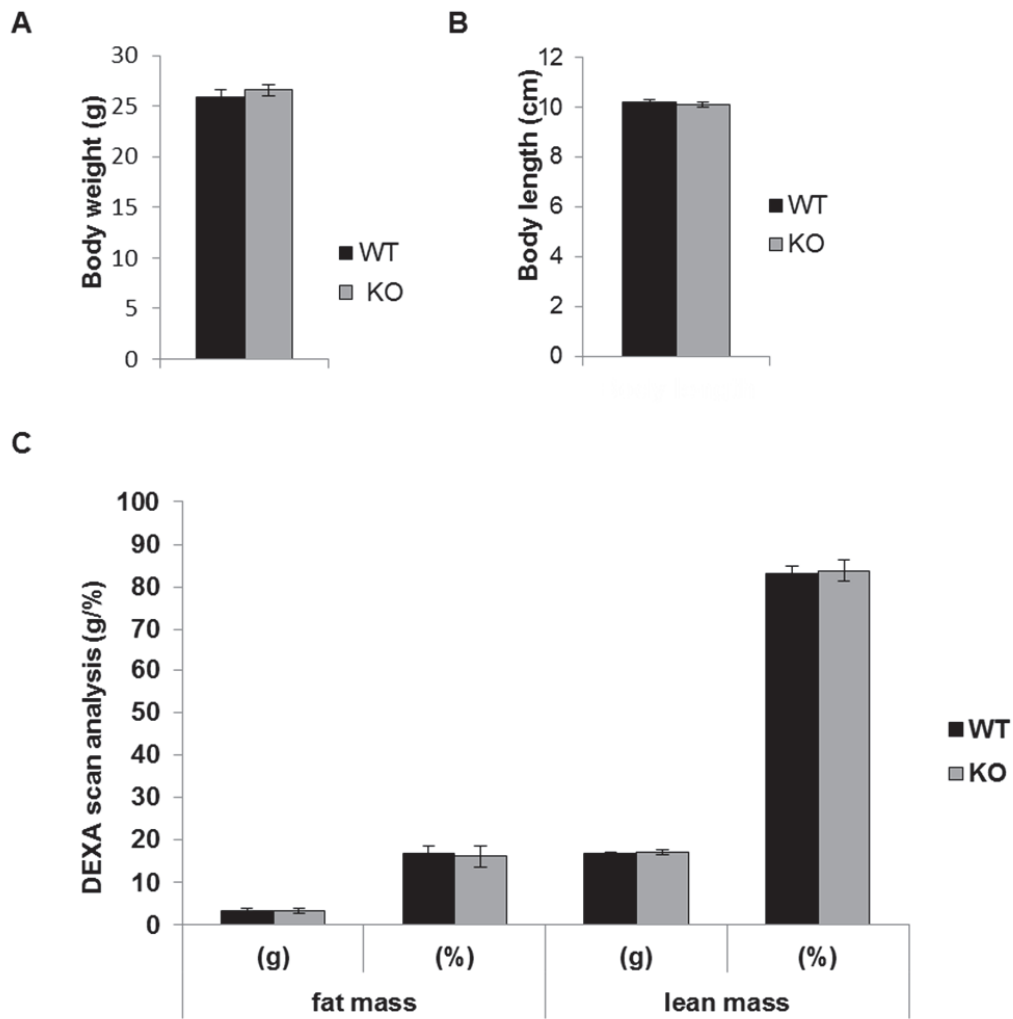


Figure 2. Body composition analysis at 12 weeks of age in *Bin1* exon 11 KO and WT littermates. (A) Body weight of KO mice did not differ from WT littermates. (B) Body length of KO and WT littermates was comparable. (C) DEXA scan analysis did not show any strong difference in the body composition when KO mice were compared to the WT. (n= minimum 7 mice per group).

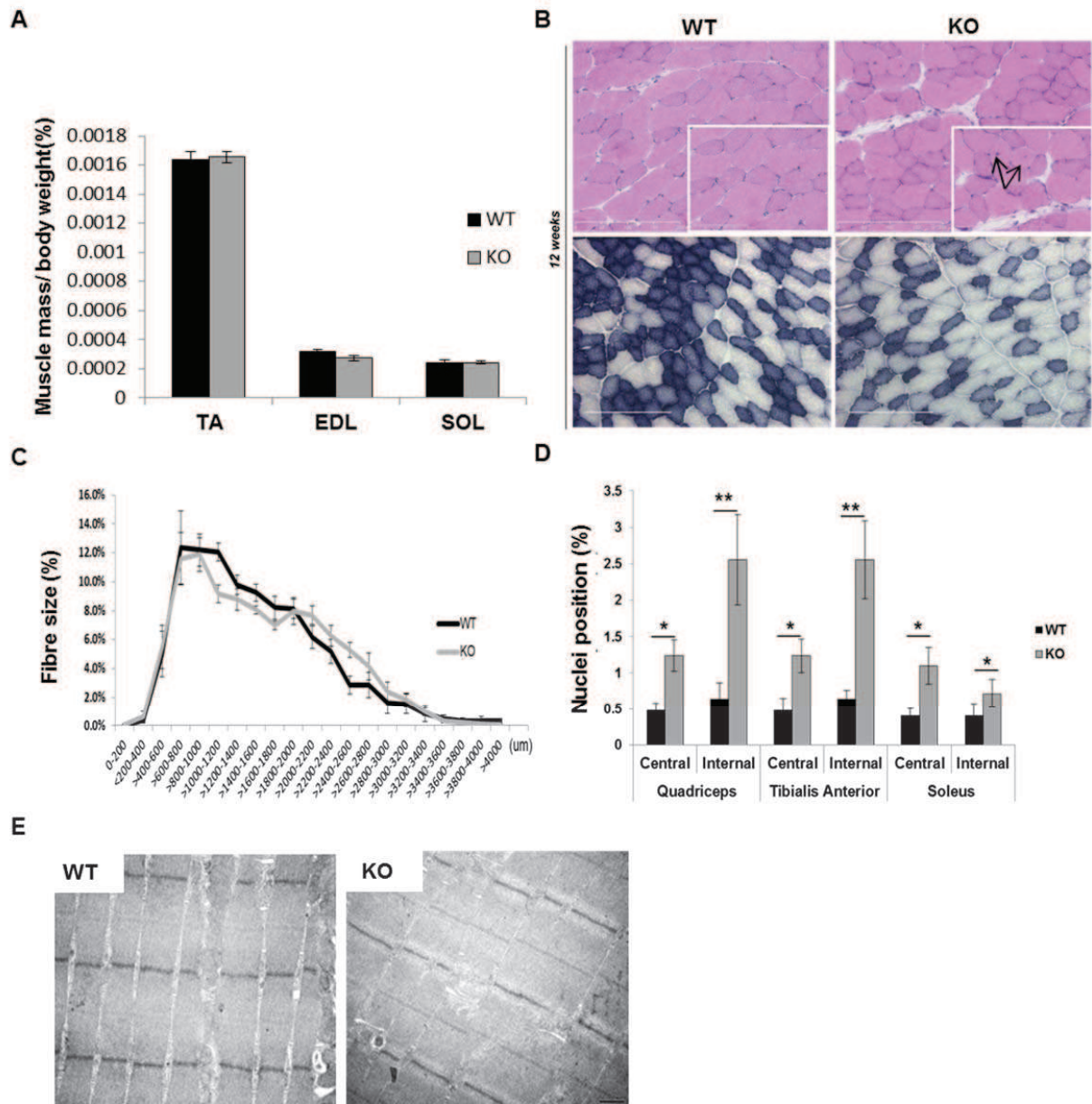


Figure 3. Characterization of the histological features in *Bin1* exon 11 KO mice at 12 weeks of age. (A) Muscle mass of the Tibialis Anterior (TA), Extensor Digitorum Longus (EDL) and Soleus (SOL) relative to body weight in the *Bin1* exon 11 KO mice compared to the WT littermates. (B) Histology of the TA muscle seen by haematoxylin and eosin (HE) (upper panel) or succinate dehydrogenase (SDH) (lower panel). Scale bar 200 μ m (100 μ m for inserted images) (C) TA muscles were analyzed for fibre area. Fibre size is grouped into 200 μ m² intervals, and represented as the percentage of total fibres in each group (n=5-7 mice). (D) The frequency of fibres with internal or central nuclei were scored (n=5 mice). Internal nuclei are defined as not subsarcolemmal nor central. All graphs depict mean \pm s.e.m. (*p<0.05, **p<0.01, ***p<0.001). (E) TA ultrastructure of WT and KO mice was analyzed by transmission electron microscopy (TEM) (n=5 mice). Scale bar 1 μ m.

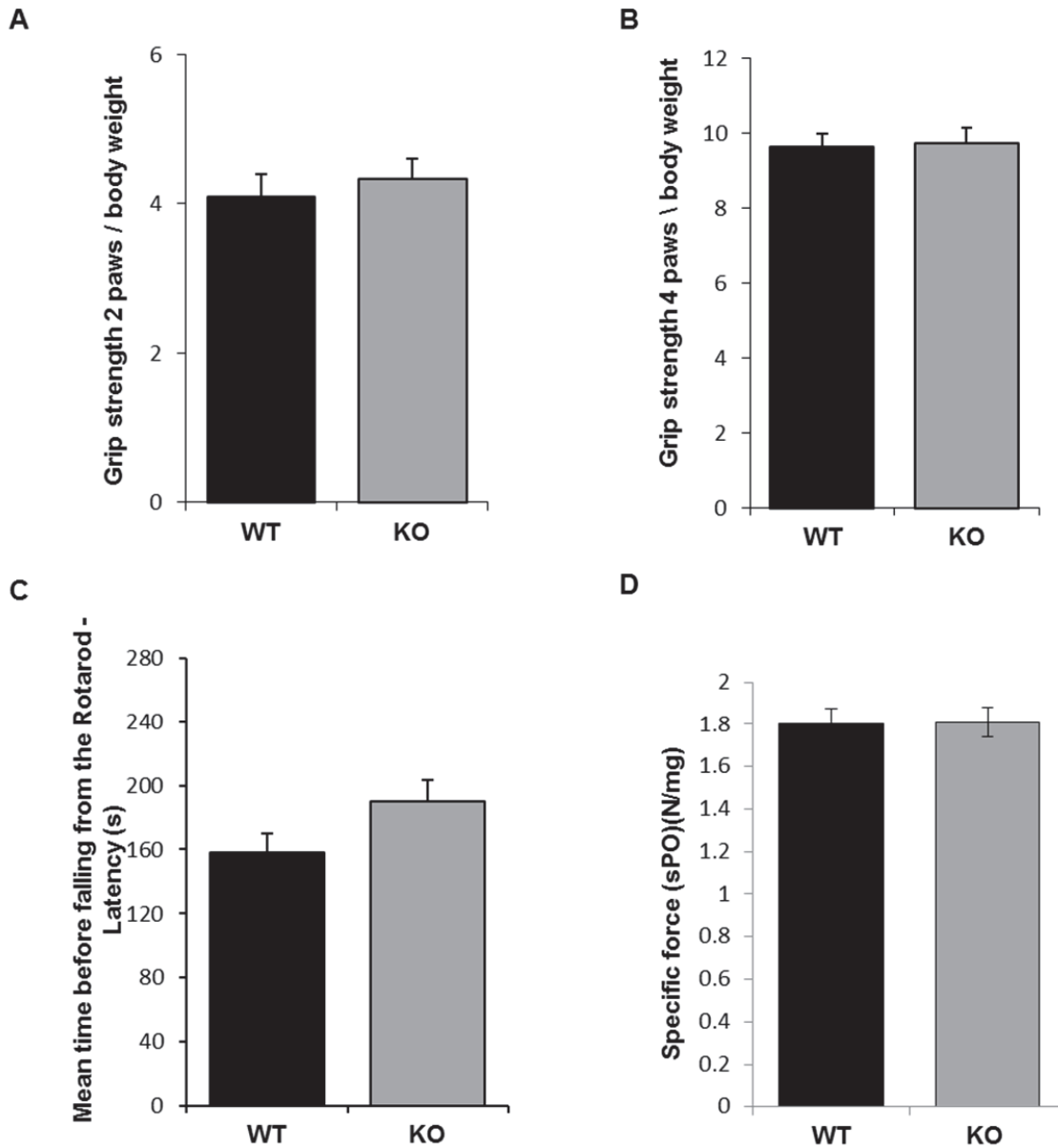


Figure 4. Muscle function analysis at 12 weeks of age. (A) The Grip test was performed using 2 (A) or 4 (B) paws and shows no difference when measured by Grip strength. (B) Further motor evaluation was done by Rotarod and the time when the mouse fell was noted. Results were comparable between the two groups of mice. (D) The specific maximal force of the TA muscle represents the absolute maximal force related to muscle weight and was not altered in KO mice. All graphs depict mean \pm s.e.m. (* $p < 0.05$, ** $p < 0.01$, *** $p < 0.001$) (n=minimum 6 mice per group).

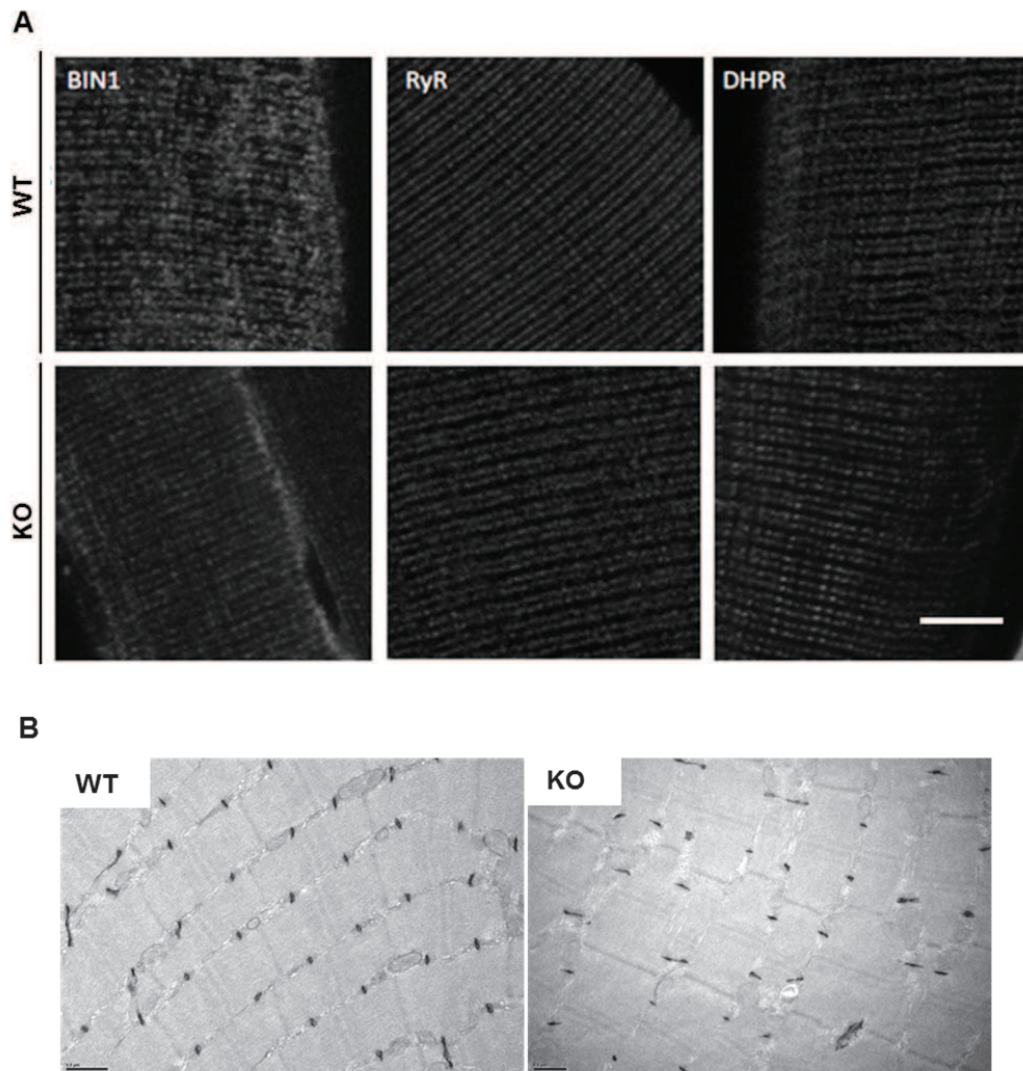


Figure 5. Localization of triads in TA muscle from 12 week old mice. (A) Isolated fibres were stained with BIN1, RyR1 (SR), or DHPR (T-tubules) antibodies and imaged by confocal microscopy. Scale bar 10 μm (B) Electron micrographs of WT and KO muscle labeled with the potassium ferrocyanide $[\text{K}_3\text{Fe}(\text{CN})_6]$ technique. Electron dense material is located within the lumen of T-tubules. Scale bar 0.5 μm .

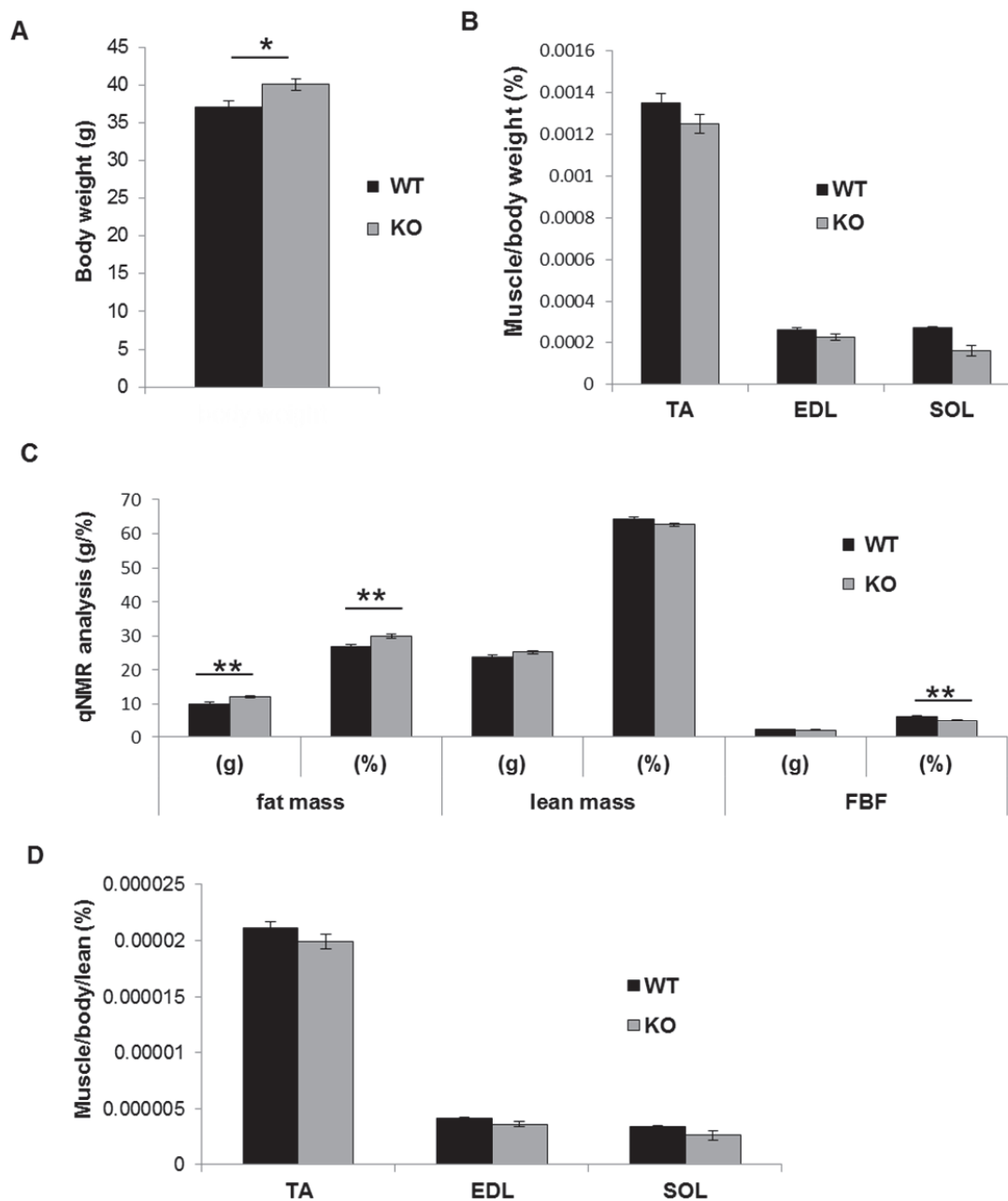


Figure 6. Body composition analysis at 12 month of age in *Bin1* exon 11 KO and WT littermates. (A) Body weight of the 12 month old KO mice shows slight increase compared to the WT littermates. (B) The increase in muscle weight does not come from an increase in muscle mass, which is comparable between the KO and the WT littermates relative to body weight. (C) qNMR analysis confirmed that in the KO mice lean mass is similar, but fat and normalized free body fluid (FBF) values are slightly increased in the KO mice. (D) Normalization of the individual muscles compared to the lean tissue. All graphs depict mean \pm s.e.m (* $p < 0.05$, ** $p < 0.01$, *** $p < 0.001$) ($n =$ minimum 7 mice per group).

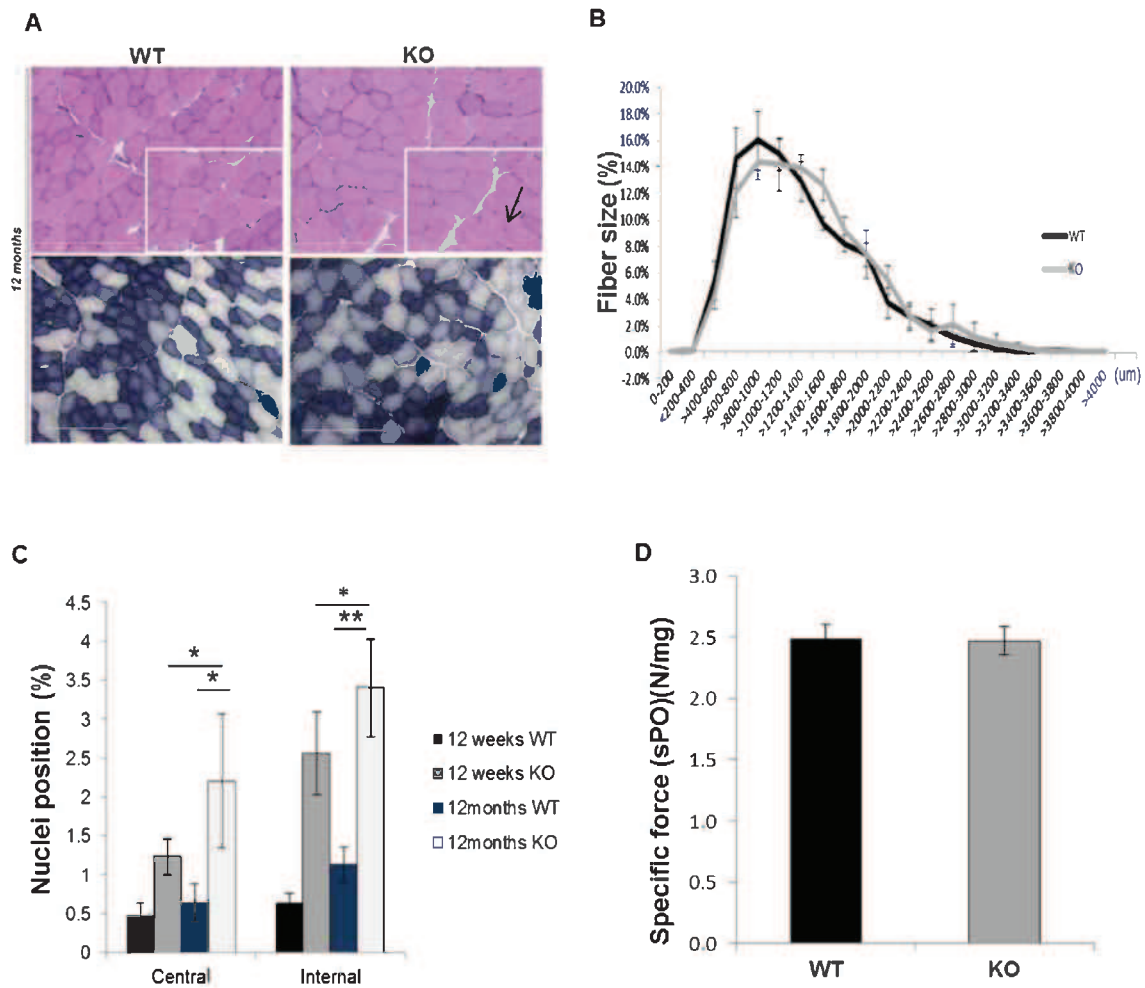


Figure 7. Characterization of the histological features in TA of *Bin1* exon 11 KO mice at 12 month of age. (A) Histology of the muscle seen by haematoxylin and eosin (HE) (upper panel) or succinate dehydrogenase (SDH) (lower panel). Scale bar 200 μm (100 μm for inserted images). (B) TA muscles were analyzed for fibre area. Fibre size is grouped into 200 μm^2 intervals, and represented as the percentage of total fibres in each group (n=5-7 mice). (C) The frequency of fibres with internal or central nuclei were scored (n=5 mice). Internal nuclei are defined as not subsarcolemmal nor central (D) The specific maximal force of the TA muscle represents the absolute maximal force related to muscle weight and was not altered in BIN1 exon 11 KO mice. All graphs depict mean \pm s.e.m. (* $p < 0.05$, ** $p < 0.01$, *** $p < 0.001$).

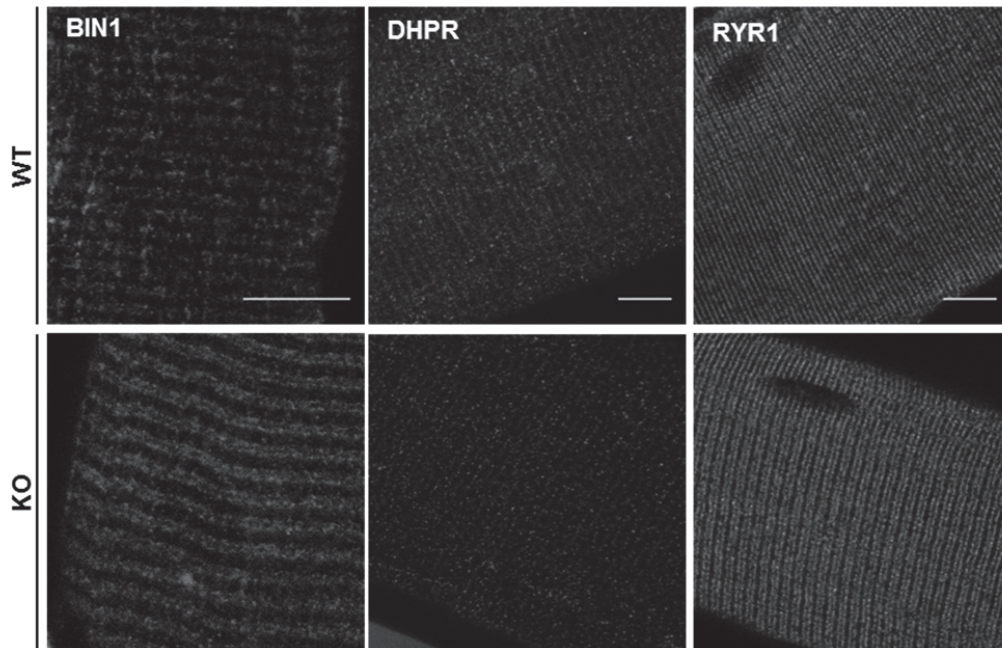


Figure 8. Localization of triad markers in EDL muscle from aged mice (10 month old). (A) Isolated fibres were stained with BIN1, DHPR or RYR1 antibodies and imaged by confocal microscopy. Labeling in *Bin1* exon 11 KO mice is comparable to WT. Scale bar 10 μ m.

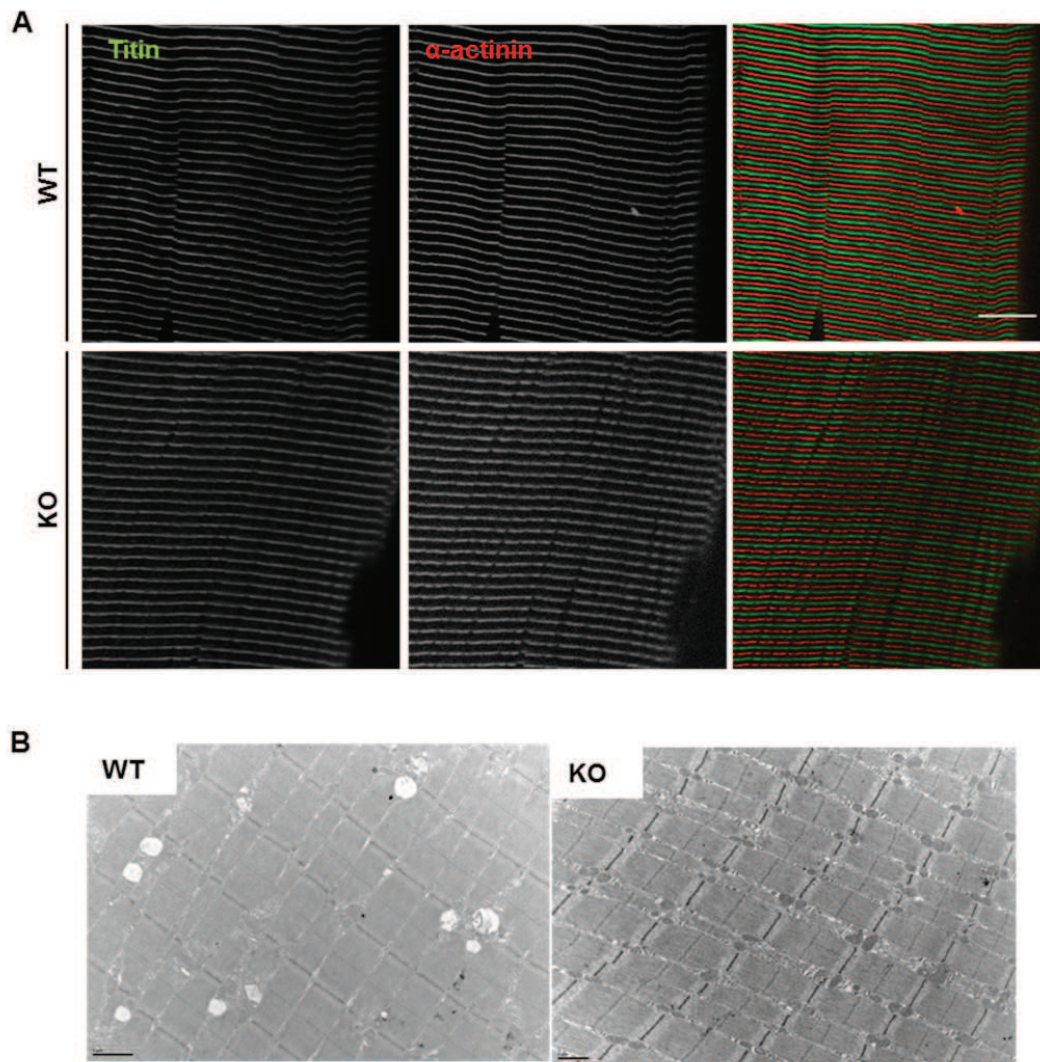


Figure 9. Sarcomere organization in aged KO and WT mice. (A) Isolated fibres of EDL from 10 month old mice were stained with titin (red) and α -actinin (green) antibodies and imaged by confocal microscopy. Scale bar 50 μm . (B) Sarcomere organization seen by transmission electron microscopy (TEM). Scale bar 1 μm .

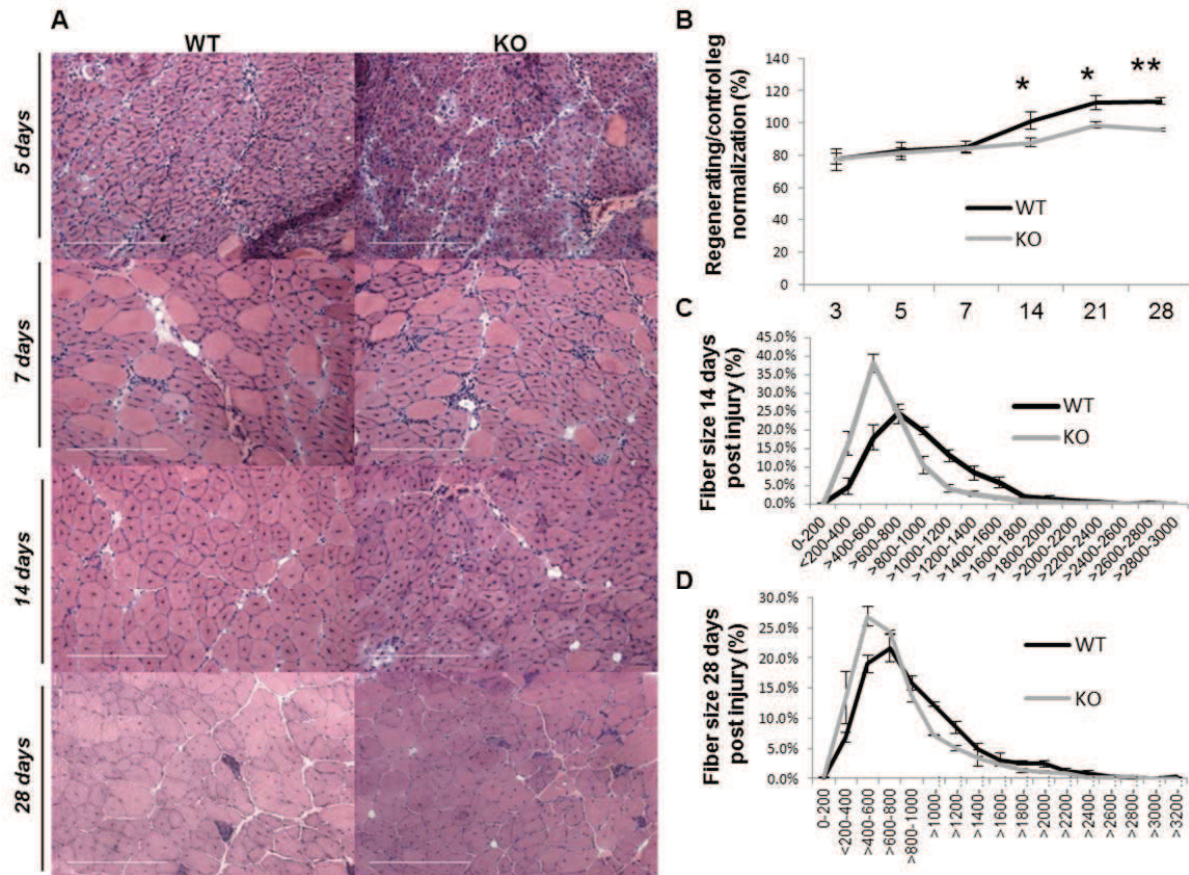


Figure 10. Regeneration test induced by notexin injection on TA of 12 weeks old *Bin1* exon 11 KO mice. (A) Histology of the muscle seen by haematoxylin and eosin (HE) observed at 3, 5, 7, 14 and 28 days after the notexin injection. Scale bar 200 μm . (B) Regenerative capacity, estimated through normalization of the injected leg to uninjected contralateral leg at different time points and represented as the percentage of recovery. (C) and (D) TA muscles were analyzed for fibre area, 14 days after notexin injection (C) and 28 days after the injury (D). Only fibres with centralized nuclei were taken into account and fibre size is grouped into 200 μm^2 intervals, and represented as the percentage of total fibres in each group ($n=5-7$ mice). All graphs depict mean \pm s.e.m. (* $p<0.05$, ** $p<0.01$, *** $p<0.001$).

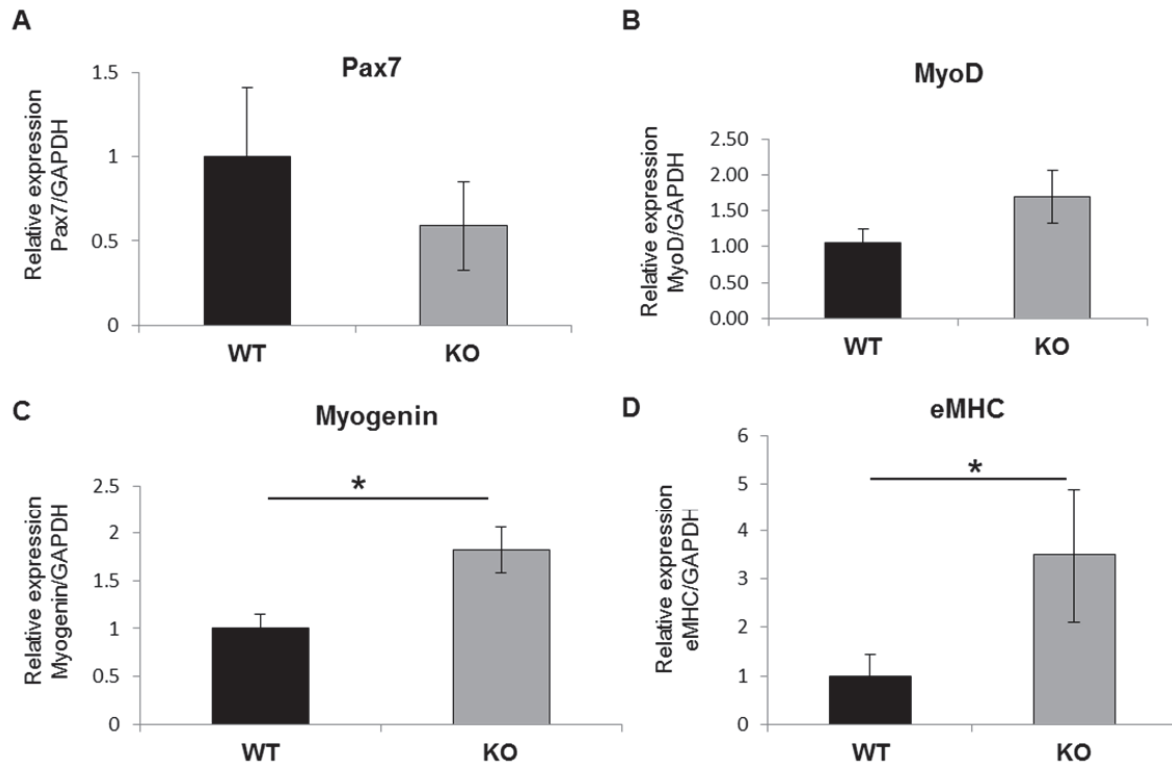


Figure 11. Regeneration markers checked by RT-qPCR at 14 days after the induced injury. No difference in the relative expression of satellite cells markers of the total satellite cell population (A) and of the activated satellite cells (B). (C) A relative myogenin and (D) eMHC expression (markers of newly regenerated fibers) show a slight but significant increase in muscle from BIN1 exon 11 KO compared to WT littermates. All graphs depict mean \pm s.e.m. (* $p < 0.05$, ** $p < 0.01$, *** $p < 0.001$). (n=3-4 mice per group).

Results IV: Altered splicing of the BIN1 muscle-specific exon in humans and dogs with a highly progressive centronuclear myopathy

IV.1. Introduction

A large cohort of patients who were clinically diagnosed with CNM still have no identified mutations. In addition our lab has the DNA of dogs, diagnosed with Inherited Great Dane myopathy, which was known myopathy present in the population of these dogs, but has no identified cause. All the CNM cases are primarily sequenced for MTM1, DNM2 and BIN1 and only if mutation is not found further approach involve widening the list in search for the new genes implicated. The candidate mutation identification is followed by extensive characterization of its impact.

IV.2. Aim

The aim of this study was to identify new mutations in CNM patients and dogs, and to characterize their impact. Additionally, we aimed to find a mammalian model for CNM other than X-linked form; and test if muscle specific exon is impaired in CNM forms as only ubiquitous exons were previously found mutated.

IV.3. Results

This work identified two novel BIN1 exon 11 splice site mutations, one in the human patients and the other in dogs clinically diagnosed with CNM. Both mutations altered the splicing of muscle specific exon 11, causing its missplicing. In human patients exon 11 coding for the PI motif was strongly reduced, but there was no impact on the total BIN1 protein level. In the affected dogs, there was a complete absence of BIN1 protein. Both patients and dogs showed late onset but rapid progression of the myopathy, untypical for the congenital myopathies. Interestingly, both human and canine histopathologies were comparable.

IV.4. Conclusion and contribution to the study

This study describes two novel splice site mutations in exon 11 of BIN1. The main common observations include general muscle weakness, muscle atrophy and

nuclei centralization, but the progression of the disease was very rapid compared to the other BIN1 ARCNM patients exon 11 missplicing was also proven to contribute to the muscle pathology in myotonic dystrophy patients (Fugier, Klein et al. 2011). Taken together this work shows the importance of exon 11 for healthy muscle functioning. I was involved in immunofluorescence characterization of biopsies.

Altered Splicing of the BIN1 Muscle-Specific Exon in Humans and Dogs with Highly Progressive Centronuclear Myopathy

Johann Böhm^{1,2,3,4,5}, Nasim Vasli^{1,2,3,4,5}, Marie Maurer^{6,7}, Belinda Cowling^{1,2,3,4,5}, G. Diane Shelton⁸, Wolfram Kress⁹, Anne Toussaint^{1,2,3,4,5}, Ivana Prokic^{1,2,3,4,5}, Ulrike Schara¹⁰, Thomas James Anderson¹¹, Joachim Weis¹², Laurent Tiret^{6,7}, Jocelyn Laporte^{1,2,3,4,5*}

1 IGBMC (Institut de Génétique et de Biologie Moléculaire et Cellulaire), Illkirch, France, **2** Inserm, U964, Illkirch, France, **3** CNRS, UMR7104, Illkirch, France, **4** Université de Strasbourg, Illkirch, France, **5** Collège de France, Chaire de Génétique Humaine, Illkirch, France, **6** Université Paris-Est Créteil, CNM project, Ecole Nationale Vétérinaire d'Alfort, Maisons-Alfort, France, **7** INRA, UMR955 de Génétique Fonctionnelle et Médicale, Maisons-Alfort, France, **8** Department of Pathology, University of California at San Diego, La Jolla, California, United States of America, **9** Department of Human Genetics, Julius-Maximilian University, Würzburg, Germany, **10** Department of Neuropediatrics, University of Essen, Essen, Germany, **11** Institute of Comparative Medicine, Division of Companion Animal Sciences, University of Glasgow Veterinary School, Glasgow, United Kingdom, **12** Institute of Neuropathology and JARA Brain Translational Medicine, RWTH Aachen University, Aachen, Germany

Abstract

Amphiphysin 2, encoded by *BIN1*, is a key factor for membrane sensing and remodelling in different cell types. Homozygous *BIN1* mutations in ubiquitously expressed exons are associated with autosomal recessive centronuclear myopathy (CNM), a mildly progressive muscle disorder typically showing abnormal nuclear centralization on biopsies. In addition, misregulation of *BIN1* splicing partially accounts for the muscle defects in myotonic dystrophy (DM). However, the muscle-specific function of amphiphysin 2 and its pathogenicity in both muscle disorders are not well understood. In this study we identified and characterized the first mutation affecting the splicing of the muscle-specific *BIN1* exon 11 in a consanguineous family with rapidly progressive and ultimately fatal centronuclear myopathy. In parallel, we discovered a mutation in the same *BIN1* exon 11 acceptor splice site as the genetic cause of the canine Inherited Myopathy of Great Danes (IMGD). Analysis of RNA from patient muscle demonstrated complete skipping of exon 11 and *BIN1* constructs without exon 11 were unable to promote membrane tubulation in differentiated myotubes. Comparative immunofluorescence and ultrastructural analyses of patient and canine biopsies revealed common structural defects, emphasizing the importance of amphiphysin 2 in membrane remodelling and maintenance of the skeletal muscle triad. Our data demonstrate that the alteration of the muscle-specific function of amphiphysin 2 is a common pathomechanism for centronuclear myopathy, myotonic dystrophy, and IMGD. The IMGD dog is the first faithful model for human *BIN1*-related CNM and represents a mammalian model available for preclinical trials of potential therapies.

Citation: Böhm J, Vasli N, Maurer M, Cowling B, Shelton GD, et al. (2013) Altered Splicing of the BIN1 Muscle-Specific Exon in Humans and Dogs with Highly Progressive Centronuclear Myopathy. *PLoS Genet* 9(6): e1003430. doi:10.1371/journal.pgen.1003430

Editor: Gregory A. Cox, The Jackson Laboratory, United States of America

Received: September 20, 2012; **Accepted:** February 18, 2013; **Published:** June 6, 2013

Copyright: © 2013 Böhm et al. This is an open-access article distributed under the terms of the Creative Commons Attribution License, which permits unrestricted use, distribution, and reproduction in any medium, provided the original author and source are credited.

Funding: This study was supported by INSERM, CNRS, University of Strasbourg, and Collège de France and by grants from Association Française contre les Myopathies (AFM), Muscular Dystrophy Association (MDA), the Myotubular Trust, Fondation Recherche Médicale (FRM), the E-rare program, Agence Nationale de la Recherche (ANR Centronucleus and CM-WES), and the CNM Project (www.laboratorcnm.com). BC was supported by FRM; JL was supported by a Contrat Hospitalier de Recherche Translationnelle from Assistance Publique - Hôpitaux de Paris. The funders had no role in study design, data collection and analysis, decision to publish, or preparation of the manuscript.

Competing Interests: The authors have declared that no competing interests exist.

* E-mail: jocelyn@igbmc.fr

Introduction

Amphiphysin 2 is one of the key factors in muscular membrane remodeling. The gene, *BIN1*, has recently been associated with two different muscle disorders: centronuclear myopathy (CNM, MIM #255200) [1] and myotonic dystrophy (DM, MIM #160900 and #602668) [2]. However, the muscle-specific role of the ubiquitous protein amphiphysin 2 and the pathological mechanisms underlying the muscle disorders are not well understood. This is mainly due to the lack of faithful animal models.

Centronuclear myopathies are characterized by a generalized muscle weakness, atrophy, predominance of type I fibers, and aberrant positioning of nuclei and mitochondria [3]. The different genetic forms are not or are only moderately progressive. The X-

linked and dominant CNM forms result from mutations in the phosphoinositide phosphatase myotubularin (*MTM1*) and the large GTPase dynamin 2 (*DNM2*), respectively [4,5]. The autosomal recessive form (ARCNM) is caused by mutations in *BIN1*, probably involving a partial loss-of-function as the protein level was found to be normal in previously described patients [1]. Amphiphysin 2, encoded by *BIN1*, contains a N-terminal amphipathic helix, a BAR (Bin/Amphiphysin/Rvs) domain, able to sense and maintain membrane curvature, a Myc-binding domain and a SH3 domain, both implicated in protein-protein interactions [6,7,8]. There are at least 12 different isoforms, mainly differing by the presence or absence of a phosphoinositide-binding domain and a clathrin-binding domain encoded by exon 11 and exons 13–16, respectively [9,10]. The clathrin-binding

Author Summary

The intracellular organization of muscle fibers relies on a complex membrane system important for muscle structural organization, maintenance, contraction, and resistance to stress. Amphiphysin 2, encoded by *BIN1*, plays a central role in membrane sensing and remodelling and is involved in intracellular membrane trafficking in different cell types. The ubiquitously expressed *BIN1*, altered in centronuclear myopathy (CNM) and myotonic dystrophy (DM), possesses a muscle-specific exon coding for a phosphoinositide binding domain. We identified splice mutations affecting the muscle-specific *BIN1* isoform in humans and dogs presenting a clinically and histopathologically comparable highly progressive centronuclear myopathy. Our functional and ultrastructural data emphasize the importance of amphiphysin 2 in membrane remodeling and suggest that the defective maintenance of the triad structure is a primary cause for the muscle weakness. The canine Inherited Myopathy of Great Danes is the first faithful mammalian model for investigating other potential pathological mechanisms underlying centronuclear myopathy and for testing therapeutic approaches.

domain is present in the brain isoforms, while the phosphoinositide-binding (PI) domain is found almost exclusively in skeletal muscle isoforms [10,11,12]. Sequencing of cDNA demonstrated that all *BIN1* skeletal muscle isoforms contain exon 11 [12]. All ARCNM mutations described to date are in ubiquitously expressed exons [1,13,14,15], raising the question about the molecular basis of the muscle-specificity of the disease. The BAR domain mutations strongly decreased the amphiphysin 2 membrane tubulating properties when expressed in cultured cells, while SH3 truncating mutations were shown to impair the binding and recruitment of dynamin 2 [1].

Mis-splicing of the *BIN1* muscle-specific exon 11 was reported in different forms of myotonic dystrophy (DM) [2]. DM is one of the most common muscular dystrophies in neonates and adults, and results from the expression of mutant RNAs with expanded CUG or CCUG repeats leading to the sequestration of splicing factors and subsequent defects in RNA splicing. Splicing alterations of the muscle chloride channel *CLCN1* are suggested to be responsible for the myotonia, whereas aberrant splicing of the insulin receptor *INSR* gene is thought to cause insulin resistance in DM patients. Complete or partial skipping of *BIN1* exon 11 in congenital and adult DM was shown to involve structural T-tubule abnormalities and subsequently muscle weakness [2]. However, there are numerous splicing defects in DM. It is therefore challenging to assess the exact contribution of *BIN1* exon 11 skipping to the DM phenotype, even though severe hypotonia, respiratory failure and histopathological features such as fiber hypotrophy and centrally located nuclei in the congenital forms of DM show intriguing similarities to CNM.

Amphiphysins are key regulators of membrane curvature and trafficking [16]. They can sense membrane curvature and presumably promote the curvature and fission of membranes [17]. Membrane binding occurs via BAR domain dimers, presenting a positively charged concave site that interacts with the negative membrane charges [17]. Amphiphysins also bind and recruit other regulators of endocytosis to sites of plasma membrane inward budding [18]. Amphiphysin 1 expression is restricted to neuronal tissues and the protein regulates synaptic vesicle recycling in the brain [19]. Amphiphysin 2 is highly expressed in adult striated muscle and its expression increases during muscle cell

maturation [10,11,20,21]. The polybasic residues encoded by *BIN1* exon 11 are required for amphiphysin 2-induced membrane tubulation when exogenously expressed in cultured cells [1,22]. In skeletal muscle, amphiphysin 2 is localized at the T-tubules, which are deep sarcolemmal invaginations enabling excitation-contraction coupling [11], i.e. the process converting an electrical stimulus into mechanical muscle work. This specific localization, together with the membrane tubulation properties of the muscle-specific isoform containing the PI domain, called iso8 or M-amphiphysin, has led to the suggestion that amphiphysin 2 is implicated in T-tubule biogenesis [22]. This is sustained by defects in the localization of nascent T-tubule markers such as caveolin 3 following *BIN1* downregulation in cultured cells [23], and by the abnormal T-tubule structure seen in drosophila with null mutations in *amph*, the unique ortholog of mammalian amphiphysins 1 and 2 [24]. While faithful animal models were previously characterized for the *MTM1* and *DNM2* related CNM forms [25], the perinatal lethality of *Bin1*-null mice precludes the analysis of the role of amphiphysin 2 in skeletal muscle [26]. Therefore, critical questions concerning the muscle-specific function of amphiphysin 2 in mammals and the pathological mechanism of *BIN1*-related CNM remain unanswered. The lack of a faithful animal model for autosomal recessive centronuclear myopathy is a hurdle for a better comprehension of the pathological mechanisms and for the development of therapeutic approaches.

In this study, we identified and characterized the first human *BIN1* mutation affecting the muscle-specific PI domain. We also identified a novel spontaneous canine model reproducing the human pathology and allowing investigations on the physiological role of amphiphysin 2 in skeletal muscle after birth. Characterization of the dog model revealed an important role for amphiphysin 2 in triad structure, and we provide the evidence for a physiological function of the membrane-deforming properties of amphiphysin 2 and its alternative splicing-dependent activity. Our data support the hypothesis that the alteration of the muscle-specific function of amphiphysin 2 on membrane remodeling is a common pathomechanism underlying several canine and human myopathies.

Results

BIN1 exon 11 splice mutation in patients with rapidly progressive centronuclear myopathy

To identify *BIN1* mutations affecting its function in skeletal muscle, we sequenced the muscle-specific exon 11 and the adjacent splice-relevant intronic regions in a cohort of 84 patients with various forms of centronuclear myopathy and without mutations in *MTM1*, *DNM2*, or in the other *BIN1* exons. We identified a homozygous *BIN1* exon 11 splice acceptor mutation (IVS10-1G>A) in two affected members from a consanguineous family from Turkey (Figure 1A and 1B). DNA was not available for the third affected member, who is expected to carry the same homozygous *BIN1* mutation as her monozygotic twin sister. The parents are healthy and do not present clinical signs of a muscle disorder. They are first-degree cousins and were found to be heterozygous for the *BIN1* exon 11 splice acceptor mutation, confirming autosomal recessive inheritance of the disease. The mutation was not found in unaffected individuals from different origins, including 37 DNAs from an ethnically matched control population, and is not listed in the SNP databases as dbSNP, 1000 genomes, or the NHLBI exome variant server.

Patients 1 and 2 are dizygotic twins. Pregnancy and birth, as well as motor and speech development were normal. General muscle weakness was diagnosed at 3.5 years. Hypotonia, muscle weakness (predominantly of the lower limbs), respiratory distress

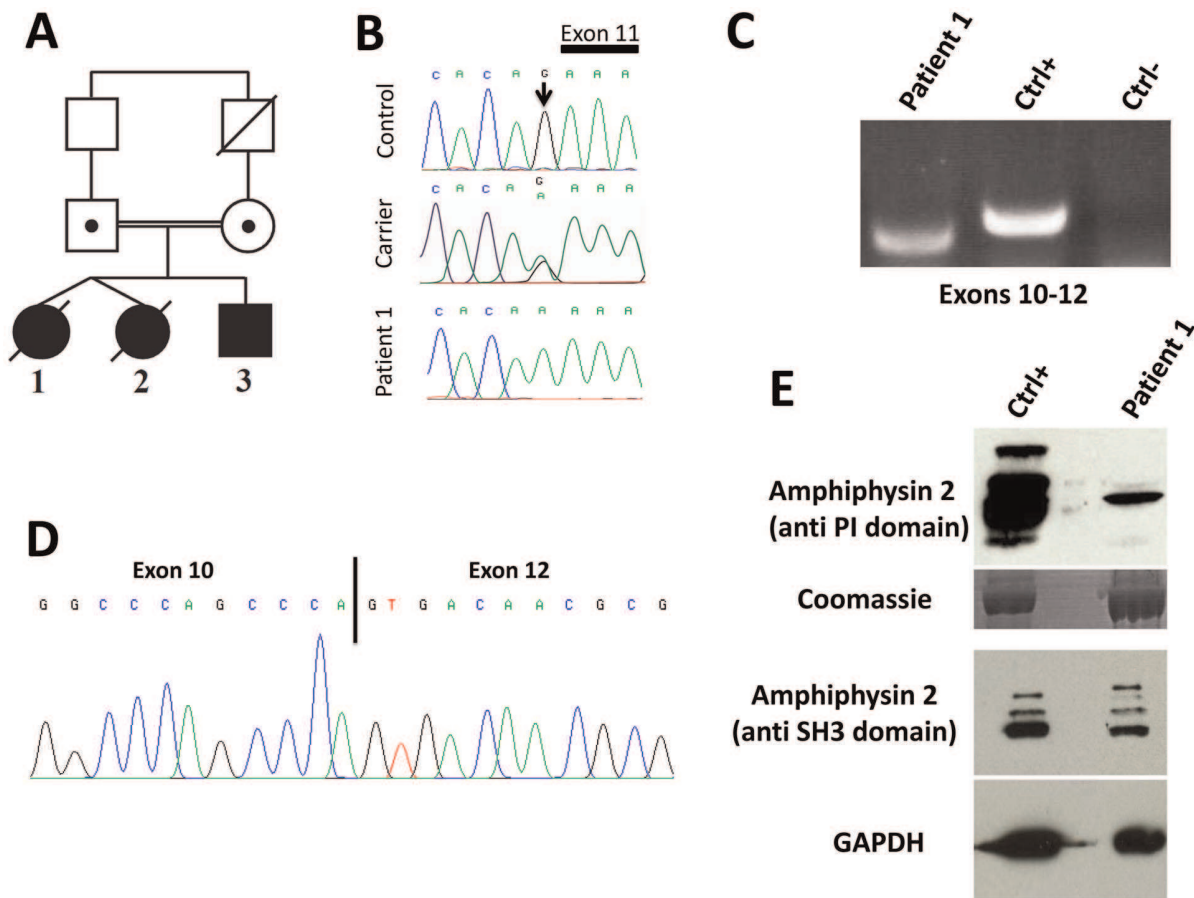


Figure 1. Human *BIN1* mutation of the exon 11 acceptor splice site and impact on splicing. (A) Pedigree and (B) Chromatophogram. Patients 1 and 3 are homozygous for the IVS10-1G>A mutation, while both parents are heterozygous carriers. DNA from patient 2 was not available. (C) RT-PCR on mRNA isolated from muscle using primers encompassing *BIN1* exons 10–12 demonstrated amplification of a shorter product in patient 1 compared to a healthy control. For the negative control (Ctrl-) PCR was performed without cDNA. (D) Sequencing of the *BIN1* cDNA from muscle demonstrated skipping of *BIN1* exon 11 in patient 1. (E) Western blot analysis of patient muscle extracts detected a strong reduction of the amphiphysin 2 isoforms containing the exon 11 encoded PI-binding domain. The level of amphiphysin 2 detected with an anti-SH3 antibody was comparable between patient 1 and control.
doi:10.1371/journal.pgen.1003430.g001

(VC 50%) and loss of motor skills were rapidly progressive and the twins died from acute pneumonia involving cardiac failure at age 5 and 7, respectively. Patient 3 is the younger brother, and as for his sisters, pregnancy, birth, motor and speech development were normal. Age of onset was 3.5 years and the myopathy was highly progressive, contrasting the slow progression of muscle weakness in the reported CNM cases with *BIN1* mutations in ubiquitous exons [1,13,14,15]. Patient 3 presented with predominant proximal muscle weakness of the lower limbs requiring a wheelchair since the age of 5 years, facial weakness, but no respiratory distress. Eye movement defects, as seen in the majority of the *MTM1*, *DNM2* and *BIN1* patients, were not noted. Deep tendon reflexes were absent and the patient had progressive contractures in knees and ankles. Electrophysiological evaluation was normal or showed only unspecific myopathic changes, with normal nerve conduction velocity. Cardiac defects were not noted and CK levels were normal. Patient 3 is now 9 years old and presented at his last medical exam in April 2012 with low MRC grades for both upper and lower limbs.

Impact of the human *BIN1* mutation on splicing

The *BIN1* IVS10-1G>A variation changes the AG acceptor splice site into AA, and is predicted to impair exon 11 splicing by

various algorithms. The wild-type acceptor site was recognized by NNSPLICE (score 0.84) and Human Splice Finder (88.5), while no acceptor splice site was predicted in the mutated sequence. To confirm an impact on exon 11 splicing, we performed RT-PCR after RNA isolation from a muscle biopsy of patient 1, amplified a fragment encompassing exons 10 to 12, and obtained a shorter product compared to the control (Figure 1C). To analyze the transcript(s), we cloned the PCR-products and sequenced the resulting clones. As we and others previously reported, the skeletal muscle *BIN1* isoforms contain exon 11, but lack exons 7 and 13 to 16. Exon 17 can be either present or absent, corresponding to isoform 8 or M-amphiphysin [10,11,12]. Among the 30 analyzed clones, only a single clone contained exon 11. Twenty-nine clones did not contain exon 11 and directly combined exon 10 with exon 12, demonstrating a major skipping of the in-frame exon 11 in the patient muscle (Figure 1D). The impact of the mutation on the amphiphysin 2 protein level in skeletal muscle was investigated by Western blot (Figure 1E). Using an anti-PI domain antibody, we detected several bands in the control as previously reported [1], most probably reflecting post-translational modifications of the different isoforms containing exon 11. In the patient muscle, we found a significant decrease of the level of the amphiphysin 2

isoform containing the PI domain, confirming exon 11 skipping in most *BIN1* muscle transcripts. The amphiphysin levels detected with the anti-SH3 domain antibody were similar in patient 1 and control. Together with the genetic data, we conclude that the rapidly progressive CNM form results from a splice mutation involving the skipping of the muscle-specific exon 11.

BIN1 exon 11 is required for membrane tubulation in muscle cells

Previous publications demonstrated the importance of the amphiphysin 2 PI domain in PtdIns(4,5)P₂ binding and membrane tubulation [1,2,22]. We transfected C2C12 cells with *BIN1* constructs including or excluding exon 11, and we induced the differentiation of the murine myoblasts into myotubes. Myotubes expressing the exon 11 containing isoform showed tubulation [22,27], whereas the isoform without exon 11 did not induce this effect (Figure 2). Quantification revealed statistical significance. Immunolabelling of actin, caveolin-3 and RYR1 did not reveal obvious differences between the differentially transfected myotubes (data not shown), suggesting that the amphiphysin 2 PI domain is important for late muscle development or maintenance, rather than for early muscle development. This hypothesis is supported by the fact that the patients were unaffected at birth and during early childhood.

BIN1 exon 11 splice mutation causes the canine Inherited Myopathy of Great Danes (IMGD)

The perinatal lethality of *Bin1*-null mice precludes investigations on the role of amphiphysin 2 in skeletal muscle maintenance [26]. To identify and characterize an animal model for *BIN1*-related CNM, we analyzed canine pedigrees with molecularly unsolved myopathies. The canine Inherited Myopathy of Great Danes (IMGD) is characterized by rapidly progressive muscle atrophy and exercise intolerance with an age of onset of about 6 months. Histological examinations of muscle biopsies from autosomal recessive cases from the UK, Canada and Australia revealed increased nuclear internalization and centralization [28,29,30], consistent with centronuclear myopathy. We excluded mutations in *MTM1* [31] and *PTPLA* [32] before sequencing the coding regions and intron/exon boundaries of the canine *BIN1* gene (XM_540990.3). We identified a homozygous AG to GG substitution of the *BIN1* exon 11 acceptor splice site in five dogs from Canada, US and UK (IVS10-2A>G; Figures 3A and 3B). CK values for the dogs were normal or slightly elevated. Pedigree reconstruction revealed a distant relationship between the US and one UK dog (Figure 3C) and a previous publication reported a common ancestor for all IMGD dogs in the UK [29]. The *BIN1* IVS10-2A>G mutation was not found in 112 healthy Great Danes and in 35 dogs from 12 other breeds, strongly suggesting its pathogenicity.

Impact of the canine *BIN1* mutation on exon 11 splicing

Like the human *BIN1* IVS10-1G>A mutation, the canine *BIN1* IVS10-2A>G variation affects the exon 11 acceptor splice site. To assess its impact on splicing, we performed RT-PCR on RNA isolated from skeletal muscle biopsies and found a strong reduction of the *BIN1* RNA level compared to healthy controls and compared to a control gene (*MTM1*, Figure 3D). We however detected a faint signal of expected size and cloned the amplicon. All three clones contained exon 11 with 27 additional upstream nucleotides, encoding the amino acid sequence ASASRPFPQ (Figure 3E). This in-frame extension results from the disposition of a weak cryptic 5' acceptor site. The intronic sequence upstream of exon 11 slightly differs between human and dog, possibly

explaining the cryptic splicing in dogs versus exon skipping in human patients (Figure 3F). To confirm the impact of the splice mutation on the amphiphysin 2 protein level, canine muscle extracts were probed with an anti-PI domain antibody on Western blot. Compared to the healthy control, amphiphysin 2 was significantly reduced in the affected dog (Figure 3G). Using an anti-SH3 antibody we detected a strong reduction of all skeletal muscle amphiphysin isoforms (Figure S1) in accordance with the RT-PCR data. We conclude that the canine Inherited Myopathy of Great Danes results from a *BIN1* exon 11 splice mutation, provoking a strong reduction of the exon 11/PI domain-containing RNA and protein.

Similar histopathology in affected humans and dogs

Vastus lateralis muscle biopsies were performed for patient 1 as well as for patient 3 at the age of 3.5 years. H&E staining revealed prominent nuclear centralization (>60%, arrow), fiber atrophy and endomysial fibrosis (Figure 4), consistent with centronuclear myopathy. Similarly, H&E staining of biceps femoris muscle biopsies from affected dogs revealed nuclear internalization (>40%) and fiber atrophy. The central areas devoid of staining reflect perinuclear regions lacking myofibrils. Of note, the transverse muscle sections of patients and affected dogs showed an unusual lobulated appearance with indentations of the sarcolemma (arrowheads). NADH staining of human and canine sections revealed dense central areas in most fibers and “spoke of wheel” appearance in 5% of the fibers. ATPase staining showed no or only a slight predominance of type I muscle fibers as compared to the age matched controls. Gomori trichrome staining did not reveal any further abnormalities (data not shown). Taken together, human and canine histopathologies were comparable.

Common ultrastructural and membrane defects in affected patients and dogs

To uncover the pathological defects underlying this highly progressive form of centronuclear myopathy and to validate the canine model, we analyzed human and dog muscle biopsies by electron microscopy. Ultrastructural analysis of the human muscle biopsy revealed centralized nuclei surrounded by an area devoid of myofibrils and containing glycogen granules and other organelles (Figure 5A, Figure S2), as commonly seen in *MTM1*, *DNM2* and *BIN1*-related CNM. Myofibrillar disintegration with occasional Z-band streaming (arrow, Figure 5A) was seen in the adjacent sarcomeres. Triad structures were found to be aberrant and we observed frequent enlarged structures, most probably originating from the sarcoplasmic reticulum (arrow, Figure 5D). We also noted other membrane alterations, including accumulations of membranes and tubules, vacuoles containing whorled membranes (arrow, Figure 5B), as well as a high number of myelin-like membranous structures suggestive of autophagosomes (arrow, Figure 5C). Likewise, ultrastructural analysis of muscle biopsies from an affected Great Dane dog showed nuclear internalization, mitochondrial accumulations around the internalized nuclei and myofibrillar disarray (Figure 5E, Figure S3). We furthermore found membranous whorls (arrow, Figure 5F) as reported for the X-linked CNM Labrador retriever model with *MTM1* mutation [31], deep membrane invaginations (arrowhead, Figure 5F), lipofuscin granules (arrow, Figure 5G), and abnormal triads in almost all fibers (arrow, Figure 5H). Sarcolemmal invaginations contained basement membranes and often pointed towards centralized nuclei. Taken together and considering the histological analysis described above, histopathology of IMGD dogs and human patients appear strikingly similar, emphasizing common alterations of membrane structures.

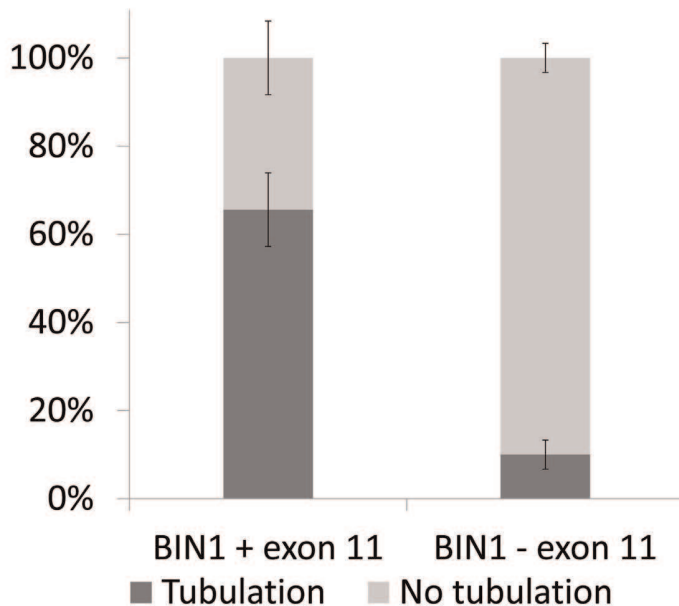
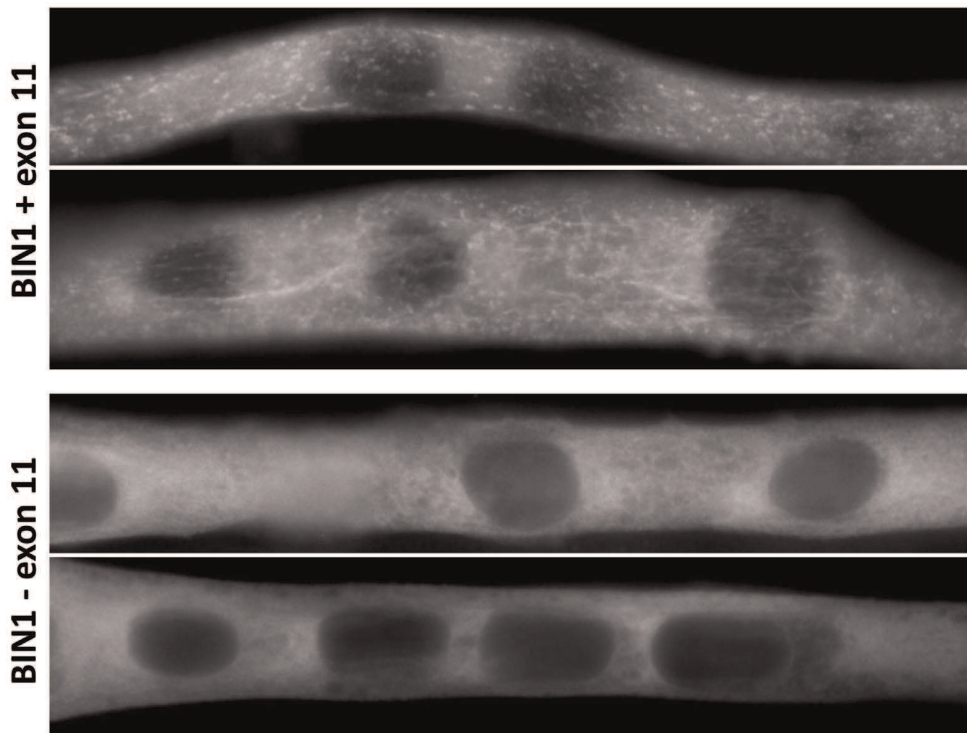


Figure 2. Essential role of *BIN1* exon 11 in membrane tubulation in myotubes. C2C12 myotubes overexpressing *BIN1* isoform 8 (including exon 11) showed strong tubulation, whereas *BIN1* isoform 9 (without exon 11) does not induce membrane tubulation 5 days post differentiation. Below: quantification of three independent experiments (>30 myotubes each) demonstrated that these findings were significant ($p < 0.01$). doi:10.1371/journal.pgen.1003430.g002

Amphiphysin 2 is present but altered in affected human and dog muscles

To further characterize the pathophysiology of the rapidly progressive human CNM and canine IMGD, we performed

immunolocalization experiments on muscle biopsies. Using the R3062 antibody recognizing most amphiphysin isoforms or the PI-domain specific R2405 antibody, signals were detected as an intracellular network in transverse sections of human and canine

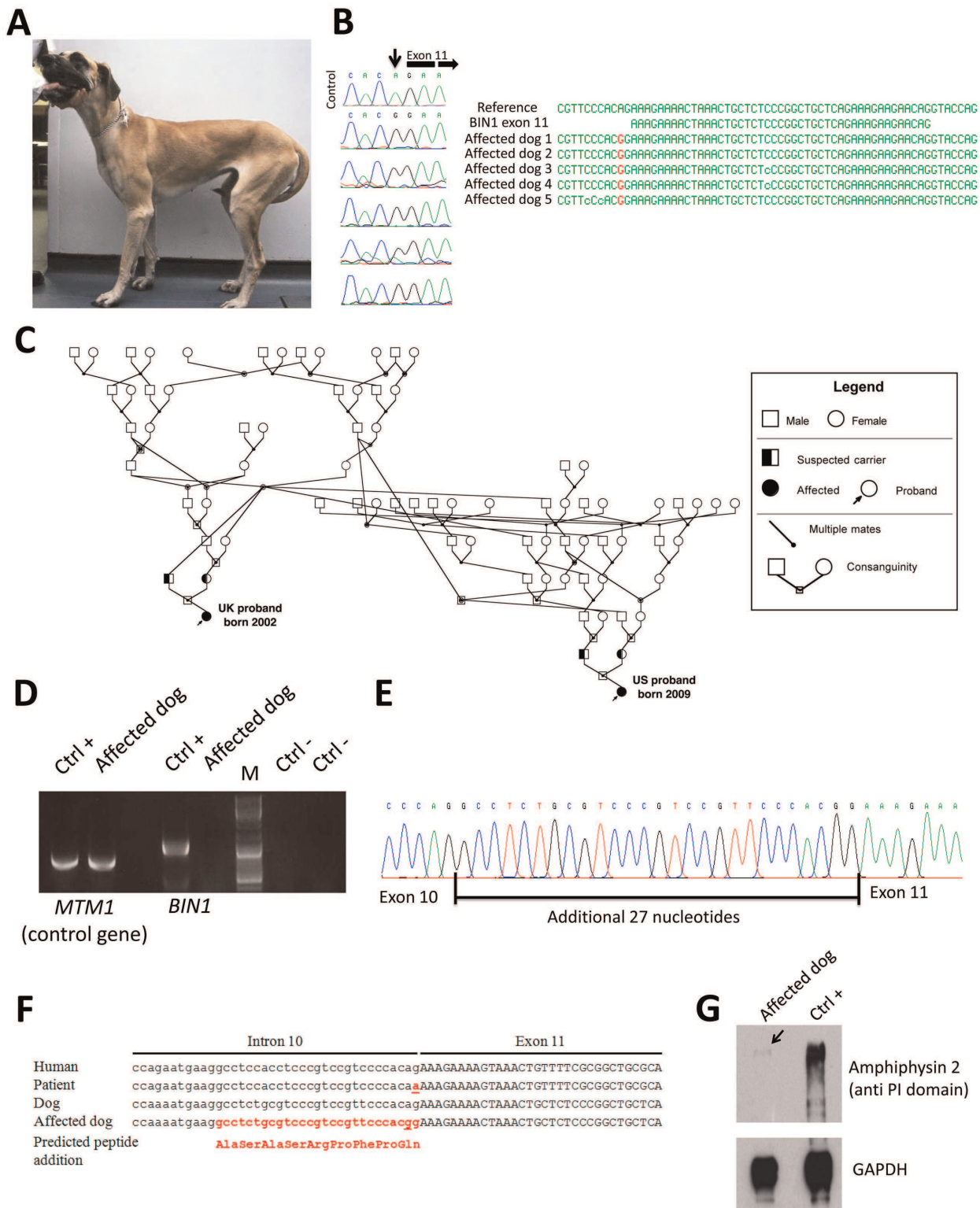


Figure 3. The canine Inherited Myopathy of Great Danes results from a *BIN1* mutation in the exon 11 acceptor splice site. (A) Picture of an affected 3-year-old Great Dane dog. (B) Chromatophorograms and sequence alignment showing the *BIN1* IVS10-2A>G mutation in 5 affected dogs. (C) Pedigree showing the distant relationship of two affected Great Dane dogs from the UK and US. (D) RT-PCR on skeletal muscle RNA showed a strong reduction of the *BIN1* RNA level in the IMGD dog compared to the healthy canine control. Amplification of a control gene (*MTM1*) was normal. M = Marker (E) Sequencing of the residual cDNA revealed the presence of 27 additional nucleotides due to the use of a weak cryptic 5' splice acceptor site. (F) Sequence alignment of human and canine *BIN1* intron/exon boundary of exon 11. (G) Western blot using an anti-PI domain antibody showed a strong decrease of the amphiphysin 2 protein level. doi:10.1371/journal.pgen.1003430.g003

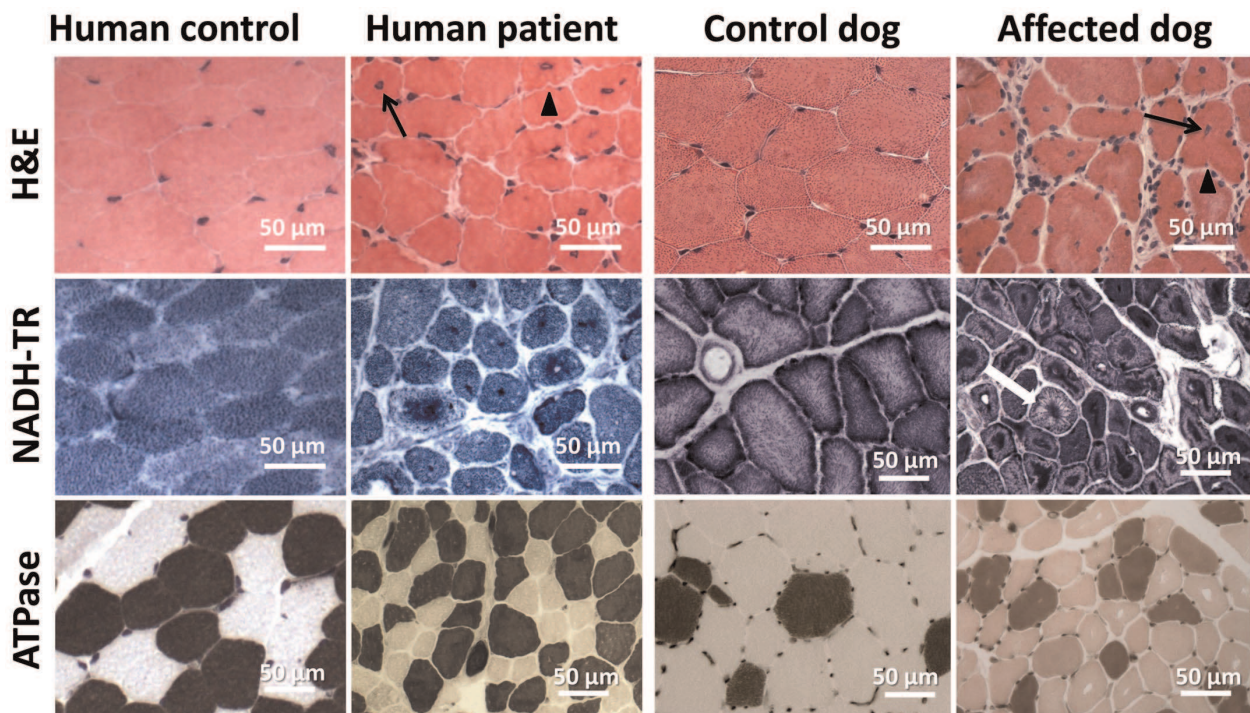


Figure 4. Histopathological comparison of muscles from human patient and IMGD dog. Human and canine muscle biopsy sections revealed nuclear centralization (arrows), fiber atrophy and lobulation as well as sarcolemmal invaginations (arrowheads) on H&E staining. NADH-TR staining demonstrated central dense areas in many fibers and “spoke of wheel” appearance in a few fibers (white arrow). ATPase staining (pH 4.3) revealed no or only a slight predominance of type I fibers compared to the age-matched controls.
doi:10.1371/journal.pgen.1003430.g004

controls (Figure 6). Signals were also detected in sections of muscles from patient and affected dog, reflecting the presence of different amphiphysin 2 isoforms as shown by Western blot. Despite the decrease of *BINI* RNA in affected dogs, the remaining mis-spliced in-frame transcripts can explain the detection of amphiphysin 2 on muscle sections, especially because immunohistochemistry is not quantitative. The amphiphysin 2 network appeared however abnormal in patient and IMGD sections. In some fibers we noted central areas without any signal, while in other fibers accumulations around centralized nuclei were observed (arrows). To determine whether these anomalies were specific for the *BINI* exon 11 splice mutation or rather a general *BINI*-related CNM feature, we analyzed a muscle biopsy from a patient with the previously reported *BINI* p.Asp151Asn mutation and a classical ARCNM phenotype [1]. We observed similar accumulations of amphiphysin 2 (Figure 6A), suggesting that different *BINI* mutations in humans and dogs lead to similar amphiphysin 2 mis-localization in muscle.

Alteration of triad and membrane trafficking regulators

Amphiphysin 2 has been proposed to be implicated in T-tubule biogenesis, but the exact link has barely been documented in mammalian skeletal muscle [22]. We therefore examined the skeletal muscle triad using antibodies against the junctional sarcoplasmic calcium channel RYR1 and the T-tubule marker DHPR in human and dog (Figure 7). Both proteins were profoundly altered, showing focal accumulations or central areas without signal in the fibers. Compared to the control longitudinal sections, the transversal orientation of RYR1-labeled triads was lost in patient and canine muscle. Similarly, the longitudinal sarcoplasmic calcium pump SERCA1 was mislocalized in sections from affected dogs.

We next wanted to know whether the aberrant triad structure was concurrent with more generalized membrane defects. Dysferlin and caveolin 3, key regulators of membrane repair and trafficking [33,34], were found to be mainly located at the sarcolemma in control muscle sections. In contrast, transverse sections of patient 1 and of an affected Great Dane dog revealed striking intracellular accumulations of dysferlin, mainly around central nuclei (Figure 7). Labeling of the sarcolemmal markers dysferlin, caveolin 3 and dystrophin confirmed the presence of numerous fibers with unusual lobulated and indented sarcolemma, representing deep sarcolemmal invaginations pointing towards the center of the fibers (arrows, Figure 7). Taken together, our data correlate the highly progressive human CNM and canine IMGD with general membrane alterations at the triad, the sarcolemma and within the fibers. However, these defects did not reflect a general disorganization of the sarcomere, as alpha-actinin labeling appeared largely normal (not shown). Staining of developmental myosin revealed no difference between affected and control dogs, indicating that there is no excessive fiber regeneration in IMGD dogs (Figure S3).

Altered myotubularin localization in BIN1-mutated canine muscles

As *MTM1* is mutated in X-linked human and canine CNM, we investigated the localization of myotubularin in muscle sections of IMGD dogs. Myotubularin formed an intracellular network in control sections and the signal was stronger in type II fibers labeled with the SERCA1 antibody (Figure 8). In both analyzed IMGD muscles, myotubularin was mainly located as concentric strands pointing to the center in both type I and type II fibers. We conclude that altered splicing of *BINI* has a strong impact on

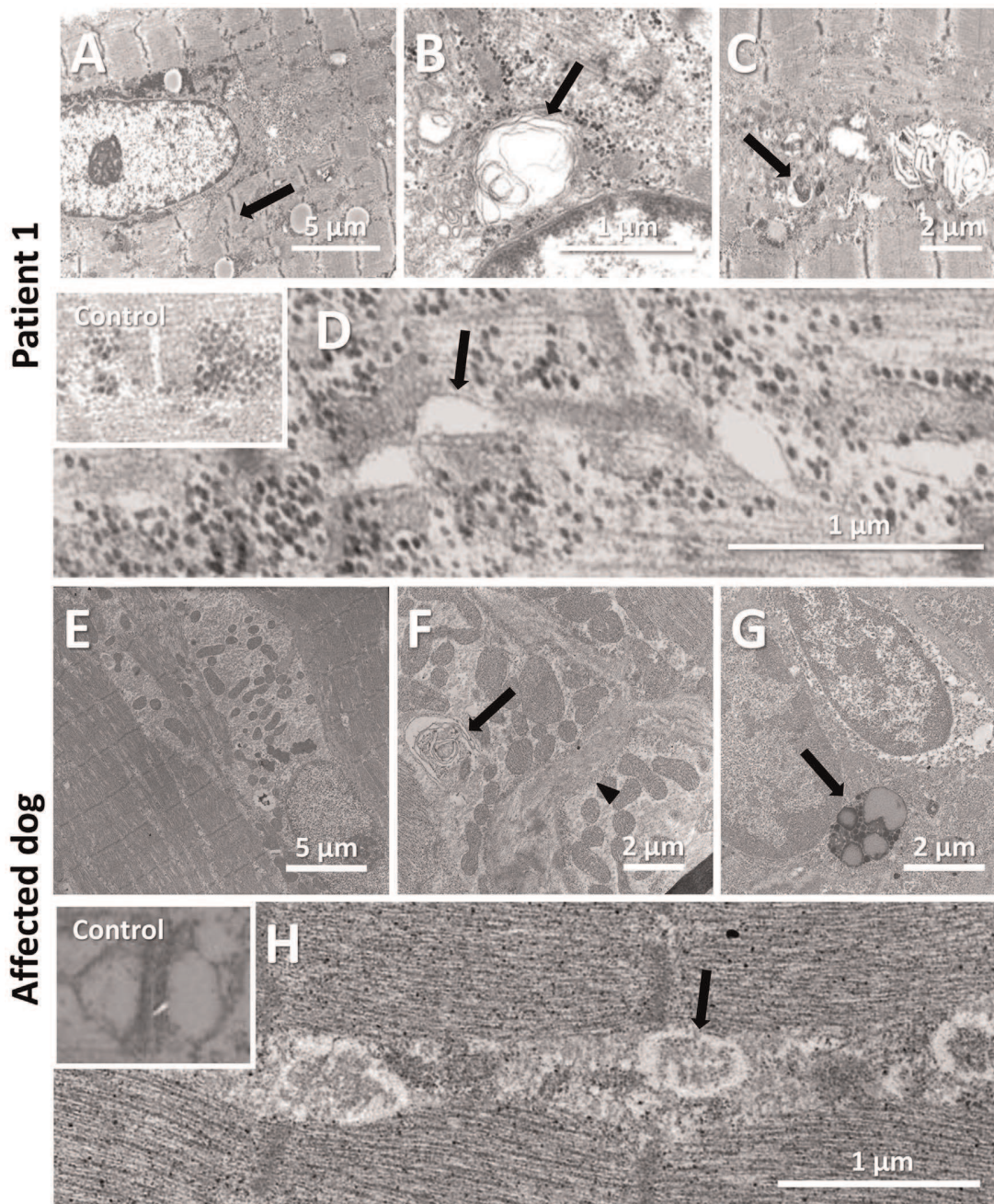


Figure 5. Common ultrastructural and membrane defects in affected human and dog. (A–D) Electron microscopic analysis of a patient biopsy showing a centralized nucleus surrounded by organelles and mild sarcomeric disarray (arrow, A), accumulations of membranes and vacuoles containing whorled membranes (arrow, B), autophagic vacuoles containing myelin-like material (arrow, C), and widened tubules at the triads (arrow, D). The inset shows normal triads in an age-matched biopsy. (E–H) Ultrastructural analysis of a IMGD dog biopsy revealed central nuclei surrounded by mitochondrial accumulations (E), membranous whorls (arrow, F), deep membrane invaginations (arrowhead, F), lipofuscin granules (arrow, G), and abnormal triads (arrow, H). The inserted picture shows a normal triad in an age-matched canine control. doi:10.1371/journal.pgen.1003430.g005

myotubularin localization in muscle, revealing a potential link between IMGD and X-linked CNM.

Discussion

In this study we identified and characterized *BIN1* mutations affecting the splicing of the muscle-specific exon 11, resulting in a

rapidly progressing myopathy in humans and dogs. The IMGD dog is the first faithful mammalian model for *BIN1*-related centronuclear myopathy and particularly for the highly progressive form, and is the only characterized mammalian model available for preclinical trials of potential therapies for this severe congenital myopathy. Our data provide strong evidence for muscle-specific functions of amphiphysin 2 in membrane struc-

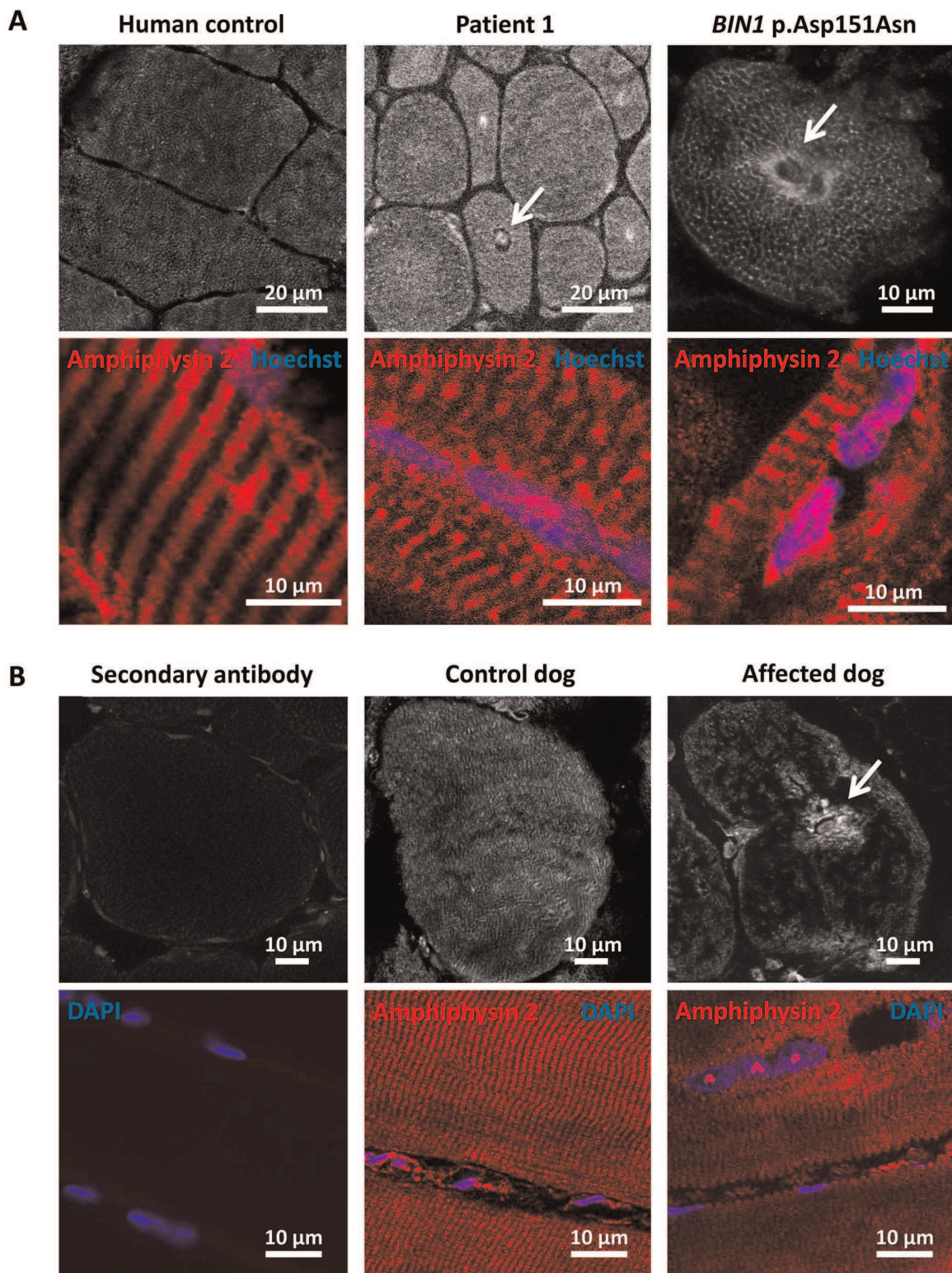


Figure 6. Amphiphysin 2 is present but altered in muscles from affected humans and dogs. (A) Amphiphysin 2 localization in control (left), patient 1 (middle) and a CNM patient with the p.Asp151Asn mutation (right). Arrows indicate abnormal accumulations of amphiphysin 2 around centralized nuclei in both patient muscles. (B) Abnormal localization of amphiphysin 2 on transversal and longitudinal muscle sections from an IMGD dog compared to a control. The secondary without the primary antibody was applied on control canine sections to withdraw non-specific background staining.
doi:10.1371/journal.pgen.1003430.g006

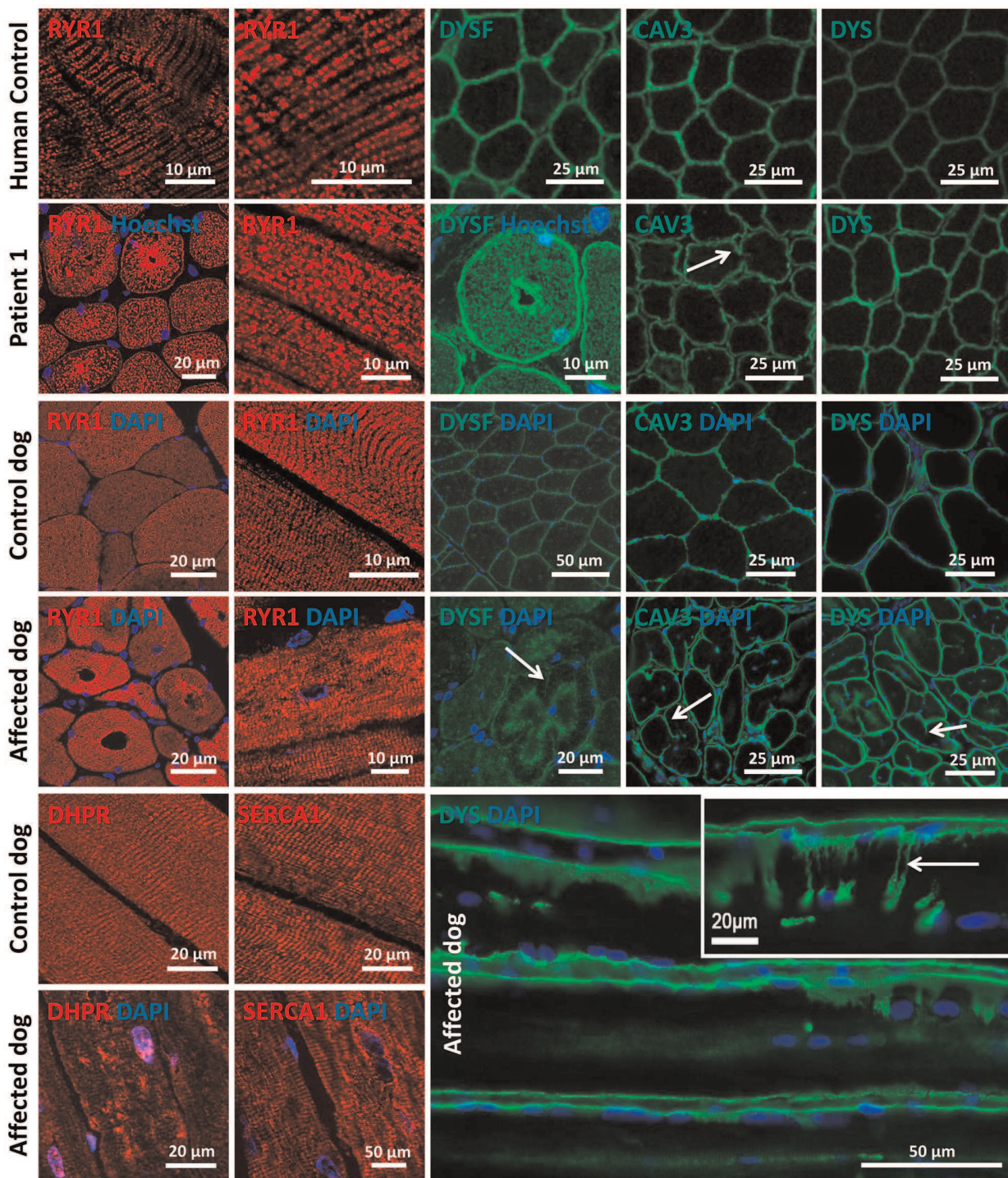


Figure 7. Alteration of triad components and proteins regulating membrane trafficking. Immunolocalization on longitudinal and transversal sections from patients and affected dogs revealed an abnormal pattern of the junctional sarcoplasmic calcium channel RYR1, the T-tubule marker DHPR and the longitudinal sarcoplasmic calcium pump SERCA1. Especially RYR1 was found to accumulate around internalized nuclei. Intracellular dysferlin signals were detected in patients and affected dogs, but not in the age-matched controls. Labeling of the sarcolemmal markers caveolin 3 and dystrophin demonstrated prominent lobulation and deep indentations of the plasma membrane in patients and affected dogs on transversal and longitudinal sections (arrows).
doi:10.1371/journal.pgen.1003430.g007

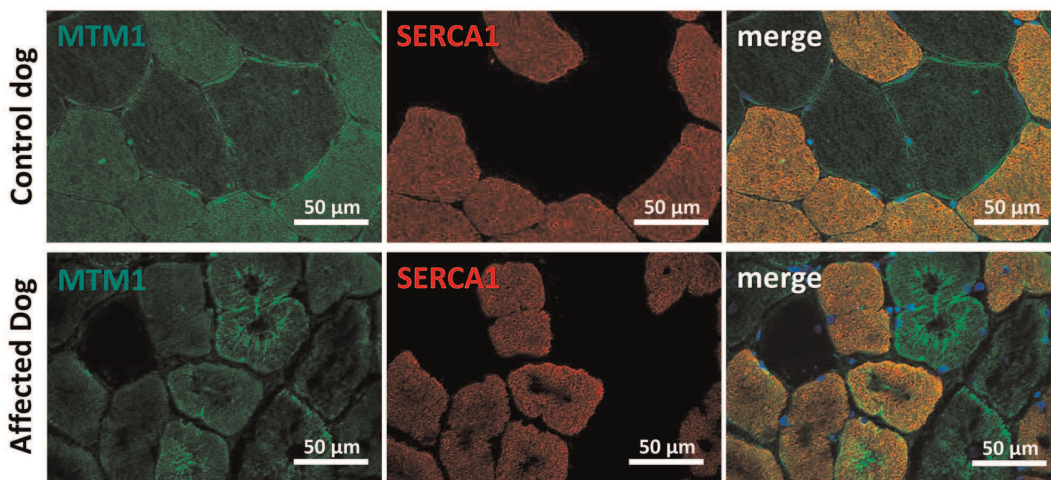


Figure 8. Myotubularin is mis-localized in IMGD muscle. In muscle sections from control dogs, myotubularin is predominantly expressed in type II fibers expressing SERCA1. In affected IMGD dogs, massive myotubularin accumulations formed a concentric network around the fiber center. doi:10.1371/journal.pgen.1003430.g008

tural organization and remodelling and allow novel insights into the overlapping pathogenesis of centronuclear myopathy and myotonic dystrophy. A schematic representation of the amphiphysin 2 protein domains and of the position of the mutations and splicing alterations causing classical autosomal recessive centronuclear myopathy, rapidly progressive human CNM and canine IMGD as well as myotonic dystrophy is shown in Figure 9.

BIN1 mutations in classical and highly progressive centronuclear myopathies

Classical *BIN1*-related ARCNM has been described with neonatal or childhood onset, hypotonia and ptosis and all mutations were found in ubiquitously expressed exons [1,13,14,15]. The muscle weakness was mildly to moderately progressive, and some patients could still walk at older age. In contrast, our patients with a splice mutation affecting the muscle-specific exon 11 showed a rapid disease progression involving strong care-dependence and leading to death within a few years, despite normal motor development and disease-onset not before 3.5 years. The histopathological findings of our patients and of the previously reported ARCNM cases partially overlap, including atrophy, prominent nuclear internalization and central dense

areas upon NADH-TR staining of muscle sections. However, there is no evidence for type I fiber predominance in the muscle biopsies of our patients. Previous RT-PCR experiments demonstrated a progressive integration of exon 11 in *BIN1* mRNA during human skeletal muscle development [2]. We therefore hypothesize that the muscle-specific exon 11 plays a major role in muscle maintenance, rather than in early muscle development. This is in accordance with the highly progressive phenotype of humans and dogs with a disease onset several months or years after birth. Consistently, we detected amphiphysin 2 in muscle tissue, but RNA analysis revealed major skipping of *BIN1* exon 11. This suggests that the patients mainly express an embryonic *BIN1* isoform, which might not be able to assume the function of the adult *BIN1* isoform, possibly explaining the more progressive phenotype compared to patients with *BIN1* mutations in the ubiquitously expressed exons.

The canine Inherited Myopathy of Great Danes is a faithful model for *BIN1*-related centronuclear myopathy

The characterization of the pathological mechanisms leading to *BIN1*-related CNM and the development of potential therapeutic approaches is obviated by the lack of a faithful animal model. *Bin1*-

Myotonic dystrophy

Centronuclear Myopathy

Progressive Centronuclear Myopathy

Inherited Myopathy of Great Danes

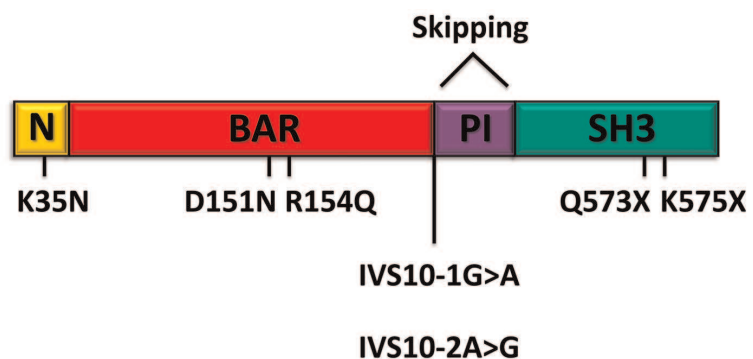


Figure 9. Schematic representation of the amphiphysin 2 domains and *BIN1* alterations in different myopathies. Schematic representation of the amphiphysin 2 protein domains and position of the known mutations causing autosomal recessive centronuclear myopathy, the new splice mutations resulting in rapidly progressive centronuclear myopathy and canine Inherited Myopathy of Great Danes. Myotonic dystrophy induces mis-splicing of *BIN1* exon 11. Nomenclature is based on isoform 1 (NM_139343). doi:10.1371/journal.pgen.1003430.g009

null mice are perinatally lethal [26], so that a comprehensive analysis of skeletal muscle alterations during disease development is not possible. We sought for dog breeds with molecularly unsolved congenital myopathies and we identified the canine Inherited Myopathy of Great Danes as a disease model reproducing the histological and physiological defects observed in *BIN1*-related CNM patients. IMGD has been reported for cases in Canada, Australia and UK and is characterized by generalized muscle atrophy, exercise intolerance, exercise-induced tremor and muscle wasting [29]. The disease typically starts before 10 months of age, is highly progressive, and most of the affected dogs are euthanized before 18 months of age due to severe debilitating muscle weakness. Histological examinations revealed internalized or central nuclei without evidence of inflammation, disruption of the sarcomeric architecture with central fiber areas devoid of myofibrils, and central accumulations of mitochondria and glycogen granules ([28,29,30] and our data). In addition, type I fiber predominance in combination with an increased expression of genes implicated in the slow-oxidative metabolism was described [35]. In this study we demonstrate that IMGD and progressive CNM have a comparable etiopathology and both conditions result from mutations of the AG acceptor splice site of the *BIN1* muscle-specific exon 11. The histopathology and the cellular organization defects of the human and canine muscle disorders are almost identical, we therefore consider IMGD as a faithful mammalian model for *BIN1*-related centronuclear myopathy.

Veterinary implications

Some dogs of our IMGD cohort were found to be negative for *BIN1* mutations, suggesting that IMGD encompasses several disorders with similar clinical and overlapping histopathological features. The proven relationship of two affected Great Dane dogs demonstrates a common origin of the *BIN1* exon 11 splice mutation, and it is likely that all five affected dogs described here can be traced back to a common ancestor. As the muscle disorder is inherited as a recessive trait, and as canine pedigrees are generally highly inbred, it is likely that the mutation can be found in Great Dane dog populations from all over the world, as recently demonstrated for another autosomal recessive CNM form in Labrador retrievers [36]. It is therefore of veterinary medical interest to sequence *BIN1* exon 11 in Great Dane dogs. Also, veterinarians and veterinary pathologists should consider *BIN1* mutations as a possible cause of any unexplained progressive myopathy in dogs, especially when the biopsy displays internal nuclei and lobulated or indented sarcolemma.

Insights into amphiphysin 2 muscle-specific functions and pathological mechanisms of centronuclear myopathy

Detailed immunohistochemical and ultrastructural analyses of muscles from patients and affected Great Dane dogs revealed common membrane alterations and abnormal accumulations of proteins regulating membrane trafficking. Similar findings were observed on biopsies from patients with *DNM2* or *MTM1* mutations [12], suggesting that mislocalization of triad proteins reflects common aberrations in CNM and that the amphiphysin 2 muscle-specific isoform plays an important role in triad formation and/or maintenance. This is in accordance with the known biochemical function of amphiphysin 2 and other N-BAR domain proteins to sense membrane curvature and to potentially induce curvature through the insertion of an amphipathic helix into the membrane bilayer. *In vitro* and cell culture experiments have led to the suggestion that the exon 11 encoded PI-binding motif is

essential for membrane tubulation in cultured muscle cells [22]. Indeed, *Drosophila* mutated for amphiphysin, the ortholog of both amphiphysin 1 and amphiphysin 2, display an abnormal T-tubule system [24]. T-tubule alterations and muscle weakness were reproduced in murine *Tibialis anterior* injected with a U7 small nuclear RNA construct harboring an antisense sequence promoting *BIN1* exon 11 skipping [2]. However, nuclear centralization and atrophy were not observed, contrasting with the IMGD model. This difference might be species-related, is possibly due to a low efficacy of the AAV-U7 method or alternatively to the examination time point 4 months post injection. As the triad is the membrane structure controlling excitation-contraction coupling, this suggests that impaired excitation-contraction coupling and subsequent calcium homeostasis defects are a primary cause of the myopathy. Of note, abnormal intracellular calcium release was observed in isolated murine muscle fibers after *BIN1* shRNA-mediated knock-down [37]. Together with the present characterization of the IMGD model, these data indicate that amphiphysin 2 has an important muscle-specific role in triad structural maintenance, and provide additional evidence that triad modifications are a common defect in centronuclear myopathies, IMGD and myotonic dystrophies [2,12].

Triads are not the only membrane compartment affected in patients and dogs harboring *BIN1* exon 11 mutations. We also noted central accumulations of caveolin 3 and dysferlin, two key regulators of membrane trafficking in skeletal muscle, numerous membranous whorls, and a peculiar remodeling of the sarcolemma, manifesting an indented fiber perimeter and invaginations towards the center of the fibers. Caveolin 3 regulates membrane tension at the sarcolemma and dysferlin controls membrane exocytosis in sarcolemmal membrane repair [33,34]. As both proteins are also present on regenerating T-tubules [38], their mislocalization resulting from a *BIN1* mutation would be in accordance with defective T-tubule regeneration. Moreover, data mainly obtained in cultured cells support a key role of amphiphysins in the formation of endocytic vesicles [16], and a study in *Caenorhabditis elegans* suggested a role of amphiphysin in vesicle recycling [39]. Defects in intracellular signaling resulting from calcium defects and impaired transport of ion channels and growth factor might explain the muscle weakness and atrophy in *BIN1*-related CNM.

Amphiphysin 2 links several forms of centronuclear myopathies and myotonic dystrophy

Our findings on the IMGD model uncovered possible links between *BIN1*-related and other forms of CNM. Altered triads and the presence of membranous whorls were reported for *MTM1* dog, mouse and zebrafish models as well as for patients with *MTM1* mutations involving protein loss [12,31,40,41,42]. Abnormal triad markers were also reported for *MTM1*-related and *DNM2*-related CNM [12,43]. Dysferlin localization was not extensively studied in *MTM1*-CNM but was increased in the cytoplasm of a mouse model and in patients with *DNM2*-CNM [44]. Moreover, we found myotubularin localization was strongly impaired in IMGD muscles. These findings suggest that myotubularin and amphiphysin 2 are in the same pathway regulating membrane remodeling in skeletal muscle and strengthen the hypothesis of a common pathological mechanism of the X-linked and the autosomal recessive CNM forms.

Alternative splicing of *BIN1* exon 11 is mis-regulated in patients with myotonic dystrophy [2]. The parallel inclusion of exon 7 was noted, but its impact has not been assessed yet. Here we report the first mutation affecting the muscle-specific exon 11 of *BIN1* and having an impact on splicing. The major clinical and histological

aspects of the patients and IMGD dogs include general muscle weakness, atrophy and nuclear centralization, consistent with the muscle phenotype in DM patients. Our data therefore support the hypothesis that mis-splicing of *BIN1* exon 11 partially accounts for the muscle-specific signs in myotonic dystrophy.

Materials and Methods

Ethics statement

Human sample collection was performed with informed consent from the patients according to the declaration of Helsinki and experimentation was performed as part of routine diagnosis. All dogs were examined with the consent of their owners. Blood and biopsies were obtained as part of routine clinical procedures for diagnostic purposes. Cheek cells were collected by owners or veterinarians using non-invasive swabs. As the data were from client-owned dogs undergoing normal veterinary exams, there was no “animal experiment” according to the legal definitions in Europe and the US. All local regulations related to clinical procedures were observed. Cryopreserved muscle specimens were processed and stored at the University of California, San Diego, under a tissue transfer approval from the institutional Animal Care and Use Committee.

Molecular genetics

Human Genomic DNA was prepared from peripheral blood by routine procedures and sequenced for all coding exons and intron/exon boundaries of *MTM1*, *DNM2*, and *BIN1* as described elsewhere [1,4,5]. Patient 1 had a normal CTG repeat length at the DMPK locus (7 and 13 repeats) and was therefore excluded for myotonic dystrophy. Control DNAs were from healthy individuals of Turkish origin.

Dog DNA samples were extracted from cheek cells, venous blood or muscle biopsy specimens (cryosections or paraffin embedded tissue) by routine procedures and sequenced for all coding exons and intron/exon boundaries of canine *MTM1* [31], *PTPLA* [32] and *BIN1* (primer sequences in Table S1). Control samples were from a world-wide collection of healthy Great Danes as well as from healthy individuals of 13 other breeds.

RNA studies

RNA was extracted from muscle biopsies by routine procedures and reverse transcribed using the SuperScript III kit (Invitrogen, Carlsbad, USA). Human and dog amplicons were cloned into the pGEM-T Easy vector (Promega, Madison, USA) and transfected into *E.coli* DH5 α cells. Blue/white selection, repeated twice, resulted in 30 clones for the human cDNA and 3 clones for the canine cDNA. Control dog was an unaffected Drahthaar (German Wirehaired Pointer). Primer sequences are listed in Table S1.

Protein studies

Western blot and immunofluorescence were performed using routine protocols. Biceps femoris and tibialis anterior biopsies from two affected dogs (14 months and 22 months, respectively) and from healthy age-matched Golden Retrievers or Belgian Shepherds as controls have been used for the analysis. Following antibodies were used for the study: R2406 (home-made rabbit anti-BIN1 PI binding domain), R2444 (home-made rabbit anti-BIN1 SH3 domain), R3062 (home-made rabbit anti-BIN1 exon 12 epitope), R2867 and R2868 (home-made rabbit anti-MTM1), mouse anti-GAPDH (Merck Millipore, Darmstadt, Germany), mouse anti-ryanodine receptor 1 (Affinity BioReagents, Golden, USA), mouse anti-SERCA 1 (Affinity BioReagents, Golden, USA),

rabbit anti-dysferlin (Euromedex, Souffelweyersheim, France), goat anti-caveolin-3 (Tebu-BIO, Le-Perray-en-Yvelines, France), rabbit anti-caveolin-3 (Affinity BioReagents, Golden, USA), mouse anti-DHPR (Affinity BioReagents, Golden, USA), and mouse anti-dystrophin (Leica Microsystems, Germany). For immunohistochemistry, transverse cryosections were prepared, fixed and stained by routine methods. Nuclei were stained with Hoechst or DAPI (Sigma-Aldrich, St. Louis, USA). Sections were mounted with slowfade antifade reagent (Invitrogen, Carlsbad, USA) and viewed using a laser scanning confocal microscope (TCS SP2; Leica Microsystems, Wetzlar, Germany) or a Zeiss Axio Observer Z.1 microscope equipped with a 20 \times , 40 \times or 63 \times lens and AxioPlan imaging with structured illumination (Carl Zeiss, Jena, Germany).

Muscle histology

For histochemical analyses, transverse sections of muscle cryosections (8 μ m) of vastus lateralis and biceps femoris muscle biopsies were stained with hematoxylin-eosin, modified Gomori trichrome, NADH-TR and myofibrillar ATPase and then assessed for centralized nuclei, fiber morphology, fiber type distribution, cores, protein accumulation and cellular infiltrations.

Electron microscopy

Muscle biopsies were processed for electron microscopy as described previously [45]. Briefly, the tissue was fixed either in 6% phosphate-buffered glutaraldehyde (human patient) or in 2.5% paraformaldehyde, 2.5% glutaraldehyde, and 50 mM CaCl₂ in 0.1 M cacodylate buffer at pH 7.4 (dog), and post-fixed with 2% OsO₄, 0.8% K₃Fe(CN)₆ in 0.1 M cacodylate buffer (pH 7.4) for 2 h at 4°C and incubated with 5% uranyl acetate for 2 h at 4°C. Samples were dehydrated in graded series of ethanol and embedded in epoxy resin 812. Ultrathin sections (70 nm) were contrasted with uranyl acetate and lead citrate.

Membrane tubulation assay

Murine C2C12 myoblasts were seeded on coverslips and transfected at 50–60% confluency using Lipofectamine 2000 (Invitrogen, Carlsbad, USA) either with GFP-BIN1 isoform 8 (including exon 11) or isoform 9 (excluding exon 11, both were a kind gift from Pietro de Camilli, Howard Hughes Medical Institute, USA). Cells were differentiated after 24 h by changing to medium containing 2% horse serum instead of FCS and fixed and stained after 5 days of differentiation by routine methods. Nuclei were stained with Hoechst/DAPI (Sigma-Aldrich, St. Louis, USA) and sections were mounted with slowfade antifade reagent and viewed using a laser scanning confocal microscope (TCS SP2; Leica Microsystems, Wetzlar, Germany).

Web resources

1000 genomes - A Deep Catalog of Human Genetic Variation (URL: <http://www.1000genomes.org/>)

Database of Single Nucleotide Polymorphisms (dbSNP). Bethesda (MD): National Center for Biotechnology Information, National Library of Medicine. (dbSNP Build ID: 134).

(URL: <http://www.ncbi.nlm.nih.gov/SNP/>)

Exome Variant Server, NHLBI Exome Sequencing Project (ESP), Seattle, WA (URL: <http://evs.gs.washington.edu/EVS/>)

Online Mendelian Inheritance in Man (OMIM) (URL: <http://www.omim.org/>)

NNsplice: prediction of splice mutations (URL: http://www.fruitfly.org/seq_tools/splice.html)

Human Splicing finder (URL: <http://www.umd.be/HSF/>)

Supporting Information

Figure S1 Western blot of canine muscle extracts using the anti-SH3 domain antibody. Compared to the control, the main skeletal muscle amphiphysin 2 isoform is strongly reduced in the IMGD dog. The protein levels of the other isoforms are also reduced, but still detectable.

(TIF)

Figure S2 Low-magnitude electron microscopy pictures of muscles from patient 1 and an affected dog demonstrate moderate Z-band streaming, mitochondriodrial accumulations and myofibrillar disarray.

(TIF)

Figure S3 Dog muscle sections labeled for developmental myosin. Signals were comparable in affected dog and control, suggesting that there is no excessive fiber regeneration.

(TIF)

References

- Nicot AS, Toussaint A, Tosch V, Kretz C, Wallgren-Pettersson C, et al. (2007) Mutations in amphiphysin 2 (BIN1) disrupt interaction with dynamin 2 and cause autosomal recessive centronuclear myopathy. *Nat Genet* 39: 1134–1139.
- Fugier C, Klein AF, Hammer C, Vassilopoulos S, Ivarsson Y, et al. (2011) Misregulated alternative splicing of BIN1 is associated with T tubule alterations and muscle weakness in myotonic dystrophy. *Nat Med* 17: 720–725.
- Jungbluth H, Wallgren-Pettersson C, Laporte J (2008) Centronuclear (myotubular) myopathy. *Orphanet J Rare Dis* 3: 26.
- Bitoun M, Maugère S, Jeannot PY, Lacene E, Ferrer X, et al. (2005) Mutations in dynamin 2 cause dominant centronuclear myopathy. *Nat Genet* 37: 1207–1209.
- Laporte J, Hu LJ, Kretz C, Mandel JL, Kioschis P, et al. (1996) A gene mutated in X-linked myotubular myopathy defines a new putative tyrosine phosphatase family conserved in yeast. *Nat Genet* 13: 175–182.
- Grabs D, Slepnev VI, Songyang Z, David C, Lynch M, et al. (1997) The SH3 domain of amphiphysin binds the proline-rich domain of dynamin at a single site that defines a new SH3 binding consensus sequence. *J Biol Chem* 272: 13419–13425.
- Itoh T, De Camilli P (2006) BAR, F-BAR (EFC) and ENTH/ANTH domains in the regulation of membrane-cytosol interfaces and membrane curvature. *Biochim Biophys Acta* 1761: 897–912.
- Sakamuro D, Elliott KJ, Wechsler-Reya R, Prendergast GC (1996) BIN1 is a novel MYC-interacting protein with features of a tumour suppressor. *Nat Genet* 14: 69–77.
- Ren G, Vajjhala P, Lee JS, Winsor B, Munn AL (2006) The BAR domain proteins: molding membranes in fission, fusion, and phagy. *Microbiol Mol Biol Rev* 70: 37–120.
- Wechsler-Reya R, Sakamuro D, Zhang J, DuHadaway J, Prendergast GC (1997) Structural analysis of the human BIN1 gene. Evidence for tissue-specific transcriptional regulation and alternate RNA splicing. *J Biol Chem* 272: 31453–31458.
- Butler MH, David C, Ochoa GC, Freyberg Z, Daniell L, et al. (1997) Amphiphysin II (SH3P9; BIN1), a member of the amphiphysin/Rvs family, is concentrated in the cortical cytomatrix of axon initial segments and nodes of Ranvier in brain and around T tubules in skeletal muscle. *J Cell Biol* 137: 1355–1367.
- Toussaint A, Cowling BS, Hnia K, Mohr M, Oldfors A, et al. (2011) Defects in amphiphysin 2 (BIN1) and triads in several forms of centronuclear myopathies. *Acta Neuropathol* 121: 253–266.
- Bohm J, Yis U, Ortac R, Cakmakci H, Kurul SH, et al. (2010) Case report of intrafamilial variability in autosomal recessive centronuclear myopathy associated to a novel BIN1 stop mutation. *Orphanet J Rare Dis* 5: 35.
- Claeys KG, Maisonobe T, Bohm J, Laporte J, Hezode M, et al. (2010) Phenotype of a patient with recessive centronuclear myopathy and a novel BIN1 mutation. *Neurology* 74: 519–521.
- Mejaddam AY, Nennesmo I, Sejersen T (2009) Severe phenotype of a patient with autosomal recessive centronuclear myopathy due to a BIN1 mutation. *Acta Myol* 28: 91–93.
- Qualmann B, Koch D, Kessels MM (2011) Let's go bananas: revisiting the endocytic BAR code. *EMBO J* 30: 3501–3515.
- Peter BJ, Kent HM, Mills IG, Vallis Y, Butler PJ, et al. (2004) BAR domains as sensors of membrane curvature: the amphiphysin BAR structure. *Science* 303: 495–499.
- Owen DJ, Wigge P, Vallis Y, Moore JD, Evans PR, et al. (1998) Crystal structure of the amphiphysin-2 SH3 domain and its role in the prevention of dynamin ring formation. *EMBO J* 17: 5273–5285.
- Di Paolo G, Sankaranarayanan S, Wenk MR, Daniell L, Perucco E, et al. (2002) Decreased synaptic vesicle recycling efficiency and cognitive deficits in amphiphysin 1 knockout mice. *Neuron* 33: 789–804.
- Mao NC, Steingrimsson E, DuHadaway J, Wasserman W, Ruiz JC, et al. (1999) The murine Bin1 gene functions early in myogenesis and defines a new region of synteny between mouse chromosome 18 and human chromosome 2. *Genomics* 56: 51–58.
- Wechsler-Reya RJ, Elliott KJ, Prendergast GC (1998) A role for the putative tumor suppressor Bin1 in muscle cell differentiation. *Mol Cell Biol* 18: 566–575.
- Lee E, Marcucci M, Daniell L, Pypaert M, Weisz OA, et al. (2002) Amphiphysin 2 (Bin1) and T-tubule biogenesis in muscle. *Science* 297: 1193–1196.
- Kojima C, Hashimoto A, Yabuta I, Hirose M, Hashimoto S, et al. (2004) Regulation of Bin1 SH3 domain binding by phosphoinositides. *Embo J* 23: 4413–4422.
- Razzaq A, Robinson IM, McMahon HT, Skepper JN, Su Y, et al. (2001) Amphiphysin is necessary for organization of the excitation-contraction coupling machinery of muscles, but not for synaptic vesicle endocytosis in *Drosophila*. *Genes Dev* 15: 2967–2979.
- Cowling BS, Toussaint A, Muller J, Laporte J (2012) Defective membrane remodeling in neuromuscular diseases: insights from animal models. *PLoS Genet* 8: e1002595.
- Muller AJ, Baker JF, DuHadaway JB, Ge K, Farmer G, et al. (2003) Targeted disruption of the murine Bin1/Amphiphysin II gene does not disable endocytosis but results in embryonic cardiomyopathy with aberrant myofibril formation. *Mol Cell Biol* 23: 4295–4306.
- Spiegelhalter C, Tosch V, Hentsch D, Koch M, Kessler P, et al. (2010) From dynamic live cell imaging to 3D ultrastructure: novel integrated methods for high pressure freezing and correlative light-electron microscopy. *PLoS One* 5: e9014.
- Davies SE, Davies DR, Richards RB, Bruce WJ (2008) Inherited myopathy in a Great Dane. *Aust Vet J* 86: 43–45.
- Lujan Feliu-Pascual A, Shelton GD, Targett MP, Long SN, Comerford EJ, et al. (2006) Inherited myopathy of great Danes. *J Small Anim Pract* 47: 249–254.
- McMillan CJ, Taylor SM, Shelton GD (2006) Inherited myopathy in a young Great Dane. *Can Vet J* 47: 891–893.
- Beggs AH, Bohm J, Snead E, Kozlowski M, Maurer M, et al. (2010) MTM1 mutation associated with X-linked myotubular myopathy in Labrador Retrievers. *Proc Natl Acad Sci U S A* 107: 14697–14702.
- Pele M, Tiret L, Kessler JL, Blot S, Panthier JJ (2005) SINE exonic insertion in the PTPLA gene leads to multiple splicing defects and segregates with the autosomal recessive centronuclear myopathy in dogs. *Hum Mol Genet* 14: 1417–1427.
- Bansal D, Miyake K, Vogel SS, Groh S, Chen CC, et al. (2003) Defective membrane repair in dysferlin-deficient muscular dystrophy. *Nature* 423: 168–172.
- Sinha B, Koster D, Ruez R, Gonnord P, Bastiani M, et al. (2011) Cells respond to mechanical stress by rapid disassembly of caveolae. *Cell* 144: 402–413.
- Chang KC, McCulloch ML, Anderson TJ (2010) Molecular and cellular insights into a distinct myopathy of Great Dane dogs. *Vet J* 183: 322–327.
- Maurer M, Mary J, Guillaud L, Fender M, Pele M, et al. (2012) Centronuclear Myopathy in Labrador Retrievers: A Recent Founder Mutation in the PTPLA Gene Has Rapidly Disseminated Worldwide. *PLoS One* 7: e46408.
- Tjondrokoesoemo A, Park KH, Ferrante C, Komazaki S, Lesniak S, et al. (2011) Disrupted membrane structure and intracellular Ca²⁺(+) signaling in adult skeletal muscle with acute knockdown of Bin1. *PLoS One* 6: e25740.

Table S1 Primer sequences.
(XLSX)

Acknowledgments

We thank Valérie Biancalana for the myotonic dystrophy testing, Pietro de Camilli for the BIN1 constructs, Anders Oldfors for the muscle biopsy of the p.Asp151Asn *BLN1* patient, Swantja Hertel and Sandra Bour for technical assistance, Inès Barthélémy, Nicolas Blanchard-Gutton, and Stéphane Blot from the UETM-ENVA for the control canine muscle biopsies, Laetitia Lagoutte, Catherine André and the Cani-DNA banking resource, Anne Thomas from Antagene, and the owners for DNAs from control Great Danes.

Author Contributions

Conceived and designed the experiments: JB LT JL. Performed the experiments: JB NV MM BC GDS WK AT LT. Analyzed the data: JB NV WK GDS US JW LT. Contributed reagents/materials/analysis tools: GDS IP TJA JW. Wrote the paper: JB JL.

38. Klinge L, Harris J, Sewry C, Charlton R, Anderson L, et al. (2010) Dysferlin associates with the developing T-tubule system in rodent and human skeletal muscle. *Muscle Nerve* 41: 166–173.
39. Pant S, Sharma M, Patel K, Caplan S, Carr CM, et al. (2009) AMPH-1/Amphiphysin/Bin1 functions with RME-1/Ehd1 in endocytic recycling. *Nat Cell Biol* 11: 1399–1410.
40. Buj-Bello A, Laugel V, Messaddeq N, Zahreddine H, Laporte J, et al. (2002) The lipid phosphatase myotubularin is essential for skeletal muscle maintenance but not for myogenesis in mice. *Proc Natl Acad Sci U S A* 99: 15060–15065.
41. Dowling JJ, Vreede AP, Low SE, Gibbs EM, Kuwada JY, et al. (2009) Loss of myotubularin function results in T-tubule disorganization in zebrafish and human myotubular myopathy. *PLoS Genet* 5: e1000372.
42. Pierson CR, Dulin-Smith AN, Durban AN, Marshall ML, Marshall JT, et al. (2012) Modeling the human MTM1 p.R69C mutation in murine *Mtm1* results in exon 4 skipping and a less severe myotubular myopathy phenotype. *Hum Mol Genet* 21: 811–825.
43. Romero NB, Bitoun M (2011) Centronuclear myopathies. *Semin Pediatr Neurol* 18: 250–256.
44. Durieux AC, Vignaud A, Prudhon B, Viou MT, Beuvin M, et al. (2010) A centronuclear myopathy-dynamamin 2 mutation impairs skeletal muscle structure and function in mice. *Hum Mol Genet* 19: 4820–4836.
45. Weis J, Schroder JM (1988) Adult polyglucosan body myopathy with subclinical peripheral neuropathy: case report and review of diseases associated with polyglucosan body accumulation. *Clin Neuropathol* 7: 271–279.

Figure S1. Western blot of canine muscle extracts using the anti-SH3 domain antibody

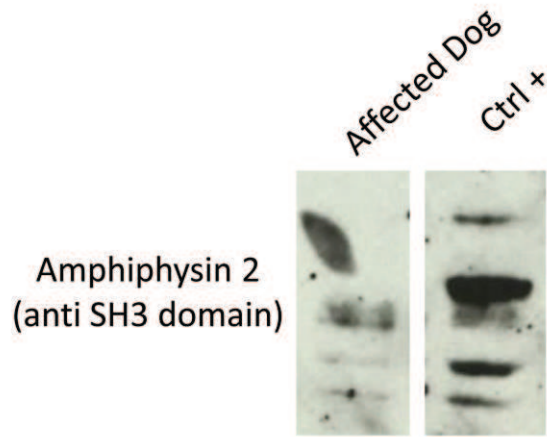


Figure S2. Low-magnitude electron microscopy pictures of muscles from patient 1 and an affected dog

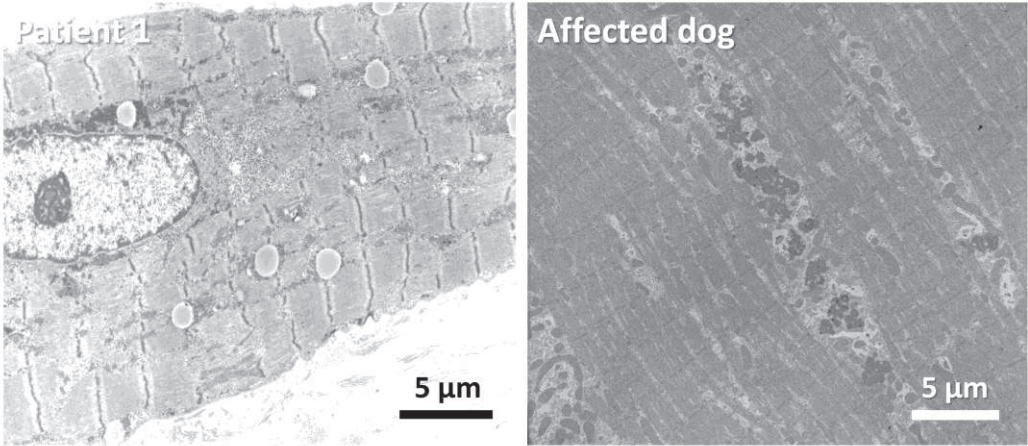


Figure S3. Dog muscle sections labeled for developmental myosin

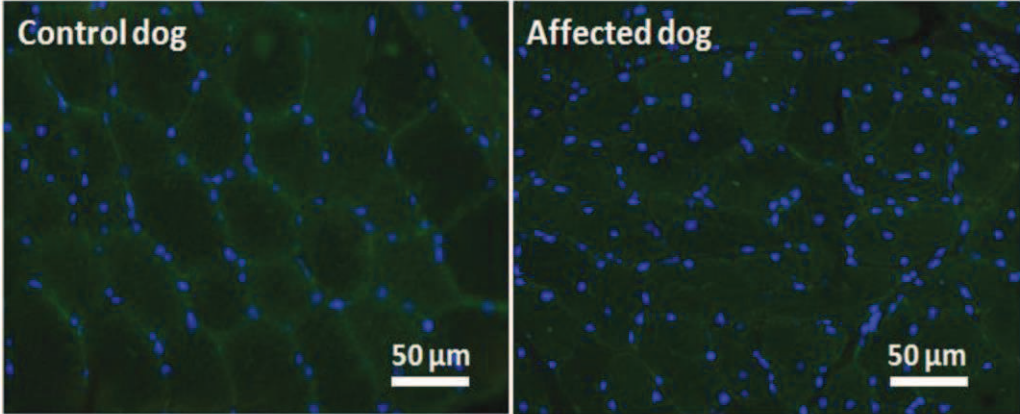


Table S1. Primer sequences

Species	5' -3'	5' -3'	Size (nt)
human	TCCTCTGAGCAGAAGGGTTG	CACTGCACACAGAGCCAGAT	266
human	GCAAGCTGGTGGACTACGACAG	ACAGTTGCTGGGAAGGTCTC	1106
human	AGAACCTCAATGATGTGCTGG	GGCTCGTGGTTGACTCTGAT	209
human	GCAAGCTGGTGGACTACGACAG	GGCTCGTGGTTGACTCTGAT	547
human	AGAACCTCAATGATGTGCTGG	ACAGTTGCTGGGAAGGTCTC	768
dog	GTCGGGGCTGCAAGATCG	TCGGGGGTGCGCGAGGTG	226
dog	GAGCCATCTGTGGTATTGG	CTTCCAGCTCGCTTACTCC	277
dog	GCGTTTGTCCACCTGAGAG	GTCCAAGAAGGTGAGGCAG	552
dog	GGAAGCAGTGGGGCTCAAG	CTTACCTCCAGTGCACAG	268
dog	CTGAACATCTCGACATCTCG	CAGTGGGCACAGCACAAGAG	263
dog	CCACTCTCCTTTGCCGTGAC	CAGGAAAGAGACTGAGCCCTC	249
dog	GACTTGGCTAGGCCTAAGC	GTGGCCACTAGTGTGTACC	539
dog	GTGCAAGGAAGGGGCTAAGATG	CTACAGCCAGGGCAGTAG	203
dog	GCTGCTGATGAGGGAACAGG	GCACCAGGCGCATGCACAG	206
dog	CTGTGGATGCACATGGTCC	CCATGAGCCCAGTGTTC	302
dog	GTGACTAACTGTGGCTTTGTC	GGAAGAAGGCCATGCACAC	286
dog	GCACCTGCCGAATGTTCC	GTGCAAGTGCATGCACCTG	775
dog	CTTGTCTCGTGCCTTGCC	GCAAATGTCTAGGTTAGAGTG	495
dog	CCATTGCAGGGACCTGAC	CAACGTCGGCTCAGATAGC	659
dog	CCTGGTGCACCATGCTTG	GCAGGGTACAGAGACAG	314
dog	GGTCCAGTGCCTCTG	GGTGTTCCTCACACGCCAG	209
dog	CAAGCAGCTGACTGAGGGCAC	GGTGTTCCTCACACGCCAG	1128
dog	CCGAGTTTCCAGTATGGCTTC	GTCTCCCTGATAACATCGAG	813

DISCUSSION and PERSPECTIVES

BIN1 is a ubiquitously expressed protein, with the highest expression found in skeletal muscle (Butler, David et al. 1997). In human, mutations in BIN1 lead to autosomal recessive centronuclear myopathy (ARCNM) (Nicot, Toussaint et al. 2007) and the missplicing of BIN1 was identified in myotonic dystrophy (MD) (Fugier, Klein et al. 2011). Additionally, downregulation of BIN1 protein level was found in patients with right ventricular cardiomyopathy (Hong, Cogswell et al. 2012). All this highlight the importance of BIN1 in muscle. Over the past years various approaches have been used in order to better understand the normal function of BIN1 in muscle and pathological mechanisms in disease. The aim of my work was to contribute to this understanding and better characterize important steps in which BIN1 is involved in muscle development, maintenance and disease.

1. Role of BIN1 in skeletal muscle

Our data confirmed that BIN1 has the highest expression level in skeletal muscle (Butler, David et al. 1997; Razzaq, Robinson et al. 2001). Moreover, we specifically localized BIN1 on triads, specifically at the T-tubules in skeletal muscle, again in agreement with published data (Butler, David et al. 1997). Previously published *Bin1* KO mice die in the first hours after birth, possibly from cardiomyopathy with no reported alteration in skeletal muscle structure (Muller, Baker et al. 2003). Although there is a possibility that the skeletal muscle defect was overseen in the *Bin1* KO mice. In our CMV model we did thorough analysis of the heart phenotype and no difference was found in the heart organization and function. This, together with the observation that total and muscle specific mice show strong decrease in BIN1 expression and die in the same time frame as the published complete KO of *Bin1* (Muller, Baker et al. 2003), argue against cardiomyopathy as a main cause of death. We believe that BIN1 is crucial for T-tubule development, a network which was lacking in muscle fibers from CMV *Bin1* exon 20 KO mice. However as low BIN1 expression is still observed (even though expressed as a truncated protein without of exon 20) in total *Bin1* exon 20 model, we cannot rule out that it might be sufficient for the normal functioning of the mice heart.

1.1. BIN1 and muscle maturation

The intracellular tubule network as observed by BIN1 immunofluorescence in C2C12 cells, was shown to be connected to the plasma membrane, therefore strongly supporting a role for BIN1 in T-tubules formation (Lee, Marcucci et al. 2002). The first *in vivo* study showing role of BIN1 in muscle development was done on *Drosophila melanogaster* with an amphiphysin mutant, which had major T-tubules malformations and were viable but flightless (Razzaq, Robinson et al. 2001). Similarly, *Bin1* exon 20 KO mice had major DHPR and RyR1 collapse of both networks which would be expected if the triads would not be able to form due to the lack of T-tubules.

Interestingly, both *in vitro* and *in vivo* expression of muscle specific exon 11 is upregulated during muscle differentiation, reaching its peak and inclusion in all muscle isoforms in mature muscle (Nicot, Toussaint et al. 2007; Fugier, Klein et al. 2011). In CHO cells overexpression of only muscle specific isoform of BIN1 and overexpression of BAR domain together with the PI motif is targeted to the cell membrane (Lee, Marcucci et al. 2002). However our *Bin1* exon 11 KO mouse model did not have detectable defects and alterations in T-tubule structure or BIN1 localization, but the defect were seen only after the muscle damage. Together this data indicates that exon 11 is not needed for T-tubule formation, and its expression pattern suggests that it might have a more important role in the muscle maintenance rather than during the development. Lee and co-workers used *in vitro* approach to address the question of a role of the PI motif in localization of the protein overexpressing different BIN1 domain constructs (Lee, Marcucci et al. 2002). *In vivo*, it is likely that other mechanisms compensate during T-tubule formation or as discussed the PI motif is important in muscle maintenance only and not needed during development. It would be interesting to use our *Bin1* exon 11 KO model and induce exon 11 deletion around the birth, when T-tubules are not yet developed. This approach may answer the question if compensatory mechanism may be activated in our KO mice due to an embryonic deletion of exon 11.

In WT differentiating muscle, *in utero* and during regeneration in adult muscle, we observed BIN1 and dynamin 2 colocalization, which was restricted to the short period of time during T-tubules reformation. *In vivo* in adult mature muscle dynamin 2 is located

on the Z-line (Cowling, Toussaint et al. 2011), whereas BIN1 localizes at the T-tubules and therefore no apparent colocalization occurs supporting the hypothesis that the interaction is transient and developmentally regulated. In vitro, BIN1 and dynamin 2 were already shown to interact and it seems that exon 7 inclusion in the BAR domain of BIN1 increases the strength of interaction compared to the BIN1 isoforms lacking exon 7 (Ellis, Barrios-Rodiles et al. 2012). Interestingly, increase in exon 7 inclusion was significant at the embryonic state compared to the adult muscle, giving a possible explanation of the colocalization observed. Preliminary data presented here suggest for the first time the possible involvement of BIN1 and dynamin 2 interaction in T-tubules formation. A fine control of BIN1 splicing may be a key for regulating dynamin 2 oligomerization and/or activity, where BIN1 would inhibit the membrane fission by interacting with dynamin 2.

1.2. BIN1 in skeletal muscle maintenance

To address if BIN1 has a role in skeletal muscle maintenance we used HSA-inducible *Bin1* exon 20 KO mice in which the recombination, therefore *Bin1* KO was triggered in adult mouse muscle. Our data showed that even 5 months after the induction of the recombination and although BIN1 protein level showed strong reduction, the analyzed muscle did not show any difference in histology or muscle function compared to the control group. This data are in contradiction with the shRNA knockdown of *Bin1* done in adult muscle fibers (Tjondrokoesoemo, Park et al. 2011), where already 14 days after the electroporation of shRNA, around 30% of muscle fibers showed swollen T-tubules and greatly reduced Ca^{2+} sparks frequency (Tjondrokoesoemo, Park et al. 2011). Using shRNA leads to protein downregulation faster than in the case of time-inducible promoter, due to which compensational mechanisms are possible. Additionally, the voltage induced Ca^{2+} was done on individual fibers, which may be susceptible to biased analysis between the groups. It could be possible that if the authors examined the complete muscle the difference would be lost.

We did not detect a phenotype different to WT littermates in *Bin1* exon 11 KO mice tested up to 12 months of age. Contrary to our results, exon 11 deletion in wild type mice, using the U7 exon skipping strategy showed a significant reduction of muscle

force together with extensive T-tubules misorganization (Fugier, Klein et al. 2011). Although exon 11 was skipped efficiently; one cannot exclude the U7 off target effects, since only the rescue with BIN1 containing exon 11 would support the specificity of the data. In our CMV *Bin1* exon 11 KO mice the deletion was specific due to the Lox P sites in the introns 10 and 11, causing excision of exon 11. Nevertheless we cannot exclude the possibility of a functional compensation in our KO model, since the deletion was done early in utero.

Patients with a splice site mutation in exon 11 present relatively late with a muscle phenotype, where up to the age of 3.5 years there was no myopathy signs detected, indicating that the motoric coordination and speech during first years developed normally (Bohm, Vasli et al. 2013). The mutation was found in 3 patients (from the same family) and in all, after the first onset of symptoms the disease progressed very rapidly and two patients died at age of 5 and 7 and the third, now 5 years old is wheelchair bound (Bohm, Vasli et al. 2013). Since the patients were not affected at birth and the first symptoms appeared in already adult muscle, this prompted us to investigate the role of exon 11 in muscle regeneration. We used notexin-induced muscle regeneration in *Bin1* exon 11 KO mice and interestingly we observed decrease in fiber size at 14 and 28 days after the muscle damage together with increase in eMHC and myogenin levels. Taken together this indicates that BIN1 exon 11 has a role in muscle maintenance, which is in agreement with its increased expression level towards the end of muscle differentiation (Nicot, Toussaint et al. 2007; Fugier, Klein et al. 2011). Additionally, it is worth noting that BIN1 was highly abundant at the myotubes fusion sites (Klinge, Laval et al. 2007) and that shRNA deletion of *Bin1* compromised myofiber membrane integrity (Tjondrokoesoemo, Park et al. 2011). Increased membrane fragility may facilitate the injury of the muscle, however there was no difference in creatine kinase level (often increased in damaged muscle) before and after the exhaustion exercise done on Treadmill (data not shown). Myotubes fusion is reacquired during muscle regeneration in order to build or repair functional myofibers and BIN1 localization on the sites of fusion points that it may be needed for the repair.

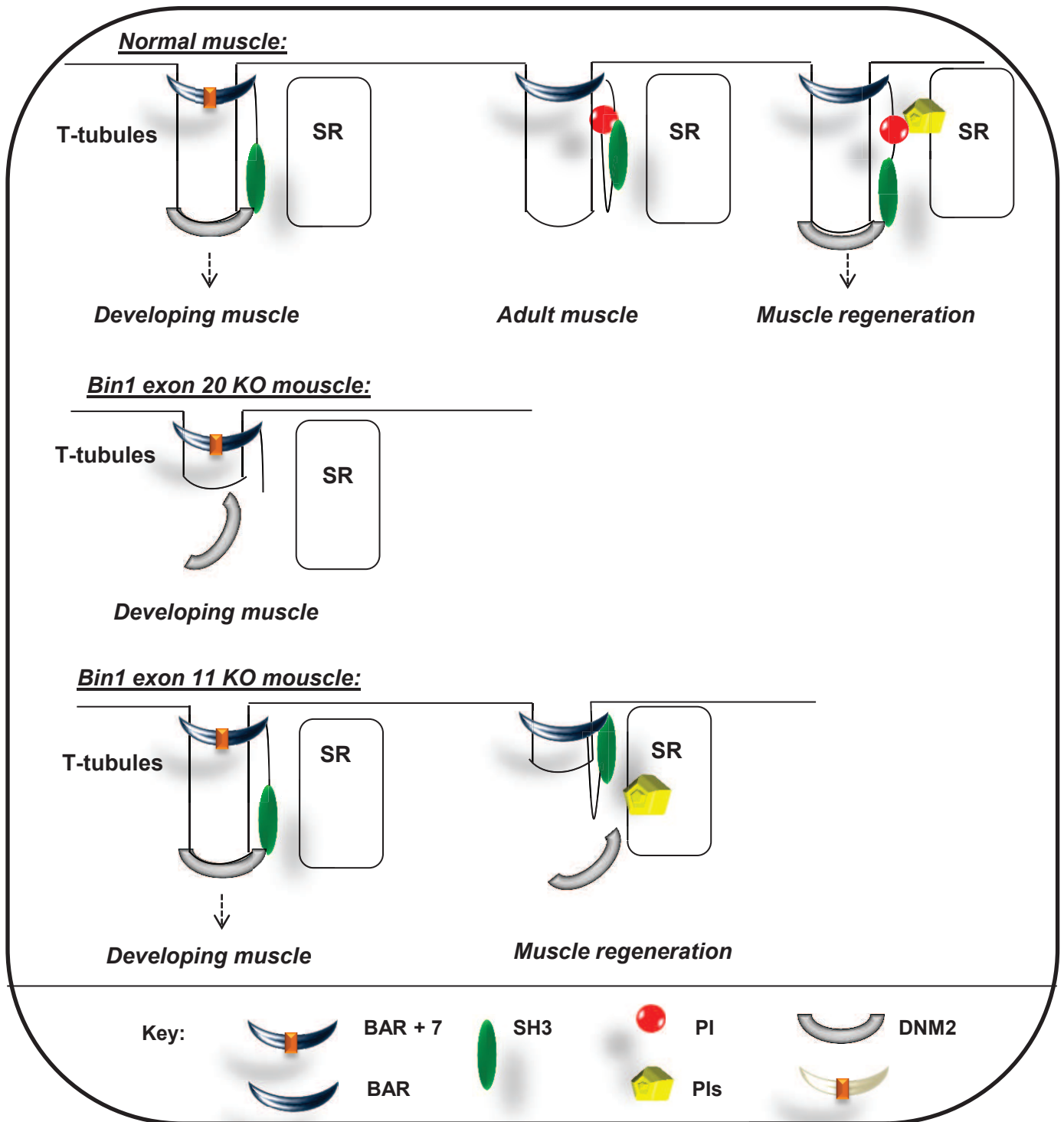


Figure 18. Model of BIN1 tubulation mechanism in normal muscle and KO models.

Functional compensation in both *Bin1* exon 11 KO mice and patients with the exon 11 splice site mutation, during the development in utero, may explain the normal muscle function observed at birth and eventually phenotype seen in the U7 skipped model, since the skipping was done after the birth. There may be a threshold of accumulated damage after which muscle is not able to tolerate it any more. Electroporation procedure in the case of shRNA knockdown may have provoked this kind of damage. Standard analysis of mice models besides the muscle tests performed is relying on sedentary, caged mice which are not exposed to strong physiological stress and whose ambulation is highly limited. Both CMV *Bin1* exon 11 and HSA inducible *Bin1* exon 20 KO mice may not have a strong phenotype due to this kind of life conditions. Additionally, mice may not live long enough to accumulate sufficient damage which will trigger the start of the disease.

1.3. Conclusion and perspectives

This work highlights the necessity of BIN1 in skeletal muscle development and maintenance. We hypothesize that the embryonic isoform of BIN1 which includes exon 7 and not the exon 11 (+7-11) is necessary for the T-tubule network formation, and then at the final steps of differentiation the adult isoform of BIN1 (-7+11) is the predominant isoform. The embryonic isoform was shown to increase binding affinity for dynamin 2. This interaction may be a key mechanism in understanding the process of T-tubule development. Previously described key proteins involved in T-tubule biogenesis such as caveolin 3 or mitostagumins when deleted in the KO models are viable but have misshaped T-tubules. Only *Bin1* exon 20 model shows a strong disruption of T-tubules network and is perinatally lethal, even when deletion was done specifically in skeletal muscle. This highlights the crucial role of BIN1 in T-tubules biogenesis. BIN1 may be involved in elongation of T-tubules together with dynamin 2 and the exon 7 inclusion may recruit dynamin 2 to the places of tubulation and the SH3 domain of BIN1 may regulate the dynamin 2 by inhibiting the fission of the membranes. In muscle maintenance the PI motif may be a place of BIN1 regulation, inhibiting this interaction, unless the SH3 domain is liberated by PtdIns binding (Figure 18). In adult muscle BIN1 localizes at the T-tubules and DNM2 on the Z-line. In developing and remodeling

muscle colocalization of the two exists. This indicates that there may be a time window in which the interaction is important. We plan by using biochemical approach to further investigate this point.

To further investigate this question, more work will need to be done. Since the T-tubules in mice start to be formed at E15 we expect that the interaction between the dynamin 2 and BIN1 may be strongest at this time point. In addition to verifying this interaction *in vivo*, it is important to identify the functional role of the isoform shift from embryonic to mature has. The future challenge would be to modulate dynamin 2 and/or BIN1 isoform expression and look at their impact. Since the T-tubule maturation in mice happens gradually and postnatally over the period of three weeks one might try inducing the deletion of exon 20 BIN1 in this time frame in HSA- inducible *Bin1* exon 20 line and observe the effect. Regarding the role of BIN1 in muscle regeneration, one could perform the regeneration test in HSA-inducible *Bin1* exon 20 KO mice. Using *Bin1* exon 11 model we showed impact on regeneration and now we plan to assess muscle function and in more detail investigate the mechanisms of BIN1 and exon 11 participation in this process. Additionally different regeneration approaches may be used, such as downhill running in order to induce damage in more physiological environment and verify the hypothesis. Primary myoblast cell culture of both *Bin1* KO models can be used as an approach to identify the BIN1 role in myoblast fusion. And eventually as mentioned previously, time inducible KO model of exon 11 could answer to the question if due to the functional compensation in embryonic muscle we don't see the phenotype before stressing the mice. It would be interesting to test regeneration capability using notexin or any other type of injury and observe the impact on the muscle in these mice.

2. BIN1 and pathophysiology

Various pathologies are associated with BIN1. BIN1 increased expression causes late-onset Alzheimer's disease (Harold D et al. 2009) and loss or misregulation of BIN1 is found in cancer (Ge, DuHadaway et al. 1999; Ge, Minhas et al. 2000). Patients with ventricular cardiomyopathy again show the reduction of BIN1 on protein level (Hong, Cogswell et al. 2012) and mutations in *BIN1* which cause autosomal recessive centronuclear myopathy (ARCNM) do not impact the level of BIN1 expression but alter BIN1's domain properties (Nicot, Toussaint et al. 2007) 2007). Additionally in myothonic dystrophy patients BIN1 is misspliced and this missplicing contributes to a skeletal muscle defects seen in the patients (Fugier, Klein et al. 2011). Our data confirms the necessity of BIN1 in skeletal muscle, and importantly highlight that this is the primary organ affected in CMV total *Bin1* KO mice.

2.1. What can murine models tell us about ARCNM?

This work is intended to investigate the muscle specific role of BIN1 in order to better understand the pathology in patients with ARCNM. Deleting the exon 20 in our KO model is meant to emphasize the effect seen in patients with stop codon mutation in exon 20 of *BIN1*. In fact two such mutations have been identified the K575X mutation (Nicot, Toussaint et al. 2007) and the Q573X (Bohm, Yis et al. 2010). Other identified mutations include the K35N mutation in the amphipathic helix of the BAR domain which is being inserted into the membranes, therefore positioning BIN1, and the D151N and R154Q mutations which are located around the middle of the BAR domain (Nicot, Toussaint et al. 2007; Claeys, Maisonobe et al. 2010). Recently a splice site mutation in exon 11 has been identified (IVS10-1G>A), removing the exon 11 whilst not changing the BIN1 protein level (Bohm, Vasli et al. 2013). Patients harboring stop codon mutations in exon 20 and the K35N patients had hypotonia at birth and delayed motor development. Two out of three patients with the K35N mutation died soon after the birth (Bohm, Yis et al. 2010). Patients with BAR mutations were affected later in childhood at 8 years (in the case of the D151N mutation) and 11 (in the case of the R154Q mutation) (Bohm, Yis et al. 2010). General histology of all the patients showed highly variable fiber size with a very high number of centralized nuclei (up to 70%) often clustered or simply

increased in size and NADH-TR staining shows oxidative staining aggregations (Toussaint, Cowling et al. 2011). Moreover the EM morphological examination showed subsarcolemmal accumulation of mitochondria and caveolae (Toussaint, Cowling et al. 2011). The majority of triads had swollen either T-tubules or SR. Immunofluorescence revealed a strong BIN1 staining around the nuclei and a weaker DHPR, RyR1, desmin and caveolin 3 staining (Romero and Bitoun 2011; Toussaint, Cowling et al. 2011). Interestingly the *Bin1* exon 20 KO model has strong BIN1, DHPR and RyR1 accumulation in the center of the fiber showing a strong collapse of the T-tubule/SR network, therefore being a good model to study the mechanisms of T-tubules and SR biogenesis. Other histological features are more difficult to assess in this models since mouse muscle maturation continues to occur after the birth whereas in human at birth muscle is mainly mature. Matured muscle is characterized by peripherally placed nuclei and well organized SR and triad junctions. It is important to mention this, since at the time of death, the muscle of the exon 20 KO mouse is not histologically comparable to the patient's muscle.

In the case of the IVS10-1G>A mutation, affected patients had normal speech and motor development. Muscle weakness was noticed at 3,5 years of age and after which the disease became highly progressive and two out of three patients died at the age of 5 and 7 and the third sibling, now 9 is wheelchair bound (Bohm, Vasli et al. 2013). The central area of the fibers similar to other BIN1 patients, was devoid of myofibrils and contains glycogen and other organelles (Bohm, Vasli et al. 2013). The triad structure was again altered which was shown by the RyR 1 and DHPR disorganization while occasionally staining was collapsed towards the center of the fiber, similarly to what was seen in other *BIN1* patients. Dysferlin staining, besides normal localization on the plasma membrane, was found in the center of the fibers, which is characteristic during the formation and regeneration process. The plasma membrane of the muscle cells was lobular with a strongly altered shape (Bohm, Vasli et al. 2013). Interestingly creatine kinase levels were normal in these patients indicating that there is no increase in plasma membrane fragility. *Bin1* exon 11 KO mice did not reproduce any of these features under normal conditions. Only induced regeneration showed a defect in fiber maturation, revealing smaller fibers with higher expressions of eMHC and myogenin.

Late onset of the disease in patients and normal muscle function until the first symptoms of the disease appeared, previously observed in affected individuals, together with altered regeneration seen in *Bin1* exon 11 KO mouse model reveal a novel exon 11 role. This is a role in muscle maintenance, and it disputes previously proposed role during muscle development. The PI motif may serve as a regulatory point through interaction with phosphoinositides. It is possible that in adult muscle, BIN1 is mainly found in its “closed” conformation, where SH3 domain is “locked” through binding with the PI motif. Control of the SH3 domain binding may be regulated through PIs levels. Recently it was shown that MTM1 enhances BIN1 tubulating activity (Royer, Hnia et al. 2013). Authors showed that enzymatically inactive MTM1 mutant strongly reduces tubulation of BIN1. This means that regulation through PtdIns production is important for the tubulation. Liberation of the SH3 domain allows it to interact with other proteins to cooperate in the process. The most obvious interactor from gathered data is DNM2, but we do not exclude that there may be some other ones also.

The missense mutation in the splice site of exon 11 (IVS10-2A>G), found in dogs, is somewhat different compared to the patients. It leads to a strong *Bin1* mRNA and protein decrease, with a small amount of protein which is still expressed and which harbors additional 9 amino acids before the PI motif (Bohm, Vasli et al. 2013). Dogs are also affected late, at 10 months of age, and most of them have to be euthanized before 18 months due to the severity of the disease. The dog’s histology reveals even more pronounced lobular fibers where invaginations go deep into the muscle and positively stain for dysferlin and caveolin 3 (Bohm, Vasli et al. 2013). Again, DHPR and RyR1 were mislocalized and EM confirmed abnormal triad organization (Bohm, Vasli et al. 2013). In dogs muscle maturation and muscle size, compared to murine, resemble those in humans more closely. Therefore the canine model will be an important tool for the future of the BIN1 therapy approach.

2.2. Pathological mechanism of ARCNM

Mislocalization of DHPR, RyR1 and caveolin 3 are indicating T-tubules defects in BIN1 patients which were confirmed by electron microscopy. Using CMV *Bin1* exon 20 KO models I have showed the necessity of BIN1 in normal muscle maturation and T-

tubules biogenesis. From different ARCNM patients and murine models we can see that all domains of BIN1 are needed for its correct functioning. I believe that BIN1 is one of the key proteins required for the T-tubules biogenesis. Mutations found in ARCNM patients do not change the protein level of BIN1 but affect its domain properties. Mutation in N-amphipathic helix may reduce the ability of BIN1 binding to plasma membrane and therefore reduce the efficiency of T-tubule formation. BAR domain mutations reduce its membrane tubulating activity (Nicot, Toussaint et al. 2007) and/or BAR domain homo and hetero dimerization. Stop codon mutations in the SH3 domain reduce binding to the SH3 domain interactors such as dynamin 2 (Nicot, Toussaint et al. 2007). We are also starting to better understand the role of the muscle specific exon 11 of BIN1. The histopathology of the patients with IVS10-1G>A and experiments on the *Bin1* exon 11 KO mouse reveal a novel BIN1 role in muscle maintenance. Muscle remodeling and muscle maintenance are constantly happening in skeletal muscle and well-coordinated and efficient machinery behind this must work perfectly. In addition to this, BIN3, another N-BAR protein which consists only of a BAR domain (similar to BIN1), was shown to be important in myogenesis through actin-dependent process (Simionescu-Bankston, Leoni et al. 2013). Interestingly the phenotype of the BIN3 KO mice was not observed before the toxin induced muscle regeneration (Simionescu-Bankston, Leoni et al. 2013). This further supports our hypothesis of the role of BIN1 during the muscle regeneration.

The exon 11 of BIN1 has the ability to bind the SH3 domain (Royer, Hnia et al. 2013). Binding leads to a conformational change of BIN1 into a close conformation, in effect locking the SH3 domain and prevents its interaction with other proteins. Why is this interaction needed in the healthy muscle? Calcium signaling and muscle contractions impact the T-tubules shape and position, but in the normal physiological conditions no or very little new T-tubules need to be made. Therefore I believe that the T-tubules in adult muscle are stable structures except in the case of injury. The interaction of the SH3 domain with the PI motif would facilitate the control of BIN1 activity. The PI motif has affinity towards PtdIns(4,5)P₂ and/or PtdIns3P and PtdIns5P (Lee, Marcucci et al. 2002; Fugier, Klein et al. 2011). Specific localization of these PIs might regulate this process and the open-close conformation of BIN1. While PtdIns3P is

implicated in vesicular trafficking, PtdIns(4,5)P₂ localizes to the T-tubules (Lee, Marcucci et al. 2002) and PtdIns3P levels were shown to modulate the SR shape (Amoasii L et al., 2013). Could this regulation be important for the triad maintenance and shape? PtdIns5P trafficking is involved in controlling of the cytoskeletal dynamics and intracellular membrane trafficking (Dang, Li et al. 2004; Lecompte, Poch et al. 2008), both important during the repair of the muscle. Interestingly in patients with the Q573X mutation, EM revealed caveolae accumulation underneath the sarcolemma and T-tubules (Toussaint, Cowling et al. 2011). Cholesterol agents disrupt both T-tubules labeled by caveolin 3 (Carozzi, Ikonen et al. 2000) and BIN1 (Lee, Marcucci et al. 2002). Dysferlin was also seen mislocalized in some patients (Bohm, Vasli et al. 2013). As dysferlin and caveolin 3 are shown to interact and both are involved in the biogenesis and regeneration of the T-tubules It was proposed that dysferlin may have a role in fusion of caveolin-3 containing vesicles during the T-tubule biogenesis (Matsuda, Hayashi et al. 2001; Among, Imamura et al. 2005). It would be interesting to look at those two proteins dynamics in a primary myoblast culture in the WT and *Bin1* exon 20 KO mice and in the regeneration model of *Bin1* exon 11 KO mice. Caveolin 3, dysferlin and BIN1 are suspected of cooperating in the process where BIN1 may be needed for the T-tubules formation while dysferlin and caveolin 3 compliment the process by bringing in and/or creating new membranes. The start of the T-tubules formation in the skeletal muscle of mice is at E15. Already at E16 T-tubules are considerably longer and the network continues to expand until the birth (Takekura, Flucher et al. 2001). In this short period, a vast amount of membranes need to be created. I believe that the T-tubule biogenesis is a synergistic process where BIN1 (perhaps together with dynamin 2) may be involved in the pulling and tubulating membranes while dysferin and caveolin 3 may be involved in adding the new ones. When the T-tubules formation is complete the BIN1 – dynamin 2 interaction is not needed anymore, and BIN1 isoform change inhibits further interaction. Possibly the same isoform shift happens in dynamin 2 but this was never investigated in my knowledge, but may be important step in understanding the underlining mechanism.

2.3. The pathological mechanism in centronuclear myopathy and myotonic dystrophies

Triad defects are a common feature in all CNMs (Toussaint, Cowling et al. 2011). As the only of the three CNM associated proteins localized on the T-tubules in skeletal muscle and a key protein needed for T-tubule formation, BIN1 makes the link between the three forms of CNM. The MTM1 and BIN1 interaction was recently published and it impacts tubulation activity of BIN1 (Royer, Hnia et al. 2013). MTM1 modulation of PtdIns3P (since it is a MTM1 substrate) and PtdIns5P (MTM1 dephosphorylates PtdIns(3,5)P₂ and produces PtdIns5P) may affect BIN1 function through the regulation of the PI motif. I have also noted the importance of the isoform switch during development. During development, the isoform that includes exon 7, increased compared to the adult muscle. We know that inclusion of this isoform enhances the interaction with dynamin 2 (Ellis, Barrios-Rodiles et al. 2012). Moreover in remodeling the muscle BIN1 and dynamin 2 colocalize. BIN1 and DNM2 interactions may be needed for the T-tubules biogenesis and reparation. As mentioned I believe that BIN1 may control the tubulation process in which DNM2 is involved. In agreement with this observation in the patients with myotonic dystrophy (DM), missplicing of BIN1 was noticed, leading to an increase in exon 7 inclusion and a decrease in exon 11 (Fugier, Klein et al. 2011) which therefore expresses an embryonic isoform of BIN1. Alterations in BIN1 isoform may be responsible for the T-tubules defects seen in DM patients.

Another new common pathway of the MAD interaction (Myotubularin 1, Amphiphysin 2 and Dynamin 2) may be autophagy where PtdIns3P is known to participate to the process (Noda, Matsunaga et al. 2010). Autophagy is a basic catabolic mechanism and it involves cell degradation of cellular components (which are dysfunctional or unnecessary). If regulated, it ensures synthesis, degradation and recycling of the cellular components (Cuervo, Bergamini et al. 2005). During the development and later during the physical exercise, the activation of autophagy is required for muscle homeostasis (Nair and Klionsky 2011). In XLCNM and ADCNM autophagy impairment were well documented in murine models of the disease (Durieux, Vassilopoulos et al. 2012; Al-Qusairi, Prokic et al. 2013). In ARCNM patients with IVS10-1G>A mutation,

accumulation of autophagosomes was detected in the cytoplasm of the muscle cells (Bohm, Vasli et al. 2013), which indicates defect in this pathway. We start to better understand the involvement of MAD proteins in autophagy but it is not clear yet whether there is any cooperation between the three or if they simply act on different levels in the same process. Henceforth this will be an important question which should be addressed in future work.

2.4. Conclusion and perspectives

BIN1 is important for healthy muscle. Patients with *BIN1* related ARCNM and MD have altered BIN1 function which leads to muscle malfunction. My work showed that BIN1 is necessary during T-tubules development embryonically and in regeneration. CMV and HSA *Bin1* exon 20 models will further help deciphering steps in T-tubules biogenesis. Additionally, I could note the importance of different BIN1 isoforms present during this process. I believe that understanding isoform modulation and specific roles and interactions may be a key point in revealing the BIN1 functions. Disadvantage of CMV and HSA *Bin1* exon 20 models is an extremely short window life after the birth. This makes it difficult to analyze and further modulate muscle function. Also it limits us from using it in testing therapeutic approaches. Besides the T-tubules defect, it would be interesting to see if other histopathological findings of ARCNM would be reproduced in the case of HSA inducible *Bin1* exon 20 KO mice where the deletion would be done right after the birth. This may be a more comprehensive model, closer representing the features found in patients. Additionally, a knockin murine model of the patient's mutations may help to better decipher the exact processes altered with specific BIN1 mutations found in patients.

3. CONCLUSION

The aim of my work was to better understand the BIN1 function in skeletal muscle and processes in which it is involved. Several different approaches *in vitro* and *in vivo* were used to tackle questions regarding its muscle specific function. BIN1 is necessary during T-tubules formation and important in muscle regeneration. Its function in muscle is tightly regulated by isoform switch and intramolecular binding. Understanding these

features will help us step forward towards successful therapy in ARCNM and MD patients. The information will guide as which pathways and protein interactions down or upstream of BIN1 are crucial and may be able to be modulated or can lead to developing exon skipping in order to modulate BIN1 function.

REFERENCES

- Adams, B. A. and K. G. Beam (1990). "Muscular dysgenesis in mice: a model system for studying excitation-contraction coupling." *FASEB journal : official publication of the Federation of American Societies for Experimental Biology* 4(10): 2809-2816.
- Al-Qusairi, L., I. Prokic, et al. (2013). "Lack of myotubularin (MTM1) leads to muscle hypotrophy through unbalanced regulation of the autophagy and ubiquitin-proteasome pathways." *FASEB J.*
- Al-Qusairi, L., N. Weiss, et al. (2009). "T-tubule disorganization and defective excitation-contraction coupling in muscle fibers lacking myotubularin lipid phosphatase." *Proc Natl Acad Sci U S A* 106(44): 18763-18768.
- Amoasii, L., D. L. Bertazzi, et al. (2012). "Phosphatase-dead myotubularin ameliorates X-linked centronuclear myopathy phenotypes in mice." *PLoS Genet* 8(10): e1002965.
- Amoasii, L., K. Hnia, et al. (2013). "Myotubularin and PtdIns3P remodel the sarcoplasmic reticulum in muscle in vivo." *J Cell Sci.*
- Ampong, B. N., M. Imamura, et al. (2005). "Intracellular localization of dysferlin and its association with the dihydropyridine receptor." *Acta myologica : myopathies and cardiomyopathies : official journal of the Mediterranean Society of Myology / edited by the Gaetano Conte Academy for the study of striated muscle diseases* 24(2): 134-144.
- Anderson, A. A., X. Altafaj, et al. (2006). "The junctional SR protein JP-45 affects the functional expression of the voltage-dependent Ca²⁺ channel Cav1.1." *Journal of cell science* 119(Pt 10): 2145-2155.
- Anderson, A. A., S. Treves, et al. (2003). "The novel skeletal muscle sarcoplasmic reticulum JP-45 protein. Molecular cloning, tissue distribution, developmental expression, and interaction with alpha 1.1 subunit of the voltage-gated calcium channel." *The Journal of biological chemistry* 278(41): 39987-39992.
- Andronache, Z., D. Ursu, et al. (2007). "The auxiliary subunit gamma(1) of the skeletal muscle L-type Ca²⁺ channel is an endogenous Ca²⁺ antagonist." *Proceedings*

- of the National Academy of Sciences of the United States of America 104(45): 17885-17890.
- Arnold, L., A. Henry, et al. (2007). "Inflammatory monocytes recruited after skeletal muscle injury switch into antiinflammatory macrophages to support myogenesis." *Journal of Experimental Medicine* 204(5): 1057-1069.
- Balagopal, P., J. C. Schimke, et al. (2001). "Age effect on transcript levels and synthesis rate of muscle MHC and response to resistance exercise." *American journal of physiology. Endocrinology and metabolism* 280(2): E203-208.
- Balghi, H., S. Sebille, et al. (2006). "Mini-dystrophin expression down-regulates IP3-mediated calcium release events in resting dystrophin-deficient muscle cells." *The Journal of general physiology* 128(2): 219-230.
- Bauer, F., M. Urdaci, et al. (1993). "Alteration of a Yeast Sh3 Protein Leads to Conditional Viability with Defects in Cytoskeletal and Budding Patterns." *Molecular and Cellular Biology* 13(8): 5070-5084.
- Bauerfeind, R., K. Takei, et al. (1997). "Amphiphysin I is associated with coated endocytic intermediates and undergoes stimulation-dependent dephosphorylation in nerve terminals." *Journal of Biological Chemistry* 272(49): 30984-30992.
- Beam, K. G., C. M. Knudson, et al. (1986). "A lethal mutation in mice eliminates the slow calcium current in skeletal muscle cells." *Nature* 320(6058): 168-170.
- Beard, N. A., M. G. Casarotto, et al. (2005). "Regulation of ryanodine receptors by calsequestrin: Effect of high luminal Ca²⁺ and phosphorylation." *Biophysical journal* 88(5): 3444-3454.
- Beard, N. A., M. M. Sakowska, et al. (2002). "Calsequestrin is an inhibitor of skeletal muscle ryanodine receptor calcium release channels." *Biophysical journal* 82(1): 310-320.
- Beggs, A. H., J. Bohm, et al. (2010). "MTM1 mutation associated with X-linked myotubular myopathy in Labrador Retrievers." *Proc Natl Acad Sci U S A* 107(33): 14697-14702.
- Begley, M. J. and J. E. Dixon (2005). "The structure and regulation of myotubularin phosphatases." *Curr Opin Struct Biol* 15(6): 614-620.

- Biancalana, V., O. Caron, et al. (2003). "Characterisation of mutations in 77 patients with X-linked myotubular myopathy, including a family with a very mild phenotype." *Hum Genet* 112(2): 135-142.
- Bitoun, M., J. A. Bevilacqua, et al. (2007). "Dynamin 2 mutations cause sporadic centronuclear myopathy with neonatal onset." *Ann Neurol* 62(6): 666-670.
- Bitoun, M., A. C. Durieux, et al. (2009). "Dynamin 2 mutations associated with human diseases impair clathrin-mediated receptor endocytosis." *Human mutation* 30(10): 1419-1427.
- Bitoun, M., S. Maugenre, et al. (2005). "Mutations in dynamin 2 cause dominant centronuclear myopathy." *Nat Genet* 37(11): 1207-1209.
- Bittner, R. E., L. V. Anderson, et al. (1999). "Dysferlin deletion in SJL mice (SJL-Dysf) defines a natural model for limb girdle muscular dystrophy 2B." *Nature genetics* 23(2): 141-142.
- Blaauw, B., P. del Piccolo, et al. (2012). "No evidence for inositol 1,4,5-trisphosphate-dependent Ca²⁺ release in isolated fibers of adult mouse skeletal muscle." *Journal of General Physiology* 140(2): 235-241.
- Block, B. A., T. Imagawa, et al. (1988). "Structural Evidence for Direct Interaction between the Molecular-Components of the Transverse Tubule Sarcoplasmic-Reticulum Junction in Skeletal-Muscle." *Journal of Cell Biology* 107(6): 2587-2600.
- Blondeau, F., J. Laporte, et al. (2000). "Myotubularin, a phosphatase deficient in myotubular myopathy, acts on phosphatidylinositol 3-kinase and phosphatidylinositol 3-phosphate pathway." *Hum Mol Genet* 9(15): 2223-2229.
- Boffoli, D., S. C. Scacco, et al. (1994). "Decline with age of the respiratory chain activity in human skeletal muscle." *Biochimica et biophysica acta* 1226(1): 73-82.
- Bohm, J., N. Vasli, et al. (2013). "Altered Splicing of the BIN1 Muscle-Specific Exon in Humans and Dogs with Highly Progressive Centronuclear Myopathy." *PLoS Genet* 9(6): e1003430.
- Bohm, J., U. Yis, et al. (2010). "Case report of intrafamilial variability in autosomal recessive centronuclear myopathy associated to a novel BIN1 stop mutation." *Orphanet J Rare Dis* 5: 35.

- Boland, R., A. Martonosi, et al. (1974). "Developmental changes in the composition and function of sarcoplasmic reticulum." *The Journal of biological chemistry* 249(2): 612-623.
- Bonangelino, C. J., J. J. Nau, et al. (2002). "Osmotic stress-induced increase of phosphatidylinositol 3,5-bisphosphate requires Vac14p, an activator of the lipid kinase Fab1p." *The Journal of cell biology* 156(6): 1015-1028.
- Boncompagni, S., M. Thomas, et al. (2012). "Triadin/Junctin double null mouse reveals a differential role for Triadin and Junctin in anchoring CASQ to the jSR and regulating Ca(2+) homeostasis." *PloS one* 7(7): e39962.
- Brabec, V. and J. Kasparkova (2005). "Modifications of DNA by platinum complexes. Relation to resistance of tumors to platinum antitumor drugs." *Drug resistance updates : reviews and commentaries in antimicrobial and anticancer chemotherapy* 8(3): 131-146.
- Brandl, C. J., N. M. Green, et al. (1986). "Two Ca²⁺ ATPase genes: homologies and mechanistic implications of deduced amino acid sequences." *Cell* 44(4): 597-607.
- Brodeur, G. M., R. C. Seeger, et al. (1984). "Amplification of N-Myc in Untreated Human Neuroblastomas Correlates with Advanced Disease Stage." *Science* 224(4653): 1121-1124.
- Brotto, M. A. P., R. Y. Nagaraj, et al. (2004). "Defective maintenance of intracellular Ca²⁺ homeostasis is linked to increased muscle fatigability in the MG29 null mice." *Cell Research* 14(5): 373-378.
- Buck, E., I. Zimanyi, et al. (1992). "Ryanodine stabilizes multiple conformational states of the skeletal muscle calcium release channel." *The Journal of biological chemistry* 267(33): 23560-23567.
- Buj-Bello, A., F. Fougousse, et al. (2008). "AAV-mediated intramuscular delivery of myotubularin corrects the myotubular myopathy phenotype in targeted murine muscle and suggests a function in plasma membrane homeostasis." *Hum Mol Genet* 17(14): 2132-2143.
- Buj-Bello, A., V. Laugel, et al. (2002). "The lipid phosphatase myotubularin is essential for skeletal muscle maintenance but not for myogenesis in mice." *Proc Natl Acad Sci U S A* 99(23): 15060-15065.

- Butler, M. H., C. David, et al. (1997). "Amphiphysin II (SH3P9; BIN1), a member of the amphiphysin/Rvs family, is concentrated in the cortical cytomatrix of axon initial segments and nodes of Ranvier in brain and around T tubules in skeletal muscle." *J Cell Biol* 137(6): 1355-1367.
- Cai, C., H. Masumiya, et al. (2009). "MG53 nucleates assembly of cell membrane repair machinery." *Nature cell biology* 11(1): 56-64.
- Cai, C. X., N. Weisleder, et al. (2009). "Membrane Repair Defects in Muscular Dystrophy Are Linked to Altered Interaction between MG53, Caveolin-3, and Dysferlin." *Journal of Biological Chemistry* 284(23): 15894-15902.
- Callaway, C., A. Seryshev, et al. (1994). "Localization of the high and low affinity [3H]ryanodine binding sites on the skeletal muscle Ca²⁺ release channel." *The Journal of biological chemistry* 269(22): 15876-15884.
- Cao, C., J. Laporte, et al. (2007). "Myotubularin lipid phosphatase binds the hVPS15/hVPS34 lipid kinase complex on endosomes." *Traffic* 8(8): 1052-1067.
- Cardenas, C., J. L. Liberona, et al. (2005). "Nuclear inositol 1,4,5-trisphosphate receptors regulate local Ca²⁺ transients and modulate cAMP response element binding protein phosphorylation." *Journal of cell science* 118(Pt 14): 3131-3140.
- Carl, S. L., K. Felix, et al. (1995). "Immunolocalization of triadin, DHP receptors, and ryanodine receptors in adult and developing skeletal muscle of rats." *Muscle & nerve* 18(11): 1232-1243.
- Carozzi, A. J., E. Ikonen, et al. (2000). "Role of cholesterol in developing T-tubules: analogous mechanisms for T-tubule and caveolae biogenesis." *Traffic* 1(4): 326-341.
- Carrasquillo, M. M., O. Belbin, et al. (2011). "Replication of BIN1 Association with Alzheimer's Disease and Evaluation of Genetic Interactions." *Journal of Alzheimers Disease* 24(4): 751-758.
- Cassimere, E. K., S. Pyndiah, et al. (2009). "The c-MYC-interacting proapoptotic tumor suppressor BIN1 is a transcriptional target for E2F1 in response to DNA damage." *Cell Death and Differentiation* 16(12): 1641-1653.
- Caswell, A. H., N. R. Brandt, et al. (1991). "Localization and partial characterization of the oligomeric disulfide-linked molecular weight 95,000 protein (triadin) which

- binds the ryanodine and dihydropyridine receptors in skeletal muscle triadic vesicles." *Biochemistry* 30(30): 7507-7513.
- Catterall, W. A. (2000). "Structure and regulation of voltage-gated Ca²⁺ channels." *Annual review of cell and developmental biology* 16: 521-555.
- Chang, M. Y., J. Boulden, et al. (2007). "Bin1 Ablation Increases Susceptibility to Cancer during Aging, Particularly Lung Cancer." *Cancer Res* 67(16): 7605-7612.
- Chapuis, J., F. Hansmannel, et al. (2013). "Increased expression of BIN1 mediates Alzheimer genetic risk by modulating tau pathology." *Molecular psychiatry*.
- Chazaud, B., C. Sonnet, et al. (2003). "Satellite cells attract monocytes and use macrophages as a support to escape apoptosis and enhance muscle growth." *Journal of Cell Biology* 163(5): 1133-1143.
- Chen, Y. J., P. J. Zhang, et al. (2004). "The stalk region of dynamin drives the constriction of dynamin tubes." *Nature Structural & Molecular Biology* 11(6): 574-575.
- Ching, L. L., A. J. Williams, et al. (2000). "Evidence for Ca(2+) activation and inactivation sites on the luminal side of the cardiac ryanodine receptor complex." *Circulation research* 87(3): 201-206.
- Claeys, K. G., T. Maisonobe, et al. (2010). "Phenotype of a patient with recessive centronuclear myopathy and a novel BIN1 mutation." *Neurology* 74(6): 519-521.
- Colwill, K., D. Field, et al. (1999). "In vivo analysis of the domains of yeast Rvs167p suggests Rvs167p function is mediated through multiple protein interactions." *Genetics* 152(3): 881-893.
- Cook, T. A., R. Urrutia, et al. (1994). "Identification of dynamin 2, an isoform ubiquitously expressed in rat tissues." *Proc Natl Acad Sci U S A* 91(2): 644-648.
- Copello, J. A., S. Barg, et al. (1997). "Heterogeneity of Ca²⁺ gating of skeletal muscle and cardiac ryanodine receptors." *Biophysical journal* 73(1): 141-156.
- Corbett, A. M., A. H. Caswell, et al. (1985). "Determinants of triad junction reformation: identification and isolation of an endogenous promoter for junction reformation in skeletal muscle." *The Journal of membrane biology* 86(3): 267-276.
- Coronado, R., J. Morrissette, et al. (1994). "Structure and function of ryanodine receptors." *The American journal of physiology* 266(6 Pt 1): C1485-1504.

- Costello, B., C. Chadwick, et al. (1986). "Characterization of the junctional face membrane from terminal cisternae of sarcoplasmic reticulum." *The Journal of cell biology* 103(3): 741-753.
- Cowling, B. S., A. Toussaint, et al. (2011). "Increased expression of wild-type or a centronuclear myopathy mutant of dynamin 2 in skeletal muscle of adult mice leads to structural defects and muscle weakness." *Am J Pathol* 178(5): 2224-2235.
- Cuervo, A. M., E. Bergamini, et al. (2005). "Autophagy and aging: the importance of maintaining "clean" cells." *Autophagy* 1(3): 131-140.
- Cui, X., I. De Vivo, et al. (1998). "Association of SET domain and myotubularin-related proteins modulates growth control." *Nat Genet* 18(4): 331-337.
- D'Antona, G., M. A. Pellegrino, et al. (2003). "The effect of ageing and immobilization on structure and function of human skeletal muscle fibres." *The Journal of physiology* 552(Pt 2): 499-511.
- Dang, H., Z. Li, et al. (2004). "Disease-related myotubularins function in endocytic traffic in *Caenorhabditis elegans*." *Mol. Biol. Cell.* 15(1): 189-196.
- Darnfors, C., H. E. Larsson, et al. (1990). "X-linked myotubular myopathy: a linkage study." *Clinical genetics* 37(5): 335-340.
- Dauber, W. (1979). "[Fiber-type morphology and function of the triads in frog (*Rana esculenta*) skeletal muscle]." *Zeitschrift fur mikroskopisch-anatomische Forschung* 93(3): 512-536.
- David, C., P. S. McPherson, et al. (1996). "A role of amphiphysin in synaptic vesicle endocytosis suggested by its binding to dynamin in nerve terminals." *Proc Natl Acad Sci U S A* 93(1): 331-335.
- De Jongh, K. S., C. Warner, et al. (1991). "Characterization of the two size forms of the alpha 1 subunit of skeletal muscle L-type calcium channels." *Proceedings of the National Academy of Sciences of the United States of America* 88(23): 10778-10782.
- Delbono, O., J. Xia, et al. (2007). "Loss of skeletal muscle strength by ablation of the sarcoplasmic reticulum protein JP45." *Proceedings of the National Academy of Sciences of the United States of America* 104(50): 20108-20113.

- Di Paolo, G. and P. De Camilli (2006). "Phosphoinositides in cell regulation and membrane dynamics." *Nature* 443(7112): 651-657.
- Di Paolo, G., S. Sankaranarayanan, et al. (2002). "Decreased synaptic vesicle recycling efficiency and cognitive deficits in amphiphysin 1 knockout mice." *Neuron* 33(5): 789-804.
- Dong, J., R. Misselwitz, et al. (2000). "Expression and purification of dynamin II domains and initial studies on structure and function." *Protein expression and purification* 20(2): 314-323.
- Doran, P., P. Donoghue, et al. (2009). "Proteomics of skeletal muscle aging." *Proteomics* 9(4): 989-1003.
- Dove, S. K., F. T. Cooke, et al. (1997). "Osmotic stress activates phosphatidylinositol-3,5-bisphosphate synthesis." *Nature* 390(6656): 187-192.
- Dove, S. K. and Z. E. Johnson (2007). "Our FABulous VACation: a decade of phosphatidylinositol 3,5-bisphosphate." *Cell Biology of Inositol Lipids and Phosphates* 74: 129-139.
- Dowling, J. J., A. P. Vreede, et al. (2009). "Loss of myotubularin function results in T-tubule disorganization in zebrafish and human myotubular myopathy." *PLoS Genet* 5(2): e1000372.
- DuHadaway, J. B., D. Sakamuro, et al. (2001). "Bin1 mediates apoptosis by c-Myc in transformed primary cells." *Cancer Res* 61(7): 3151-3156.
- Durieux, A. C., S. Vassilopoulos, et al. (2012). "A centronuclear myopathy--dynamin 2 mutation impairs autophagy in mice." *Traffic* 13(6): 869-879.
- Durieux, A. C., A. Vignaud, et al. (2010). "A centronuclear myopathy-dynamin 2 mutation impairs skeletal muscle structure and function in mice." *Human molecular genetics* 19(24): 4820-4836.
- Eastwood, A. B., C. Franzini-Armstrong, et al. (1982). "Structure of membranes in crayfish muscle: comparison of phasic and tonic fibres." *Journal of muscle research and cell motility* 3(3): 273-294.
- Eccleston, J. F., D. D. Binns, et al. (2002). "Oligomerization and kinetic mechanism of the dynamin GTPase." *European biophysics journal* : EBJ 31(4): 275-282.

- Elliott, K., K. Ge, et al. (2000). "The c-Myc-interacting adaptor protein Bin1 activates a caspase-independent cell death program." *Oncogene* 19(41): 4669-4684.
- Elliott, K., D. Sakamuro, et al. (1999). "Bin1 functionally interacts with Myc and inhibits cell proliferation via multiple mechanisms." *Oncogene* 18(24): 3564-3573.
- Ellis, J. D., M. Barrios-Rodiles, et al. (2012). "Tissue-Specific Alternative Splicing Remodels Protein-Protein Interaction Networks." *Molecular Cell* 46(6): 884-892.
- Engel, A. G. and C. Franzini-Armstrong (2004). *Myology*, McGraw-Hill.
- Farsad, K., N. Ringstad, et al. (2001). "Generation of high curvature membranes mediated by direct endophilin bilayer interactions." *J Cell Biol* 155(2): 193-200.
- Felder, E., F. Protasi, et al. (2002). "Morphology and molecular composition of sarcoplasmic reticulum surface junctions in the absence of DHPR and RyR in mouse skeletal muscle." *Biophysical Journal* 82(6): 3144-3149.
- Ferguson, S. M., A. Raimondi, et al. (2009). "Coordinated actions of actin and BAR proteins upstream of dynamin at endocytic clathrin-coated pits." *Dev Cell* 17(6): 811-822.
- Fernando, P., J. S. Sandoz, et al. (2009). "Bin1 SRC homology 3 domain acts as a scaffold for myofiber sarcomere assembly." *J Biol Chem* 284(40): 27674-27686.
- Fetalvero, K. M., Y. Yu, et al. (2013). "Defective autophagy and mTORC1 signaling in myotubularin null mice." *Molecular and cellular biology* 33(1): 98-110.
- Fetalvero, K. M., Y. Yu, et al. (2013). "Defective autophagy and mTORC1 signaling in myotubularin null mice." *Mol Cell Biol* 33(1): 98-110.
- Fill, M. and J. A. Copello (2002). "Ryanodine receptor calcium release channels." *Physiological reviews* 82(4): 893-922.
- Fischer, D., M. Herasse, et al. (2006). "Characterization of the muscle involvement in dynamin 2-related centronuclear myopathy." *Brain* 129(Pt 6): 1463-1469.
- Fliegel, L., M. Ohnishi, et al. (1987). "Amino acid sequence of rabbit fast-twitch skeletal muscle calsequestrin deduced from cDNA and peptide sequencing." *Proceedings of the National Academy of Sciences of the United States of America* 84(5): 1167-1171.
- Flucher, B. E. (1992). "Structural analysis of muscle development: transverse tubules, sarcoplasmic reticulum, and the triad." *Developmental biology* 154(2): 245-260.

- Flucher, B. E., S. B. Andrews, et al. (1994). "Molecular organization of transverse tubule/sarcoplasmic reticulum junctions during development of excitation-contraction coupling in skeletal muscle." *Molecular biology of the cell* 5(10): 1105-1118.
- Flucher, B. E. and C. Franzini-Armstrong (1996). "Formation of junctions involved in excitation-contraction coupling in skeletal and cardiac muscle." *Proceedings of the National Academy of Sciences of the United States of America* 93(15): 8101-8106.
- Flucher, B. E., M. E. Morton, et al. (1990). "Localization of the alpha 1 and alpha 2 subunits of the dihydropyridine receptor and ankyrin in skeletal muscle triads." *Neuron* 5(3): 339-351.
- Flucher, B. E., H. Takekura, et al. (1993). "Development of the excitation-contraction coupling apparatus in skeletal muscle: association of sarcoplasmic reticulum and transverse tubules with myofibrils." *Developmental biology* 160(1): 135-147.
- Flucher, B. E., M. Terasaki, et al. (1991). "Biogenesis of transverse tubules in skeletal muscle in vitro." *Developmental biology* 145(1): 77-90.
- Fourest-Lieuvin, A., J. Rendu, et al. (2012). "Role of triadin in the organization of reticulum membrane at the muscle triad." *Journal of cell science* 125(14): 3443-3453.
- Franzini-Armstrong, C. (1991). "Simultaneous maturation of transverse tubules and sarcoplasmic reticulum during muscle differentiation in the mouse." *Developmental biology* 146(2): 353-363.
- Franzini-Armstrong, C. and A. O. Jorgensen (1994). "Structure and development of E-C coupling units in skeletal muscle." *Annual review of physiology* 56: 509-534.
- Franzini-Armstrong, C., L. J. Kenney, et al. (1987). "The structure of calsequestrin in triads of vertebrate skeletal muscle: a deep-etch study." *The Journal of cell biology* 105(1): 49-56.
- Franzini-Armstrong, C. and G. Nunzi (1983). "Junctional feet and particles in the triads of a fast-twitch muscle fibre." *Journal of muscle research and cell motility* 4(2): 233-252.

- Frontera, W. R., D. Suh, et al. (2000). "Skeletal muscle fiber quality in older men and women." *American journal of physiology. Cell physiology* 279(3): C611-618.
- Frost, A., V. M. Unger, et al. (2009). "The BAR domain superfamily: membrane-molding macromolecules." *Cell* 137(2): 191-196.
- Fugier, C., A. F. Klein, et al. (2011). "Misregulated alternative splicing of BIN1 is associated with T tubule alterations and muscle weakness in myotonic dystrophy." *Nat Med* 17(6): 720-725.
- Galbiati, F., J. A. Engelman, et al. (2001). "Caveolin-3 null mice show a loss of caveolae, changes in the microdomain distribution of the dystrophin-glycoprotein complex, and T-tubule abnormalities." *Journal of Biological Chemistry* 276(24): 21425-21433.
- Gatti, G., P. Podini, et al. (1997). "Overexpression of calsequestrin in L6 myoblasts: Formation of endoplasmic reticulum subdomains and their evolution into discrete vacuoles where aggregates of the protein are specifically accumulated." *Molecular biology of the cell* 8(9): 1789-1803.
- Ge, K., J. DuHadaway, et al. (1999). "Mechanism for elimination of a tumor suppressor: aberrant splicing of a brain-specific exon causes loss of function of Bin1 in melanoma." *Proc Natl Acad Sci U S A* 96(17): 9689-9694.
- Ge, K., J. Duhadaway, et al. (2000). "Losses of the tumor suppressor BIN1 in breast carcinoma are frequent and reflect deficits in programmed cell death capacity." *Int J Cancer* 85(3): 376-383.
- Ge, K., F. Minhas, et al. (2000). "Loss of heterozygosity and tumor suppressor activity of Bin1 in prostate carcinoma." *Int J Cancer* 86(2): 155-161.
- Ghaneie, A., V. Zemba-Palko, et al. (2007). "Bin1 attenuation in breast cancer is correlated to nodal metastasis and reduced survival." *Cancer Biology & Therapy* 6(2): 192-194.
- Giannini, G. and V. Sorrentino (1995). "Molecular structure and tissue distribution of ryanodine receptors calcium channels." *Medicinal research reviews* 15(4): 313-323.

- Gilbert, R., J. A. Cohen, et al. (1999). "Identification of the A-band localization domain of myosin binding proteins C and H (MyBP-C, MyBP-H) in skeletal muscle." *Journal of cell science* 112 (Pt 1): 69-79.
- Gillooly, D. J., I. C. Morrow, et al. (2000). "Localization of phosphatidylinositol 3-phosphate in yeast and mammalian cells." *Embo J* 19(17): 4577-4588.
- Gold, E. S., D. M. Underhill, et al. (1999). "Dynamin 2 is required for phagocytosis in macrophages." *J Exp Med* 190(12): 1849-1856.
- Golini, L., C. Chouabe, et al. (2011). "Junctophilin 1 and 2 proteins interact with the L-type Ca²⁺ channel dihydropyridine receptors (DHPRs) in skeletal muscle." *The Journal of biological chemistry* 286(51): 43717-43725.
- Gouadon, E., R. P. Schuhmeier, et al. (2006). "A possible role of the junctional face protein JP-45 in modulating Ca²⁺ release in skeletal muscle." *The Journal of physiology* 572(Pt 1): 269-280.
- Grelle, G., S. Kostka, et al. (2006). "Identification of VCP/p97, carboxyl terminus of Hsp70-interacting protein (CHIP), and amphiphysin II interaction partners using membrane-based human proteome arrays." *Molecular & Cellular Proteomics* 5(2): 234-244.
- Hagiwara, Y., T. Sasaoka, et al. (2000). "Caveolin-3 deficiency causes muscle degeneration in mice." *Human molecular genetics* 9(20): 3047-3054.
- Hain, J., S. Nath, et al. (1994). "Phosphorylation modulates the function of the calcium release channel of sarcoplasmic reticulum from skeletal muscle." *Biophysical journal* 67(5): 1823-1833.
- Hamao, K., M. Morita, et al. (2009). "New function of the proline rich domain in dynamin-2 to negatively regulate its interaction with microtubules in mammalian cells." *Experimental cell research* 315(7): 1336-1345.
- Harris, J. B., M. A. Johnson, et al. (1974). "Proceedings: Histological and histochemical aspects of the effect of notexin on rat skeletal muscle." *British journal of pharmacology* 52(1): 152P.
- He, B., R. H. Tang, et al. (2012). "Enhancing muscle membrane repair by gene delivery of MG53 ameliorates muscular dystrophy and heart failure in delta-Sarcoglycan-

- deficient hamsters." *Molecular therapy : the journal of the American Society of Gene Therapy* 20(4): 727-735.
- Henley, J. R., E. W. Krueger, et al. (1998). "Dynamin-mediated internalization of caveolae." *The Journal of cell biology* 141(1): 85-99.
- Herman, G. E., K. Kopacz, et al. (2002). "Characterization of mutations in fifty North American patients with X- linked myotubular myopathy." *Hum Mutat* 19(2): 114-121.
- Herrmann-Frank, A. and M. Varsanyi (1993). "Enhancement of Ca²⁺ release channel activity by phosphorylation of the skeletal muscle ryanodine receptor." *FEBS letters* 332(3): 237-242.
- Hidalgo, C. and P. Donoso (1995). "Luminal calcium regulation of calcium release from sarcoplasmic reticulum." *Bioscience reports* 15(5): 387-397.
- Hinshaw, J. E. and S. L. Schmid (1995). "Dynamin self-assembles into rings suggesting a mechanism for coated vesicle budding." *Nature Cell Biol.* 374: 190-192.
- Hirata, Y., M. Brotto, et al. (2006). "Uncoupling store-operated Ca²⁺ entry and altered Ca²⁺ release from sarcoplasmic reticulum through silencing of junctophilin genes." *Biophysical Journal* 90(12): 4418-4427.
- Hnia, K., H. Tronchere, et al. (2011). "Myotubularin controls desmin intermediate filament architecture and mitochondrial dynamics in human and mouse skeletal muscle." *J Clin Invest* 121(1): 70-85.
- Hnia, K., I. Vaccari, et al. (2012). "Myotubularin phosphoinositide phosphatases: cellular functions and disease pathophysiology." *Trends Mol Med* 18(6): 317-327.
- Hofmann, P. A., M. L. Greaser, et al. (1991). "C-Protein Limits Shortening Velocity of Rabbit Skeletal-Muscle Fibers at Low-Levels of Ca²⁺ Activation." *Journal of Physiology-London* 439: 701-715.
- Hofmann, S. L., J. L. Goldstein, et al. (1989). "Molecular-Cloning of a Histidine-Rich Ca²⁺-Binding Protein of Sarcoplasmic-Reticulum That Contains Highly Conserved Repeated Elements." *Journal of Biological Chemistry* 264(30): 18083-18090.
- Hogarty, M. D., X. Liu, et al. (2000). "BIN1 inhibits colony formation and induces apoptosis in neuroblastoma cell lines with MYCN amplification." *Med Pediatr Oncol* 35(6): 559-562.

- Hong, T. T., R. Cogswell, et al. (2012). "Plasma BIN1 correlates with heart failure and predicts arrhythmia in patients with arrhythmogenic right ventricular cardiomyopathy." *Heart Rhythm* 9(6): 961-967.
- Hong, T. T., J. W. Smyth, et al. (2012). "BIN1 is reduced and Cav1.2 trafficking is impaired in human failing cardiomyocytes." *Heart Rhythm* 9(5): 812-820.
- Hong, T. T., J. W. Smyth, et al. (2010). "BIN1 localizes the L-type calcium channel to cardiac T-tubules." *PLoS Biol* 8(2): e1000312.
- Hu, X. L., E. Pickering, et al. (2011). "Meta-Analysis for Genome-Wide Association Study Identifies Multiple Variants at the BIN1 Locus Associated with Late-Onset Alzheimer's Disease." *Plos One* 6(2).
- Iles, D. E., F. Lehmann-Horn, et al. (1994). "Localization of the gene encoding the alpha 2/delta-subunits of the L-type voltage-dependent calcium channel to chromosome 7q and analysis of the segregation of flanking markers in malignant hyperthermia susceptible families." *Human molecular genetics* 3(6): 969-975.
- Inesi, G., M. Kurzmack, et al. (1980). "Cooperative calcium binding and ATPase activation in sarcoplasmic reticulum vesicles." *The Journal of biological chemistry* 255(7): 3025-3031.
- Ishikawa, H. (1968). "Formation of elaborate networks of T-system tubules in cultured skeletal muscle with special reference to the T-system formation." *The Journal of cell biology* 38(1): 51-66.
- Ito, K., S. Komazaki, et al. (2001). "Deficiency of triad junction and contraction in mutant skeletal muscle lacking junctophilin type 1." *The Journal of cell biology* 154(5): 1059-1067.
- Jay, S. D., A. H. Sharp, et al. (1991). "Structural Characterization of the Dihydropyridine-Sensitive Calcium-Channel Alpha-2-Subunit and the Associated Delta-Peptides." *Journal of Biological Chemistry* 266(5): 3287-3293.
- Jayaraman, T., A. M. Brillantes, et al. (1992). "FK506 binding protein associated with the calcium release channel (ryanodine receptor)." *The Journal of biological chemistry* 267(14): 9474-9477.
- Jeannet, P. Y., G. Bassez, et al. (2004). "Clinical and histologic findings in autosomal centronuclear myopathy." *Neurology* 62(9): 1484-1490.

- Jones, L. R., Y. J. Suzuki, et al. (1998). "Regulation of Ca²⁺ signaling in transgenic mouse cardiac myocytes overexpressing calsequestrin." *The Journal of clinical investigation* 101(7): 1385-1393.
- Jones, L. R., L. Zhang, et al. (1995). "Purification, primary structure, and immunological characterization of the 26-kDa calsequestrin binding protein (junctin) from cardiac junctional sarcoplasmic reticulum." *The Journal of biological chemistry* 270(51): 30787-30796.
- Jorgensen, A. O., A. C. Y. Shen, et al. (1993). "The Ca²⁺-Release Channel Ryanodine Receptor Is Localized in Junctional and Corbular Sarcoplasmic-Reticulum in Cardiac-Muscle." *Journal of Cell Biology* 120(4): 969-980.
- Joubert, R., A. Vignaud, et al. (2013). "Site-specific Mtm1 mutagenesis by an AAV-Cre vector reveals that myotubularin is essential in adult muscle." *Human Molecular Genetics* 22(9): 1856-1866.
- Jungbluth, H., C. Wallgren-Pettersson, et al. (2008). "Centronuclear (myotubular) myopathy." *Orphanet J Rare Dis* 3: 26.
- Kadi, F., N. Charifi, et al. (2004). "Satellite cells and myonuclei in young and elderly women and men." *Muscle & nerve* 29(1): 120-127.
- Kadlec, L. and A. M. Pendergast (1997). "The amphiphysin-like protein 1 (ALP1) interacts functionally with the cABL tyrosine kinase and may play a role in cytoskeletal regulation." *Proceedings of the National Academy of Sciences of the United States of America* 94(23): 12390-12395.
- Kennah, E., A. Ringrose, et al. (2009). "Identification of tyrosine kinase, HCK, and tumor suppressor, BIN1, as potential mediators of AHI-1 oncogene in primary and transformed CTCL cells." *Blood* 113(19): 4646-4655.
- Kessels, M. M., A. E. Engqvist-Goldstein, et al. (2001). "Mammalian Abp1, a signal-responsive F-actin-binding protein, links the actin cytoskeleton to endocytosis via the GTPase dynamin." *The Journal of cell biology* 153(2): 351-366.
- Kim, E., D. W. Shin, et al. (2003). "Increased Ca²⁺ storage capacity in the sarcoplasmic reticulum by overexpression of HRC (histidine-rich Ca²⁺ binding protein)." *Biochemical and biophysical research communications* 300(1): 192-196.

- Kim, K. C., A. H. Caswell, et al. (1990). "Identification of a new subpopulation of triad junctions isolated from skeletal muscle; morphological correlations with intact muscle." *The Journal of membrane biology* 113(3): 221-235.
- Kinney, E. L., S. Tanida, et al. (2008). "Adenovirus E1A oncoprotein liberates c-Myc activity to promote cell proliferation through abating Bin1 expression via an Rb/E2F1-dependent mechanism." *Journal of cellular physiology* 216(3): 621-631.
- Klein, D. E., A. Lee, et al. (1998). "The pleckstrin homology domains of dynamin isoforms require oligomerization for high affinity phosphoinositide binding." *The Journal of biological chemistry* 273(42): 27725-27733.
- Klinge, L., J. Harris, et al. (2010). "Dysferlin associates with the developing T-tubule system in rodent and human skeletal muscle." *Muscle & nerve* 41(2): 166-173.
- Klinge, L., S. Laval, et al. (2007). "From T-tubule to sarcolemma: damage-induced dysferlin translocation in early myogenesis." *FASEB journal : official publication of the Federation of American Societies for Experimental Biology* 21(8): 1768-1776.
- Knudson, C. M., K. K. Stang, et al. (1993). "Biochemical characterization of ultrastructural localization of a major junctional sarcoplasmic reticulum glycoprotein (triadin)." *The Journal of biological chemistry* 268(17): 12637-12645.
- Kobayashi, Y. M., B. A. Alseikhan, et al. (2000). "Localization and characterization of the calsequestrin-binding domain of triadin 1. Evidence for a charged beta-strand in mediating the protein-protein interaction." *The Journal of biological chemistry* 275(23): 17639-17646.
- Kockskemper, J., A. V. Zima, et al. (2008). "Emerging roles of inositol 1,4,5-trisphosphate signaling in cardiac myocytes." *Journal of molecular and cellular cardiology* 45(2): 128-147.
- Kojima, C., A. Hashimoto, et al. (2004). "Regulation of Bin1 SH3 domain binding by phosphoinositides." *Embo J* 23(22): 4413-4422.
- Komazaki, S., K. Ito, et al. (2002). "Deficiency of triad formation in developing skeletal muscle cells lacking junctophilin type 1." *FEBS letters* 524(1-3): 225-229.
- Komazaki, S., M. Nishi, et al. (1999). "Immunolocalization of mitsugumin29 in developing skeletal muscle and effects of the protein expressed in amphibian

- embryonic cells." *Developmental dynamics : an official publication of the American Association of Anatomists* 215(2): 87-95.
- Komazaki, S., M. Nishi, et al. (2001). "Abnormal formation of sarcoplasmic reticulum networks and triads during early development of skeletal muscle cells in mitsugumin29-deficient mice." *Development, growth & differentiation* 43(6): 717-723.
- Kreitzer, G., A. Marmorstein, et al. (2000). "Kinesin and dynamin are required for post-Golgi transport of a plasma-membrane protein." *Nature cell biology* 2(2): 125-127.
- Kurebayashi, N. and Y. Ogawa (1991). "Discrimination of Ca(2+)-ATPase activity of the sarcoplasmic reticulum from actomyosin-type ATPase activity of myofibrils in skinned mammalian skeletal muscle fibres: distinct effects of cyclopiazonic acid on the two ATPase activities." *Journal of muscle research and cell motility* 12(4): 355-365.
- Labeit, S. and B. Kolmerer (1995). "The complete primary structure of human nebulin and its correlation to muscle structure." *Journal of molecular biology* 248(2): 308-315.
- Lacerda, A. E., H. S. Kim, et al. (1991). "Normalization of current kinetics by interaction between the alpha 1 and beta subunits of the skeletal muscle dihydropyridine-sensitive Ca²⁺ channel." *Nature* 352(6335): 527-530.
- Lai, F. A., M. Dent, et al. (1992). "Expression of a cardiac Ca(2+)-release channel isoform in mammalian brain." *The Biochemical journal* 288 (Pt 2): 553-564.
- Lai, F. A., H. P. Erickson, et al. (1988). "Purification and reconstitution of the calcium release channel from skeletal muscle." *Nature* 331(6154): 315-319.
- Lambert, J. C., D. Zelenika, et al. (2011). "Evidence of the association of BIN1 and PICALM with the AD risk in contrasting European populations." *Neurobiology of Aging* 32(4).
- Laporte, J., F. Bedez, et al. (2003). "Myotubularins, a large disease-associated family of cooperating catalytically active and inactive phosphoinositides phosphatases." *Hum Mol Genet* 12 Spec No 2: R285-292.

- Laporte, J., V. Biancalana, et al. (2000). "MTM1 mutations in X-linked myotubular myopathy." *Hum Mutat* 15(5): 393-409.
- Laporte, J., F. Blondeau, et al. (2002). "The PtdIns3P phosphatase myotubularin is a cytoplasmic protein that also localizes to Rac1-inducible plasma membrane ruffles." *J Cell Sci* 115(Pt 15): 3105-3117.
- Laporte, J., L. J. Hu, et al. (1996). "A gene mutated in X-linked myotubular myopathy defines a new putative tyrosine phosphatase family conserved in yeast." *Nat Genet* 13(2): 175-182.
- Larsson, L., X. Li, et al. (1997). "Effects of aging on shortening velocity and myosin isoform composition in single human skeletal muscle cells." *The American journal of physiology* 272(2 Pt 1): C638-649.
- Lau, Y. H., A. H. Caswell, et al. (1977). "Isolation of transverse tubules by fractionation of triad junctions of skeletal muscle." *The Journal of biological chemistry* 252(15): 5565-5574.
- Laver, D. R., T. M. Baynes, et al. (1997). "Magnesium inhibition of ryanodine-receptor calcium channels: evidence for two independent mechanisms." *The Journal of membrane biology* 156(3): 213-229.
- Lawlor, M. W., M. S. Alexander, et al. (2012). "Myotubularin-deficient myoblasts display increased apoptosis, delayed proliferation, and poor cell engraftment." *Am J Pathol* 181(3): 961-968.
- Lawlor, M. W., M. S. Alexander, et al. (2012). "Myotubularin-deficient myoblasts display increased apoptosis, delayed proliferation, and poor cell engraftment." *The American journal of pathology* 181(3): 961-968.
- Leberer, E., B. G. Timms, et al. (1990). "Purification, calcium binding properties, and ultrastructural localization of the 53,000- and 160,000 (sarcalumenin)-dalton glycoproteins of the sarcoplasmic reticulum." *The Journal of biological chemistry* 265(17): 10118-10124.
- Lecompte, O., O. Poch, et al. (2008). "PtdIns5P regulation through evolution: roles in membrane trafficking?" *Trends Biochem Sci* 33(10): 453-460.
- Lee, E., M. Marcucci, et al. (2002). "Amphiphysin 2 (Bin1) and T-tubule biogenesis in muscle." *Science* 297(5584): 1193-1196.

- Lee, H. G., H. Kang, et al. (2001). "Interaction of HRC (histidine-rich Ca²⁺-binding protein) and triadin in the lumen of sarcoplasmic reticulum." *The Journal of biological chemistry* 276(43): 39533-39538.
- Lee, J. H., R. Cheng, et al. (2011). "Identification of Novel Loci for Alzheimer Disease and Replication of CLU, PICALM, and BIN1 in Caribbean Hispanic Individuals." *Archives of neurology* 68(3): 320-328.
- Lee, K. J., C. S. Park, et al. (2012). "Mitsugumin 53 attenuates the activity of sarcoplasmic reticulum Ca²⁺-ATPase 1a (SERCA1a) in skeletal muscle." *Biochemical and biophysical research communications* 428(3): 383-388.
- Leprince, C., F. Romero, et al. (1997). "A new member of the amphiphysin family connecting endocytosis and signal transduction pathways." *Faseb Journal* 11(9): A928-A928.
- Lin, H. C., B. Barylko, et al. (1997). "Phosphatidylinositol (4,5)-bisphosphate-dependent activation of dynamins I and II lacking the proline/arginine-rich domains." *The Journal of biological chemistry* 272(41): 25999-26004.
- Lin Shiau, S. Y., M. C. Huang, et al. (1976). "Mechanism of action of cobra cardiotoxin in the skeletal muscle." *The Journal of pharmacology and experimental therapeutics* 196(3): 758-770.
- Littlefield, R., A. Almenar-Queralt, et al. (2001). "Actin dynamics at pointed ends regulates thin filament length in striated muscle." *Nature Cell Biology* 3(6): 544-551.
- Liu, Y. W., M. C. Surka, et al. (2008). "Isoform and splice-variant specific functions of dynamin-2 revealed by analysis of conditional knock-out cells." *Molecular Biology of the Cell* 19(12): 5347-5359.
- Lo, H. P., S. T. Cooper, et al. (2008). "Limb-girdle muscular dystrophy: diagnostic evaluation, frequency and clues to pathogenesis." *Neuromuscular disorders : NMD* 18(1): 34-44.
- Ma, J., K. Anderson, et al. (1993). "Effects of perchlorate on the molecules of excitation-contraction coupling of skeletal and cardiac muscle." *The Journal of general physiology* 102(3): 423-448.

- MacLennan, D. H., C. J. Brandl, et al. (1985). "Amino-acid sequence of a Ca^{2+} + Mg^{2+} -dependent ATPase from rabbit muscle sarcoplasmic reticulum, deduced from its complementary DNA sequence." *Nature* 316(6030): 696-700.
- MacLennan, D. H. and P. T. Wong (1971). "Isolation of a calcium-sequestering protein from sarcoplasmic reticulum." *Proceedings of the National Academy of Sciences of the United States of America* 68(6): 1231-1235.
- Maier, O., M. Knoblich, et al. (1996). "Dynamin II binds to the trans-Golgi network." *Biochemical and biophysical research communications* 223(2): 229-233.
- Malouf, N. N. and P. E. Wilson (1986). "Proliferation of the surface-connected intracytoplasmic membranous network in skeletal muscle disease." *The American journal of pathology* 125(2): 358-368.
- Mao, N. C., E. Steingrimsson, et al. (1999). "The murine Bin1 gene functions early in myogenesis and defines a new region of synteny between mouse chromosome 18 and human chromosome 2." *Genomics* 56(1): 51-58.
- Marks, A. R., M. B. Taubman, et al. (1991). "The Ryanodine Receptor Junctional Channel Complex Is Regulated by Growth-Factors in a Myogenic Cell-Line." *Journal of Cell Biology* 114(2): 303-312.
- Marks, B. and H. T. McMahon (1998). "Calcium triggers calcineurin-dependent synaptic vesicle recycling in mammalian nerve terminals." *Molecular Biology of the Cell* 9: 341a-341a.
- Martonosi, A. (1982). "The development of sarcoplasmic reticulum membranes." *Annual review of physiology* 44: 337-355.
- Marty, I., J. Faure, et al. (2009). "Triadin: what possible function 20 years later ?" *Journal of Physiology-London* 587(13): 3117-3121.
- Marty, I., D. Thevenon, et al. (2000). "Cloning and characterization of a new isoform of skeletal muscle triadin." *The Journal of biological chemistry* 275(11): 8206-8212.
- Masoodi, T. A., S. A. Al Shammari, et al. (2013). "Exploration of deleterious single nucleotide polymorphisms in late-onset Alzheimer disease susceptibility genes." *Gene* 512(2): 429-437.

- Matsuda, C., Y. K. Hayashi, et al. (2001). "The sarcolemmal proteins dysferlin and caveolin-3 interact in skeletal muscle." *Human molecular genetics* 10(17): 1761-1766.
- Mauro, A. (1961). "Satellite cell of skeletal muscle fibers." *The Journal of biophysical and biochemical cytology* 9: 493-495.
- McEntagart, M., G. Parsons, et al. (2002). "Genotype-phenotype correlations in X-linked myotubular myopathy." *Neuromuscul Disord* 12(10): 939-946.
- McMahon, H. T., P. Wigge, et al. (1997). "Clathrin interacts specifically with amphiphysin and is displaced by dynamin." *Febs Letters* 413(2): 319-322.
- McPherson, P. S., E. P. Garcia, et al. (1996). "A presynaptic inositol-5-phosphatase." *Nature* 379(6563): 353-357.
- Meunier, B., M. Quaranta, et al. (2009). "The membrane-tubulating potential of amphiphysin 2/BIN1 is dependent on the microtubule-binding cytoplasmic linker protein 170 (CLIP-170)." *Eur J Cell Biol* 88(2): 91-102.
- Meyer-Ficca, M. L., R. G. Meyer, et al. (2005). "Poly(ADP-ribose) polymerases: managing genome stability." *The international journal of biochemistry & cell biology* 37(5): 920-926.
- Micheva, K. D., A. R. Ramjaun, et al. (1997). "SH3 domain dependent interactions of endophilin with amphiphysin (vol 414, pg 308, 1997)." *Febs Letters* 419(1): 150-150.
- Mikami, A., K. Imoto, et al. (1989). "Primary structure and functional expression of the cardiac dihydropyridine-sensitive calcium channel." *Nature* 340(6230): 230-233.
- Minetti, C., F. Sotgia, et al. (1998). "Mutations in the caveolin-3 gene cause autosomal dominant limb-girdle muscular dystrophy." *Nature genetics* 18(4): 365-368.
- Morton, M. E., J. M. Caffrey, et al. (1988). "Monoclonal antibody to the alpha 1-subunit of the dihydropyridine-binding complex inhibits calcium currents in BC3H1 myocytes." *The Journal of biological chemistry* 263(2): 613-616.
- Muhlberg, A. B., D. E. Warnock, et al. (1997). "Domain structure and intramolecular regulation of dynamin GTPase." *The EMBO journal* 16(22): 6676-6683.
- Muller, A. J., J. F. Baker, et al. (2003). "Targeted disruption of the murine Bin1/Amphiphysin II gene does not disable endocytosis but results in embryonic

- cardiomyopathy with aberrant myofibril formation." *Mol Cell Biol* 23(12): 4295-4306.
- Munn, A. L., B. J. Stevenson, et al. (1995). "End5, End6, and End7 - Mutations That Cause Actin Delocalization and Block the Internalization Step of Endocytosis in *Saccharomyces-Cerevisiae*." *Molecular Biology of the Cell* 6(12): 1721-1742.
- Nair, U. and D. J. Klionsky (2011). "Activation of autophagy is required for muscle homeostasis during physical exercise." *Autophagy* 7(12): 1405-1406.
- Nakata, T., A. Iwamoto, et al. (1991). "Predominant and developmentally regulated expression of dynamin in neurons." *Neuron* 7(3): 461-469.
- Nakata, T., R. Takemura, et al. (1993). "A Novel Member of the Dynamin Family of Gtp-Binding Proteins Is Expressed Specifically in the Testis." *Journal of Cell Science* 105: 1-5.
- Nakayama, H., M. Taki, et al. (1991). "Identification of 1,4-Dihydropyridine Binding Regions within the Alpha-1 Subunit of Skeletal-Muscle Ca²⁺ Channels by Photoaffinity-Labeling with Diazipine." *Proceedings of the National Academy of Sciences of the United States of America* 88(20): 9203-9207.
- Negorev, D., H. Riethman, et al. (1996). "The Bin1 Gene Localizes to Human Chromosome 2q14 by PCR Analysis of Somatic Cell Hybrids and Fluorescence in Situ Hybridization." *Genomics* 33(2): 329-331.
- Nicot, A. S. and J. Laporte (2008). "Endosomal phosphoinositides and human diseases." *Traffic* 9(8): 1240-1249.
- Nicot, A. S., A. Toussaint, et al. (2007). "Mutations in amphiphysin 2 (BIN1) disrupt interaction with dynamin 2 and cause autosomal recessive centronuclear myopathy." *Nat Genet* 39(9): 1134-1139.
- Nishi, M., S. Komazaki, et al. (1999). "Abnormal features in skeletal muscle from mice lacking mitsugumin29." *The Journal of cell biology* 147(7): 1473-1480.
- Noda, T., K. Matsunaga, et al. (2010). "Regulation of membrane biogenesis in autophagy via PI3P dynamics." *Seminars in cell & developmental biology* 21(7): 671-676.

- Noda, Y., T. Nakata, et al. (1993). "Localization of dynamin: widespread distribution in mature neurons and association with membranous organelles." *Neuroscience* 55(1): 113-127.
- Oddoux, S., J. Brocard, et al. (2009). "Triadin deletion induces impaired skeletal muscle function." *The Journal of biological chemistry* 284(50): 34918-34929.
- Owen, D. J., P. Wigge, et al. (1998). "Crystal structure of the amphiphysin-2 SH3 domain and its role in the prevention of dynamin ring formation." *Embo Journal* 17(18): 5273-5285.
- Pan, K., X. T. Liang, et al. (2012). "Characterization of Bridging Integrator 1 (BIN1) as a Potential Tumor Suppressor and Prognostic Marker in Hepatocellular Carcinoma." *Molecular Medicine* 18(3): 507-518.
- Pant, S., M. Sharma, et al. (2009). "AMPH-1/Amphiphysin/Bin1 functions with RME-1/Ehd1 in endocytic recycling." *Nat Cell Biol* 11(12): 1399-1410.
- Parton, R. G., M. Way, et al. (1997). "Caveolin-3 associates with developing T-tubules during muscle differentiation." *The Journal of cell biology* 136(1): 137-154.
- Peachey, L. D. (1965). "The sarcoplasmic reticulum and transverse tubules of the frog's sartorius." *The Journal of cell biology* 25(3): Suppl:209-231.
- Peng, M., H. Fan, et al. (1994). "Structural diversity of triadin in skeletal muscle and evidence of its existence in heart." *FEBS letters* 348(1): 17-20.
- Perez-Reyes, E., A. Castellano, et al. (1992). "Cloning and expression of a cardiac/brain beta subunit of the L-type calcium channel." *The Journal of biological chemistry* 267(3): 1792-1797.
- Person, V., S. Kostin, et al. (2000). "Antisense oligonucleotide experiments elucidate the essential role of titin in sarcomerogenesis in adult rat cardiomyocytes in long-term culture." *Journal of cell science* 113 Pt 21: 3851-3859.
- Peter, B. J., H. M. Kent, et al. (2004). "BAR domains as sensors of membrane curvature: the amphiphysin BAR structure." *Science* 303(5657): 495-499.
- Piccolo, F., S. A. Moore, et al. (2000). "Intracellular accumulation and reduced sarcolemmal expression of dysferlin in limb-girdle muscular dystrophies." *Annals of Neurology* 48(6): 902-912.

- Pincon-Raymond, M., F. Rieger, et al. (1985). "Abnormal transverse tubule system and abnormal amount of receptors for Ca²⁺ channel inhibitors of the dihydropyridine family in skeletal muscle from mice with embryonic muscular dysgenesis." *Developmental biology* 112(2): 458-466.
- Pineda-Lucena, A., C. S. W. Ho, et al. (2005). "A structure-based model of the c-Myc/Bin1 protein interaction shows alternative splicing of Bin1 and c-Myc phosphorylation are key binding determinants." *Journal of Molecular Biology* 351(1): 182-194.
- Porter, K. R. and G. E. Palade (1957). "Studies on the endoplasmic reticulum. III. Its form and distribution in striated muscle cells." *The Journal of biophysical and biochemical cytology* 3(2): 269-300.
- Posterino, G. S. and G. D. Lamb (2003). "Effect of sarcoplasmic reticulum Ca²⁺ content on action potential-induced Ca²⁺ release in rat skeletal muscle fibres." *The Journal of physiology* 551(Pt 1): 219-237.
- Praefcke, G. J. and H. T. McMahon (2004). "The dynamin superfamily: universal membrane tubulation and fission molecules?" *Nat Rev Mol Cell Biol* 5(2): 133-147.
- Prendergast G.C, M. A. J., Ramalingam A and Chang M.Y (2009). "Bar the door : cancer suppression by amphiphysin-like genes." *Biochemica et Biophysica Acta* 1795(1): 25-36.
- Protasi, F., C. Franzini-Armstrong, et al. (1998). "Role of ryanodine receptors in the assembly of calcium release units in skeletal muscle." *The Journal of cell biology* 140(4): 831-842.
- Protasi, F., C. Franzini-Armstrong, et al. (1997). "Coordinated incorporation of skeletal muscle dihydropyridine receptors and ryanodine receptors in peripheral couplings of BC3H1 cells." *The Journal of cell biology* 137(4): 859-870.
- Protasi, F., X. H. Sun, et al. (1996). "Formation and maturation of the calcium release apparatus in developing and adult avian myocardium." *Developmental biology* 173(1): 265-278.

- Protasi, F., H. Takekura, et al. (2000). "RYR1 and RYR3 have different roles in the assembly of calcium release units of skeletal muscle." *Biophysical Journal* 79(5): 2494-2508.
- Pyndiah, S., S. Tanida, et al. (2011). "c-MYC Suppresses BIN1 to Release Poly(ADP-Ribose) Polymerase 1: A Mechanism by Which Cancer Cells Acquire Cisplatin Resistance." *Science Signaling* 4(166).
- Qualmann, B., J. Roos, et al. (1999). "Syndapin I, a synaptic dynamin binding protein that associates with the neural Wiskott-Aldrich syndrome protein." *Molecular Biology of the Cell* 10(2): 501-513.
- Raj, T., J. M. Shulman, et al. (2012). "Alzheimer disease susceptibility loci: evidence for a protein network under natural selection." *American journal of human genetics* 90(4): 720-726.
- Ramalingam, A., G. E. Farmer, et al. (2007). "Bin1 interacts with and restrains the DNA end-binding protein complex Ku." *Cell cycle* 6(15): 1914-1918.
- Ramjaun, A. R. and P. S. McPherson (1998). "Multiple amphiphysin II splice variants display differential clathrin binding: identification of two distinct clathrin-binding sites." *J Neurochem* 70(6): 2369-2376.
- Ramjaun, A. R., K. D. Micheva, et al. (1997). "Identification and characterization of a nerve terminal-enriched amphiphysin isoform." *J Biol Chem* 272(26): 16700-16706.
- Razzaq, A., I. M. Robinson, et al. (2001). "Amphiphysin is necessary for organization of the excitation-contraction coupling machinery of muscles, but not for synaptic vesicle endocytosis in *Drosophila*." *Genes Dev* 15(22): 2967-2979.
- Rezgui, S. S., S. Vassilopoulos, et al. (2005). "Triadin (Trisk 95) overexpression blocks excitation-contraction coupling in rat skeletal myotubes." *The Journal of biological chemistry* 280(47): 39302-39308.
- Rieger, F., M. Pincon-Raymond, et al. (1987). "Excitation-contraction uncoupling in the developing skeletal muscle of the muscular dysgenesis mouse embryo." *Biochimie* 69(4): 411-417.
- Ringstad, N., Y. Nemoto, et al. (1997). "The SH3p4/Sh3p8/SH3p13 protein family: Binding partners for synaptojanin and dynamin via a Grb2-like Src homology 3

- domain." *Proceedings of the National Academy of Sciences of the United States of America* 94(16): 8569-8574.
- Rios, E., J. J. Ma, et al. (1991). "The mechanical hypothesis of excitation-contraction (EC) coupling in skeletal muscle." *Journal of muscle research and cell motility* 12(2): 127-135.
- Rizo, J. and T. C. Sudhof (1998). "C2-domains, structure and function of a universal Ca²⁺-binding domain." *The Journal of biological chemistry* 273(26): 15879-15882.
- Robb, S. A., C. A. Sewry, et al. (2011). "Impaired neuromuscular transmission and response to acetylcholinesterase inhibitors in centronuclear myopathies." *Neuromuscular disorders : NMD* 21(6): 379-386.
- Romero, N. B. (2010). "Centronuclear myopathies: a widening concept." *Neuromuscul Disord* 20(4): 223-228.
- Romero, N. B. and M. Bitoun (2011). "Centronuclear myopathies." *Semin Pediatr Neurol* 18(4): 250-256.
- Romero, N. B. and N. F. Clarke (2013). "Congenital myopathies." *Handbook of clinical neurology* 113: 1321-1336.
- Romero, N. B. and J. Laporte (2013). *Muscle disease: Pathology and Genetics; Chapter 13: Centronuclear myopathies*, Wiley & Blackwell
- Routhier, E. L., P. S. Donover, et al. (2003). "hob1+, the fission yeast homolog of Bin1, is dispensable for endocytosis or actin organization, but required for the response to starvation or genotoxic stress." *Oncogene* 22(5): 637-648.
- Royer, B., K. Hnia, et al. (2013). "The myotubularin-amphiphysin 2 complex in membrane tubulation and centronuclear myopathies." *EMBO reports*.
- Sakamuro, D., K. J. Elliott, et al. (1996). "BIN1 is a novel MYC-interacting protein with features of a tumour suppressor." *Nature Genetics* 14(1): 69-77.
- Sato, Y., D. G. Ferguson, et al. (1998). "Cardiac-specific overexpression of mouse cardiac calsequestrin is associated with depressed cardiovascular function and hypertrophy in transgenic mice." *Journal of Biological Chemistry* 273(43): 28470-28477.

- Schafer, D. A., S. A. Weed, et al. (2002). "Dynamin2 and cortactin regulate actin assembly and filament organization." *Current biology : CB* 12(21): 1852-1857.
- Schaletzky, J., S. K. Dove, et al. (2003). "Phosphatidylinositol-5-phosphate activation and conserved substrate specificity of the myotubularin phosphatidylinositol 3-phosphatases." *Curr Biol* 13(6): 504-509.
- Schiaffino, S., M. Cantini, et al. (1977). "T-system formation in cultured rat skeletal tissue." *Tissue & cell* 9(3): 437-446.
- Schredelseker, J., V. Di Biase, et al. (2005). "The beta(1a) subunit is essential for the assembly of dihydropyridine-receptor arrays in skeletal muscle." *Proceedings of the National Academy of Sciences of the United States of America* 102(47): 17219-17224.
- Seeger, R. C., G. M. Brodeur, et al. (1985). "Association of Multiple Copies of the N-Myc Oncogene with Rapid Progression of Neuroblastomas." *New England Journal of Medicine* 313(18): 1111-1116.
- Selcen, D., G. Stilling, et al. (2001). "The earliest pathologic alterations in dysferlinopathy." *Neurology* 56(11): 1472-1481.
- Seshadri, S., A. L. Fitzpatrick, et al. (2010). "Genome-wide analysis of genetic loci associated with Alzheimer disease." *JAMA : the journal of the American Medical Association* 303(18): 1832-1840.
- Sever, S., A. B. Muhlberg, et al. (1999). "Impairment of dynamin's GAP domain stimulates receptor-mediated endocytosis." *Nature* 398(6727): 481-486.
- Shen, X., C. Franzini-Armstrong, et al. (2007). "Triadins modulate intracellular Ca(2+) homeostasis but are not essential for excitation-contraction coupling in skeletal muscle." *The Journal of biological chemistry* 282(52): 37864-37874.
- Shpetner, H. S. and R. B. Vallee (1989). "Identification of Dynamin, a Novel Mechanochemical Enzyme That Mediates Interactions between Microtubules." *Cell* 59(3): 421-432.
- Shupliakov, O., P. Low, et al. (1997). "Synaptic vesicle endocytosis impaired by disruption of dynamin-SH3 domain interactions." *Science* 276(5310): 259-263.

- Simionescu-Bankston, A., G. Leoni, et al. (2013). "The N-BAR domain protein, Bin3, regulates Rac1- and Cdc42-dependent processes in myogenesis." *Developmental biology*.
- Sitsapesan, R. and A. J. Williams (1990). "Mechanisms of caffeine activation of single calcium-release channels of sheep cardiac sarcoplasmic reticulum." *The Journal of physiology* 423: 425-439.
- Sitsapesan, R. and A. J. Williams (1997). "Regulation of current flow through ryanodine receptors by luminal Ca²⁺." *Journal of Membrane Biology* 159(3): 179-185.
- Slepnev, V. I., G. C. Ochoa, et al. (1998). "Role of phosphorylation in regulation of the assembly of endocytic coat complexes." *Science* 281(5378): 821-824.
- Smirnova, E., D. L. Shurland, et al. (1999). "A model for dynamin self-assembly based on binding between three different protein domains." *Journal of Biological Chemistry* 274(21): 14942-14947.
- Smith, J. S., R. Coronado, et al. (1985). "Sarcoplasmic reticulum contains adenine nucleotide-activated calcium channels." *Nature* 316(6027): 446-449.
- Sparks, A. B., N. G. Hoffman, et al. (1996). "Cloning of ligand targets: systematic isolation of SH3 domain-containing proteins." *Nature biotechnology* 14(6): 741-744.
- Spiegelhalter, C., V. Tosch, et al. (2010). "From dynamic live cell imaging to 3D ultrastructure: novel integrated methods for high pressure freezing and correlative light-electron microscopy." *PLoS One* 5(2): e9014.
- Spiro, A. J., G. M. Shy, et al. (1966). "Myotubular myopathy. Persistence of fetal muscle in an adolescent boy." *Arch Neurol* 14(1): 1-14.
- Srivastava, S., Z. Li, et al. (2005). "The phosphatidylinositol 3-phosphate phosphatase myotubularin-related protein 6 (MTMR6) is a negative regulator of the Ca²⁺-activated K⁺ channel KCa3.1." *Mol Cell Biol* 25(9): 3630-3638.
- Sun, X. H., F. Protasi, et al. (1995). "Molecular architecture of membranes involved in excitation-contraction coupling of cardiac muscle." *The Journal of cell biology* 129(3): 659-671.
- Takei, K., V. I. Slepnev, et al. (1999). "Functional partnership between amphiphysin and dynamin in clathrin-mediated endocytosis." *Nat Cell Biol* 1(1): 33-39.

- Takekura, H., B. E. Flucher, et al. (2001). "Sequential docking, molecular differentiation, and positioning of T-Tubule/SR junctions in developing mouse skeletal muscle." *Developmental biology* 239(2): 204-214.
- Takekura, H., X. Sun, et al. (1994). "Development of the excitation-contraction coupling apparatus in skeletal muscle: peripheral and internal calcium release units are formed sequentially." *Journal of muscle research and cell motility* 15(2): 102-118.
- Takekura, H., S. Komazaki, et al. (2000). "Junctophilins: a novel family of junctional membrane complex proteins." *Molecular cell* 6(1): 11-22.
- Takekura, H., M. Shimuta, et al. (1998). "Mitsugumin29, a novel synaptophysin family member from the triad junction in skeletal muscle." *The Biochemical journal* 331 (Pt 1): 317-322.
- Tan, M. S., J. T. Yu, et al. (2013). "Bridging integrator 1 (BIN1): form, function, and Alzheimer's disease." *Trends in molecular medicine*.
- Tanabe, K. and K. Takei (2009). "Dynamic instability of microtubules requires dynamin 2 and is impaired in a Charcot-Marie-Tooth mutant." *Journal of Cell Biology* 185(6): 939-948.
- Tanabe, T., K. G. Beam, et al. (1988). "Restoration of excitation-contraction coupling and slow calcium current in dysgenic muscle by dihydropyridine receptor complementary DNA." *Nature* 336(6195): 134-139.
- Tanabe, T., H. Takeshima, et al. (1987). "Primary structure of the receptor for calcium channel blockers from skeletal muscle." *Nature* 328(6128): 313-318.
- Tang, Z. L., P. E. Scherer, et al. (1994). "The primary sequence of murine caveolin reveals a conserved consensus site for phosphorylation by protein kinase C." *Gene* 147(2): 299-300.
- Tanida, S., T. Mizoshita, et al. (2012). "Mechanisms of Cisplatin-Induced Apoptosis and of Cisplatin Sensitivity: Potential of BIN1 to Act as a Potent Predictor of Cisplatin Sensitivity in Gastric Cancer Treatment." *International journal of surgical oncology* 2012: 862879.
- Tanner, S. M., K. H. Orstavik, et al. (1999). "Skewed X-inactivation in a manifesting carrier of X-linked myotubular myopathy and in her non-manifesting carrier mother." *Hum Genet* 104(3): 249-253.

- Taylor, M. J., D. Perrais, et al. (2011). "A High Precision Survey of the Molecular Dynamics of Mammalian Clathrin-Mediated Endocytosis." *Plos Biology* 9(3).
- Thomas, N. S., H. Williams, et al. (1990). "X linked neonatal centronuclear/myotubular myopathy: evidence for linkage to Xq28 DNA marker loci." *Journal of medical genetics* 27(5): 284-287.
- Thompson, H. M., H. Cao, et al. (2004). "Dynamin 2 binds gamma-tubulin and participates in centrosome cohesion." *Nature cell biology* 6(4): 335-342.
- Tidball, J. G. (1991). "Myotendinous junction injury in relation to junction structure and molecular composition." *Exercise and sport sciences reviews* 19: 419-445.
- Tidball, J. G. (1995). "Inflammatory cell response to acute muscle injury." *Medicine and science in sports and exercise* 27(7): 1022-1032.
- Tjondrokoesoemo, A., N. Li, et al. (2013). "Type 1 inositol (1,4,5)-trisphosphate receptor activates ryanodine receptor 1 to mediate calcium spark signaling in adult mammalian skeletal muscle." *The Journal of biological chemistry* 288(4): 2103-2109.
- Tjondrokoesoemo, A., K. H. Park, et al. (2011). "Disrupted membrane structure and intracellular Ca(2)(+) signaling in adult skeletal muscle with acute knockdown of Bin1." *PLoS One* 6(9): e25740.
- Toussaint, A., B. S. Cowling, et al. (2011). "Defects in amphiphysin 2 (BIN1) and triads in several forms of centronuclear myopathies." *Acta Neuropathol* 121(2): 253-266.
- Toussaint, A., A. S. Nicot, et al. (2007). "[Mutations in amphiphysin 2 (BIN1) cause autosomal recessive centronuclear myopathy]." *Med Sci (Paris)* 23(12): 1080-1082.
- Trappe, S., P. Gallagher, et al. (2003). "Single muscle fibre contractile properties in young and old men and women." *The Journal of physiology* 552(Pt 1): 47-58.
- Treves, S., G. Feriotto, et al. (2000). "Molecular cloning, expression, functional characterization, chromosomal localization, and gene structure of junctate, a novel integral calcium binding protein of sarco(endo)plasmic reticulum membrane." *The Journal of biological chemistry* 275(50): 39555-39568.

- Tripathy, A. and G. Meissner (1996). "Sarcoplasmic reticulum luminal Ca^{2+} has access to cytosolic activation and inactivation sites of skeletal muscle Ca^{2+} release channel." *Biophysical journal* 70(6): 2600-2615.
- Tripathy, A., L. Xu, et al. (1995). "Calmodulin activation and inhibition of skeletal muscle Ca^{2+} release channel (ryanodine receptor)." *Biophysical journal* 69(1): 106-119.
- Tsujita, K., T. Itoh, et al. (2004). "Myotubularin regulates the function of the late endosome through the gram domain-phosphatidylinositol 3,5-bisphosphate interaction." *J Biol Chem* 279(14): 13817-13824.
- Tsutsui, K., Y. Maeda, et al. (1997). "cDNA cloning of a novel amphiphysin isoform and tissue-specific expression of its multiple splice variants." *Biochemical and Biophysical Research Communications* 236(1): 178-183.
- van der Ven, P. F., J. W. Bartsch, et al. (2000). "A functional knock-out of titin results in defective myofibril assembly." *Journal of cell science* 113 (Pt 8): 1405-1414.
- Vassilopoulos, S., S. Oddoux, et al. (2010). "Caveolin 3 Is Associated with the Calcium Release Complex and Is Modified via in Vivo Triadin Modification." *Biochemistry* 49(29): 6130-6135.
- Vassilopoulos, S., D. Thevenon, et al. (2005). "Triadins are not triad-specific proteins: two new skeletal muscle triadins possibly involved in the architecture of sarcoplasmic reticulum." *The Journal of biological chemistry* 280(31): 28601-28609.
- Wagenknecht, T., R. Grassucci, et al. (1989). "Three-dimensional architecture of the calcium channel/foot structure of sarcoplasmic reticulum." *Nature* 338(6211): 167-170.
- Wang, S., W. R. Trumble, et al. (1998). "Crystal structure of calsequestrin from rabbit skeletal muscle sarcoplasmic reticulum." *Nature structural biology* 5(6): 476-483.
- Wang, Y., X. Li, et al. (2009). "Altered stored calcium release in skeletal myotubes deficient of triadin and junctin." *Cell calcium* 45(1): 29-37.
- Wang, Z. M., M. L. Messi, et al. (2000). "L-Type Ca^{2+} channel charge movement and intracellular Ca^{2+} in skeletal muscle fibers from aging mice." *Biophysical Journal* 78(4): 1947-1954.

- Warnock, D. E., T. Baba, et al. (1997). "Ubiquitously expressed dynamin-II has a higher intrinsic GTPase activity and a greater propensity for self-assembly than neuronal dynamin-I." *Molecular Biology of the Cell* 8(12): 2553-2562.
- Warnock, D. E. and S. L. Schmid (1996). "Dynamin GTPase, a force-generating molecular switch." *BioEssays : news and reviews in molecular, cellular and developmental biology* 18(11): 885-893.
- Weaver, A. M., A. V. Karginov, et al. (2001). "Cortactin promotes and stabilizes Arp2/3-induced actin filament network formation." *Current biology : CB* 11(5): 370-374.
- Wechsler-Reya, R. J., K. J. Elliott, et al. (1998). "A role for the putative tumor suppressor Bin1 in muscle cell differentiation." *Mol Cell Biol* 18(1): 566-575.
- WechslerReya, R., D. Sakamuro, et al. (1997). "Structural analysis of the human BIN1 gene - Evidence for tissue-specific transcriptional regulation and alternate RNA splicing." *Journal of Biological Chemistry* 272(50): 31453-31458.
- Weed, S. A., A. V. Karginov, et al. (2000). "Cortactin localization to sites of actin assembly in lamellipodia requires interactions with F-actin and the Arp2/3 complex." *The Journal of cell biology* 151(1): 29-40.
- Wei, L., E. M. Gallant, et al. (2009). "Junctin and triadin each activate skeletal ryanodine receptors but junctin alone mediates functional interactions with calsequestrin." *International Journal of Biochemistry & Cell Biology* 41(11): 2214-2224.
- Weisleder, N., N. Takizawa, et al. (2012). "Recombinant MG53 protein modulates therapeutic cell membrane repair in treatment of muscular dystrophy." *Science translational medicine* 4(139): 139ra185.
- Weiss, R. G., K. M. O'Connell, et al. (2004). "Functional analysis of the R1086H malignant hyperthermia mutation in the DHPR reveals an unexpected influence of the III-IV loop on skeletal muscle EC coupling." *American journal of physiology. Cell physiology* 287(4): C1094-1102.
- Whalen, R. G., J. B. Harris, et al. (1990). "Expression of myosin isoforms during notexin-induced regeneration of rat soleus muscles." *Developmental biology* 141(1): 24-40.
- Wigge, P., K. Kohler, et al. (1997). "Amphiphysin heterodimers: potential role in clathrin-mediated endocytosis." *Mol Biol Cell* 8(10): 2003-2015.

- Wijsman, E. M., N. D. Pankratz, et al. (2011). "Genome-Wide Association of Familial Late-Onset Alzheimer's Disease Replicates BIN1 and CLU and Nominates CUGBP2 in Interaction with APOE." *Plos Genetics* 7(2).
- Witke, W., A. V. Podtelejnikov, et al. (1998). "In mouse brain profilin I and profilin II associate with regulators of the endocytic pathway and actin assembly." *The EMBO journal* 17(4): 967-976.
- Wu, K. D., W. S. Lee, et al. (1995). "Localization and quantification of endoplasmic reticulum Ca(2+)-ATPase isoform transcripts." *The American journal of physiology* 269(3 Pt 1): C775-784.
- Wuytack, F., B. Papp, et al. (1994). "A Sarco/Endoplasmic Reticulum Ca²⁺ Atpase 3-Type Ca²⁺ Pump Is Expressed in Platelets, in Lymphoid-Cells, and in Mast-Cells (Vol 269, Pg 1410, 1994)." *Journal of Biological Chemistry* 269(17): 13056-13056.
- Wuytack, F., L. Raeymaekers, et al. (1992). "Ca²⁺-Transport Atpases and Their Regulation in Muscle and Brain." *Annals of the New York Academy of Sciences* 671: 82-91.
- Yamada, H., E. Ohashi, et al. (2007). "Amphiphysin 1 Is Important for Actin Polymerization during Phagocytosis." *Mol Biol Cell*.
- Yamada, H., S. Padilla-Parra, et al. (2009). "Dynamic interaction of amphiphysin with N-WASP regulates actin assembly." *J Biol Chem* 284(49): 34244-34256.
- Yeates, T. O. (2002). "Structures of SET domain proteins: Protein lysine methyltransferases make their mark." *Cell* 111(1): 5-7.
- Yoshida, M., S. Minamisawa, et al. (2005). "Impaired Ca²⁺ store functions in skeletal and cardiac muscle cells from sarcolumenin-deficient mice." *The Journal of biological chemistry* 280(5): 3500-3506.
- Yu, H. T., J. K. Chen, et al. (1994). "Structural Basis for the Binding of Proline-Rich Peptides to Sh3 Domains." *Cell* 76(5): 933-945.
- Yuan, S., W. Arnold, et al. (1990). "Biogenesis of transverse tubules: immunocytochemical localization of a transverse tubular protein (TS28) and a sarcolemmal protein (SL50) in rabbit skeletal muscle developing in situ." *The Journal of cell biology* 110(4): 1187-1198.

- Zammit, P. S., L. Heslop, et al. (2002). "Kinetics of myoblast proliferation show that resident satellite cells are competent to fully regenerate skeletal muscle fibers." *Experimental cell research* 281(1): 39-49.
- Zampighi, G., J. Vergara, et al. (1975). "On the connection between the transverse tubules and the plasma membrane in frog semitendinosus skeletal muscle. Are caveolae the mouths of the transverse tubule system?" *The Journal of cell biology* 64(3): 734-740.
- Zanoteli, E., A. S. Guimaraes, et al. (2000). "Temporomandibular joint involvement in a patient with centronuclear myopathy." *Oral surgery, oral medicine, oral pathology, oral radiology, and endodontics* 90(1): 118-121.
- Zhang, L., C. Franzini-Armstrong, et al. (2001). "Structural alterations in cardiac calcium release units resulting from overexpression of junctin." *Journal of molecular and cellular cardiology* 33(2): 233-247.
- Zhang, L., J. Kelley, et al. (1997). "Complex formation between junctin, triadin, calsequestrin, and the ryanodine receptor. Proteins of the cardiac junctional sarcoplasmic reticulum membrane." *The Journal of biological chemistry* 272(37): 23389-23397.
- Zhang, P. and J. E. Hinshaw (2001). "Three-dimensional reconstruction of dynamin in the constricted state." *Nature cell biology* 3(10): 922-926.
- Zhang, Y. L., J. Fujii, et al. (1995). "Characterization of cDNA and genomic DNA encoding SERCA1, the Ca²⁺-ATPase of human fast-twitch skeletal muscle sarcoplasmic reticulum, and its elimination as a candidate gene for Brody disease." *Genomics* 30(3): 415-424.
- Zhong, X. L., D. J. Hoelz, et al. (2009). "Bin1 Is Linked to Metastatic Potential and Chemosensitivity in Neuroblastoma." *Pediatric Blood & Cancer* 53(3): 332-337.
- Zoncu, R., R. M. Perera, et al. (2007). "Loss of endocytic clathrin-coated pits upon acute depletion of phosphatidylinositol 4,5-bisphosphate." *Proceedings of the National Academy of Sciences of the United States of America* 104(10): 3793-3798.
- Zorzato, F., A. A. Anderson, et al. (2000). "Identification of a novel 45 kDa protein (JP-45) from rabbit sarcoplasmic-reticulum junctional-face membrane." *The Biochemical journal* 351 Pt 2: 537-543.

Zubrzycka, E. and D. H. MacLennan (1976). "Assembly of the sarcoplasmic reticulum. Biosynthesis of calsequestrin in rat skeletal muscle cell cultures." *The Journal of biological chemistry* 251(24): 7733-7738.

APPENDIX I: Resume de la these de doctorat

Mécanismes pathologiques des myopathies centronucléaires autosomales récessives

INTRODUCTION

Les myopathies centronucléaires forment un groupe de maladies congénitales caractérisées par une hypotonie et une biopsie du muscle squelettique typique présentant de petites fibres rondes avec des noyaux centraux. Plusieurs formes ont été documentées (Laporte, Biancalana et al. 2000 ; Bitoun, Maugendre et al. 2005 ; Nicot, Toussaint et al. 2007). La forme néonatale liée à l'X, aussi appelée myopathie myotubulaire (XLCNM, OMIM 310400) est une forme très sévère caractérisée par une faiblesse musculaire généralisée chez les nouveau-nés de sexe masculin. Les patients décèdent généralement au cours de la première année d'une insuffisance respiratoire. Le gène muté, MTM1, code pour la myotubularine. La forme autosomique dominante (ADCNM, OMIM 160150) en général cliniquement moins sévère. La maladie se déclare le plus souvent à l'âge adulte et les patients présentent une faiblesse musculaire diffuse lentement progressive qui peut être accompagnée d'une hypertrophie musculaire. La plupart des patients portent des mutations dans le gène DNM2, codant pour la dynamine 2. Les formes autosomiques récessives (ARCNM, OMIM 255200) se déclarent généralement durant l'enfance ou la petite enfance, bien que des cas d'hypotonie dès la naissance aient été reportés. Les ARCNM peuvent être subdivisées en trois groupes : une forme précoce avec ophtalmoparésie, une forme précoce sans ophtalmoparésie et une forme tardive sans ophtalmoparésie. Ce travail se concentre sur les ARCNM et le gène muté associé : *BIN1*.

Jusqu'à présent, trois mutations faux-sens (K35N, D151N et R154Q) et deux mutations non-sens (K575X et Q573X) ont été reportées dans le gène Bin1 (Nicot, Toussaint et al. 2007; Toussaint, Nicot et al. 2007 ; Cowling, Toussaint et al. 2012). De plus, trois variants homozygotes ont été identifiés chez quatre individus affectés faisant partie de trois familles consanguines.

BIN1 code pour l'amphiphysine 2, qui est une protéine connue pour être impliquée dans le trafic membranaire. L'amphiphysine 2 est régulée par les phosphoinositides et joue un rôle dans la biogénèse des tubules T dans le muscle squelettique (Lee, Marcucci et al. 2002). Des défauts dans les tubules T sont fréquemment trouvés pour les trois formes de CNM et ont été observés chez le modèle murin de l'XLCNM (Al-Qusairi, Weiss et al. 2009 ; Cowling, Toussaint et al. 2011 ; Toussaint, Cowling et al. 2011). De plus, des défauts de la protéine orthologue chez *Drosophila melanogaster* conduisent à des altérations du muscle squelettique (Zelhof, Bao et al. 2001). Les domaines de la protéine codée par *BIN1* sont impliqués dans la tubulation membranaire et dans l'interaction avec des lipides et d'autres protéines. L'hélice amphipathique N-terminale s'insère vraisemblablement dans la membrane plasmique et induit la courbure de la membrane, et le domaine BAR homodimerise sous forme de banane pour sentir et maintenir la courbure. L'hélice N-terminale et le domaine BAR forment le domaine N-BAR. Le domaine SH3 C-terminal permet l'interaction avec de nombreuses protéines comme la synaptojanine ou la dynamine. L'isoforme de *BIN1* spécifique du muscle contient un résidu polybasique en C-terminal du domaine BAR. Ce résidu est codé par l'exon 11 et lie des phosphoinositides, permettant la tubulation membranaire dans des cellules cultivées (Lee, Marcucci et al. 2002).

BIN1 est également impliqué dans la myotonie dystrophique congénitale (cDM) (Fugier, Klein et al. 2011). La plupart des défauts musculaires sont comparables entre cDM et CNM. Les fibres musculaires sont atrophiques et présentent une centralisation des noyaux qui n'est pas due aux cycles répétitifs de nécrose/régénération comme pour d'autres pathologies musculaires avec noyaux centraux. Il a été démontré que l'épissage de *BIN1* est altéré chez les patients cDM, causant l'excision de l'exon 11 spécifique du muscle (Fugier, Klein et al. 2011). Le *knockout* (KO) complet de *Bin1*, généré préalablement, entraîne une perte totale de la protéine (délétion de l'exon 3) et une létalité périnatale due à une cardiomyopathie (Muller, Baker et al. 2003).

L'importance de *BIN1* dans la formation des tubules T dans le muscle squelettique de mammifère et son rôle dans la pathogenèse de CNM reste à être déterminée.

OBJECTIFS

Les objectifs de cette étude sont de mieux comprendre le rôle de BIN1/amphiphysine2 dans le muscle normal ou atteint de myopathie centronucléaire, ainsi que d'identifier de nouvelles cibles thérapeutiques pour un traitement potentiel de l'ARCNM.

RESULTATS

Pour mieux comprendre la fonction de BIN1, nous avons généré et caractérisé deux lignées de *Bin1* KO avec délétion de l'exon 11 ou délétion de l'exon 20.

🚧 L'exon 11, spécifique du muscle, n'est pas nécessaire pour la formation du muscle

Pour étudier le lien entre BIN1 et MTM1, ainsi qu'entre BIN1 et les substrats phosphoinositidiques (PIs) de MTM1, nous avons généré des cellules ES avec délétion de l'exon 11. Cet exon est en phase et code pour le domaine liant les PIs. L'isoforme sans exon 11 existe dans les myoblastes et est remplacée par l'isoforme contenant l'exon 11 durant la myogénèse, isoforme majoritaire dans le muscle squelettique adulte (Fugier, Klein et al. 2011). La délétion de l'exon 11 devrait empêcher la régulation de BIN1 par les PIs et potentiellement le lien avec MTM1.

Nous avons utilisé le promoteur CMV pour induire la délétion de l'exon 11. L'épissage des exons adjacents n'était pas perturbé par la délétion. Au niveau protéique, nous avons confirmé l'expression de BIN1 sans exon 11 en utilisant un anticorps contre l'exon 11 et un anticorps détectant toutes les isoformes. L'espérance de vie de ces souris KO n'était pas réduite comparé aux souris sauvages (WT) de la même portée. Nous avons choisi d'analyser des souris à 12 semaines et à 12 mois. Nous n'avons pas observé de différences physiques majeures et la force spécifique du muscle tibialis anterior (TA) était comparable entre les souris KO et WT. L'analyse de la taille des fibres n'a montré aucune différence significative entre les deux groupes et les colorations H&E et SDH n'ont pas révélé d'altérations majeures. Néanmoins, nous avons remarqué une augmentation légère, mais significative du mauvais positionnement des noyaux (4% contre 1% à 12 semaines et 6% contre 2% à 12 mois).

L'immunohistochimie a montré que la délétion de l'exon 11 n'avait pas d'effet sur le positionnement de BIN1, RYR1 (réticulum sarcoplasmique) ou de DHPR (Tubules T) chez la souris de 12 semaines. L'ultrastructure du muscle squelettique a été évaluée par microscopie électronique (EM). Encore une fois, nous n'avons pas observé de grandes différences entre les souris KO et WT à 12 semaines et 12 mois. Finalement, pour étudier les capacités régénératives des souris *Bin1* exon 11 KO, nous avons provoqué la dégénérescence du TA en injectant de la notexine, et analysé le muscle 3, 5, 7 et 14 jours post-injection. Au cours des premiers stades de régénération musculaire (3, 5, 7 jours), nous n'avons observé aucune différence au niveau de la masse musculaire et au niveau de la coloration H&E du TA. A un stade plus tardif (14 jours), le TA du KO a pris moins de masse que le TA de la souris WT. De plus, nous avons remarqué une atrophie prononcée du muscle KO à 14 jours. Nous avons analysé la population de cellules satellites par qRT-PCR. Il n'y avait pas de différence concernant les marqueurs Pax7 et MyoD dans la population totale ou la population activée des cellules satellites. Néanmoins, le niveau de myogénine était plus élevé chez les KO que chez le groupe contrôle, ce qui pourrait indiquer une différence dans l'étape de maturation, qui serait incomplète ou plus lente.

En plus du modèle murin de l'exon 11, nous avons caractérisé deux nouvelles mutations d'épissage de l'exon 11 de BIN1. La première mutation d'épissage (IVS10-1G>A) a été trouvée chez trois patients appartenant à une famille consanguine. La deuxième mutation d'épissage de l'exon 11 (IVS10-2A>G) a été trouvée chez 5 chiens de race dogue allemand. Concernant les patients humains, le niveau d'expression de BIN1 avec exon 11 était fortement réduit, mais il n'y avait pas d'impact sur le niveau total de protéine. La faiblesse musculaire est apparue vers l'âge de 3 ans et demi avec une progression très rapide entraînant le décès de deux des patients, à 5 et 7 ans, respectivement. Le troisième patient est toujours en vie et présente une faiblesse musculaire avec une prédominance au niveau des muscles proximaux, une faiblesse des muscles faciaux, mais pas de détresse respiratoire. L'analyse histologique (coloration H&E) a révélé une grande proportion de noyaux centraux, une atrophie des fibres musculaires et une fibrose endomysiale modérée. La coloration NADH-TR a montré une atrophie prédominante des fibres de type I. Ces anomalies sont des

marqueurs de CNM. Chez les chiens atteints, la maladie débute à 8 mois et progresse également rapidement. L'expression de l'isoforme BIN1 avec exon 11 était totalement absente. La coloration H&E du muscle *biceps femoris* de chiens atteints a révélé une internalisation nucléaire ainsi qu'une atrophie des fibres musculaires. Les zones centrales sans coloration ont été observées, et reflètent des régions exemptes de myofibrilles. En résumé, les histologies humaines et canines étaient comparables.

✚ L'exon 20 est nécessaire pendant le développement, mais pas pour le maintien du muscle

Nous avons généré un deuxième modèle murin pour BIN1. La délétion de l'exon 20 (dernier exon de BIN1) détruit le domaine SH3, qui est impliqué dans l'interaction avec différentes protéines comme la dynamine 2. Cette délétion est comparable au codon stop prématuré trouvé chez deux patients. Nous avons caractérisé des lignées KO constitutif (CMV), spécifique du muscle (HSA) et inductible (HSA-ERT2), générées par recombinaison homologue ciblée de l'exon 20 de BIN1 dans les cellules ES.

La délétion de l'exon 20 en utilisant les promoteurs CMV ou HSA induit une létalité périnatale. Les nouveau-nés mouraient dans les 12 heures suivant la naissance, certainement en raison d'une incapacité à se nourrir. En effet, les souriceaux étaient hypoglycémiques et leurs estomacs ne contenaient pas de lait. Le niveau de la protéine BIN1 était réduit, et l'organisation longitudinale typique de BIN1 dans les fibres musculaires était absente. La localisation du canal calcique DHPR aux tubules T dans les fibres isolées de souris KO était également perturbée. Ceci suggère l'importance de BIN1 et de son domaine SH3 dans la formation correcte des tubules T.

Nous avons utilisé les souris KO inductibles, sous le contrôle du promoteur HSA, pour étudier le rôle de BIN1 dans le maintien du muscle chez la souris adulte. La recombinaison a été induite à l'âge de 7 semaines par injection de tamoxifen. Nous avons analysé l'impact de cette délétion jusqu'à 25 semaines post-induction. Même si la réduction au niveau protéique était forte (70%), nous n'avons pas observé d'anomalies aux niveaux physiologiques et histologiques.

DISCUSSION ET PERSPECTIVES

Jusqu'à présent, il n'existait pas de modèle murin pour étudier le rôle de BIN1 dans le muscle squelettique. Il a précédemment été montré que le KO total de *Bin1* est létal puisque les nouveau-nés meurent d'une cardiomyopathie à la naissance. C'est pourquoi notre approche a consisté à supprimer différentes régions de BIN1 en utilisant plusieurs promoteurs (CMV, HSA, HSA ER^{T2}) afin de mieux décrypter le rôle des différents domaines.

Il a été montré que l'exon 11 joue un rôle dans la tubulation de BIN1. En effet, des altérations du site d'épissage de cet exon ont été identifiées chez des patients ainsi que chez un modèle de chien naturellement affecté. Chez la souris, il a été montré que le saut de l'exon 11 (U7) entraîne une forte réduction de la force spécifique et que sa diminution au niveau protéique affecte les tubules T et la localisation de DHPR. Dans notre laboratoire, le modèle murin KO de l'exon 11 sous le contrôle du promoteur CMV ne présente pas de phénotype évident. Ces divergences par rapport aux données publiées peuvent avoir différentes explications. Pour U7, le saut de l'exon 11 a été réalisé chez la souris adulte et le phénotype n'est apparu qu'après quatre mois. De plus, le saut d'exon 11 a été induit après la naissance, alors que la délétion génétique chez la souris KO *Bin1* exon 11 est présente dès l'embryogenèse. Cela peut avoir déclenché des mécanismes compensatoires au cours de l'embryogenèse. U7 peut aussi avoir créé des défauts d'épissage aspécifiques. D'autre part, n'oublions pas que le développement musculaire ne se produit pas de la même façon chez les patients, les chiens et les souris. Les humains et les chiens naissent avec des muscles déjà pleinement matures alors que chez les souris, la maturation continue durant les trois premières semaines après la naissance. Ceci a un impact majeur lorsque l'on extrapole des données provenant de modèles murins. Les patients et les chiens qui portent des mutations dans l'exon 11 développent la maladie plus tardivement que les autres cas d'ARCNM et restent très actifs. D'après ces données, l'exon 11 n'est pas nécessaire pour le muscle. Cela concorde avec le fait que l'exon 11 commence à être exprimé vers la naissance (Fugier, Klein et al. 2011). Avant l'apparition de la maladie chez les patients et les chiens, il pourrait y avoir un mécanisme compensatoire. Il pourrait aussi y avoir une certaine limite (âge, activité...) au-delà de laquelle le muscle n'est plus

capable de tolérer cette perte. Dans les conditions de laboratoire, les souris sont assez sédentaires et les mécanismes tels que la régénération musculaire et même le maintien du muscle sont moins visibles que dans leur mode de vie naturel. Les dernières expériences faites chez la souris KO *Bin1x11*, qui présentent des troubles pendant la régénération induite par la toxine, confirment cela. Nous avons montré que, bien qu'aucune différence au niveau des cellules satellites n'ait été observée, il existe une réduction de la capacité de régénération du muscle. Les mécanismes impliqués dans ce processus devront être étudiés plus en détail.

Nous avons pu voir, grâce à la souris *Bin1x20* ER^{T2} que BIN1 n'est pas nécessaire pour le maintien du muscle, puisque même après une réduction significative, la souris ne présente pas de phénotype. Il se pourrait que le phénotype ne soit pas visible, en raison de l'activité restreinte des souris, qui sont logées dans de petites cages. Dans un autre contexte et dans des conditions plus naturelles, les résultats pourraient être différents. Pour pallier à ce problème, nous pourrions induire un stress musculaire en utilisant des tapis roulants, ou tester la capacité de régénération par injection de notexine.

Pour conclure, nous avons confirmé le rôle de BIN1 comme un acteur clé dans la formation des tubules T. L'exon 11, spécifique du muscle, pourrait être important dans le processus de régénération musculaire, mais n'est pas nécessaire pour la formation du muscle squelettique. Enfin, nous avons identifié une nouvelle cible thérapeutique pour l'ARCNM.

Mécanismes pathologiques des myopathies centronucléaires autosomales récessives

Résumé

BIN1 est une protéine qui tubule les membranes. Elle est composée de plusieurs domaines : un domaine BAR, qui lie les membranes et possède une propriété de tubulation; un motif PI qui lie les phosphoinositides et est uniquement exprimé dans le muscle squelettique; un domaine CLAP qui lie la clathrin et AP2 et qui n'est présent que dans les isoformes de BIN1 exprimées dans le cerveau; un domaine MBD impliqué dans la liaison à c-Myc; et un domaine SH3 impliqué dans les interactions avec les protéines riches en prolines. BIN1 est une protéine ubiquitaire, et l'organe où elle est le plus fortement exprimée est le muscle squelettique. Il a été montré que des mutations dans l'amphiphysine 2/BIN1 causent une myopathie centronucléaire récessive (ARCNM, OMIM 255200). Les mutations trouvées chez les patients sont réparties dans tous les domaines de la protéine, et deux d'entre elles aboutissent à un codon stop prématuré dans l'exon 20, dernier exon de la protéine. Le motif PI, codé par l'exon 11, est régulé positivement pendant la myogenèse. Le but de cette recherche était de mieux comprendre le rôle de BIN1 dans le muscle sain et dans le cas de myopathie centronucléaire. Nous avons donc utilisé la technique de recombinaison homologue ciblée dans les cellules ES pour générer deux lignées de souris knockout: BIN1 exon 11 (délétion de l'exon 11) et BIN1 exon 20 (délétion de l'exon 20). La délétion de l'exon 20 détruit le domaine SH3, qui permet l'interaction de BIN1 avec différentes protéines, dont la dynamine 2, et induit une baisse considérable de l'expression de BIN1 au niveau protéique. Les délétions totales et spécifiques du muscle de l'exon 20 provoquent une létalité périnatale. Nous avons observé une perturbation de l'organisation des tubules T chez les souris KO, ce qui montre l'importance de BIN1 pendant la biogenèse des tubules T. Cependant, l'induction de la délétion chez la souris adulte n'a affecté ni la fonction ni l'organisation du muscle. Pour comprendre le rôle du motif PI, qui est spécifique du muscle, nous avons caractérisé les souris BIN1 KO exon 11. Même à 12 mois, la fonction du muscle n'était pas compromise chez ces souris. En revanche, nous avons observé des problèmes de régénération du muscle squelettique. Ce travail révèle, qu'in vivo, BIN1 est nécessaire pour la biogenèse des tubules T, mais pas indispensable pour le maintien du muscle. D'autre part, le domaine PI, spécifique du muscle, est impliqué dans la régénération musculaire. Sa fonction dans les muscles est régulée finement par l'expression de différentes isoformes et par des interactions intra-moléculaires. Comprendre ces caractéristiques nous aiderait à développer de nouvelles thérapies pour les patients atteints de ARCNM et de MD.

Résumé en anglais

BIN1 is a membrane tubulating protein and it consists of the BAR domain which binds membranes and has tubulating property; the PI motif which binds phosphoinositides and is expressed only in skeletal muscle; the CLAP domain binds clathrin and AP2 and is present exclusively in brain isoforms of BIN1; the MBD is involved in c-Myc binding and the SH3 domain is involved in interactions with prolin-rich proteins. BIN1 is an ubiquitously expressed protein with the highest expression in skeletal muscle. Mutations in amphiphysin 2 / BIN1 were found to cause autosomal recessive centronuclear myopathy (ARCNM, OMIM 255200). Mutations in patients were found in all the protein domains and include two mutations leading to a premature stop codon in the last exon 20. The PI motive, encoded by exon 11, is upregulated during myogenesis. The aim of this research was to better understand the role of BIN1 in healthy muscle and in the pathology of CNM. For this purpose, by using targeted homologous recombination in ES cells, we generated two knockout mouse models: BIN1 exon 11 and BIN1 exon 20, with exon 11 and 20 deleted, respectively. The deletion of exon 20 disrupts the SH3 domain, involved in interactions with different proteins, amongst which is dynamin 2 and induced a considerable loss of the total BIN1 protein expression. The total and muscle specific deletions of exon 20 were perinatally lethal. A disrupted T-tubules organization was observed in knockout mice, showing an importance of BIN1 during the T-tubule biogenesis. Interestingly, deletion induced in adult mice did not affect muscle function and organization. In order to understand the role of the muscle specific PI motif, we characterized the BIN1 exon 11 KO mice. Even at 12 months of age the muscle function in mice was not compromised by this deletion. However, further examination showed impairment of skeletal muscle regeneration. This work revealed that in vivo, BIN1 is necessary during the T-tubules biogenesis and dispensable for muscle maintenance, whereas the skeletal muscle specific PI motif of BIN1 is involved in muscle regeneration. Its function in muscle is tightly regulated by isoform switch and intramolecular binding. Understanding these features will help us step forward towards successful therapy in ARCNM and MD patients.